



Test of MicroShades and calibration and use of models of MicroShades



Technological Institute

**Test of MicroShades and
calibration and use of models of MicroShades**

**Søren Østergaard Jensen
Energy and Climate Division
Technological Institute**

July 2010

Preface

This report describes the results from measurements in two test rooms – one with MicroShades in the windows, the results from calibration of a computer model of the test rooms and the results from simulation of the thermal performance of MicroShades. The work performed is part of the project “PowerShades II – optimization and validation of highly transparent photovoltaic” project no. 2008-1-0044 financed by Energinet.dk.

The following persons have participated in this part of the project:

Søren Østergaard Jensen, M.Sc., Danish Technological Institute

Alicia Johanson, Phd., PhotoSolar Aps

Eik Bezzel, M.Sc., PhotoSolar Aps

Lars Olsen, Phd., Danish Technological Institute

Marcin Blazniak Andersen, M.Sc., Danish Technological Institute

Test of MicroShades and calibration and use of models of MicroShades

1st printing, 1st edition, 2010

© Danish Technological Institute

Energy and Climate Division

ISBN: 87-7756-776-5

ISSN: 1600-3780

List of contents

1.	Introduction	4
1.1.	The work of the present project	5
2.	Comparison between measured and calculated solar radiation through a window with MicroShades	6
2.1	Periods chosen for the comparison	7
2.2.	Radiation on the façade	8
2.3.	Comparison between measured and calculated solar radiation through the MicroShade window	17
2.4	Conclusions	32
3.	Comparison between two ways of calculating solar radiation through a traditional low-E window	33
4.	Test of the measurements of solar radiation through the windows	35
4.1.	Test of solar radiation measurements	36
4.1.1.	Test of the transmittance across the MicroShade window	44
4.1.2.	Test of the pyranometer in room B	47
4.2.	Conclusions	49
5.	Tutorial for including MicroShades in esp-r (version 11.8) simulations ...	50
6.	Case study: Malling school	53
6.1.	Parametric study	58
6.2.	Exposure to the sun	65
6.3.	CFD simulations	65
6.4.	Conclusions	69
7.	The effect of solar radiation through windows on thermal comfort	71
7.1.	MicroShades	73
7.2.	Experiments in the two test rooms	75
7.3.	Conclusions	80
8.	Daylight measurements	81
9.	Temperatures in windows with MicroShades	85
9.1.	MicroShade low-E window	85
9.2.	MicroShade low E window with a single layer of glass in front	87
9.3.	3 pane low-E window	91
9.4.	MicroShade low-E roof window	94
9.5.	Conclusions	97
10.	Evaluation of measurements from the test rooms	98
10.1.	Temperatures in the test rooms	98
10.1.1.	Comparison with the Velfac window	100
10.1.2.	Comparison with the low-E window	105
10.2.	Solar radiation to the test rooms	105
10.3.	Conclusions	111

11.	Conclusions	113
12.	References	115
Appendix A	Paper to IBPSA BS2009 – 27 th -30 th July, Glasgow, Scotland	116
Appendix B	Comparison between measured and calculated radiation through the MicroShade window with scattering factor of 0, 1 and 2 %	126
Appendix C	Brochure on applying MicroShades in windows at Malling school ...	145
Appendix D	Description of two class rooms at Malling school	151
Appendix E	Daylight measurements from [Jensen, 2008b]	156

1. Introduction

MicroShadeTM is a microstructure of small holes. Figure 1.1 shows an example of MicroShade. MicroShade consists of many small super elliptic shaped holes manufactured in a thin stainless steel sheet – see figure 1.1. The holes have a tilting angle and resemble the way Venetian Blinds function. However, the appearance is different and so is the view out as seen in figure 1.2. The screening off and view out through MicroShade are determined by the shape and tilting angle of the holes in figure 1.1.

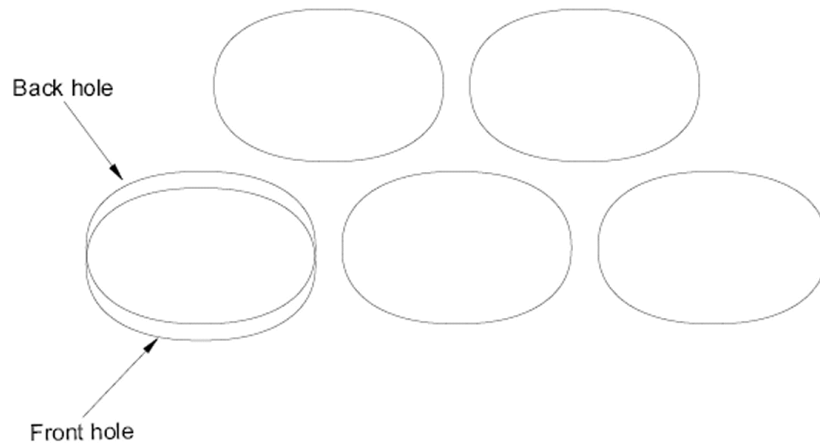


Figure 1.1. Example of the holes in MicroShade. The width of the holes is less than 1 mm.



Figure 1.2. A photo through a window with MicroShades. MicroShades are manufactured in a role to role production. The width of the foil is 140 mm. The vertical stripes in figure is 3 mm opaque areas for mounting of the MicroShades.

Figure 1.2 shows MicroShade imbedded in a low-e window. The name of this product is MicroShadeTM IG (Insulated Glazing) but will in the following be referred to as MicroShade windows.

The here described work is a continuation of the work from the project “PowerShades – Development and pilot demonstration of new transparent photo voltaic module” project no. 2006-1-6322 also financed by Energinet.dk. This work is reported in (Jensen, 2008a) and (Jensen, 2008b). The main findings from (Jensen, 2008b) were in 2009 reported in a paper to the IBPSA BS2009 conference. The paper is enclosed in Appendix A.

1.1. The work of the present project

The work of the project has consisted of several not necessarily interconnected subjects:

Chapter 2 describes the result from the continuation of validating the model of MicroShade windows.

In chapter 3 is investigated if the simulation program esp-r used for the validation in chapter 2 interpret the matrix developed to describe MicroShade windows correctly. This is done by comparing the results from simulation both with the detailed matrix description of a traditional low-E window with the normal more simple description.

In chapter 4 it is investigated if the solar measurements behind the windows in the test rooms are correct.

The simulation program esp-r is used in the present work. In chapter 5 is given a tutorial on how to incorporate MicroShade windows in esp-r models of building.

Chapter 6 contains the results for a case study on a real building where MicroShade windows has been installed.

In chapter 7 it is investigated how the comfort level is influenced when a person sitting next to a window is hit by the sun.

Chapter 8 gives the results from daylight measurements on the MS-A type of MicroShade.

In chapter 9 esp-r models are applied to investigate the temperature level of windows with MicroShades.

Finally some evaluation of the measurements in the two test rooms is given in chapter 10.

2. Comparison between measured and calculated solar radiation through a window with MicroShade

In the following the incoming solar radiation through a window with MicroShades on the inside surface of the outer layer of glass in a low-E window (see figure 2.1) is investigated by comparing the measured incoming radiation with the calculated radiation. The latter using the simulation program esp-r [ESRU, 2001] applying the special module for bi-directional calculation of the optical properties in a window.

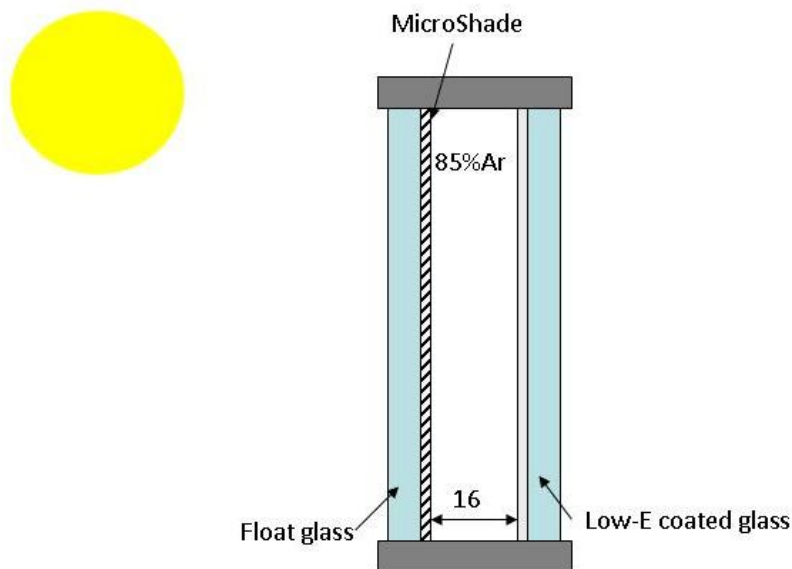


Figure 2.1. The window with MicroShades.

The bi-directional module demands a matrix with the optical properties of the window. The top of such a matrix is shown in figure 2.2. The 9 columns after the starting text contains the total direct transmission, the absorption in each layer of the window and the enhancement of incoming diffuse radiation due to the scattering of direct radiation in the MicroShades. The values are listed for combinations of the horizontal and vertical incidence angle at steps of 5° . At line 8 is located the transmittance of the diffuse radiation. For further information on the bi-directional file see [Jensen, 2008b].

The nine columns of the matrix are calculated by a special purpose program. However, there is as yet no theory for calculation of the transmittance of the diffuse radiation. This has to be measured [Jensen, 2008b], and is the ratio between the incoming radiation through the window and the radiation hitting the façade on cloudy days. For the investigated period – most part of the first half year of 2010 - the transmittance for overcast days are shown in figure 2.3. The mean value of the shown values is 0,185. This will be used as the transmittance of diffuse radiation of the investigated window.

There is further not yet a theory for the scattering of the direct solar radiation in the MicroShades so in the following the values of the ninth column are set to either 0, 1, 2 or 3%.

```

*BIDIRECTIONAL
*types,1
*item,121107
*layers,5,glass1,shading,glass2,air,glass3
*sets,1 # there is only this set of optical data
*start_set
*diffuse_abs,0.036,0.372,0.013,0.000,0.042
*diffuse_tm,0.12 ← diffuse transmittance
*direct_angs,37,37
*data
#Incidence angle, Total Glass 1, Shading device, Glass 2, Air, Glass 3, Converted diffuse fraction
#HorizontVertical, Transmittance, Absorb, Absorb, Absorb, Absorb, Absorb, Direct-diffuse
#Degrees, Degrees
-90 -90 0 0 0 0 0 0
-90 -85 0 0 0 0 0 0
-90 -80 0 0 0 0 0 0
-90 -75 0 0 0 0 0 0
-90 -70 0 0 0 0 0 0
-90 -65 0 0 0 0 0 0
-90 -60 0 0 0 0 0 0
-90 -55 0 0 0 0 0 0
-90 -50 0 0 0 0 0 0
-90 -45 0 0 0 0 0 0
-90 -40 0 0 0 0 0 0
-90 -35 0 0 0 0 0 0
-90 -30 0 0 0 0 0 0
-90 -25 0 0 0 0 0 0
-90 -20 0 0 0 0 0 0
-90 -15 0 0 0 0 0 0
-90 -10 0 0 0 0 0 0
-90 -5 0 0 0 0 0 0
-90 0 0 0 0 0 0 0
-90 5 0 0 0 0 0 0
-90 10 0 0 0 0 0 0
-90 15 0 0 0 0 0 0
-90 20 0 0 0 0 0 0
-90 25 0 0 0 0 0 0
-90 30 0 0 0 0 0 0
-90 35 0 0 0 0 0 0
-90 40 0 0 0 0 0 0
-90 45 0 0 0 0 0 0
-90 50 0 0 0 0 0 0
-90 55 0 0 0 0 0 0
-90 60 0 0 0 0 0 0
-90 65 0 0 0 0 0 0
-90 70 0 0 0 0 0 0
-90 75 0 0 0 0 0 0
-90 80 0 0 0 0 0 0
-90 85 0 0 0 0 0 0
-90 90 0 0 0 0 0 0
-85 -90 0 0 0 0 0 0
-85 -85 0 0.022 0 0 0 0
-85 -80 0 0.039 0.003 0 0 0
-85 -75 0 0.039 0.02 0 0 0 0.001
-85 -70 0 0.039 0.035 0 0 0 0.002
-85 -65 0 0.039 0.05 0 0 0 0.003

```

1th column: azimuth
2th column: solar height
3th column: total direct transmittance
4th column: absorption in the outer layer of glass
5th column: absorption in the PowerShade foil
6th column: absorption in the in the glass behind the MicroShade foil
– not used in the investigated window
7th column: absorption in the air gab of the window
8th column: absorption in the inner layer of glass
9th column: enhancement of diffuse radiation due to scattering of direct radiation in the PowerShade fail

MicroShade foil

outer glass air gab inner glass

low-E coating

Figure 2.2. Example of a MicroShade matrix. The matrix covers azimuths and solar heights from -90 to 90° with steps of 5°.

The MicroShades mounted in the window was of the type MS-A. The applied matrix is MS-A-220610_clearprem+ms.

2.1. Periods chosen for the comparison

Three periods has been chosen for the comparison:

Winter: 27/1-21/2, 2010 – 26 days

Spring: 4/3-25/4, 2010 – 52 days

Summer: 2/6-17/6, 2010 – 16 days

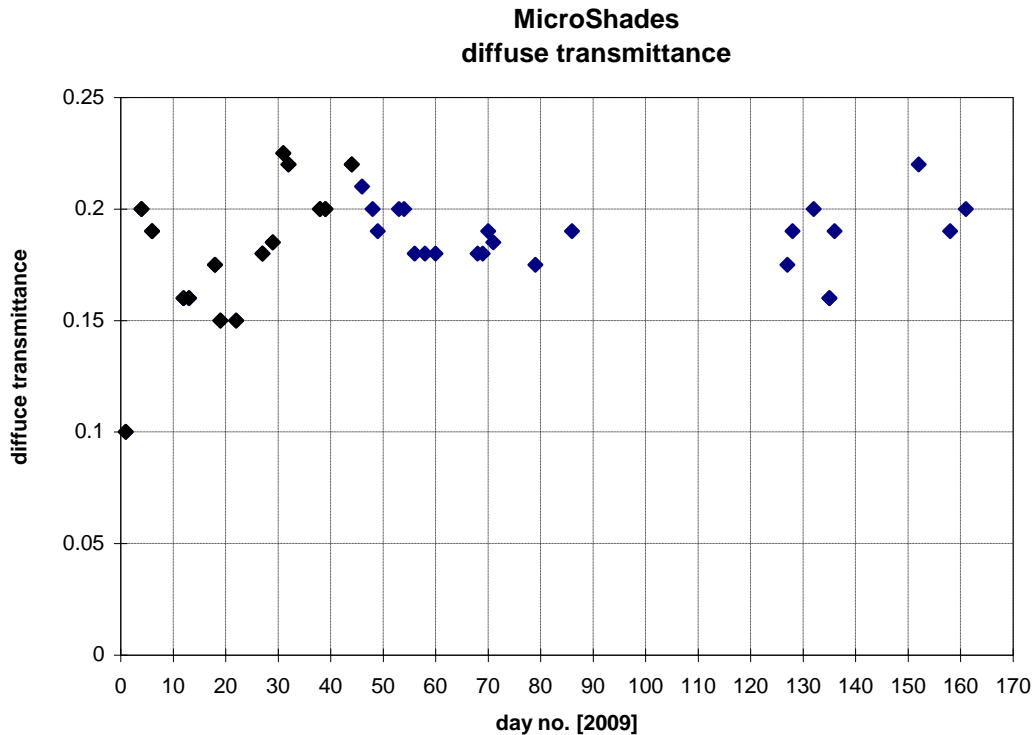


Figure 2.3. Diffuse radiation through the MicroShade window on overcast days.

2.2. Radiation on the facade

The radiation on the façade is calculated using the measured global and horizontal diffuse radiation - for further details see [Jensen, 2008a-b]. There is as seen in figures 2.4-2.15 a rather good agreement between measured and calculated solar radiation on the façade.

Another way to show the agreement between measurements and calculations is to plot the values against each other as correlation plots. This is shown in figures 2.16-18 for the three periods. The green line in these figures represents a perfect correlation between the values.

Figures 2.16-18 shows a very scattered picture for the winter period and spring period while less scattered during the summer period. Figure 2.19 shows part of the reason for the scattering. The figure shows a close up of February 12, 2010. At the start of the day much more solar radiation is calculated – see green circle in figure 2.19. This could be caused by the fact that the calculations do not incorporate the shade from a building situated to the left [Jensen, 2008b]. However, introducing shading does not change the “over calculation” in the morning. When looking at figures 2.4-2.15 this problem occurs, however, seldom and only during the winter period. There are minor discrepancies in the morning and afternoon of the two other periods, but this is related to the difficulties in calculating the solar radiation at large incidence angles – and as the energy amount at these angles is low and that MicroShades cut off radiation at large incidence angles, this will not be regarded as a problem. Day 47 and 50 (figure 2.7) and day 70 and 71 (figure 2.10) shows that the model sometimes have difficulties in predicting the solar radiation during drifting clouds while eg day 41 and 43 (figure 2.6) show good agreement.

Winter period

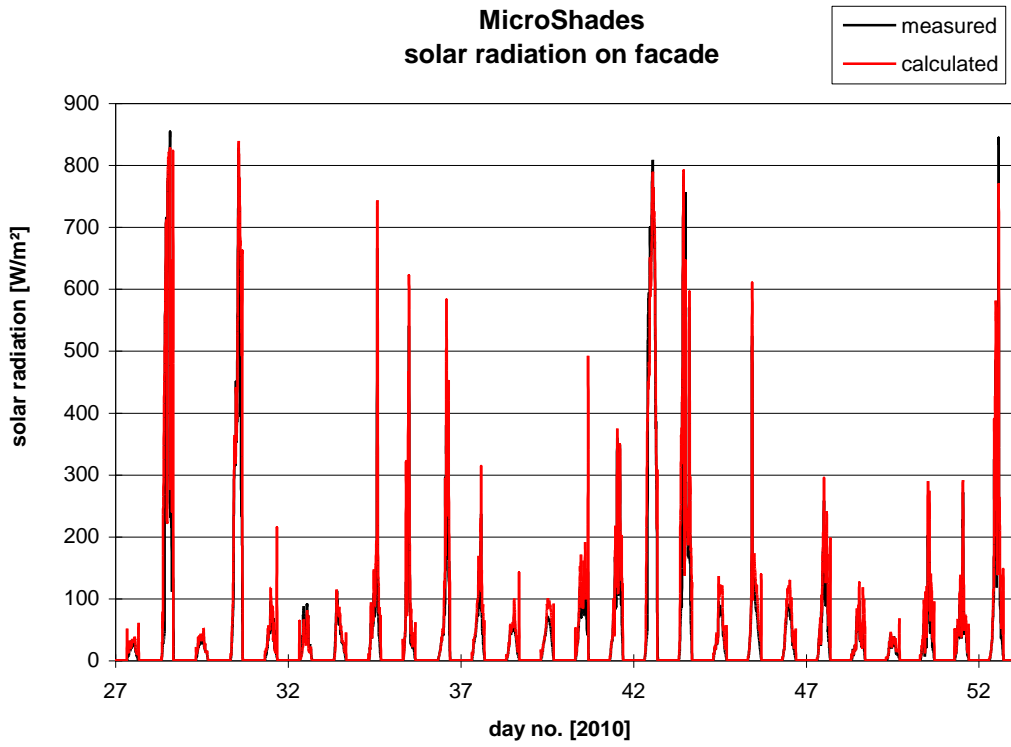


Figure 2.4. Solar radiation on the façade during the winter period.

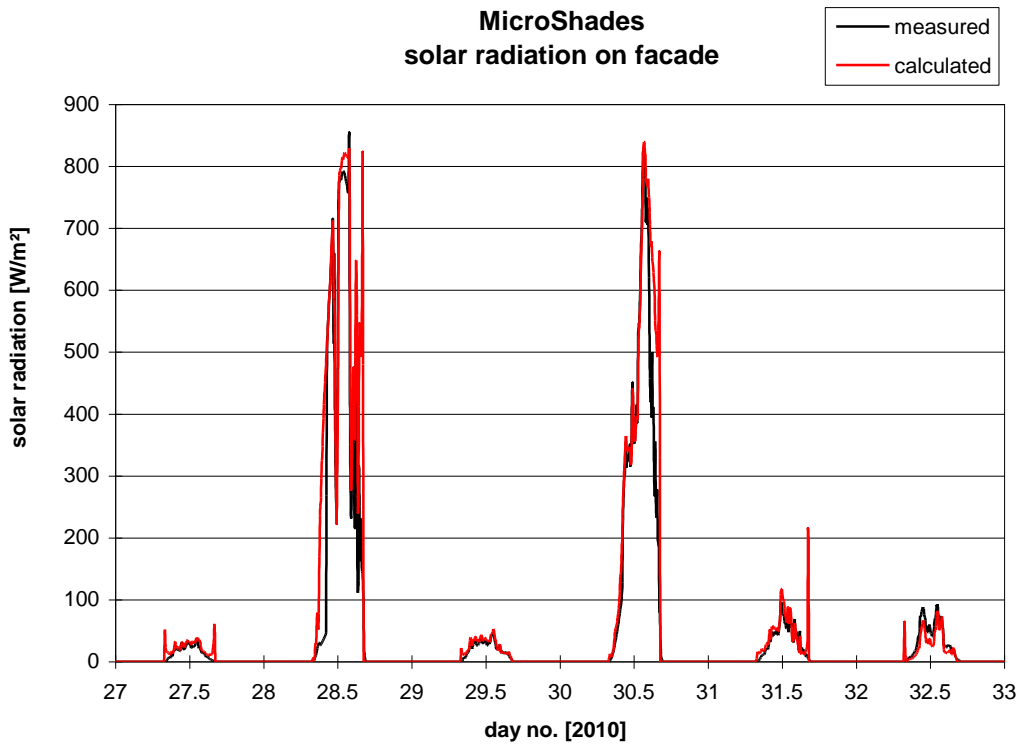


Figure 2.5. Solar radiation on the façade for 5 days in the winter (January 27-February 1, 2010).

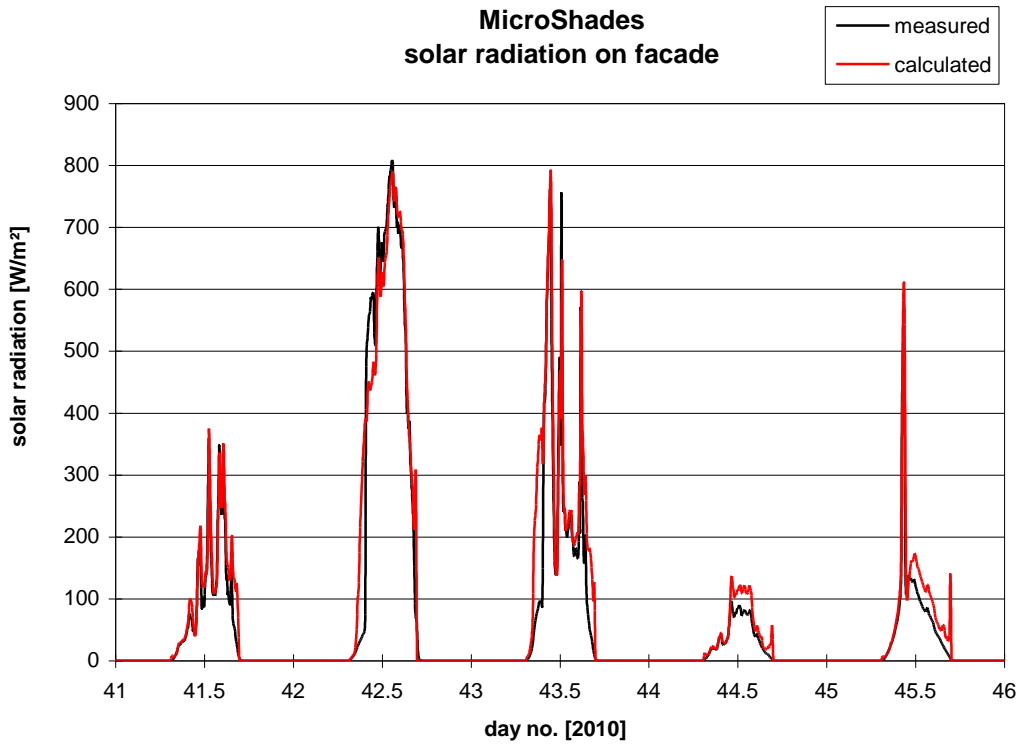


Figure 2.6. Solar radiation on the façade for 5 days in the winter (February 11-14, 2010).

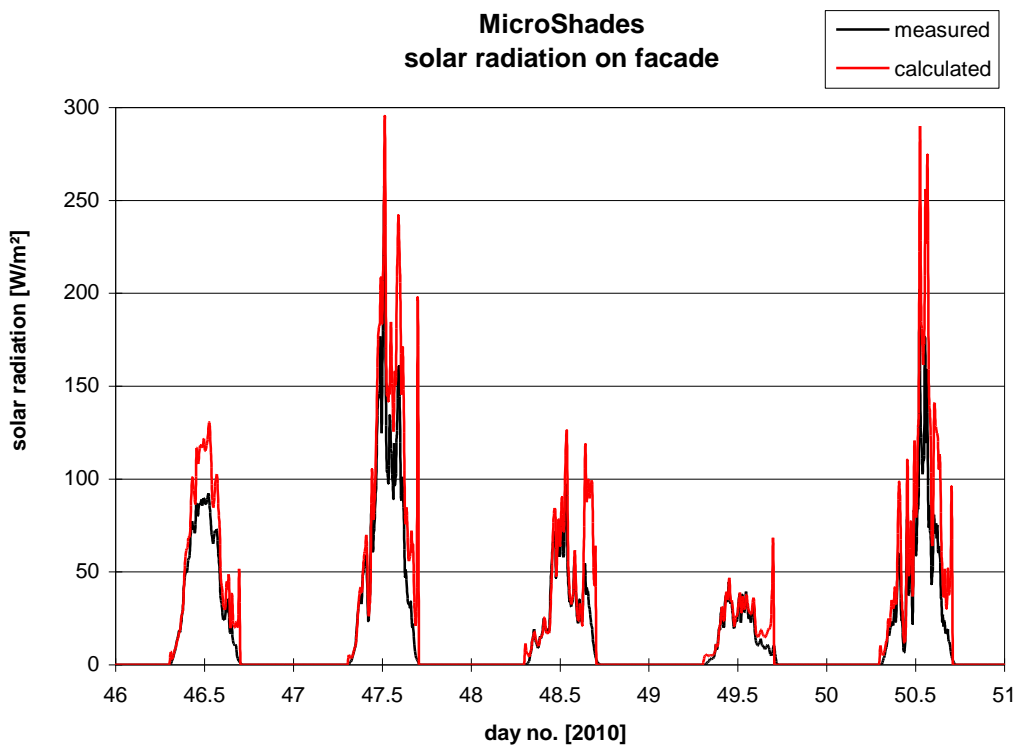


Figure 2.7. Solar radiation on the façade for 5 days in the winter (February 15-19, 2010). Special focus on diffuse radiation – note the lower units on the y-axis.

Spring period

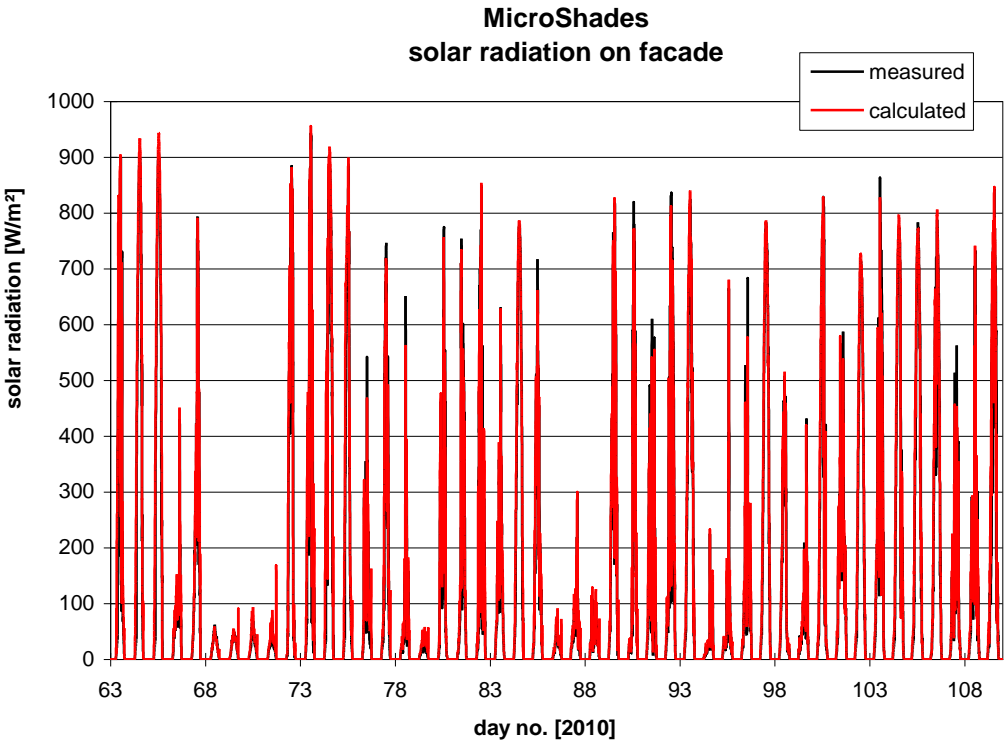


Figure 2.8. Solar radiation on the façade during the spring period.

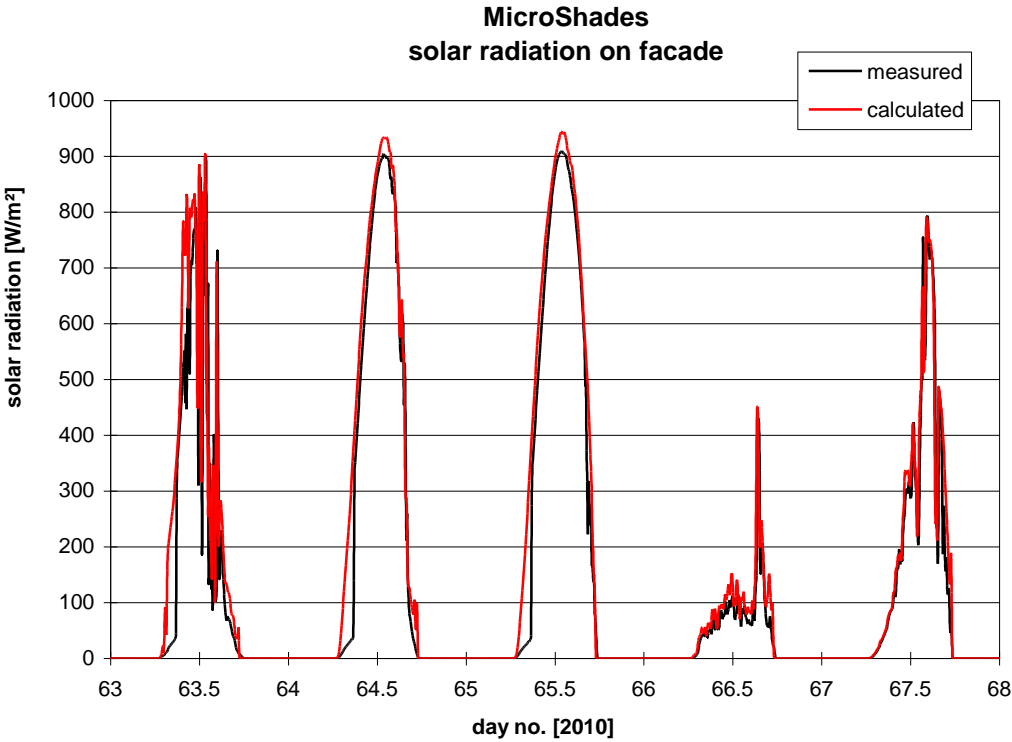


Figure 2.9. Solar radiation on the façade for 5 days in the spring (March 4-8, 2010).

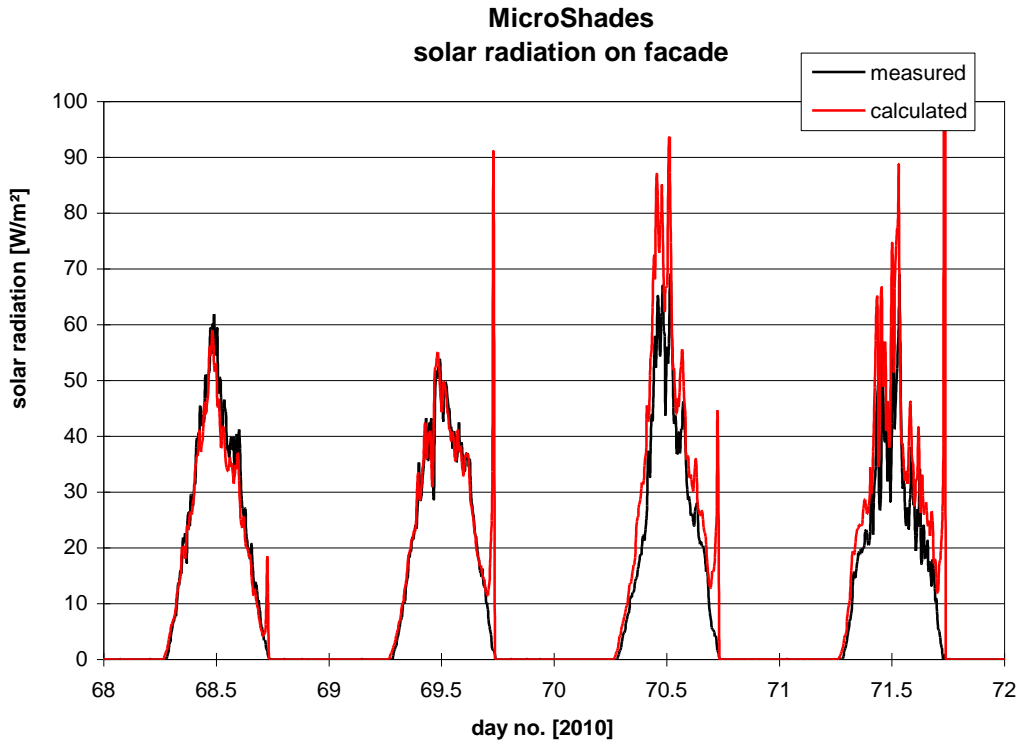


Figure 2.10. Solar radiation on the façade for 4 days in the spring (March 9-12, 2010). Special focus on diffuse radiation – note the lower units on the y-axis.

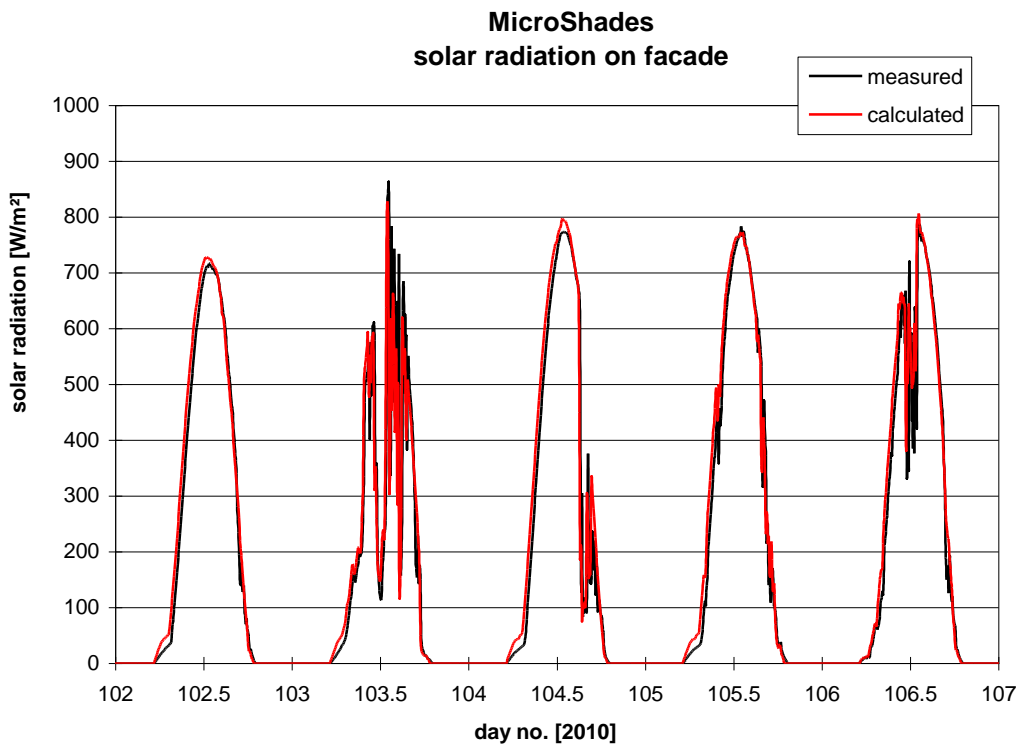


Figure 2.11. Solar radiation on the façade for 5 days in the spring (April 12-16, 2010).

Summer period

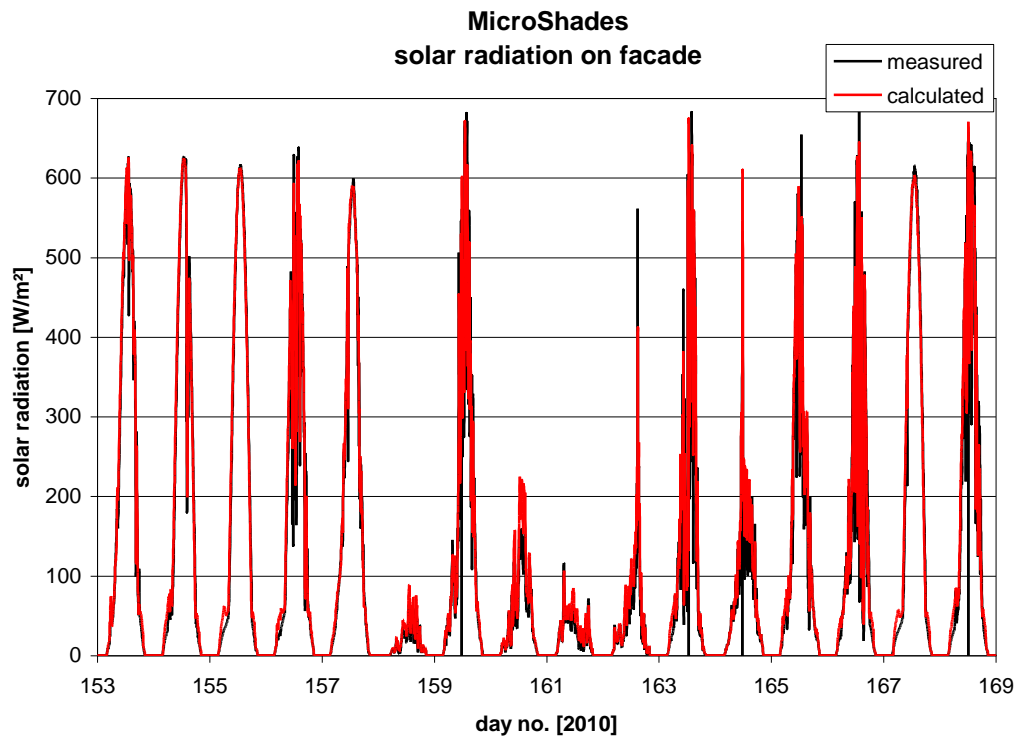


Figure 2.12. Solar radiation on the façade during the summer period.

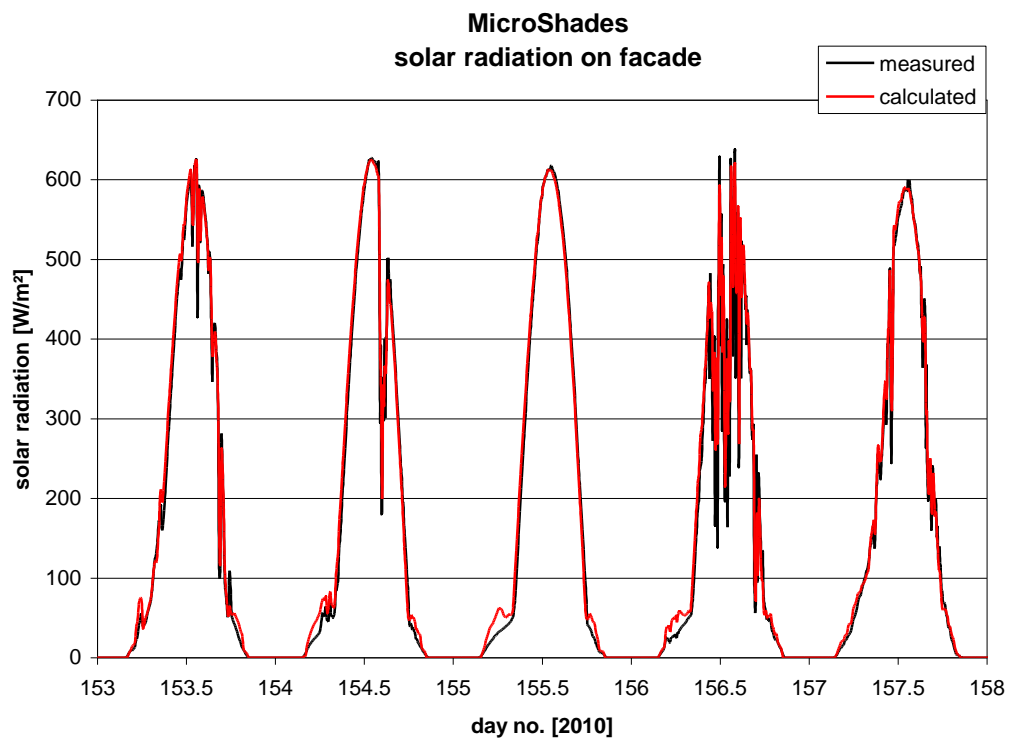


Figure 2.13. Solar radiation on the façade for 5 days in the summer (June 2-6, 2010).

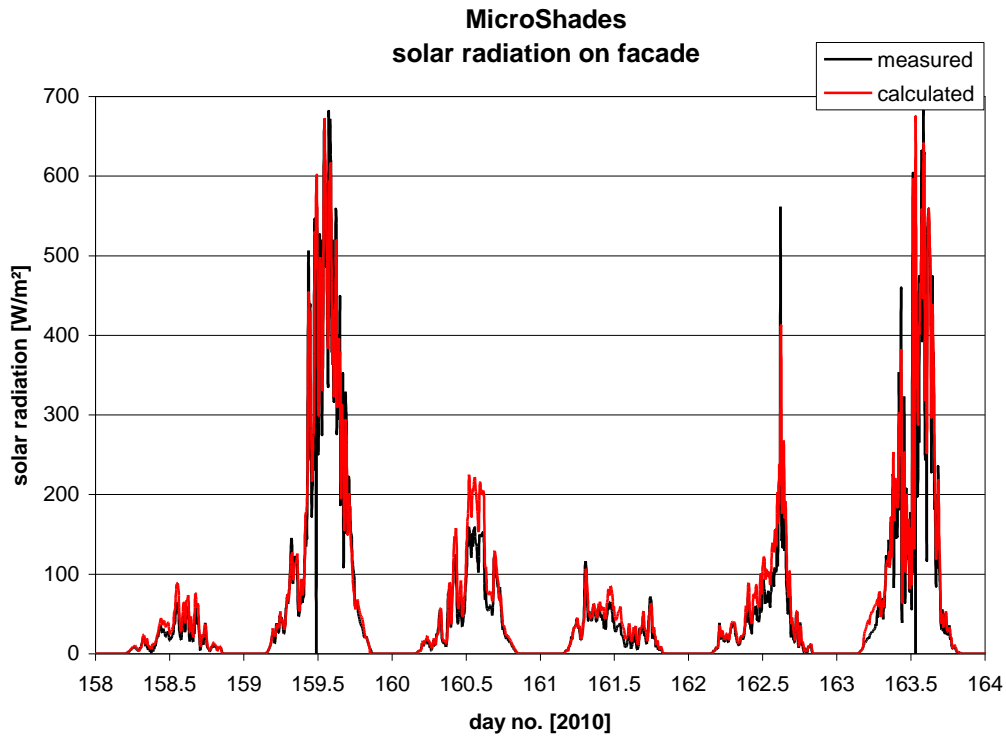


Figure 2.14. Solar radiation on the façade for 6 days in the summer (June 7-12, 2010). Special focus on diffuse radiation.

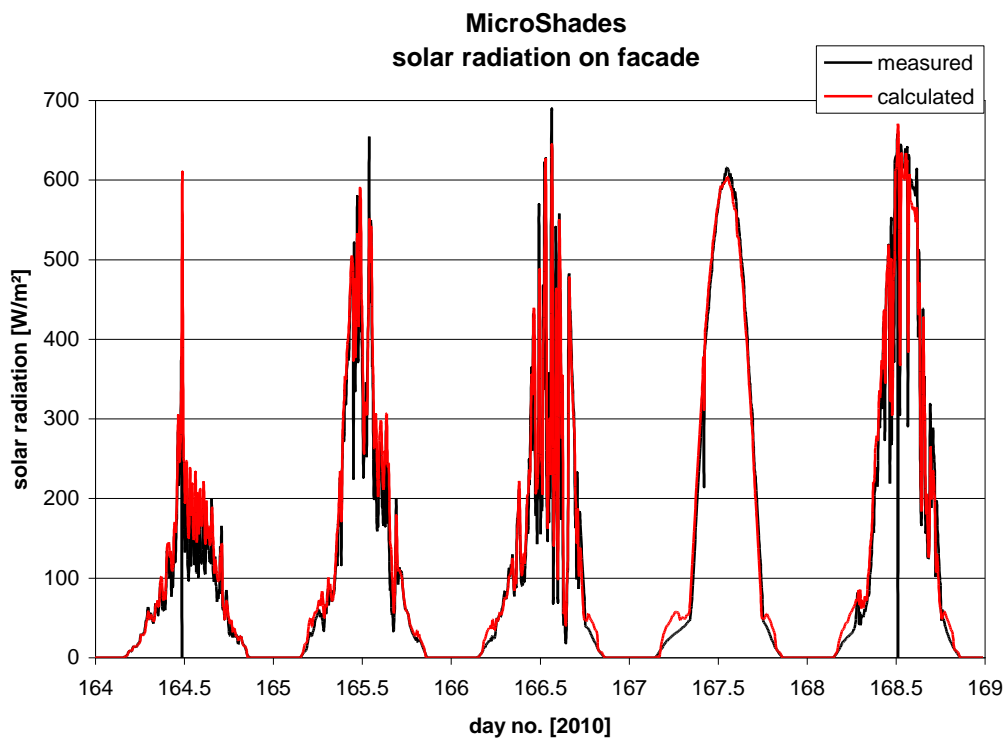


Figure 2.15. Solar radiation on the façade for 5 days in the summer (June 13-17, 2010).

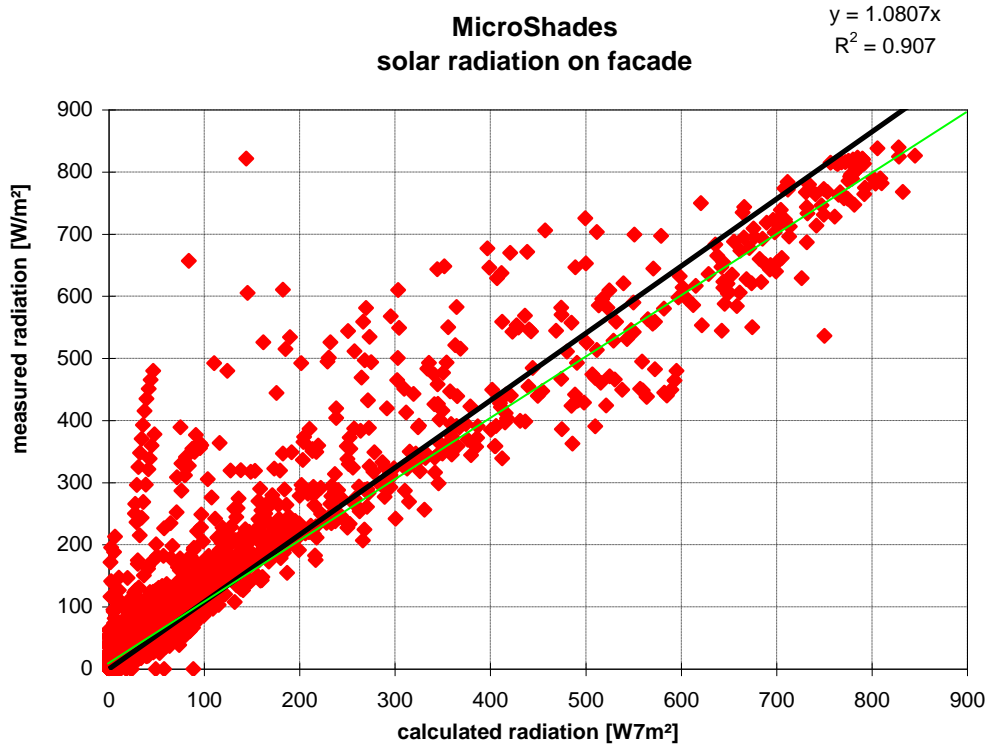


Figure 2.16. The measured solar radiation on the façade plotted against the calculated solar radiation for the winter period.

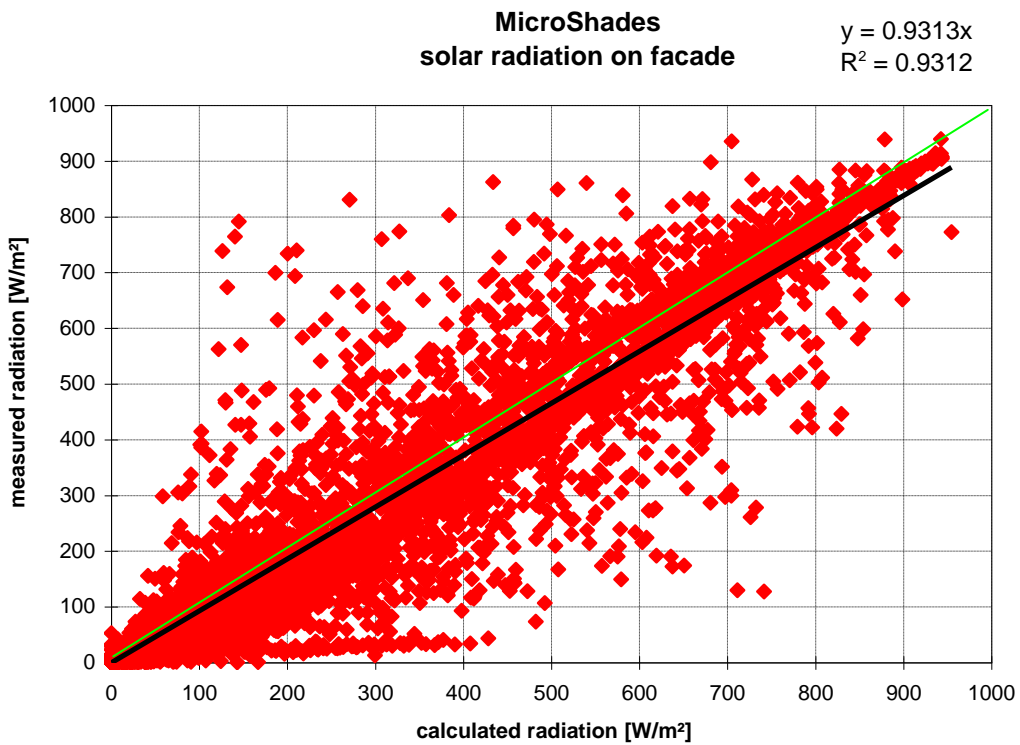


Figure 2.17. The measured solar radiation on the façade plotted against the calculated solar radiation for the spring period.

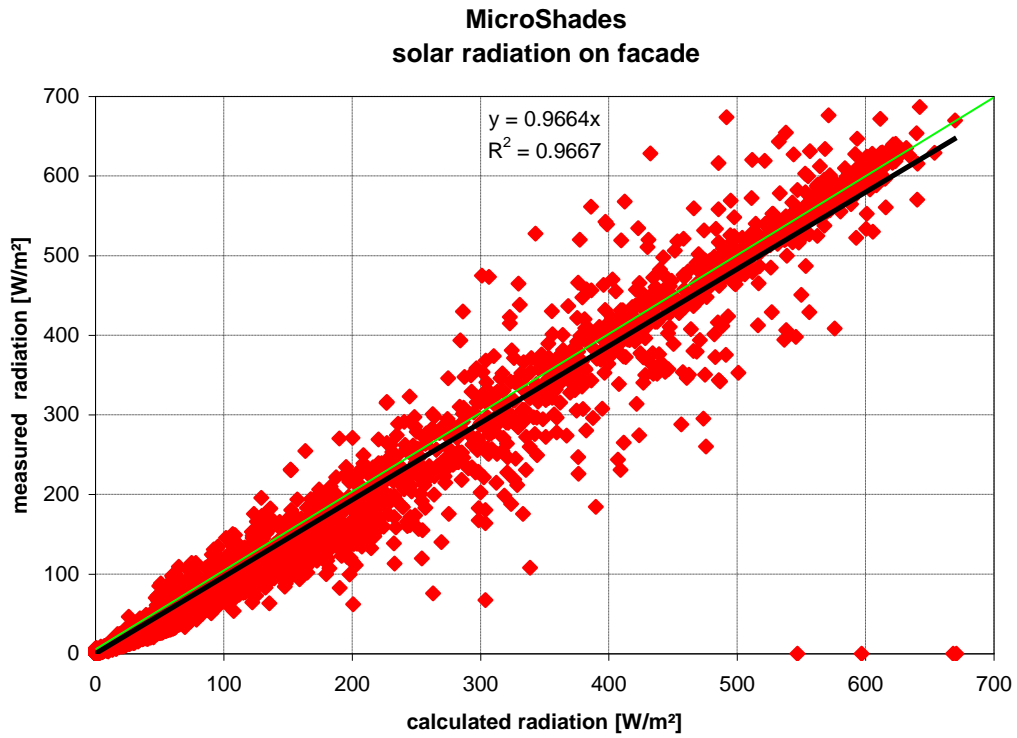


Figure 2.18. The measured solar radiation on the façade plotted against the calculated solar radiation for the summer period.

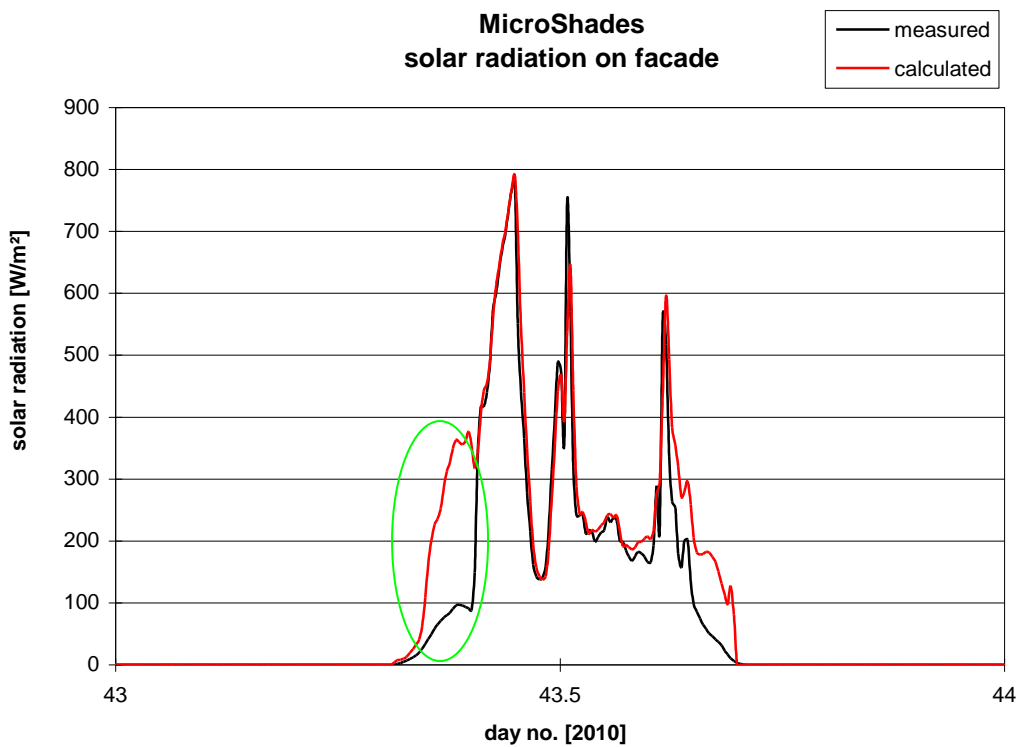


Figure 2.19. Solar radiation on the façade for February 12, 2010).

Further, the purpose of the comparison is not to investigate the solar radiation on the façade, so if the same scattering is obtained when comparing the incoming solar radiation through the window then we know that the scattering is obtained from the radiation on the façade and not from the bi-directional module of esp-r. And it is instead possible to concentrate on the regression lines also shown in figures 2.16-18. The green line is for the case of a regression coefficient of 1.

Figure 2.16 shows that the calculated radiation is in mean 7.5% $((1-1/1.0807)*100)$ lower than the measured radiation – but at high values there is a very good agreement between measurements and calculations. Figure 2.17 shows that the calculated radiation in the spring period in mean is 7.4% $((1-1/0.9313)*100)$ higher than the measured radiation – this is also indicated on figure 2.9. Figure 2.18 shows that the calculated radiation in the summer period in mean is 3.5% $((1-1/0.9664)*100)$ higher than the measured radiation. A discrepancy of $\pm 7.5\%$ is very satisfactory when considering the uncertainty on measuring solar radiation plus on the transformation of horizontal solar radiation to radiation on a vertical surface.

The above should be remembered when comparing measured and calculated incoming solar radiation through the MicroShade window.

2.3. Comparison between measured and calculated solar radiation through the MicroShade window

Based on the findings in [Jensen, 2008b] – too high calculated incoming solar radiation through the window – it was decided to develop a new and more refined program for generation of the matrix describing windows with MicroShades. It is matrixes generated with this program which will be evaluated in the following.

The applied matrixes is referred to as MS-A-220610-x-diff185 – where MS-A is the type of the MicroShades, 220610 is the date of the generation of the matrix, -x- is either 0, 1, 2 or 3 and refer to the percentages of the direct solar radiation hitting the window which is scattered and thus transformed into diffuse radiation, diff185 refers to a transmittance of the outside diffuse radiation of 0,185.

Comparisons between measured and calculated radiation through the MicroShade window have been carried out for the same periods as shown in figures 2.4-2.15 with a scattering factor of 0, 1, 2 and 3%. In the following are only shown figures for a scattering factor of 3 % (figures 2.20-2.31) as all four scattering factors lead to an overwhelming number of graphs. Graphs with scattering factors of 0, 1 and 2 % are, however, shown in Appendix B.

Figures 2.20-2.31 show rather good agreement between measured and calculated values. The dynamic is captured very well by the simulations and the overcast conditions are also well imitated. During cleat sky conditions the agreement varies: there is eg:

- good agreement for the days 64 and 65 (figure 2.25), 104 (figure 2.27) and 157 (figure 2.29)
- under prediction for the days 102 and 105 (figure 2.27) and
- over prediction for the days 154 and 155 (figure 2.29) and 167 (figure 2.30)

The same picture is seen in Appendix B but with different levels of discrepancies between measurements and calculations.

Winter period – scattering factor 3%

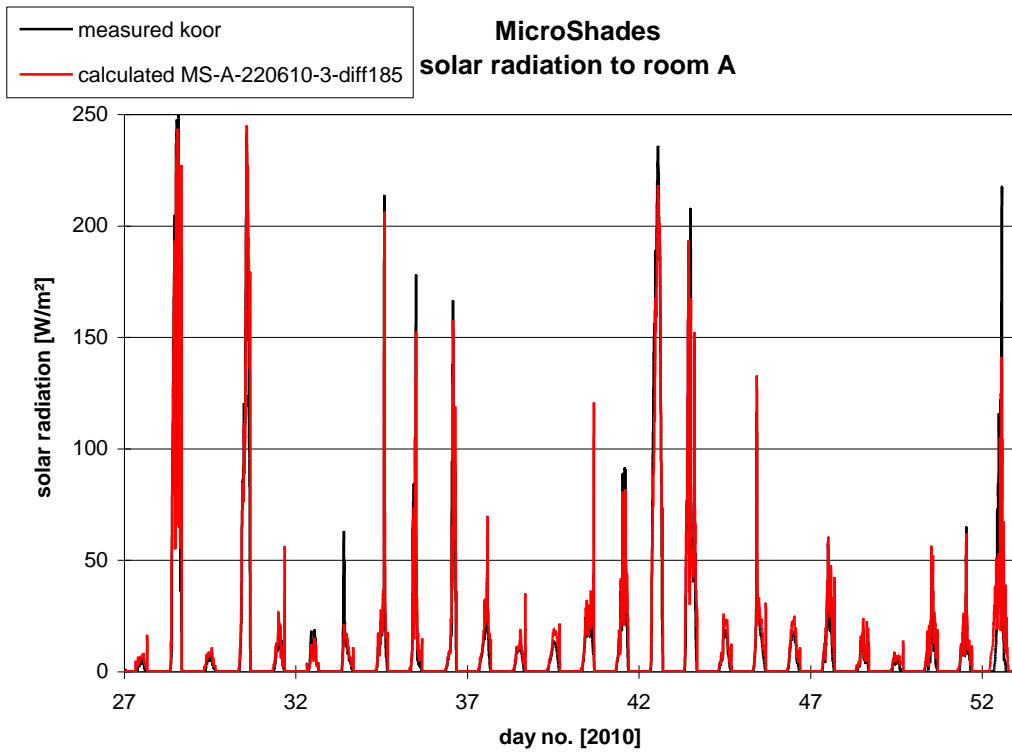


Figure 2.20. Solar radiation through the MicroShade window during summer period. Scattering factor: 3%.

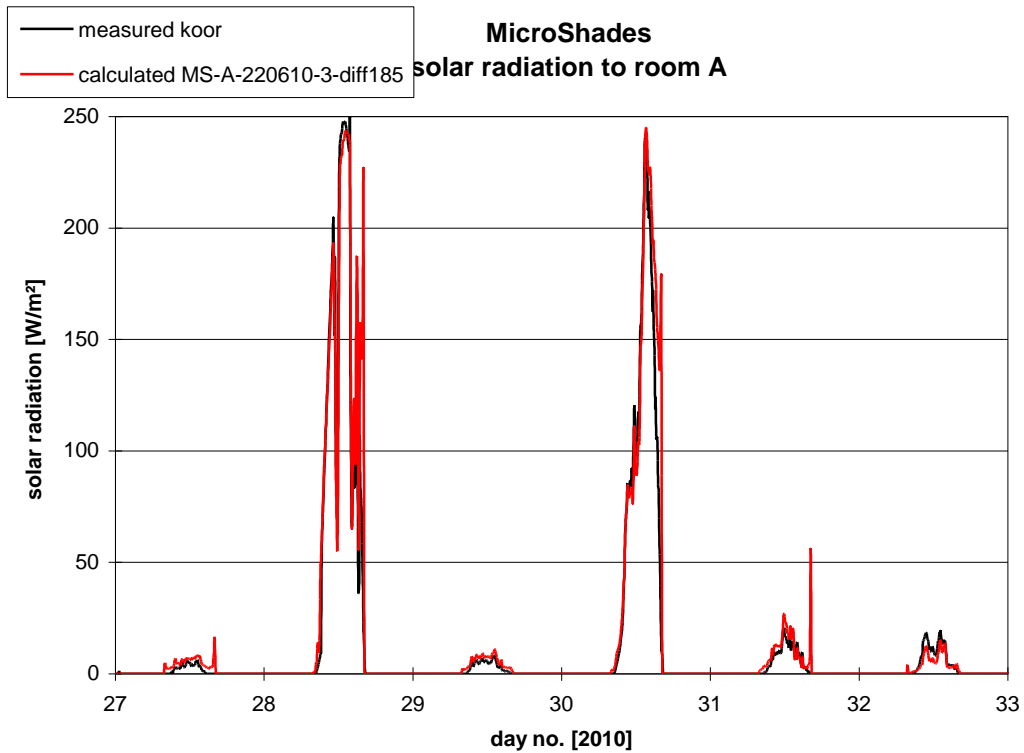


Figure 2.21. Solar radiation through the MicroShade for 5 days in the winter (January 27-February 1, 2010). Scattering factor: 3%.

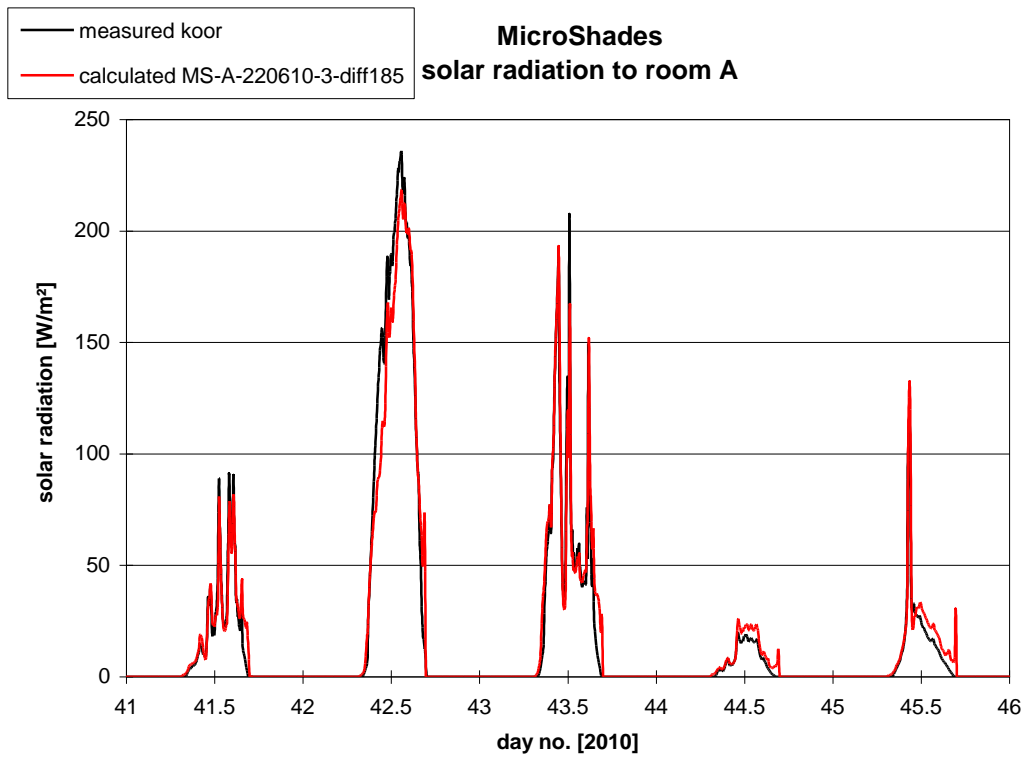


Figure 2.22. Solar radiation through the MicroShade for 5 days in the winter (February 11-14, 2010). Scattering factor: 3%.

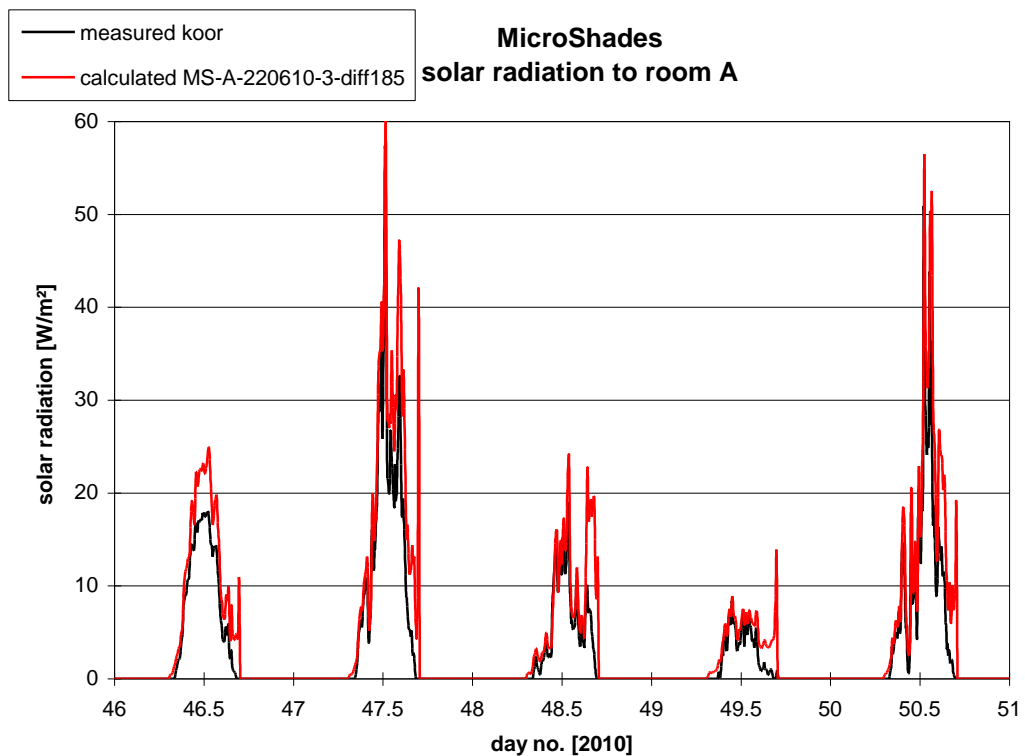


Figure 2.23. Solar radiation through the MicroShade for 5 days in the winter (February 15-19, 2010). Scattering factor: 3%.

Spring period – scattering factor 3%

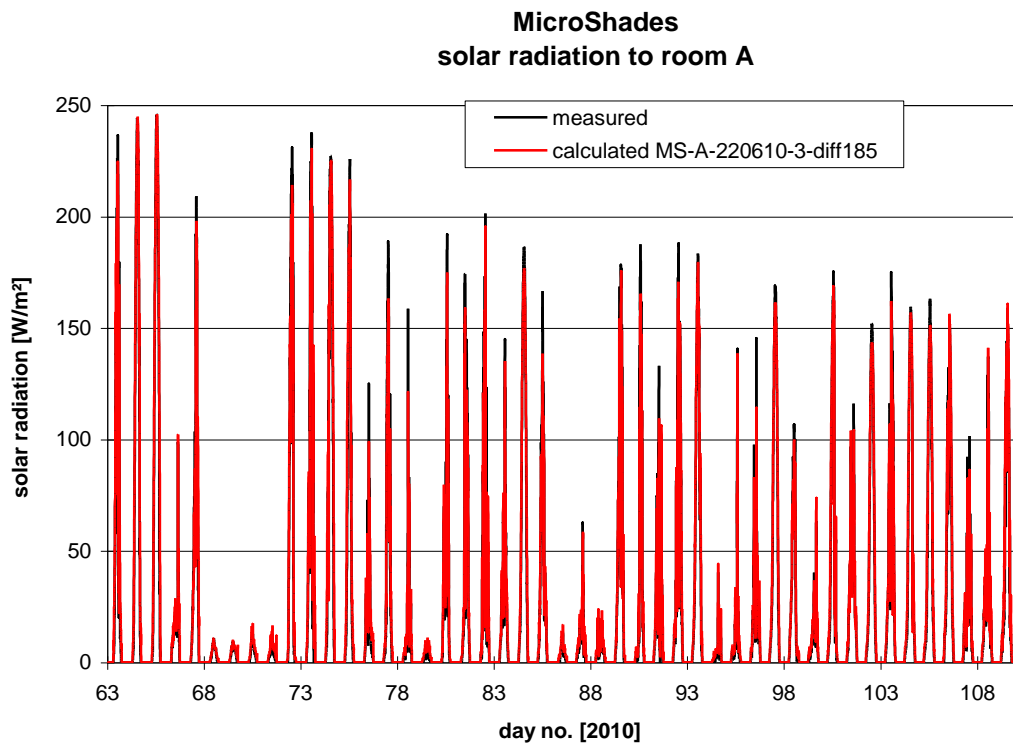


Figure 2.24. Solar radiation through the MicroShade window during spring period. Scattering factor: 3%.

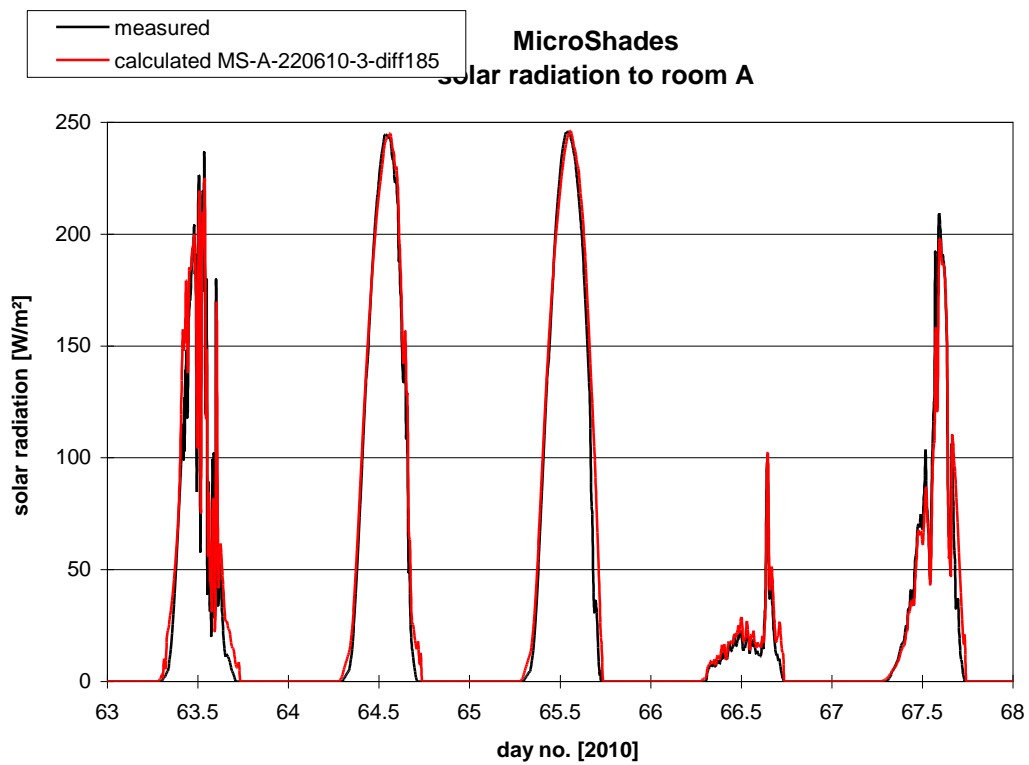


Figure 2.25. Solar radiation through the MicroShade for 4 days in the spring (March 4-8, 2010). Scattering factor: 3%.

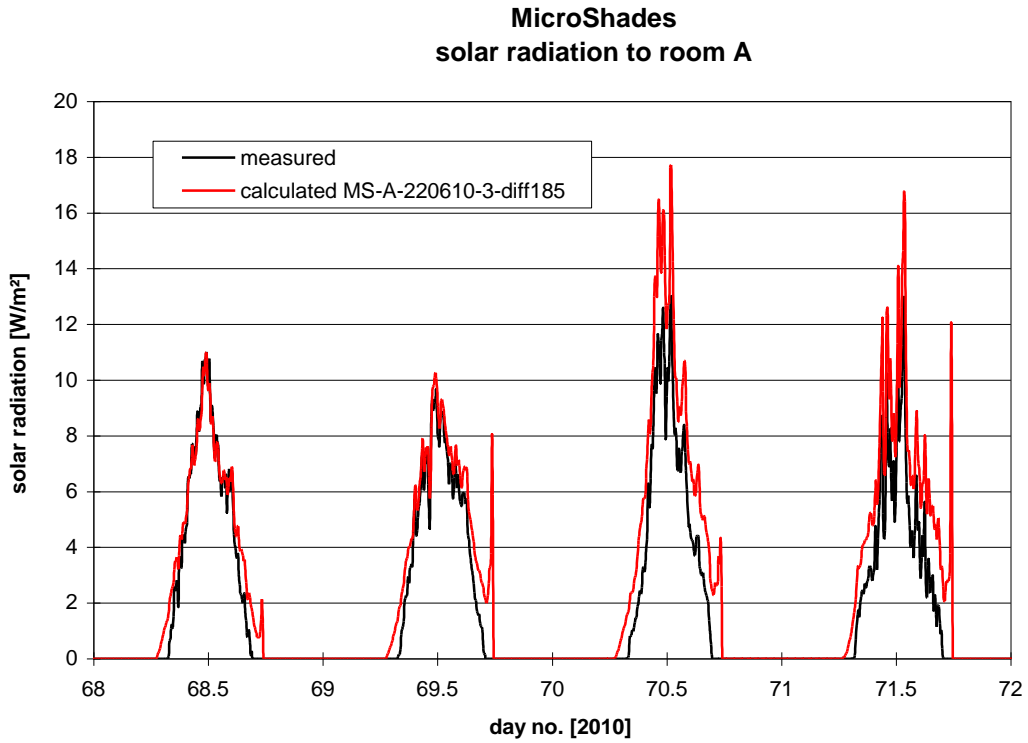


Figure 2.26. Solar radiation through the MicroShade for 5 days in the spring (March 12-16, 2010). Scattering factor: 3%.

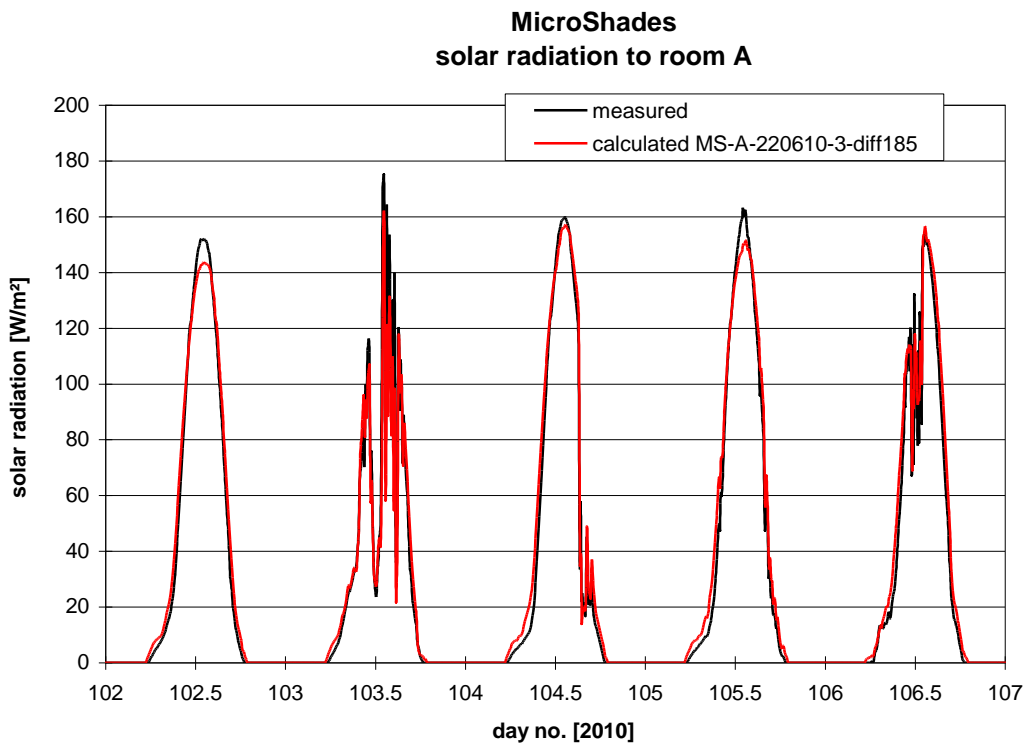


Figure 2.27. Solar radiation through the MicroShade for 5 days in the spring (April 12-16, 2010). Scattering factor: 3%.

Summer period – scattering factor 3%

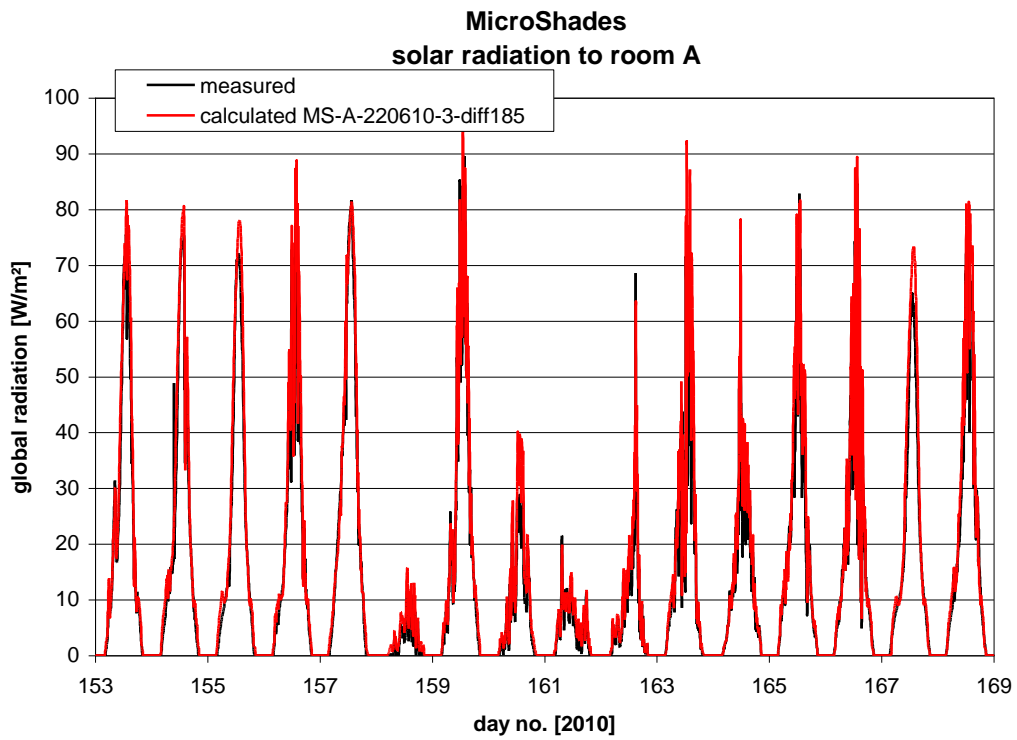


Figure 2.28. Solar radiation through the MicroShade window during summer period. Scattering factor: 3%.

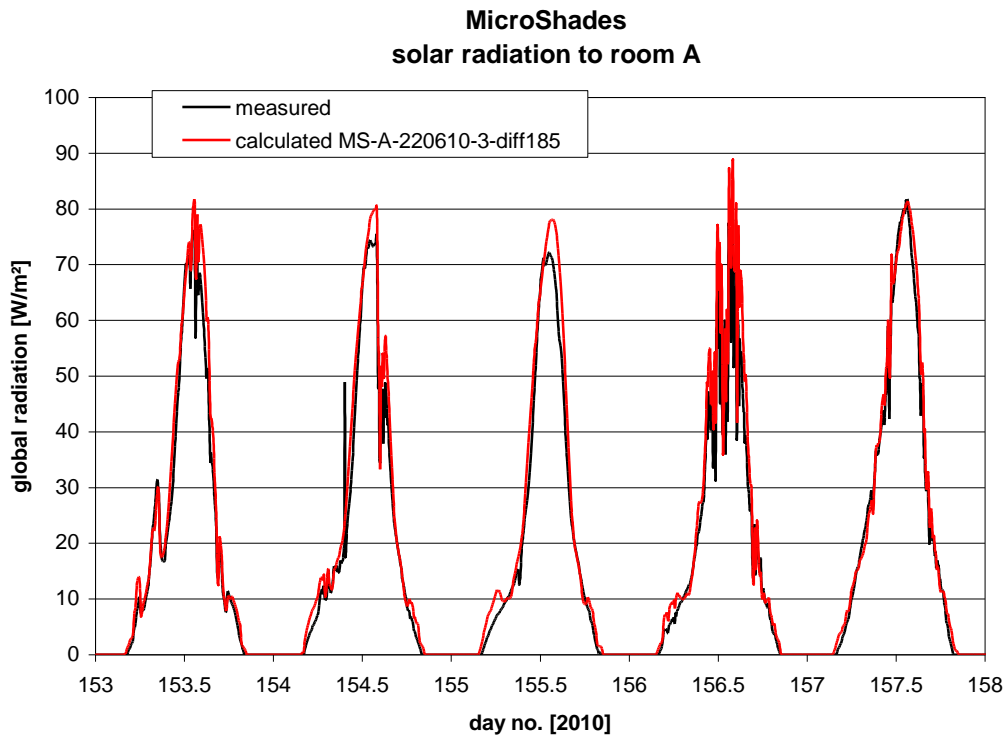


Figure 2.29. Solar radiation through the MicroShade for 5 days in the summer (June 2-6, 2010). Scattering factor: 3%.

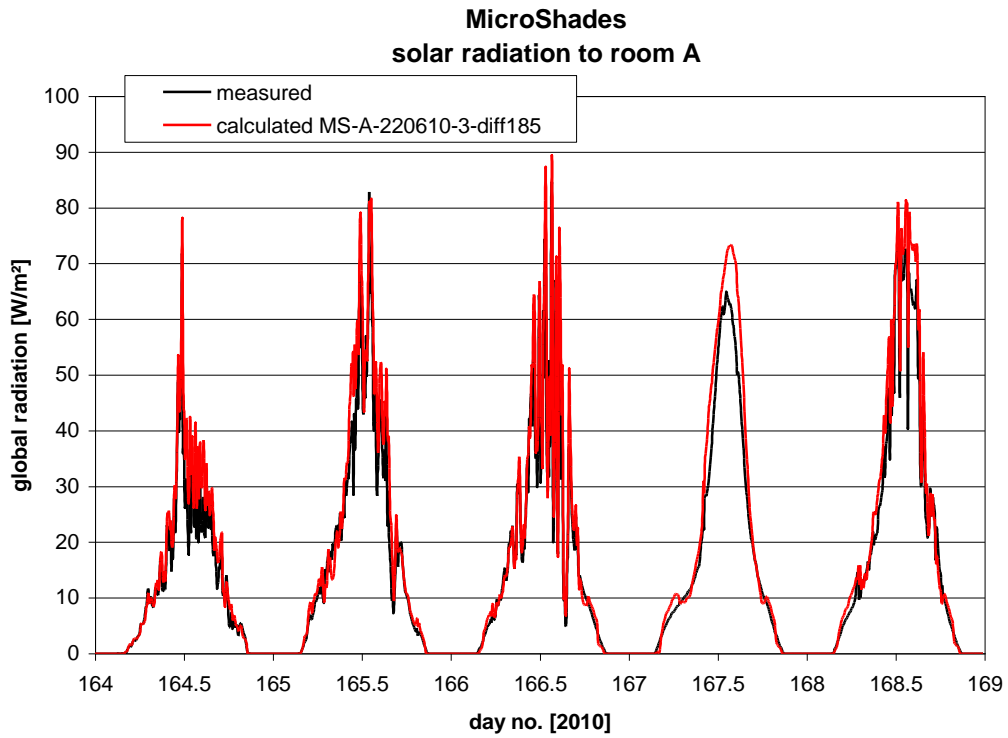


Figure 2.30. Solar radiation through the MicroShade for 6 days in the summer (June 7-12, 2010). Scattering factor: 3%.

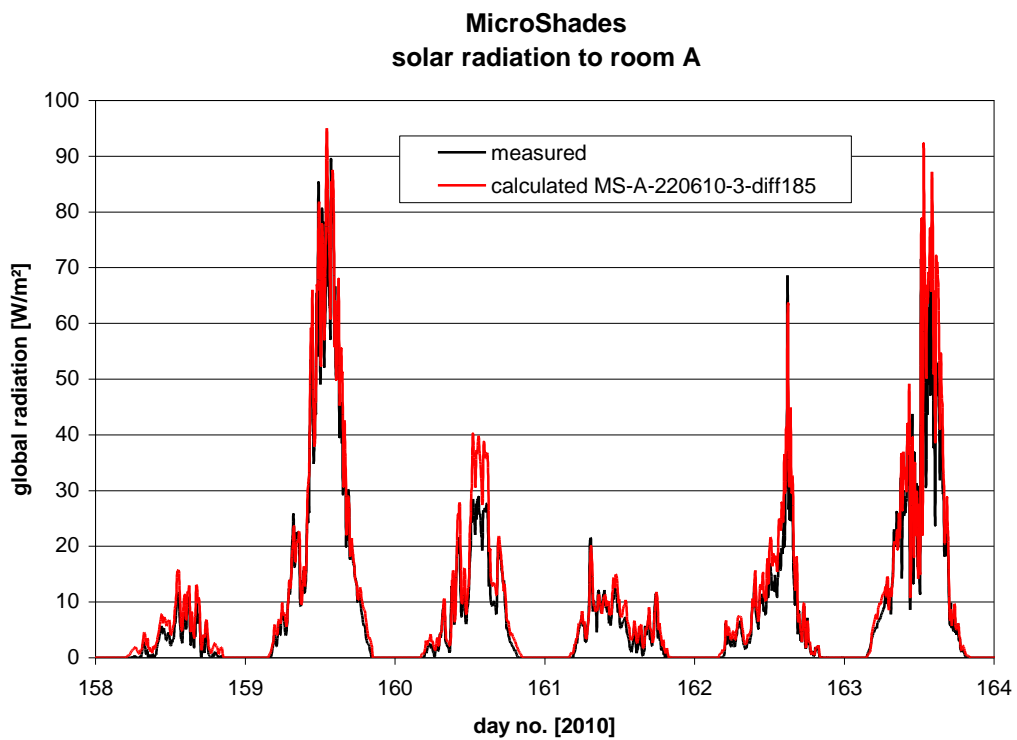


Figure 2.31. Solar radiation through the MicroShade for 5 days in the summer (June 13-17, 2010). Scattering factor: 3%.

As both good agreement and under prediction is seen for days next to each other (figure 2.27) and good agreement and over prediction for days next to each other (figure 2.29) it tells that there is something the model do not account for. However, for the time being it is judge that this is the best we can do.

In the comparison in figures 2.20-2.31 is not accounted for the fact that the input to the model – the solar radiation on the façade – is also subject to uncertainties as shown in the earlier section. To include this in the comparison correlation plots as for the radiation on the façade have been generated in figures 2.32-2.43.

Figures 2.32-2.43 shows less scattering than figures 2.16-2.18. This is because the calculation of the incoming solar radiation through the windows cuts of solar radiation at large horizontal solar angles (azimuths) where it further is difficult to calculate the radiation hitting the façade. However, the scattering in figures 2.32-2.43 occurs in the same areas as in figures 2.16-2.18. Based on this it is concluded that it is possible to concentrate on the regression lines in figures 9-20 instead of on the scattering.

Table 2.1 shows the discrepancies between measurements and calculations – ie the difference in the constant of the regression equations. The first row shows the difference between measured and calculated radiation on the façade while row 2-5 shows the difference between measured and calculated solar radiation through the MicroShade window. The red circles show where the difference for the solar radiation through the window is equal to the difference for the solar radiation on the façade. Based on table 2.1 it can be stated that a scattering factor of 2 % in mean is the best value to use.

	winter %	spring %	summer %
on facade	-7.5	7.4	3.5
scattering: 0%	-8.7	-7.1	-6.1
scattering: 1%	-6.2	-3.6	-0.8
scattering: 2%	-3.6	-0.1	4.4
scattering: 3%	-3.2	3.4	9.7

Table 2.1. Comparison of the difference in the constant of the regression equations. Positive values means that the calculations give higher values than measured.

However, in figures 2.16-2.18 and 2.32-2.43 the regression line is forced to start at 0,0. So another way of looking at it is to compare the measured and calculated amount of energy on the façade and through the window. This is done in table 2.2. Table 2.2 shows the measured and calculated solar radiation through the window integrated for the three periods.

The values in brackets in the first row of values is based on table 2.3 where the integrated measured and calculated solar radiation on the façade is shown incl. the differences. The values in brackets in table 2.2 are obtained by increasing the measured solar radiation through the window with the difference from table 2.3. The red circles in table 2.2 show at which scattering factor the best agreement is obtained between the calculations and the enhanced measured radiation in brackets while blue circles show at which scattering factor the best agreement is obtained between the calculations and the real measured radiation.

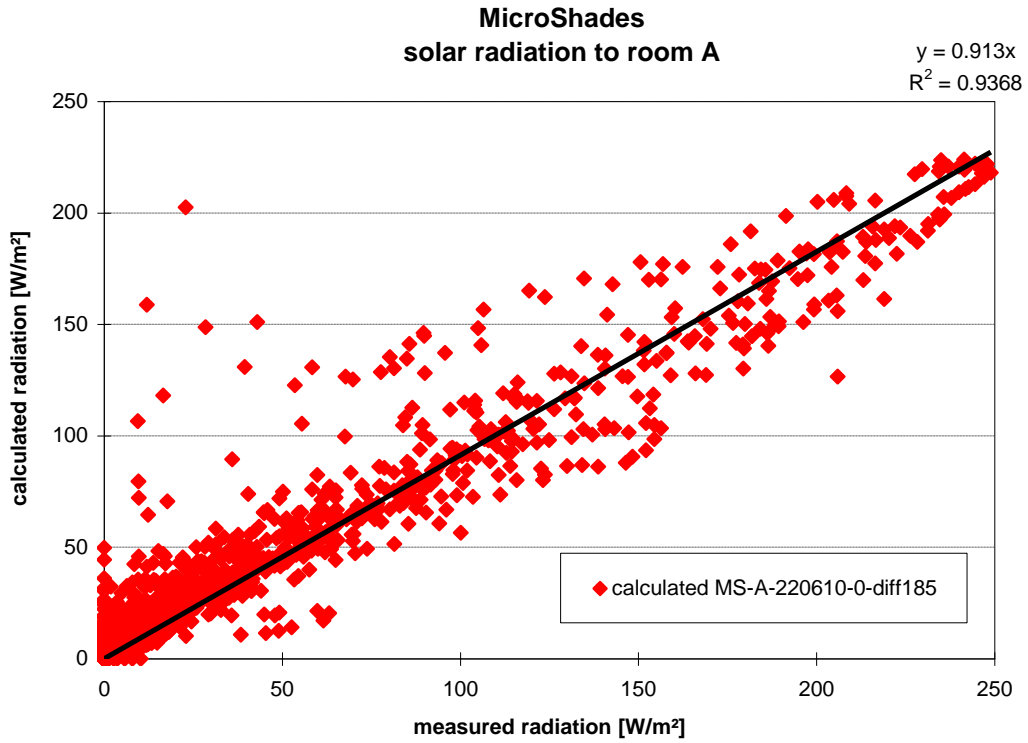


Figure 2.32. The calculated solar radiation through the MicroShade window plotted against the measured solar radiation for the winter period and with a scattering factor of 0%.

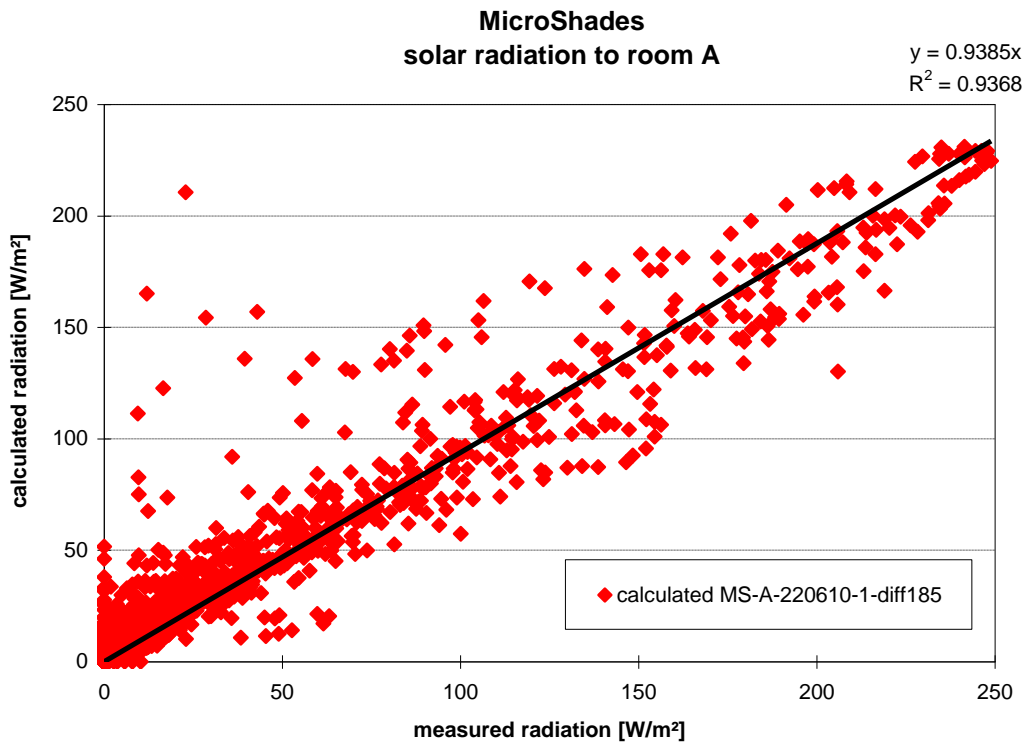


Figure 2.33. The calculated solar radiation through the MicroShade window plotted against the measured solar radiation for the winter period and with a scattering factor of 1%.

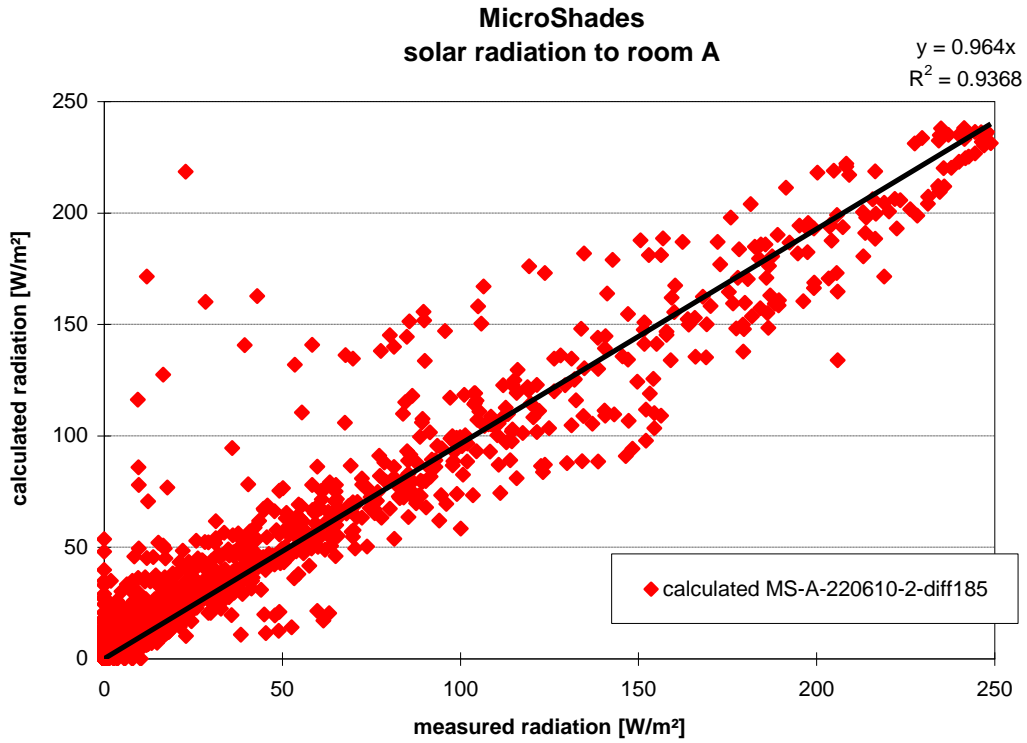


Figure 2.34. The calculated solar radiation through the MicroShade window plotted against the measured solar radiation for the winter period and with a scattering factor of 2%.

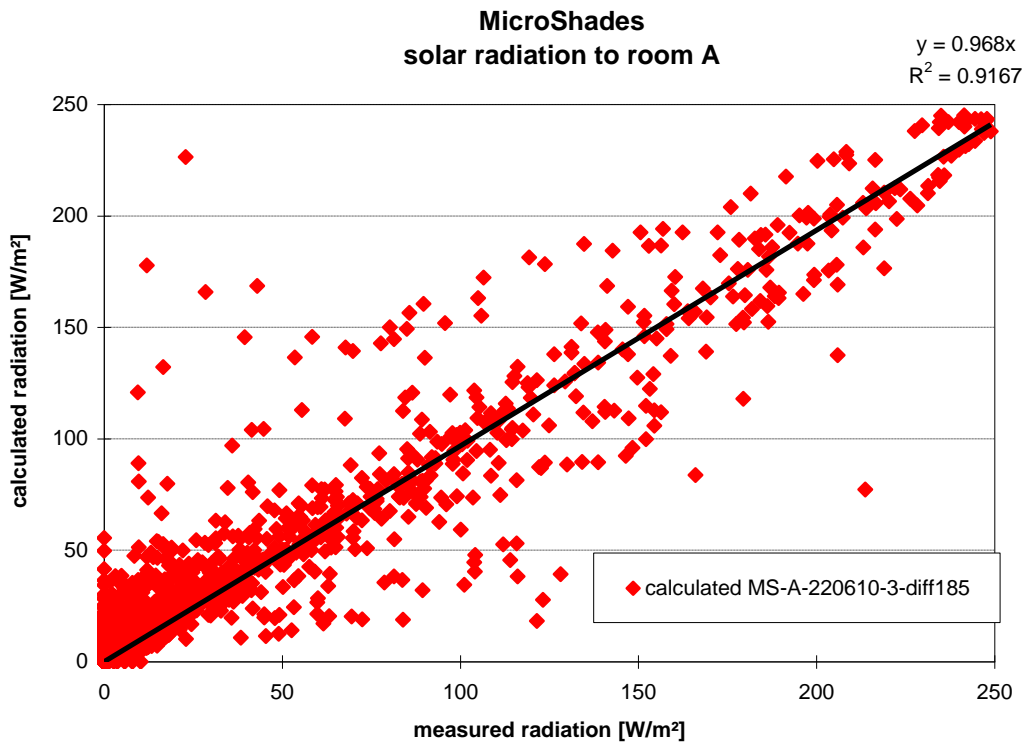


Figure 2.35. The calculated solar radiation through the MicroShade window plotted against the measured solar radiation for the winter period and with a scattering factor of 3%.

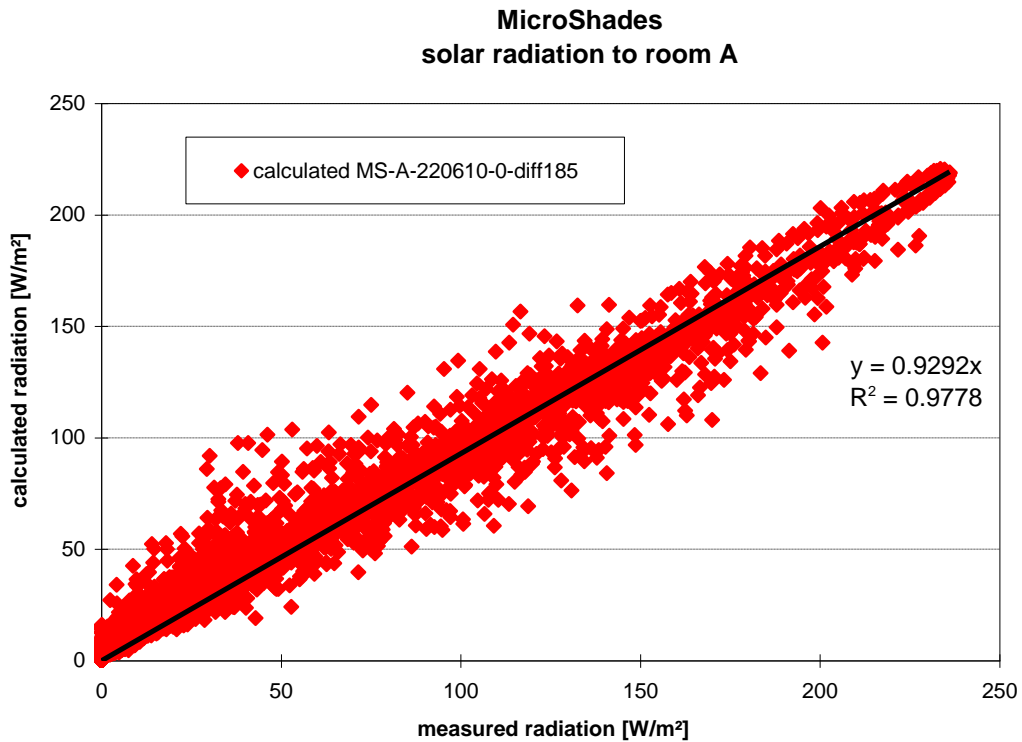


Figure 2.36. The calculated solar radiation through the MicroShade window plotted against the measured solar radiation for the spring period and with a scattering factor of 0%.

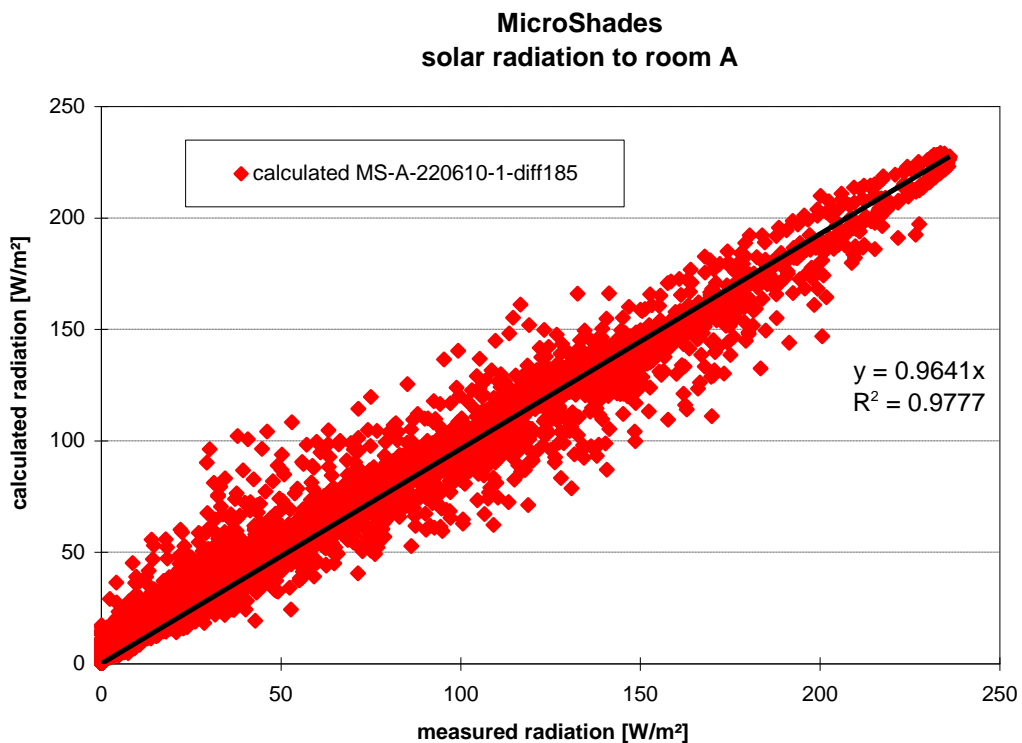


Figure 2.37. The calculated solar radiation through the MicroShade window plotted against the measured solar radiation for the spring period and with a scattering factor of 1%.

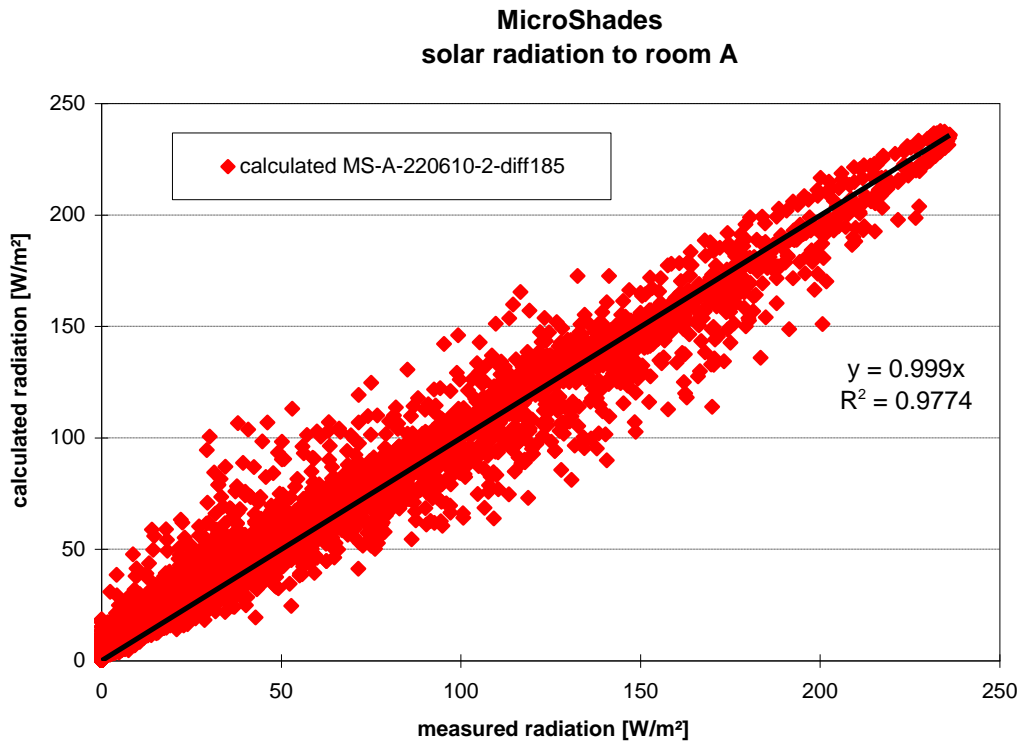


Figure 2.38. The calculated solar radiation through the MicroShade window plotted against the measured solar radiation for the spring period and with a scattering factor of 2%.

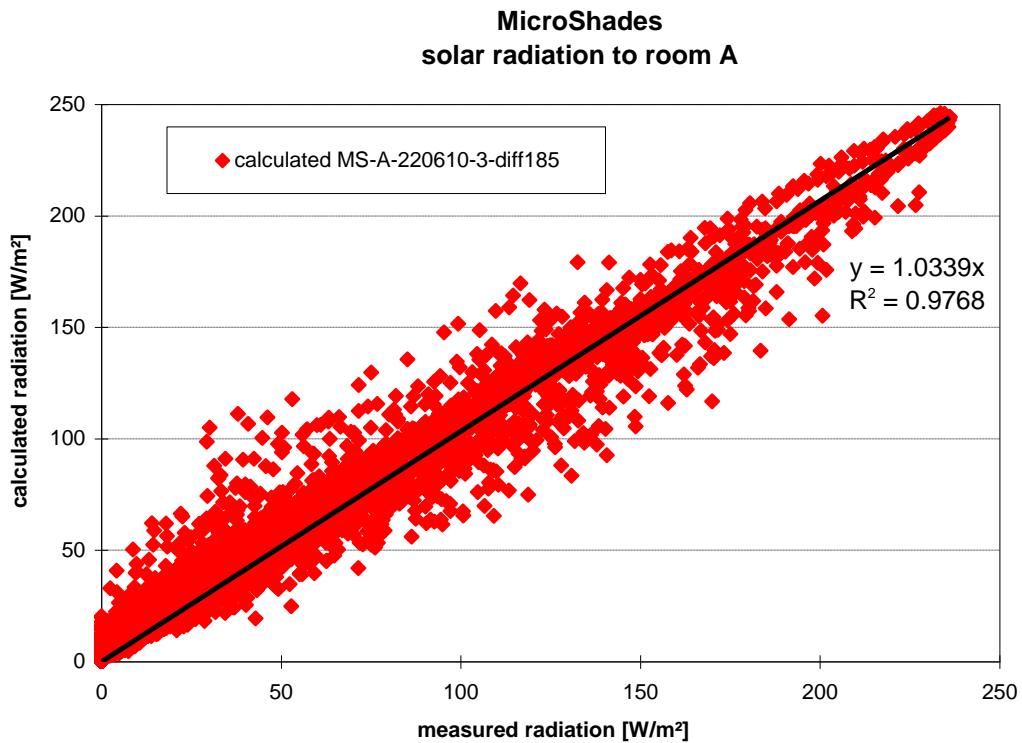


Figure 2.39. The calculated solar radiation through the MicroShade window plotted against the measured solar radiation for the spring period and with a scattering factor of 3%.

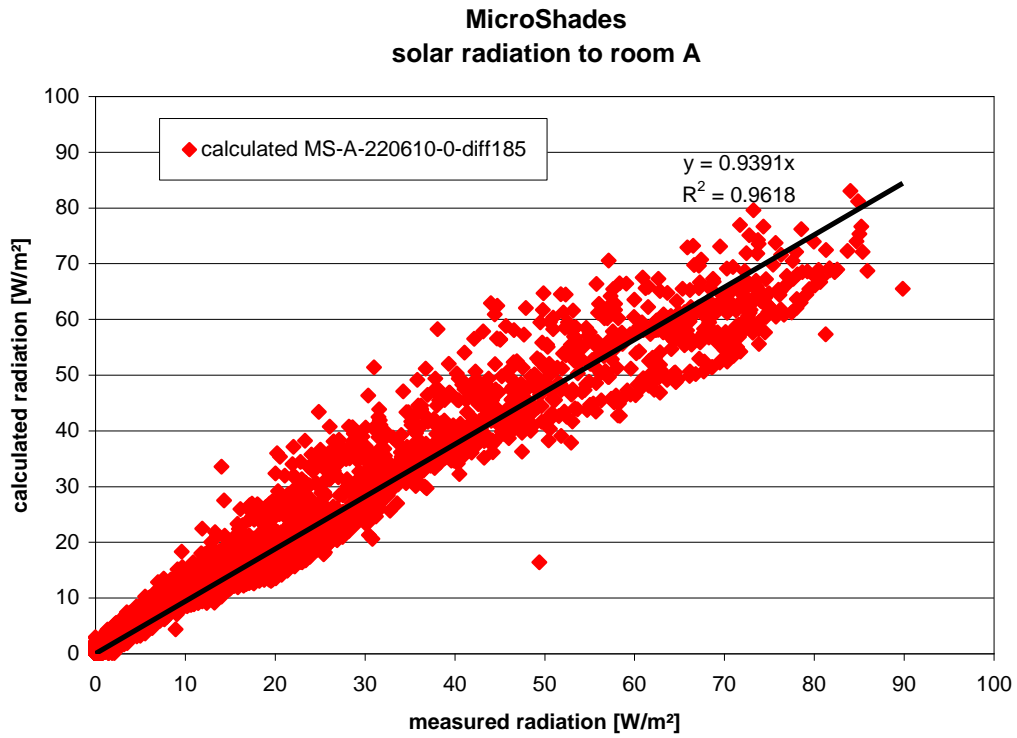


Figure 2.40. The calculated solar radiation through the MicroShade window plotted against the measured solar radiation for the summer period and with a scattering factor of 0%.

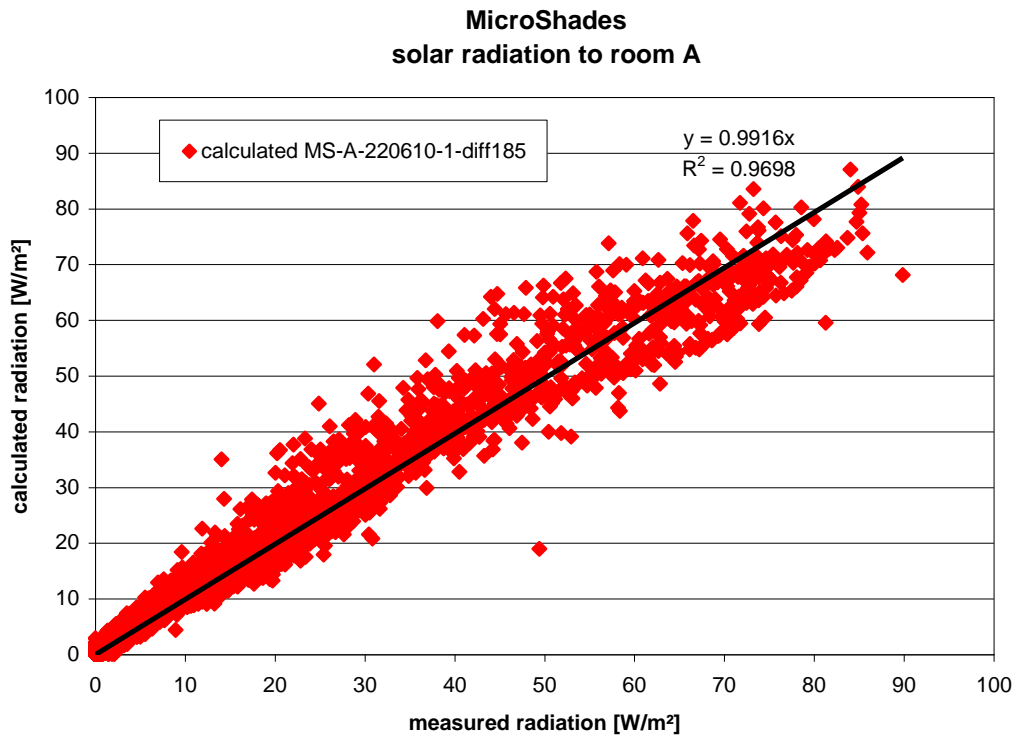


Figure 2.41. The calculated solar radiation through the MicroShade window plotted against the measured solar radiation for the summer period and with a scattering factor of 1%.

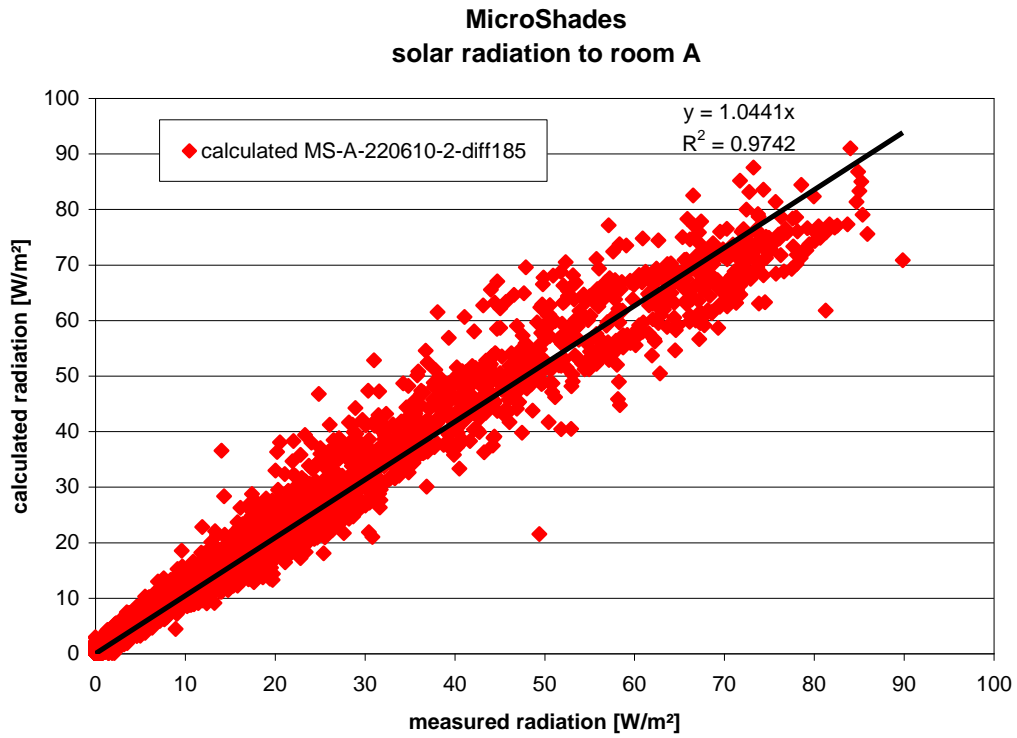


Figure 2.42. The calculated solar radiation through the MicroShade window plotted against the measured solar radiation for the summer period and with a scattering factor of 2%.

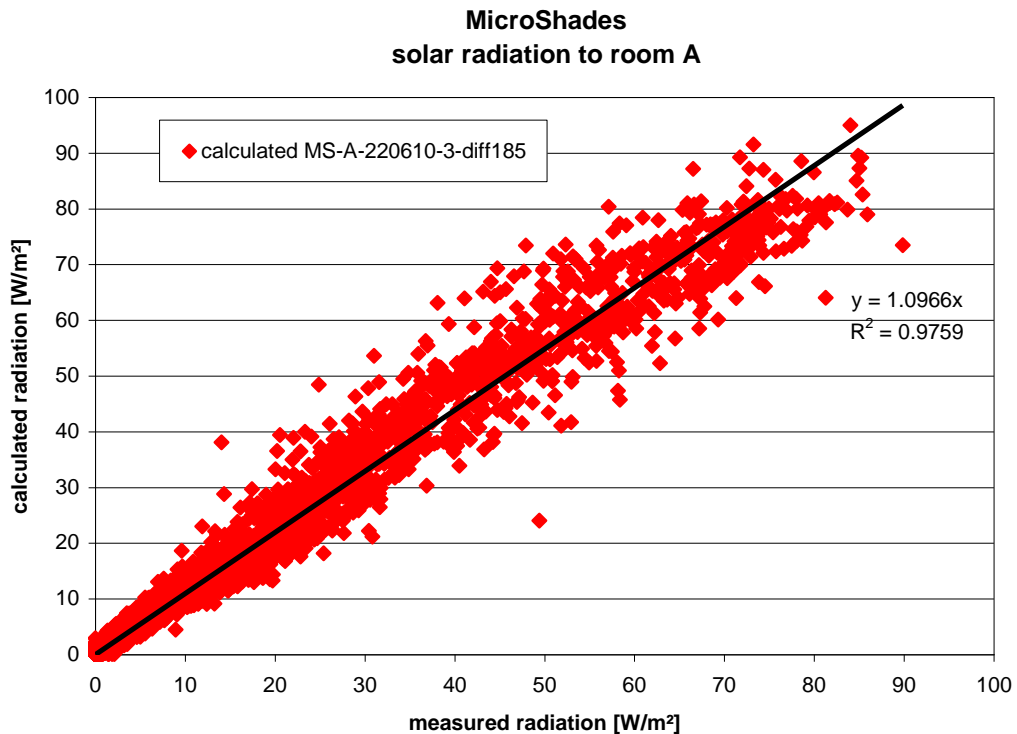


Figure 2.43. The calculated solar radiation through the MicroShade window plotted against the measured solar radiation for the summer period and with a scattering factor of 3%.

solar radiation through the window	winter kWh/m ²	spring kWh/m ²	summer kWh/m ²
measured	6,096 (7,629)	26,501 (28,955)	5,428 (5,770)
scattering: 0%	6,458	23,648	5,385
scattering: 1%	6,592	24,441	5,622
scattering: 2%	6,725	25,233	5,860
scattering: 3%	6,819	26,025	6,098

Table 2.2. Integrated measured and calculated solar radiation through the window for the three periods.

solar radiation on the facade	winter kWh/m ²	spring kWh/m ²	summer kWh/m ²
measured	23,805	142,919	42,578
calculated	29,810	156,271	45,258
difference	25 %	9,3 %	6,3 %

Table 2.3. Integrated measured and calculated solar radiation on the facade for the three periods.

Table 2.2 shows that a scattering factor of 1.5 % gives a good agreement for the summer period when comparing with the value in brackets while a scattering factor of 0.5 % is best when comparing with the real measurements. A scattering factor of above 3 % in both cases is necessary for the spring period. For the winter period a scattering factor below 0 % is necessary when comparing with the real measurements, while a scattering factor of above 3% is necessary when comparing with the value in brackets. A scattering factor of 3 % gives a difference between calculated solar radiation and the measured values and the enhanced measurements (in brackets) in table 2.2 of:

period	measured values	enhanced measured values	mean of the two former columns
winter	11.9 %	-10.5 %	0.7 %
spring	-1.8 %	-10.1 %	-6.0 %
summer	12.3 %	5.7 %	9.0 %

Table 2.4. Difference between measured (both as measured and enhanced) and calculated solar radiation through the window

As a large part of the excess calculated radiation on the facade occurs in the morning and in the afternoon – see eg figures 2.9-2.11 and 2.19 where large part of the radiation is reflected at the outer glass and screen off by the MicroShade it is believed that the right difference is somewhere in between the values in the two first columns of table 2.4. The last column of table 2.4 is therefore the mean value of the two former columns.

During the winter the solar radiation is low while during the summer large part of the solar radiation is cut off by the MicroShade – see table 2.2. Main focus should, therefore, be put on

fitting the scattering value for the spring period and secondly on the summer period especially if mechanical cooling is necessary in a building.

Based on the above considerations it is concluded that when using a fixed scattering factor, 3 % is the best choice. A better agreement would probably be obtained if the scattering factor was made angular dependent. Although the agreement in figure 2.4 is acceptable one may consider for future work to investigate the angular dependency of the scattering factor.

2.4. Conclusions

Modelling of MicroShades is as shown here and in [Jensen, 2008a-b] a non trivial task. A program for generation of a matrix representing the optical properties of windows with MicroShades has been developed. Measurements at both the Technological University of Denmark and University of Basel, Switzerland shows good agreement with the model for direct solar radiation. However, there is as yet no theory for determination of the transmittance of diffuse radiation and scattering in the MicroShades of the direct radiation.

The transmittance of diffuse radiation has for overcast conditions been measured for the MS-A MicroShades in a low-E window to 0,185 which shows good agreement for overcast conditions when comparing with measurements. However, the transmittance of diffuse radiation has also a rather large impact on the calculated radiation through a MicroShade window during clear sky conditions. The transmittance of diffuse radiation should, therefore, be investigated further in order to come up with a theory for calculation of this value for the matrix.

A fixed scattering factor of 3 % was chosen as the best value for the MS-A MicroShades in a low-E window, however, this value may very well be angular dependent – both vertical and horizontal. The scattering should, therefore, be investigated further in order to come up with a theory for calculation of this value for the matrix.

Although much work can be done in order to fully understand the optical properties of MicroShades it may be concluded that the investigated model of MicroShades very well represent the optical performance of MicroShades and may be used to investigate the thermal performance of MicroShade windows in real buildings.

3. Comparison between two ways of calculating solar radiation through a traditional low-E window

In [Jensen, 2008a-b] it was concluded that the simple representation of the optical properties of a low-E window with solar control coating gave very good agreement between measurements and calculations. The simple representation is the optical properties – total transmittance and absorptance in each layer – at 5 incidence angles – see table 3.1.

However, in order to test how esp-r interprets the matrix from the former chapter a matrix for a traditional low-E window was developed. The name of the matrix is 080610-fs3. The optical properties for an azimuth of 0° (ie the horizontal incidence angle is 0°) is shown in figure 3.1. The properties in figure 3.1 is used as the simple representation of the window – the values are shown in table 3.1.

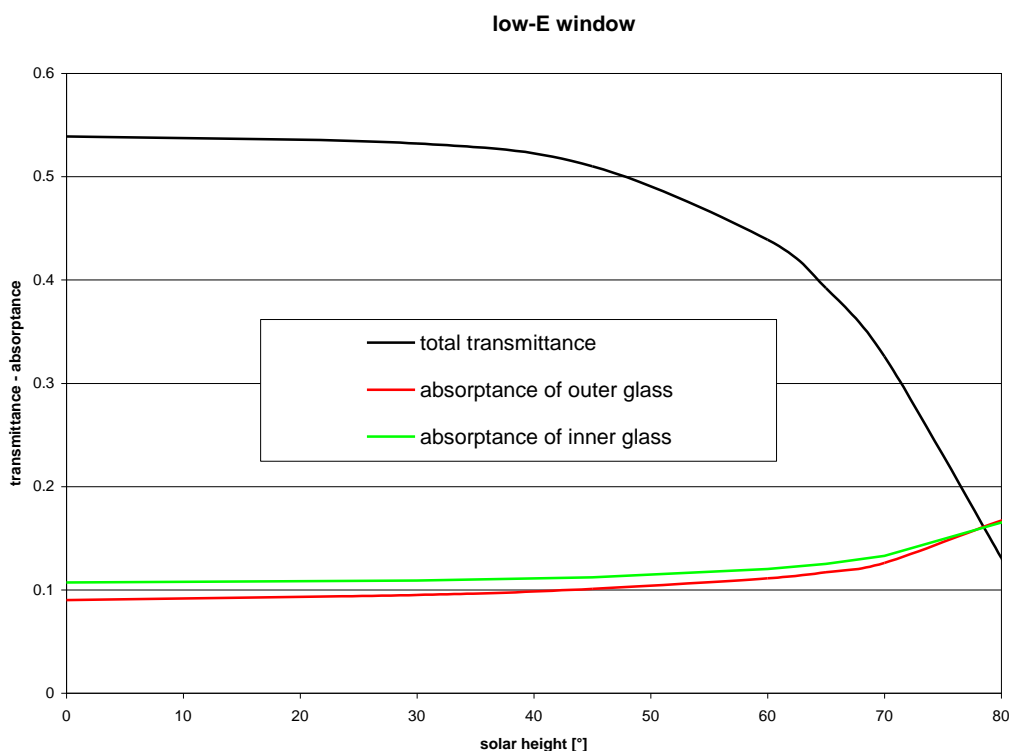


Figure 3.1. Optical properties of a low-E window for an azimuth of 0° (ie the horizontal incidence angle is 0°) for different solar heights (ie vertical incidence angles).

	incidence angle $^\circ$				
	0	40	55	70	80
Total transmittance	0.539	0.520	0.472	0.326	0.131
Absorption in outer glass pane	0.090	0.099	0.107	0.126	0.167
Absorption in inner glass pane	0.107	0.111	0.117	0.133	0.165

Table 3.1. The simple representation of the low-E window. The values is obtained from the matrix 080610-fs3 at an azimuth of 0° .

The test rooms from chapter 2 was in an esp-r simulation equipped with the matrix for room A and the simple representation for room B. A simulation was run for the spring period in chapter 2: 4/3-24/3, 2010 – 52 days. Figure 3.2 shows a comparison for 10 days – March 1-10, 2010.

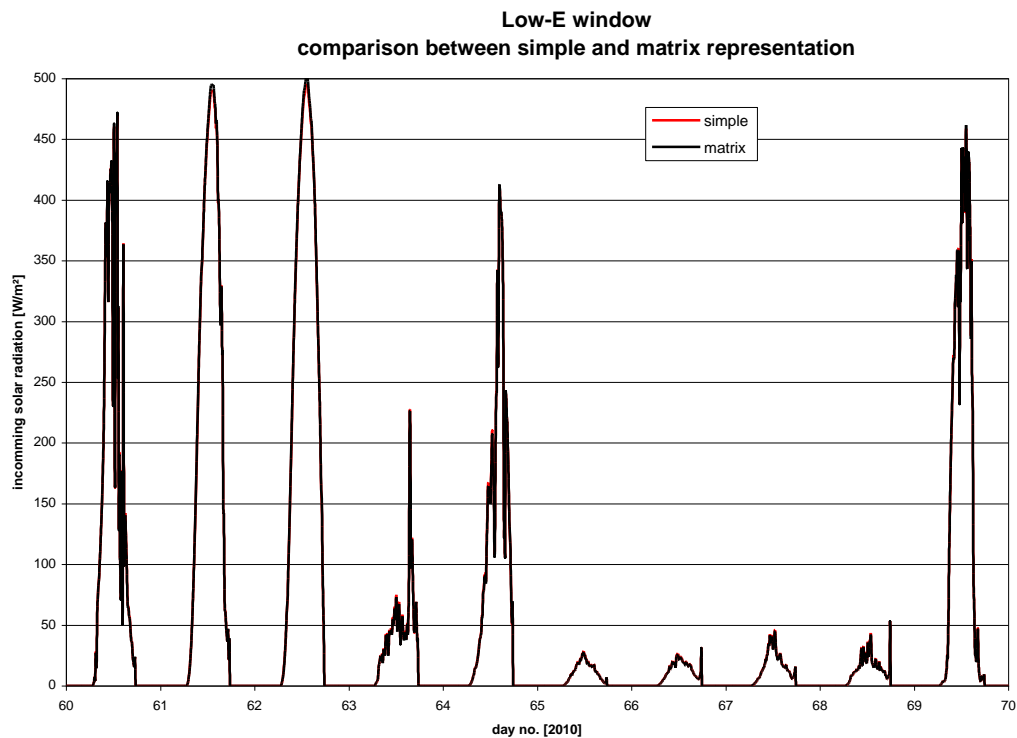


Figure 3.2. Comparison of the solar radiation through a traditional low-E window calculated either using a detailed matrix or a simple representation of the optical properties of the window.

Figure 3.2 shows nearly no difference between the two ways of representing the window. When summarizing the incoming solar radiation for the whole period nearly no difference is seen:

Simple representation: 898,863 kWh/m²
 Matrix representation: 894,769 kWh/m²

which is a difference of less than 0,5 %.

It can, therefore, be concluded that the interpretation of esp-r of the matrix is correct – at least for a traditional window. However, based on the good results in chapter 2 it can also be concluded that the interpretation of the matrix for MicroShade windows also seems to be correct.

4. Test of the measurements of solar radiation through the windows

When calibrating models for calculation of solar radiation through a window it is of course crucial that the uncertainty of pyranometer behind the window is low. The pyranometers in the two test rooms were calibrated based on readings from at calibrated pyranometer – see [Jensen, 2008a]. The calibration of the pyranometers was in [2008a] performed without a window in front of the pyranometers located in the two test rooms.

The question accose: how does a window close in front of a pyranometer influence the measurements?

Figure 4.1 shows the high precision Epply pyranometer located in room A. The pyranometer is as seen equipped with a white screen in order to avoid the pyranometer in heating up. But does this screen influence the measurements?



Figure 3.1. The Epply pyranometer applied for measuring the solar radiation through the MicroShade window in test room A. The Epply pyranometer is shown together with the original pc-pyranometer which turned out to be less applicable for measuring solar radiation through MicroShades due to a too low measuring band width – it cannot measure solar radiation above 2000 nm.

Three questions have to be answered:

- will inter-reflections between the window and the glass dome of the pyranometer increase the readings
- will inter-reflections between the window and the white screen of the pyranometer increase the readings and
- will diffuse radiation from the room behind the pyranometer increase the readings.

A series of test were carried out in order to answer the above questions.

4.1. Tests of solar radiation measurements

A high precision Kipp & Zonen pyranometer was applied – in the following referred to as Kipp & Zonen while the original pyranometer is referred to as Epply.

In the first test Kipp & Zonen was installed next to Epply. Kipp & Zonen was as Epply equipped with a white screen – see figure 4.1. The result of this experiment is shown in figure 4.1. The following figures consists of at the top a picture of the test arrangement followed by a graph showing the correlation between the measurements of the two pyranometers and a graph showing the test condition in the form of the solar radiation on the façade.

Figure 4.1 shows that the readings from the two pyranometers are nearly identical with a mean difference of less than 2 %, which is far within the uncertainty of the measurements. The uncertainty of an extremely well calibrated pyranometer is ± 3 % while in normal use the uncertainty is rather ± 5 %. When using two pyranometers the uncertainty on the difference is the square root of the sum of the square of the two uncertainties – ie here 7.1 %.

Figure 4.2 shows the next test which was the same arrangement but without the white screen on Kipp & Zonen. Figure 4.2 shows a difference of $(1-0.9261)*100 = 7.4$ %. With the difference from figure 4.1 this gives a difference of $(1-0.9261/0.9818)*100 = 5.7$ % with and without a white screen.

However, diffuse radiation from the room may influence the reading. Figure 4.3 shows a third experiment where a black screen was mounted on Kipp & Zonen. The black screen was as shown in figure 4.3 equipped with a black ring between the screen and the window in order to avoid diffuse radiation from the room in hitting the pyranometer. Due to the black screen the pyranometer may heat up which might influence the reading. In order to avoid this a fan was blowing air at the pyranometer – see figure 4.3.

On day 167 (16/6, 2010) surface temperatures was measured on the house of the pyranometer behind the black screen and to the left and right on the black screen. The latter because the fan blew air in from the left, while the right part of the black screen was shaded by the house of the pyranometer:

time	room temp.	temp. of pyranometer	temp. left screen	temp right screen
12:23	24.4	25.3	26	27.6
13:05	25.3	26.6	27.3	28.4

The house of the pyranometer had in mean an 1.1 K higher temperature than the room, while the black screen was in mean 1.8 K (left) and 3.2 K (right) warmer than the room. These temperature differences will only have minor influence on the readings.

Figure 4.3 shows a difference of $(1-0.9489)*100 = 5.1$ % or with the difference from 4.1 $(1-0.9489/0.9818)*100 = 3.3$ % which is lower than in experiment 4.2.

The reason for this may be that although mat black the black screen may still reflect some radiation. However, this shows that the diffuse radiation from the room is not influencing the readings as figure 4.2 else should have shown higher readings than figure 4.3.

Being located next to each other may, however, have influenced the reading – so a new series of test was carried out.

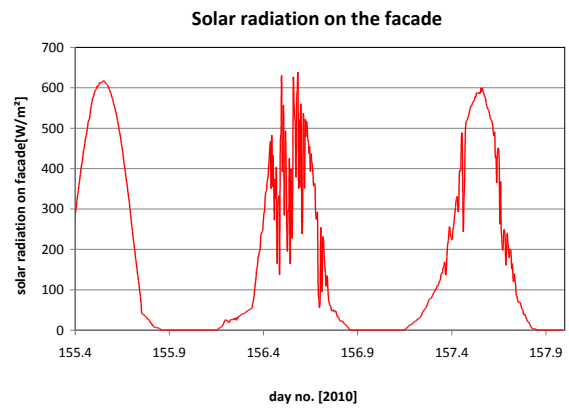
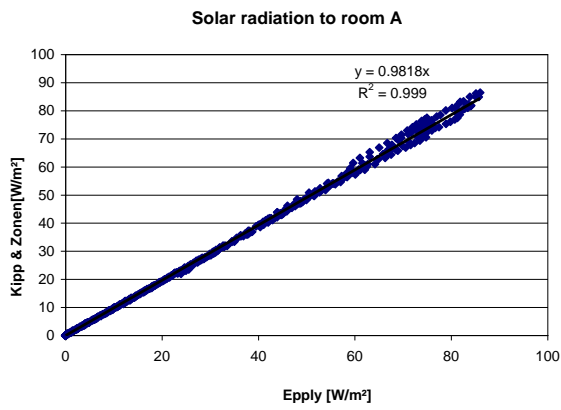


Figure 4.1. The two pyranometers located next to each other – both with white screens.

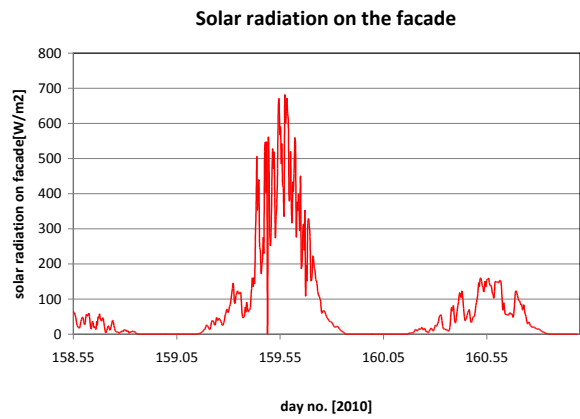
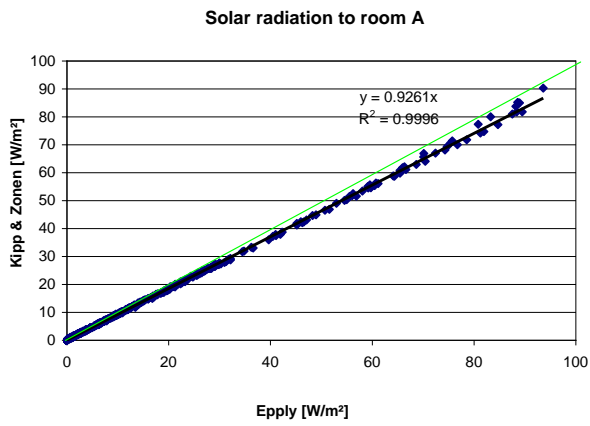


Figure 4.2. The two pyranometers located next to each other – Kipp & Zonen without screen.

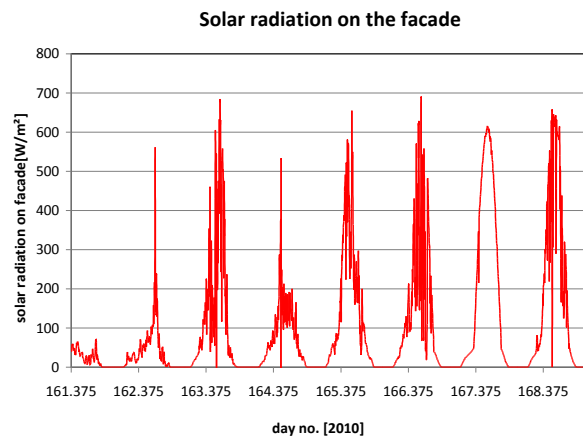
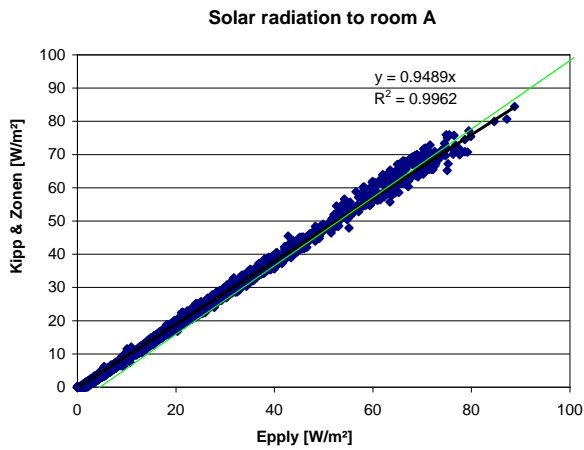


Figure 4.3. The two pyranometers located next to each other – Kipp & Zonen with black screen and ventilation.

The tests in figures 4.1-4.3 were repeated but with Kipp & Zonen located in the other window of test room A as seen in figures 4.4-4.7. The order of the test was opposite than in figures 4.1-4.3.

Figure 4.6 shows a difference of the readings from the two pyranometers of $(1-0.872)*100 = 12.8 \%$ which is more than 10 percent point from figure 4.1. This could be explained by differences in the MicroShades. However, the manufacture PhotoSolar states that the max difference in transmittance is 5 %. This is dealt with in the following section 4.1.1.

The test from figure 4.2 is repeated in figure 4.5 for the new location. The difference in 4.5 is corrected for the difference in figure 4.6 $(1-0.8357/0.872)*100 = 4.2 \%$ which is very similar to the difference after correction of 5.6 % from figure 4.2. This shows that the location next to each other in the first three test does not effect the measurements.

The test in figure 4.3 was repeated in figure 4.4. The corrected difference is her found to $(1-0.8764/0.872)*100 = -0.7 \%$ which means that the measurements with the black screen here gives identical measurements as Epply with white screen – which is odd as figure 4.3 showed a difference of 5.1 %.

All the uncertainties are, however, within the uncertainty of the measurements which means that the readings from Epply with white screen may be correct. But there is a trend that the readings with Kipp & Zonen without screen and with black screen gives lower values than Epply.

It is based on the above judged that Epply with white screen gives 4 % too high readings. Based on this the measurements used in chapter 2 has been multiplied with 0,96 before used in the comparison between measured and calculated solar radiation through the MicroShade window in room A.

In order to test the result of figure 4.4 which were a bit odd this test was repeated but without the fan flowing air at the pyranometer. The result is shown in figure 4.7. The regression constant is here 0.8945 while this constant in figure 4.4 was 0.8764 – ie a difference of 2 %.

The surface temperatures were on day 183 and 184 (June 2-3) measured to:

time	room temp.	temp. of pyranometer	black screen
12:31	28.5	30.8	35
12:28	28.8	31.4	34.9

ie a bit higher ΔT between housing/screen and room temperature than in figure 4.1. But the 2 % of difference in readings is negligible. The manufacture of Kip & Zonen also states that this type of pyranometer is temperature compensated. The temperature dependence of sensitivity (-20 to +50°C) is $\pm 1 \%$.

The test in figure 4.2 was also repeated but with ventilation on the pyranometer without screen. While the regression coefficient in figure 4.2 is 0.9261 the regression coefficient with a ventilated pyranometer was 0.9306 or less than 0.5 % higher than in figure 4.2. So the cooling of the pyranometer has no influence on the pyranometer without screen.

Based on the above it may be concluded that the inter-refletring between the window and the white screen of the pyranometer and diffuse radiation from the room behind the pyranometer has only a minor influence on the readings from the pyranometer – mostly within the uncertainty of the experiments.

The inter-reflection between the window and glass dome of the pyranometer cannot be investigated by experiments but via geometrical considerations it is judged that this has negligible influence on the readings from the pyranometer.

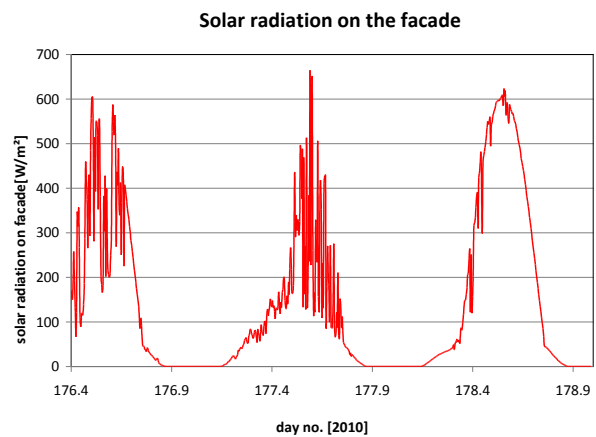
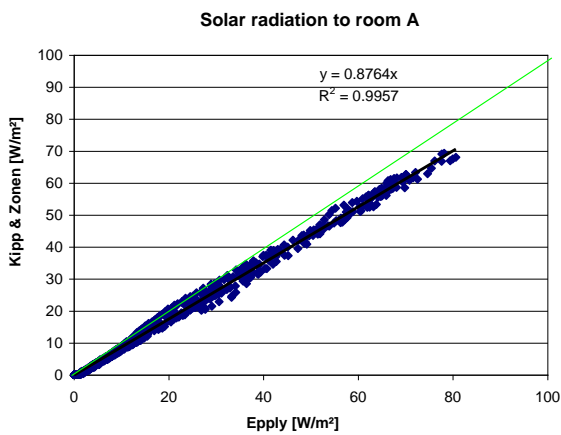


Figure 4.4. The two pyranometers located in different windows – Kipp & Zonen with black screen and ventilation.

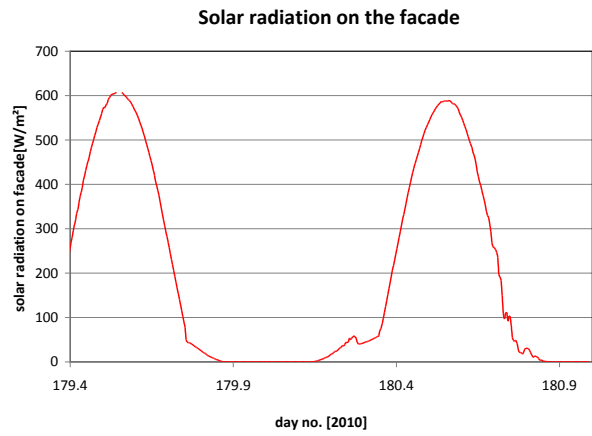
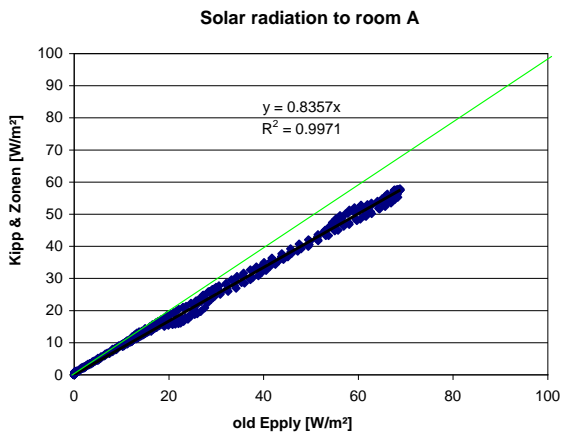


Figure 4.5. The two pyranometers located in different windows – Kipp & Zonen without screen and ventilation.

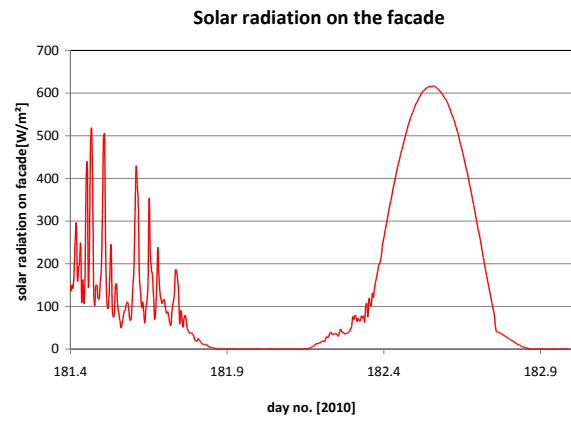
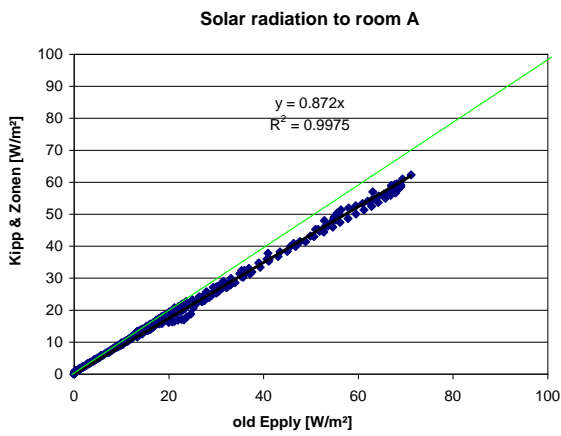


Figure 4.6. The two pyranometers located in different windows – both with white screens and ventilation.

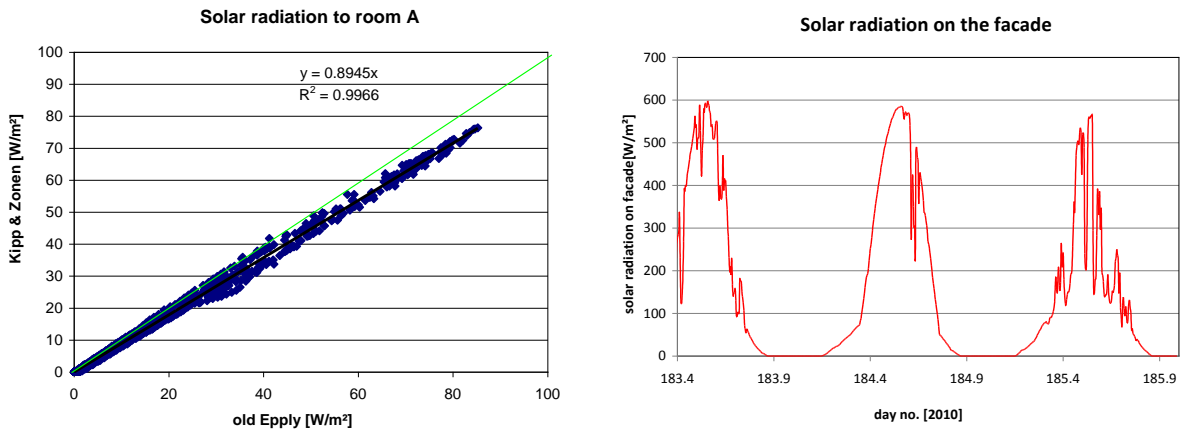


Figure 4.7. The two pyranometers located in different windows – Kipp & Zonen with black screen. No fan blowing air at Kipp & Zonen.

4.1.1. Test of the transmittance across the MicroShade window

A difference of above 10 % was observed between the two series of tests. The difference may be due to differences in the transmittance of the single stripes of MicroShades in the window. In order to test this the relative transmittance of the single stripes was measured by a fast reacting Lux meter which could be fast and easily held close to and parallel with the window.

Due to changes in the light level the experiment utilized relative difference rather than absolute values – ie the lux of a single stripe was always compared to a reference stripe. The latter being the stripe where the Epply pyranometer is mounted. The single stripes were labelled as shown in figure 4.8. The reference stripe is thus “right 6”.

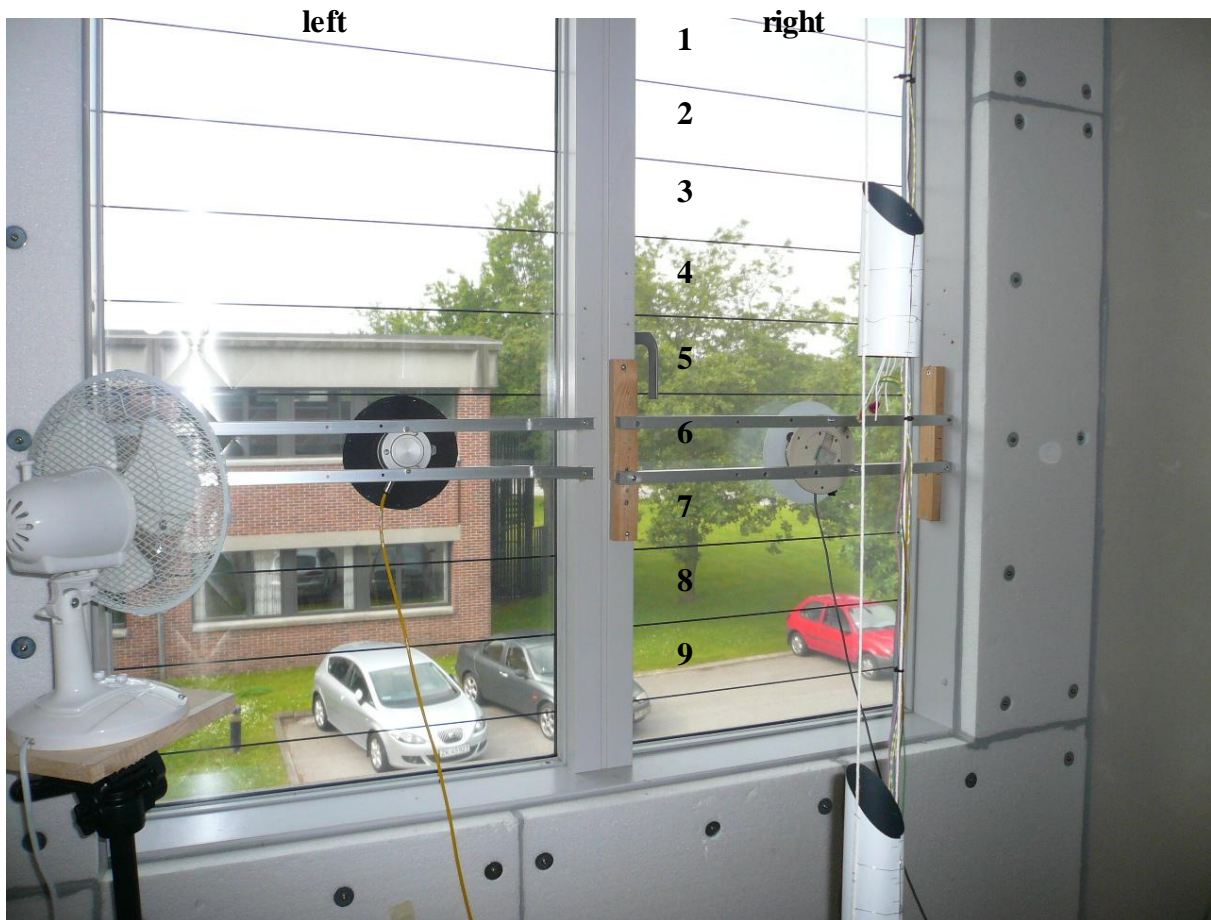


Figure 4.8. The labelling of the Lux measurements.

Figure 4.9 shows the results of the measurements during an overcast day. The Lux values for “right 6” varied over the 5 minutes measuring period between: 3020 and 3220 or 6.5 %. This is more or less the differences obtained in figure 4.9, so it was necessary to work with relative differences rather than absolute values.

Except for level 1 and 2 the discrepancy is below 5.3 %. The lower values at level 1 and 2 are caused by the external overhang above the window. These values should thus be disregarded.

Figure 4.10 shows the same as figure 4.9 but for clear sky conditions (lux at reference between 10300 and 10910 – ie a variation of 6 %). Figure 4.10 shows more clearly the influence of the overhang on the transmitted light at level 1 and 2. Figure 4.10 does not show the same pattern as figure 4.9 and the difference compared to the reference is now up to 9.2 %. This can either mean that the measurements are rather uncertain or the diffuse and direct light are transmitted differently through MicroShades. This could be subject for further investigations but will not be dealt with more here.

Both figures show a difference at “left 6” – where the Kipp & Zonen pyranometer was located – of 5 %. This explains about half de difference observed in figures 4.1 and 4.6.

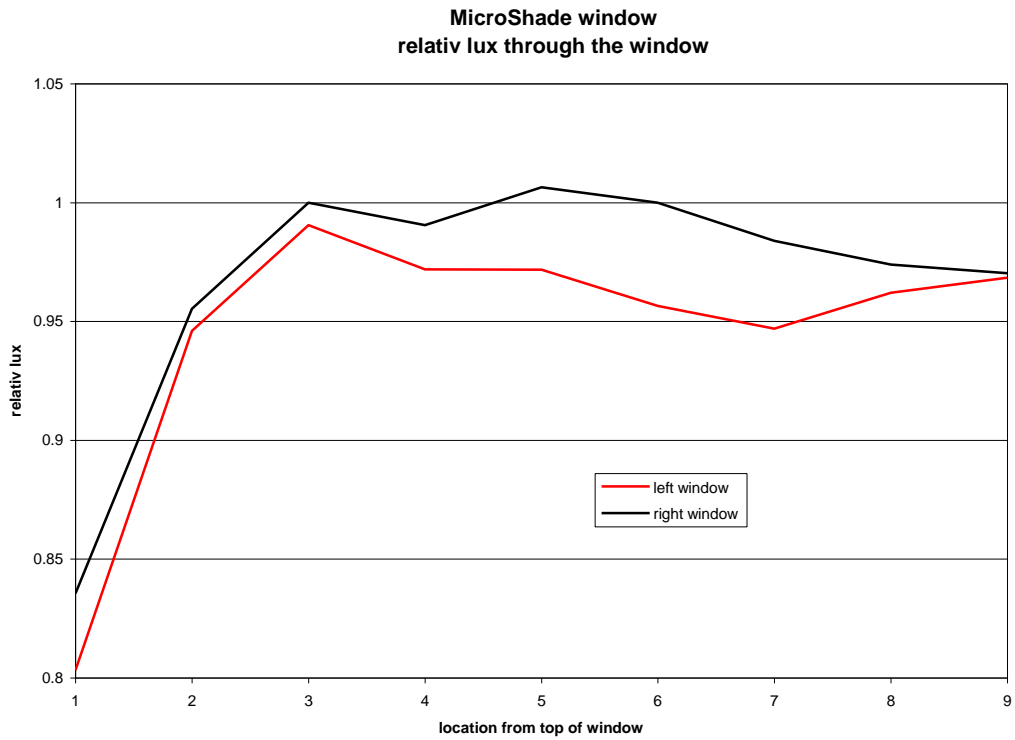


Figure 4.9. Relative Lux through the MicroShade window on an overcast day.

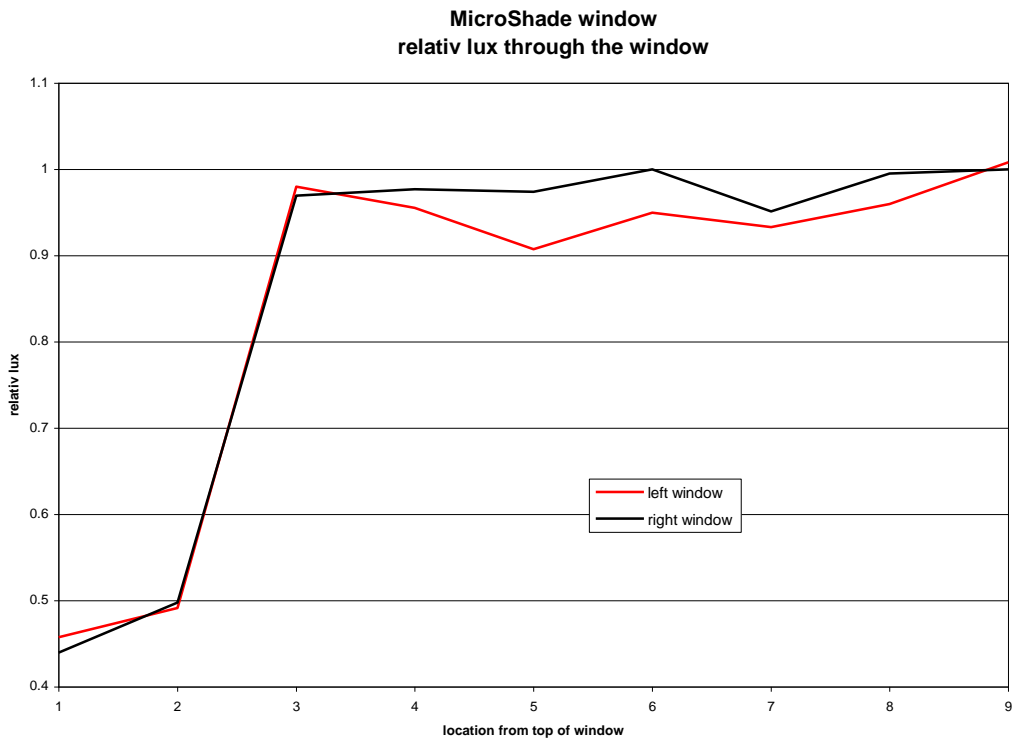


Figure 4.10. Relative Lux through the MicroShade window on a day with direct solar radiation.

4.1.2. Test of the pyranometer in room B

The pyranometer in room B is a calibrated pv pyranometer [Jensen, 2008a] – see figure 4.1. However this pyranometer was calibrated for the original Velfac window with solar control coating. First in May 2010 this window was replaced by a traditional low-E window in order to allow more solar radiation into room B among others to enhance the measurements described in chapter 7.

So a recalibration was carried out – the test arrangement is shown in figure 4.11. Figure 4.12 show a good agreement around 1 %. The calibration in figure 4.12 was, however, carried out with the white screen on Kipp & Zonen. So the calibration was repeated with the black screen on Kipp & Zonen. The result is shown in figure 4.13.



Figure 4.11. The arrangement for testing the measurements of incoming solar radiation through the traditional low-E window.

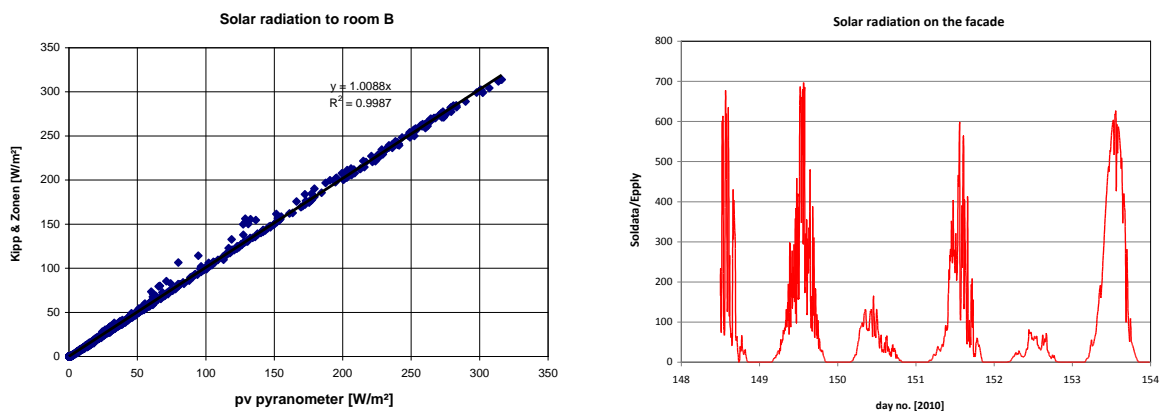


Figure 4.12. Calibration of the pv pyranometer in room B. Kipp & Zonen with white screen.

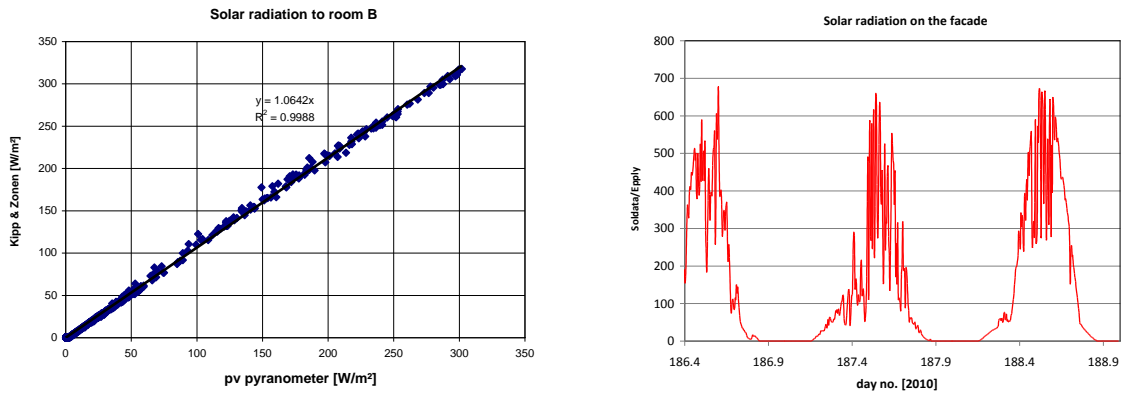


Figure 4.13. Calibration of the pv pyranometer in room B. Kipp & Zonen with black screen.

Surprisingly figure 4.13 shows 6.4 % higher values measured with Kipp & Zonen with the black screen than with the pv pyranometer. The opposite was expected. A new test now without screen on the Kipp & Zonen pyranometer was conducted. The result from this test is shown in figure 4.14. Figure 4.14 also shows higher values for the Kipp & Zonen than for the pv pyranometer: 5.2 % higher values which is within 1% identical to the test with the black screen.

The discrepancies are within the uncertainties of the measurements so one could state that the readings of the two pyranometers with and without screens are the same within the uncertainty. However, as a final check the test in figure 4.12 (with the white screen) was repeated. The result is shown in figure 4.15. Figure 4.15 shows that in this test the Kipp & Zonen gives 8.6 % higher readings than the pv-pyranometer. So this is in line with the measurements in figure 4.13-14 and with the findings for the MicroShade window.

The difference between the results in figure 4.15 and 4.12 illustrates the uncertainty of the measurements – ie. the same experiment performed with 1½ months between the experiments shows 7.5 % difference - is more or less within the uncertainty of the experiment as stated earlier.

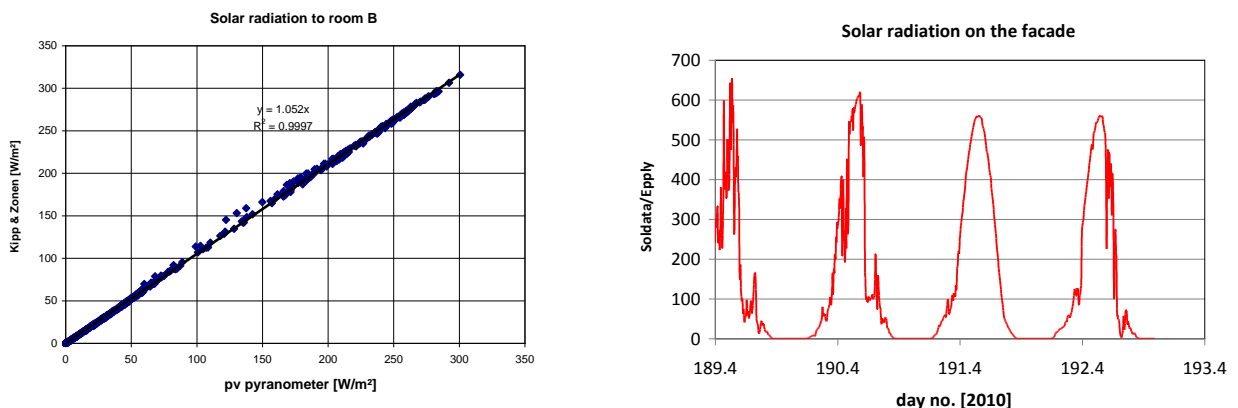


Figure 4.14. Calibration of the pv pyranometer in room B. Kipp & Zonen without screen.

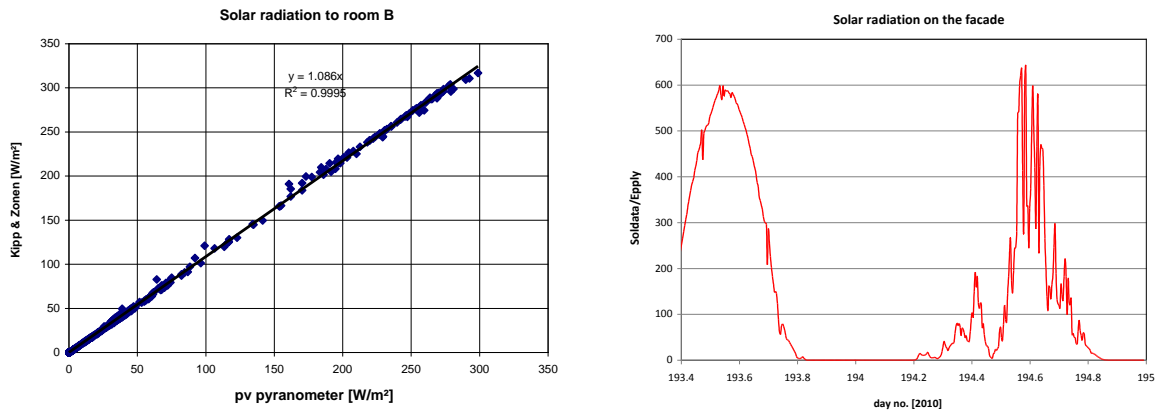


Figure 4.15. Calibration of the pv pyranometer in room B. Kipp & Zonen with white screen.

Figures 4.13-4.15 gives the following differences between the readings of the two pyranometers:

- with white screen: 8.6 %
- with black screen: 6.4 %
- without screen: 5.2 %

ie a max difference of 3 % which means that the measurements within the uncertainty is identical. The influence of inter-reflections and diffuse radiation from the room behind the pyranometers is thus negligible for the pv-pyranometer. This further support the conclusion that the inter-reflection between the window and the dome of the Epply pyranometer is negligible.

Based on the above it is concluded that the pv-pyranometer may underestimate the incoming solar radiation with up to about 5 %.

4.2. Conclusions

The tests show that the influence of inter-reflections between the pyranometer/white screen of the Epply pyranometer may lead to a over estimation of the incoming solar radiation of 4 % while it seems to have no influence on the readings from the pv-pyranometer. The diffuse radiation from the room behind also seems to have negligible influence – ie this radiation is mostly transmitted through the windows to the ambient.

Based on the above it is assumed that the readings of the Epply pyranometer should be multiplied with 0.96 while the readings from the pv-pyranometer should be multiplied with 1.05. However, the observed difference is within the uncertainty of the experiments so one could just as well claim that readings from the two pyranometers are correct and should thus not be reduced/enhanced.

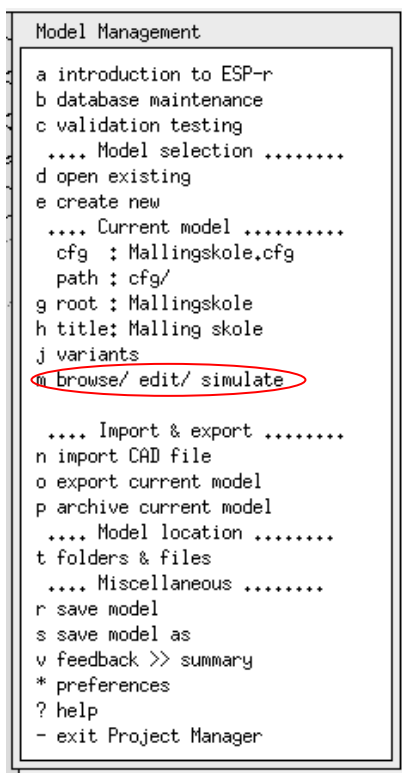
Simple measurements of the light coming through the MicroShade window show difference of up to 9.2 % between the different stripes of MicroShades. However, more precise measurements is necessary in order to come up with firm conclusions.

5. Tutorial for including MicroShades in esp-r (version 11.8) simulations

In the following it is described how the detailed matrix describing MicroShade windows may be introduced in esp-r models of buildings – in esp-r referred to as bi-directional attributes.

First: create a normal model of the room or building where transparent surfaces which include MicroShades are defined as TMCs (transparent multilayered constructions). The optical TMC properties for the surfaces including MicroShades can be chosen randomly as these are overridden by the values in the bi-directional matrix.

When the above model is created go to “m browse/edit/simulate” on the first menu of esp-r – see below:



```
Model Management
a introduction to ESP-r
b database maintenance
c validation testing
  .... Model selection .....
d open existing
e create new
  .... Current model .....
  cfg : Mallingskole.cfg
  path : cfg/
g root : Mallingskole
h title: Mallingskole
j variants
m browse/ edit/ simulate
  .... Import & export .....
n import CAD file
o export current model
p archive current model
  .... Model location .....
t folders & files
  .... Miscellaneous .....
r save model
s save model as
v feedback >> summary
* preferences
? help
- exit Project Manager
```

After this go to ”c composition” on the following menu – see below:


```
Browse/ Edit/ Simulate

  cfg file: Mallingskole.cfg
  a model domains >> building only
  b model context

-----
  ... Zones.....(12 defined)
  c composition
  ... Networks.....( 0 defined)
  d plant & systems
  e network flow
  f electrical
  g contaminant
  ... Controls.....( 0 defined)
  j zones
  k plant & systems
  l network flow
  m optics
  n global system
  o complex fenestration

-----
  p define uncertainties

-----
  ... Actions.....
  q visualisation
  r simulation
  s results analysis
  t results & QA reporting

-----
  ! save model
  ? help
  - exit this menu
```

Then choose "o advanced optics" on the following menu – see below:

```
Zones Composition

.... Zones ....( 12 defined)
a geometry & attribution
b construction materials
c operational details

-----
.... Topology ..( 86 connects)
d surface connections & boundary
e anchors (groups of surfaces)

-----
.... Options ....
f shading & insolation
g convection coefficients
h view factors & radiant sensors
i casual gain control
j computational fluid dynamics
k adaptive gridding & moisture

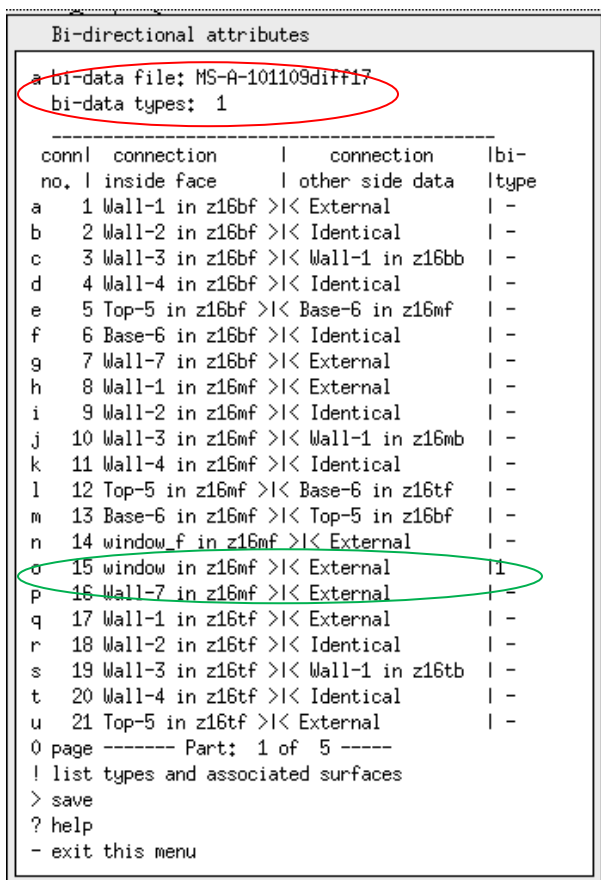
-----
.... Special components ....
m integrated renewables
n active materials
o advanced optics

-----
* global tasks
? help
- exit this menu
```

The menu for defining which transparent surfaces include MicroShades is then reached – see below.

Under “a Bi-directional file” is inserted the name of the file which contains the matrix with the optical properties of the chosen window with MicroShades. If the file is located in the cfg library of the model it is only necessary to give the name of the bi-directional file as seen in the below figure where the name of the bidirectional files is: MS-A-101109diff17. The matrix for windows including MicroShades may be obtained from PhotoSolar (www.PhotoSolar.dk). The “bi-data type” should be 1.

After this the surfaces including MicroShades is chosen by clicking at the appropriate surfaces – in the below figure “p 15 window in z16mf >|< External” - where an “1” will appear to the right of the menu when chosen for bi-directional simulation. “z16mf” is in the figure below one zone of the building which contains the surfaces from h to p.



Remember to save before leaving the above menu.

After specifying which surfaces include Microshades a simulation may run the normal way. When introducing MicroShades in the model there will be no control function associated with this, as it cannot change optical properties as e.g. venetian blinds. Therefore, a warning message will be shown during the simulation, but this can be ignored.

6. Case study: Malling school

In [Jensen, 2008b] a case study of applying MicroShades in an office building was investigated – see Appendix A. Here it is chosen to investigate the influence of MicroShades installed in a school.

The school chosen for the case study is Malling school in the town Malling in the eastern Jutland, Denmark. MicroShades have already been tried out in the school with success as seen in Appendix C (main part of Appendix C is unfortunately in Danish).

The case study considers two South facing class rooms: room 16 and 17 as seen in figure D.1 in Appendix D. Room 16 has MicroShade in the South facing windows while room 17 has solar control coating in the windows. All windows are low-E double glazed windows.

The dimensions of the class rooms are – see Appendix D:

width: 8.1 m
depth: 6.m
height: 3.1 m

There are as seen in figure 6.1 three windows in the rooms. Each window has four transparent areas of $0.782 \times 0.906 \text{ m}^2$ - ie in total a transparent area of 8.5 m^2 or a window to floor ration of 0.175.



Figure 6.1. The windows of one of the class rooms.

The constructions of the rooms are – see Appendix D:

Back wall: 260 mm concrete
 Side walls: 150 mm concrete
 Façade: 360 mm hollow brick wall
 Floor slab: 150 concrete with 15 mm asphalt finish on top
 Ceiling: Rockfon, wood, 200 mm mineral wool

Based on the above information a model of the two class rooms has been created in esp-r – see figure 6.2.

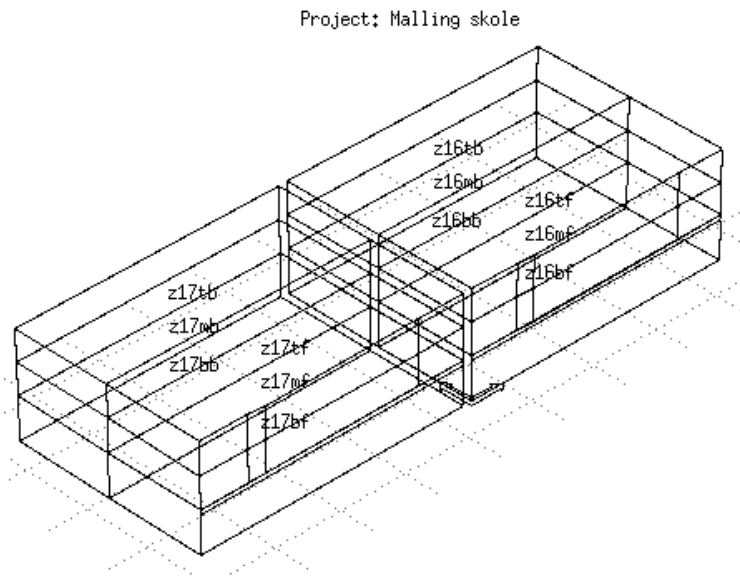


Figure 6.2. Wire model of the model of the two class rooms at Malling school.

The labelling of the 6 zones in a class room is shown more clearly in figure 6.3.

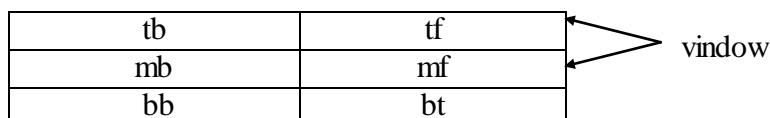


Figure 6.3. Labeling of the zones in the simulation model of a class room.
 first letter: t: top, m: middle and b: bottom
 second letter: b: back and f: front.

The models used for the two window types is:

MircoShade window: MS-A-220810-3-diff185 from chapter 2
 Solar control window: The Velfac sun 1/clear – the first window in test room B – see [Jensen, 2008a]. Solar transmittance at 0°: 0.34.

Appendix C shows temperature measurements from September 1 – see also figure 6.4. Figure 6.4 shows a max temperature difference between the two rooms of up to 2 K. It is informed that there were some clouds on the day of figure 6.4.

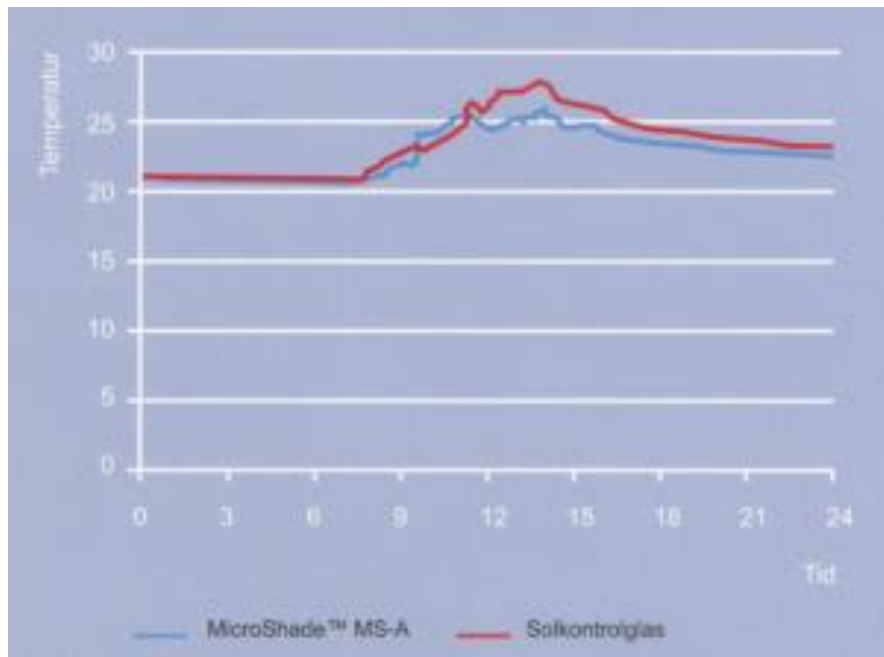


Figure 6.4. Air temperatures in the two rooms during September 1.

Figures 6.6-6.8 shows the results of simulations with the esp-r model of the two class rooms for the period August 25-September 5. The air change of the rooms is assumed to be only infiltration as no mechanical ventilation is present in the rooms – excess ventilation of the rooms are done by opening of windows. There are no persons in the room. The applied weather conditions are the weather for Copenhagen in esp-r. Figure 6.5 shows the weather conditions for the chosen period. There is no heating or cooling in the rooms.

Figures 6.6-6.8 show that the air temperature increased during the day due to the solar radiation and decreases during the night due to a lower ambient temperature. However, the figures also show that there is a general difference about 1 K between the rooms during the night which is caused by the thermal mass and the fact that more solar radiation is entering room 17. The heat loss is too low to reach the same temperature level as in room 16.

The values in figure 6.4 are part of a measuring series of 5 days. The measured values, however, only exist as plots as shown in figure 6.9. The measured values are shielded air temperature in the two rooms and a non shielded temperature where the sun was allowed to hit the temperature sensor. These values are by hand draws into figures 6.10-11. The sensors were located approx 300 mm above a table.

Figures 6.10-11 shows general problems in the interpretation of figure 6.4. The temperature of the room with the solar control window (room 17) is for the first two days lower or equal to the temperature in the room with the MicroShade window (room 16) during the day but up to 3 K lower during the night. This can be due to both higher ventilation rate or fewer pupils in room 17 compared to room 16. This is not known.

However, at September 1 the two class rooms starts at the same room temperature. The simulations in figures 6.6-6.8 has therefore been forced to start at the same temperature at day 241 – August 29. A day with clear sky conditions.

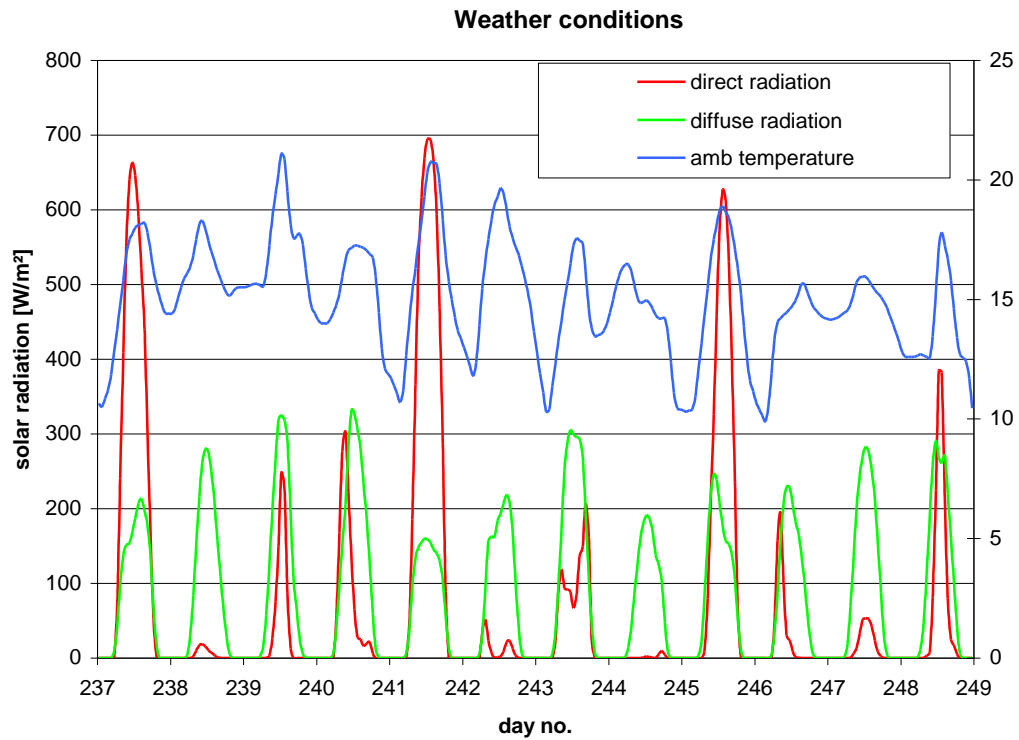


Figure 6.5. The weather conditions applied in the simulations.

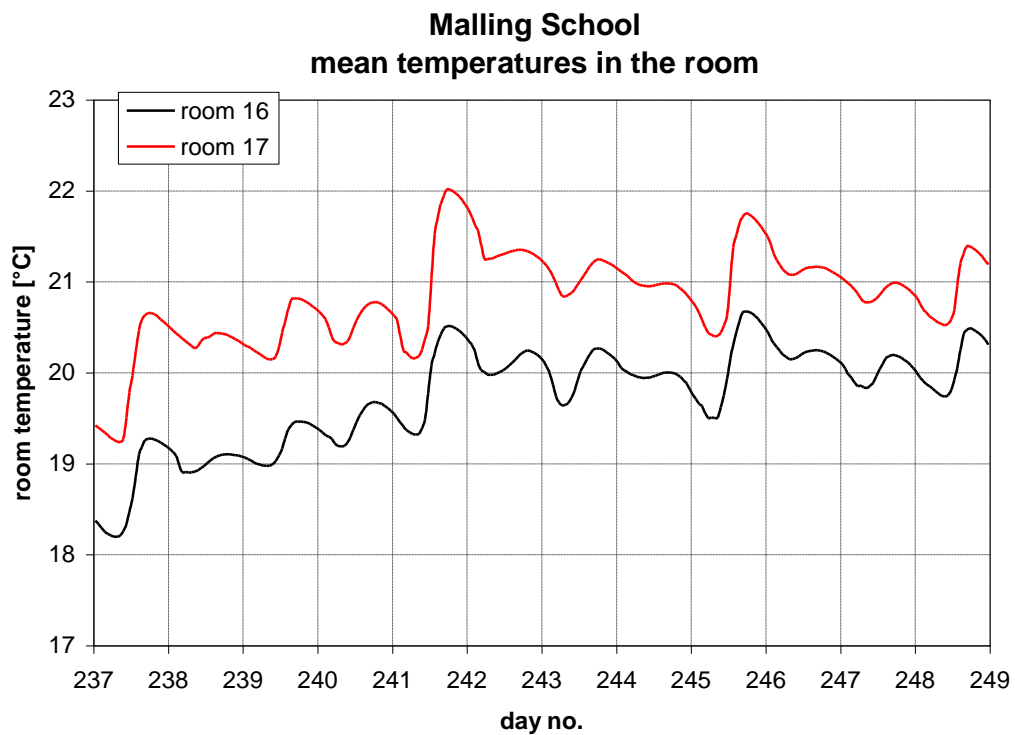


Figure 6.6. The mean temperature of the two class rooms.

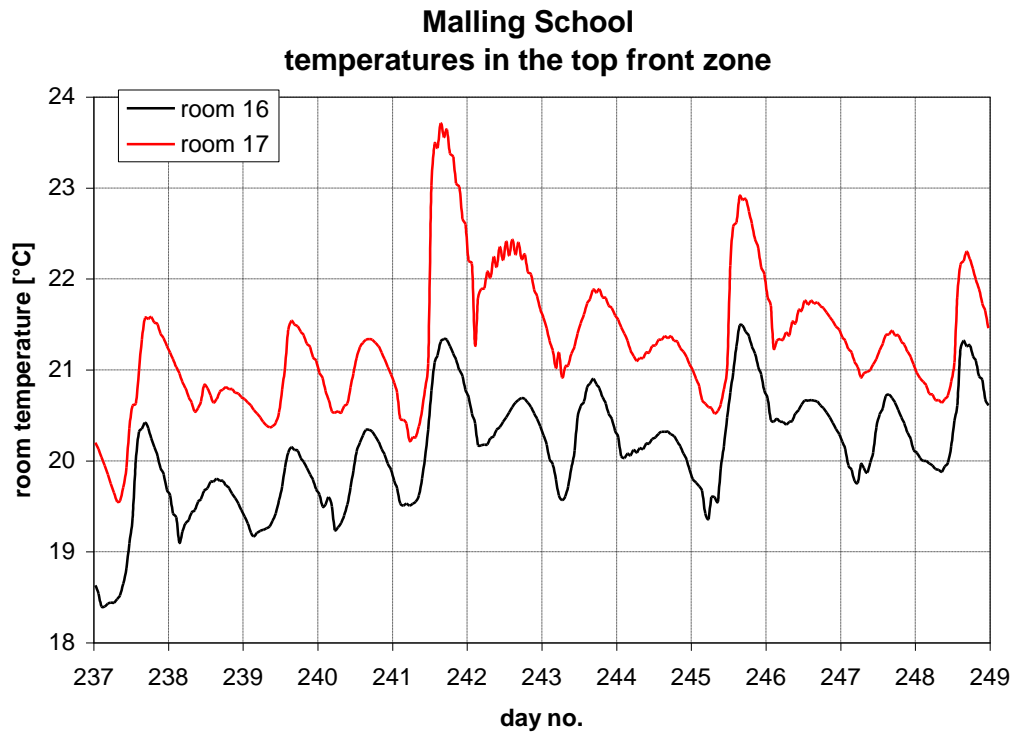


Figure 6.7. The temperature of the front top zones – tf in figure 6.3.

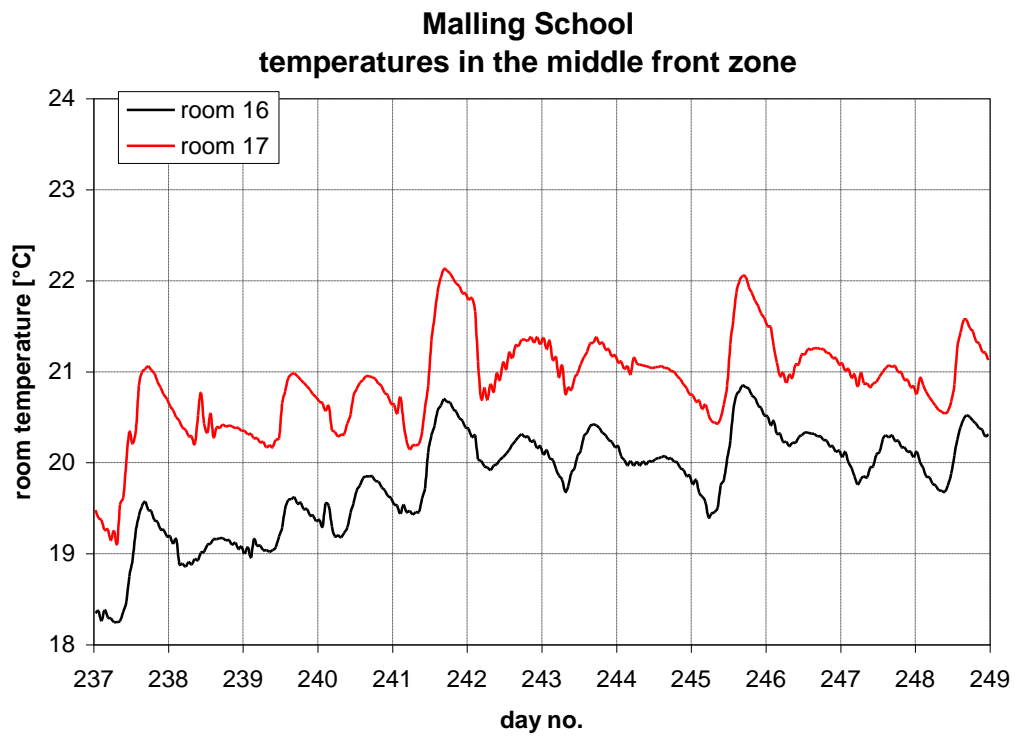


Figure 6.8. The temperature of the middle front zones – mf in figure 6.3.

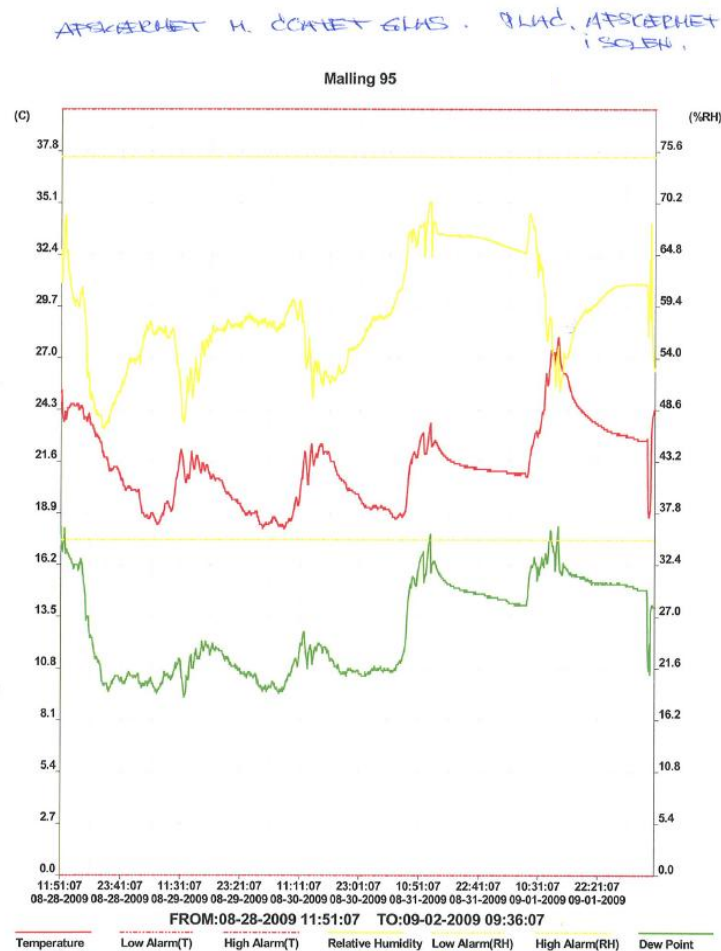


Figure 6.9. Plot of temperature and relative humidity measurements – room 17.

Figures 6.12-6.14 show a max temperature difference between the two class rooms of approx 0.5 K which is a lower than found in figure 6.4 – but when considering that the temperature sensors were located above a table which give somewhat higher readings due to the heating up of the table (see section 6.3) – higher than the mean temperature (and simulated by esp-r) in that particular vertical zoned as the tables covers only a smaller part of the floor area – the comparison is more acceptable.

Figures 6.15-6.16 shows the simulated temperature stratification in the two rooms when it is assumed that the solar radiation hits a table covering the entire top of zone bf (figure 6.3). Room 16 shows a vertical temperature stratification of up to 1.5 K, while the temperature stratification in room 17 is up to 2.5 K. There is also a small horizontal temperature stratification.

A vertical temperature stratification of up to around 2 K is quite normal.

6.1. Parametric studies

However, it is difficult to conclude on the simulations as the conditions in the two rooms during the measurements in figure 6.4 and 6.10 are not known. But, when looking at figure 6.15

showing the relative humidity during the measurements in figure 6.10 one can state a bit on the ventilation.

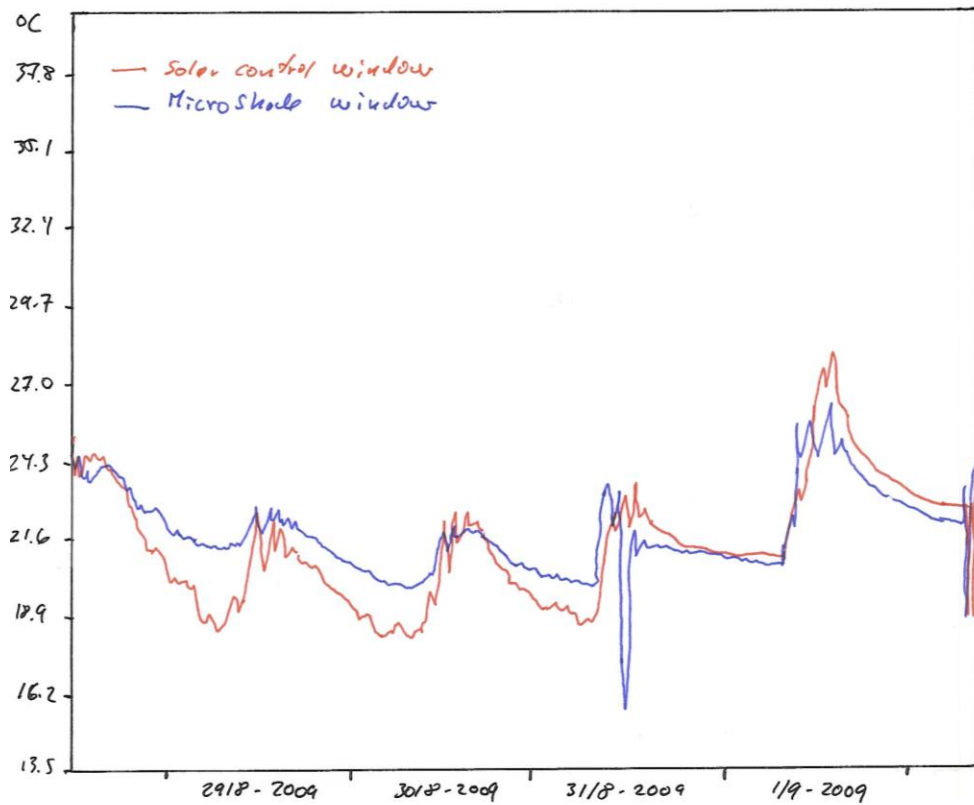


Figure 6.10. Measured shielded air temperatures in the two rooms.

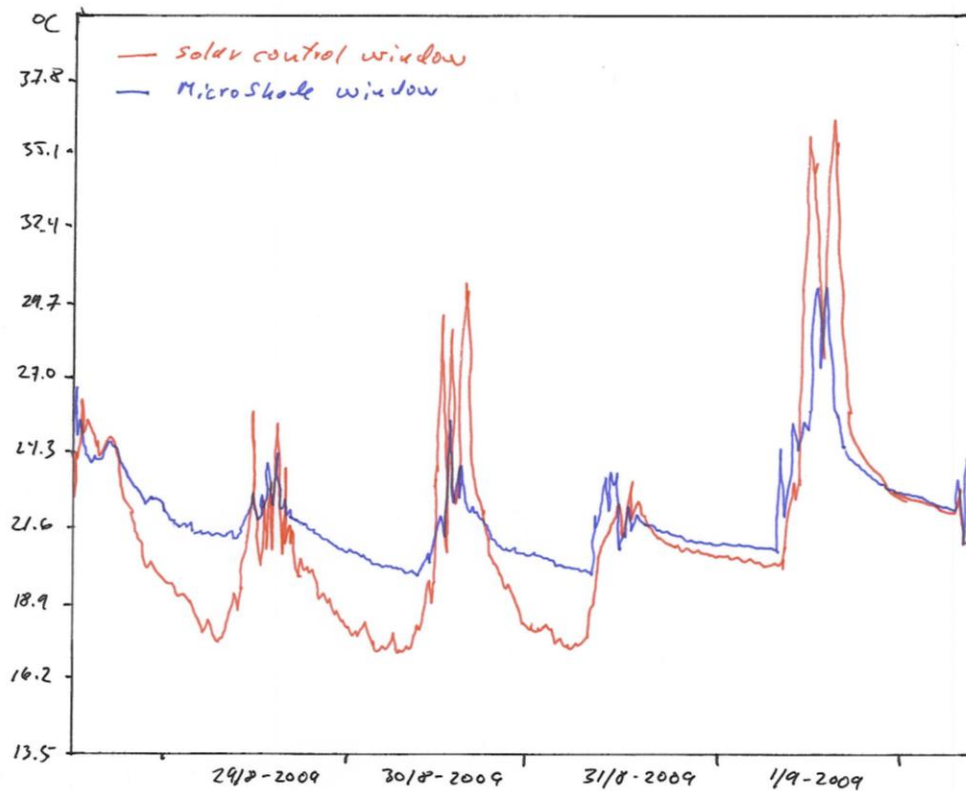


Figure 6.11. Measured temperatures where the sun was allow to hit the temperature sensor.

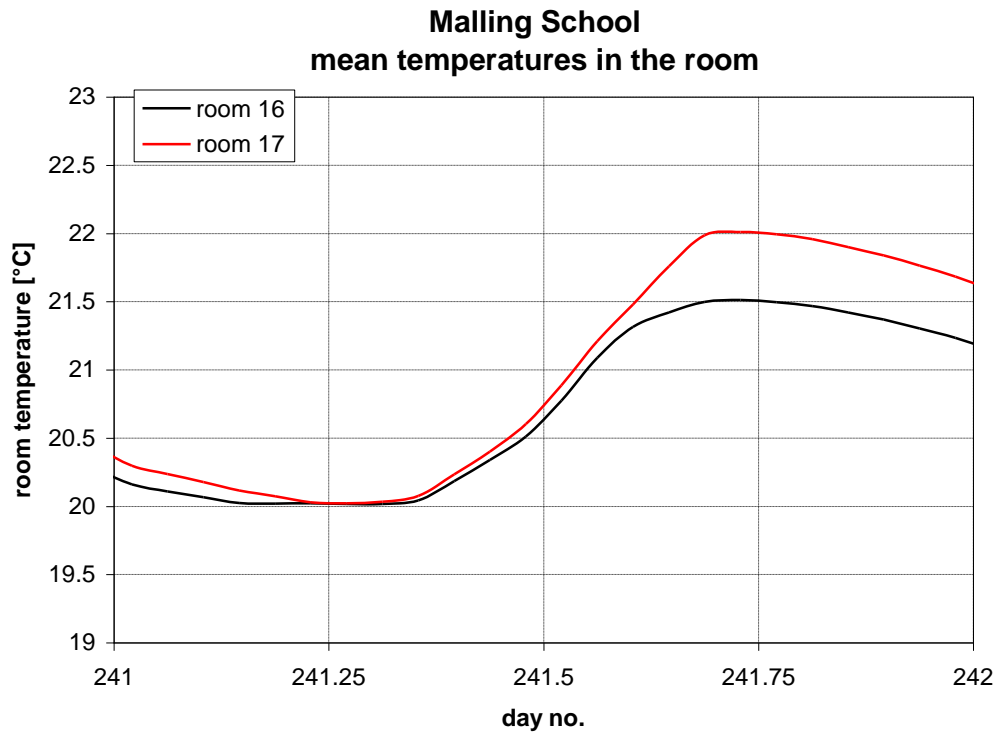


Figure 6.12. The mean temperature of the two class rooms for August 28.

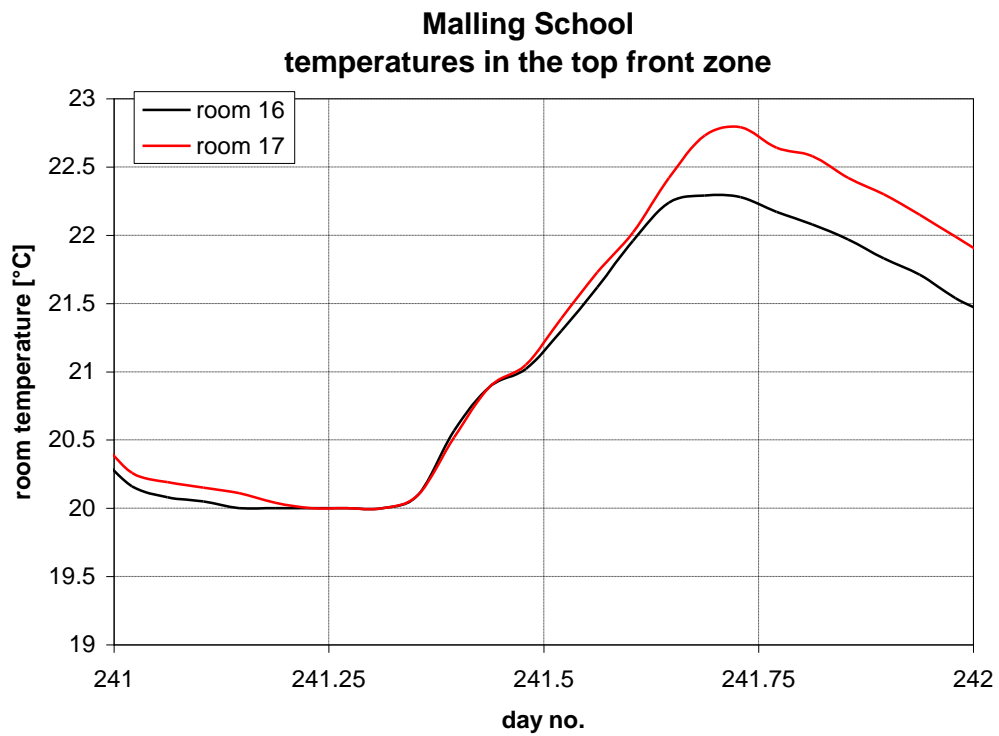


Figure 6.13. The temperature of the front top zones – tf in figure 6.3 for August 28.

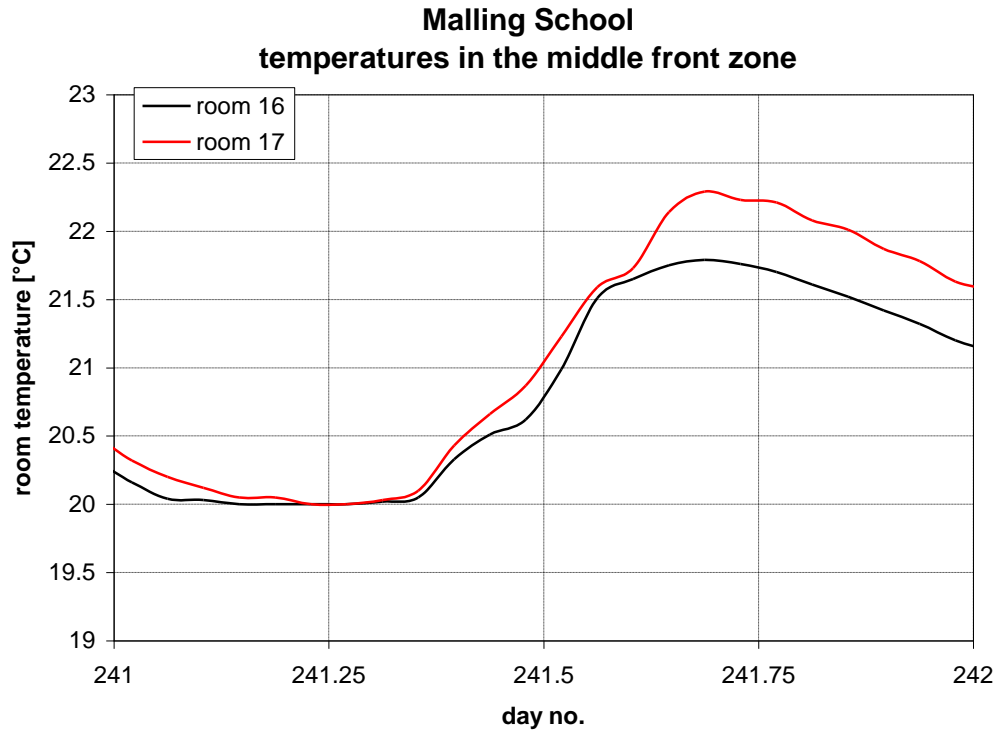


Figure 6.14. The temperature of the middle front zones – mf in figure 6.3 for August 28.

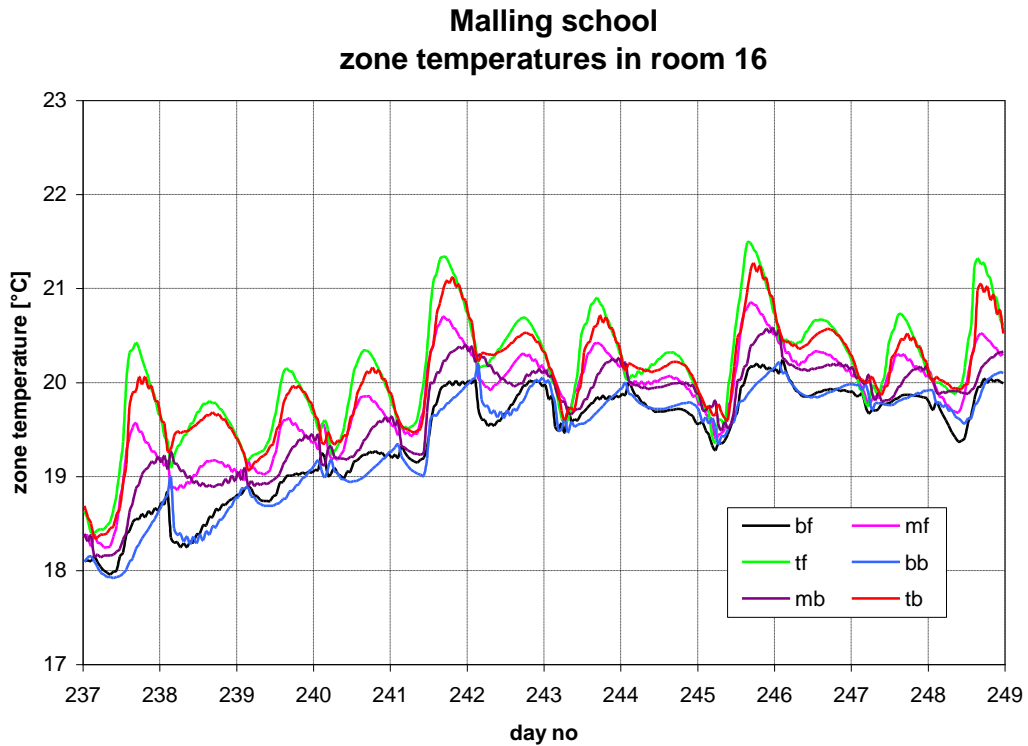


Figure 6.15. The temperature stratification in room 16.

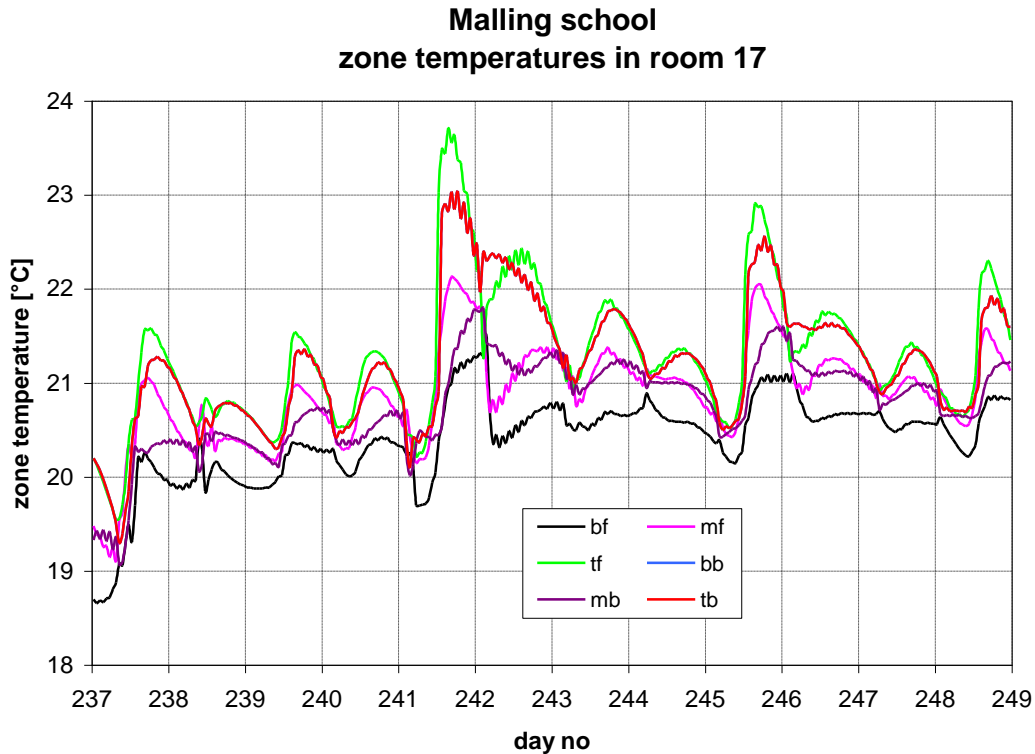


Figure 6.16. The temperature stratification in room 17.

The relative humidity increases with increasing air temperature and decreases with increased ventilation. Based on a comparison of figure 6.10 and 6.15 it is assumed that ventilation did occur during the periods at the blue circles in both rooms while at the red circle only in room 17. However, the air change rate is not known. And so is the numbers of pupils in the rooms.

So a couple of parametric runs with the simulation program have been carried out:

- a. a constant ventilation flow rate (day and night) of 225 m³/h – half the required flow rate in the Danish Building code with 21 persons in the room. This lower flow rate is used as the windows are manually operated so a lower flow rates than required is expected
- b. 20 pupil and one teacher in the room of 80 W each = 1.68 kW from 8:00 to 16:00
- c. the solar control window is replaced with at traditional low-E window with a transmittance of 0.54 at an incidence angle of 0°. Identical to the window installed in test room B in May 2010 – see chapter 2 and 3.

Figures 6.18-20 shows the results of the parametric study. For each cases are shown the mean air temperature.

- a. the extra ventilation decreases only a little the temperature level and the max temperature difference between the two rooms. The max temperature difference is decreased from approx 0.5 to 0.4 K. The influence of the ventilation air is low for this particular day as the ambient temperature as seen in figure 6.5 went above 20°C which decreases the cooling effect.

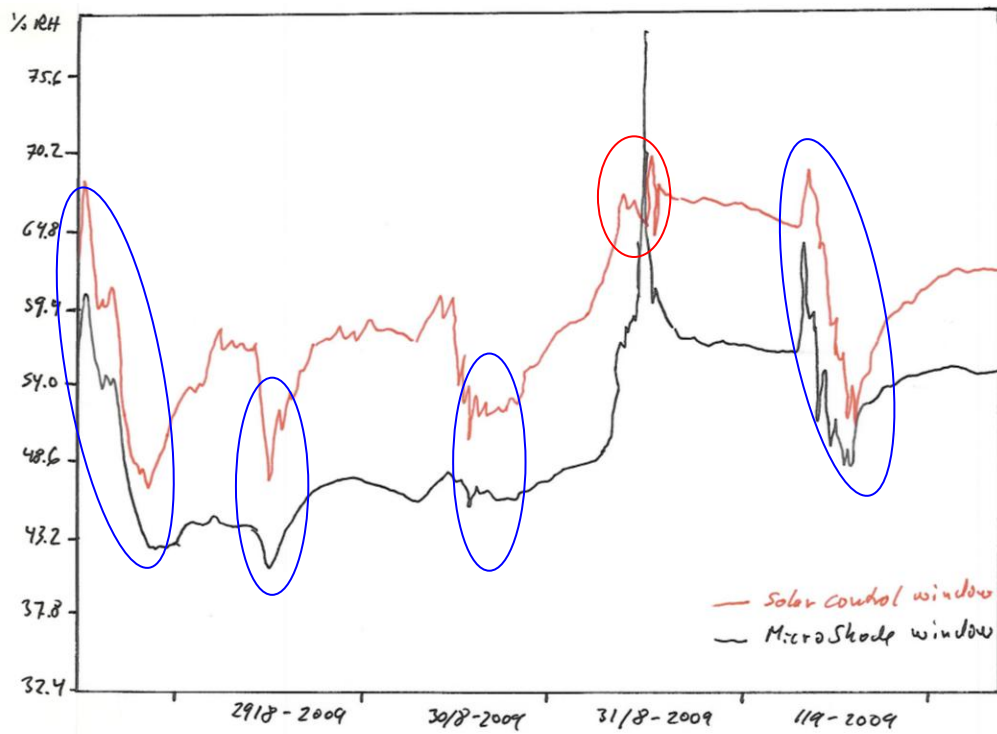


Figure 6.17. The relative humidity in the rooms during the measurements in figure 6.10.

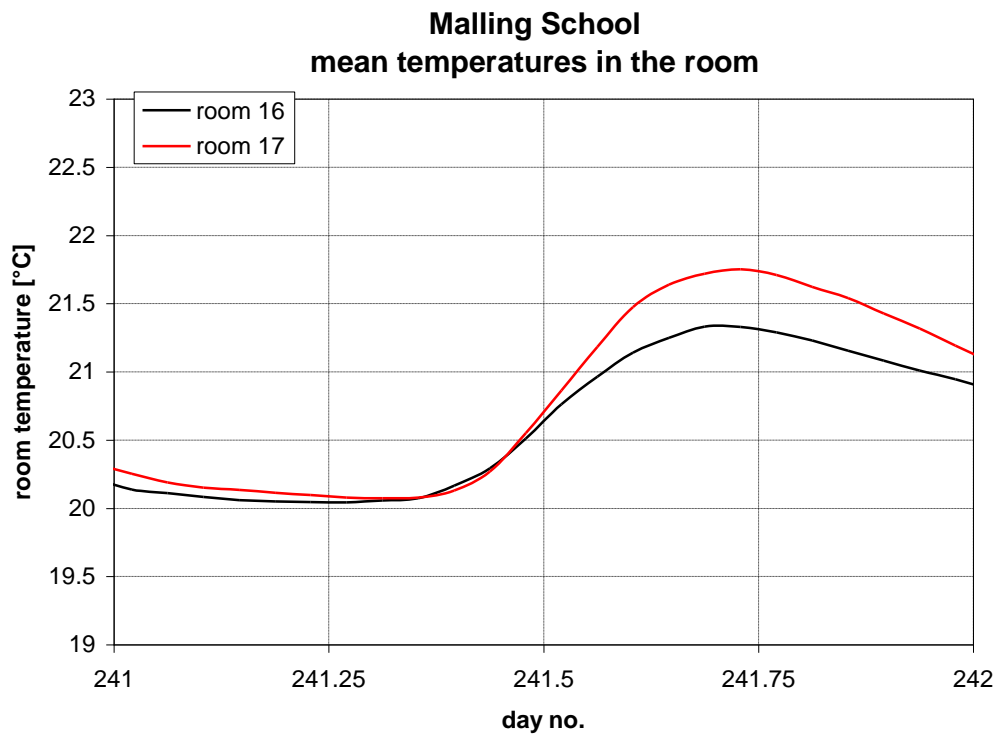


Figure 6.18. The mean temperature of the two class rooms for August 28 with at ventilation flow rate of 225 m³/h.

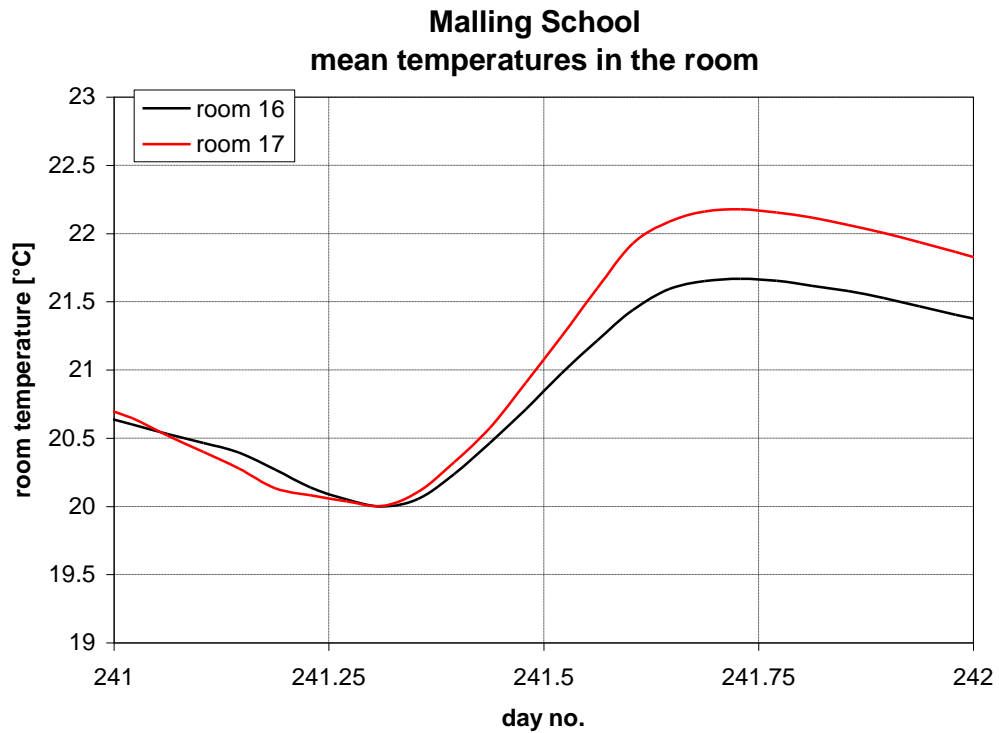


Figure 6.19. The mean temperature of the two class rooms for August 28 with pupils in the rooms.

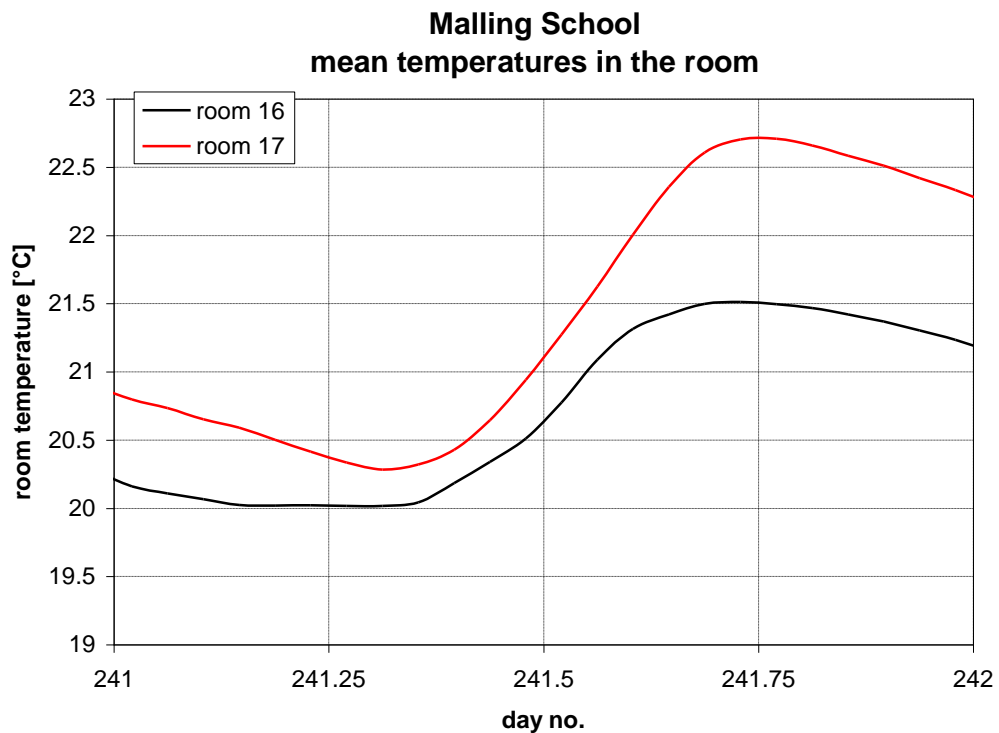


Figure 6.20. The mean temperature of the two class rooms for August 28 with a traditional low-E window without solar control.

- b. the internal heat load from pupils leads to a small increase in the air temperature while the max temperature difference is kept. This was expected.
- c. the more incoming solar radiation to room 17 leads in figure 6.20 to an increase of the max difference in mean air temperatures from 0.5 to 1.25 K. However, due to the higher incoming solar radiation an air temperature by the start of the day could not be kept. If this 0.5 K difference in the morning is subtracted the increase of the max temperature difference is from 0.5 to 0.75 K – ie an increase of 66 % which is similar to the increase in solar transmittance between the two windows (without and with solar control): $(1-0.54/0.34)*100 = 59 \%$. So this is as expected.

6.2. Exposure to the sun

Appendix C reports a temperature difference of up to 4-5 K. From figures 6.10-6.11 this large temperature difference is when exposed to direct solar radiation. Figures 6.10 and 6.11 show large differences between the readings from the shielded and the non shielded temperature sensor. The large difference is of course due to the fact that the non shielded temperature sensor was heated up by the sun. This again means that the comfort level of a person sitting next to a window will be influenced if the person is hit by the sun. This is dealt with in the next chapter.

6.3. CFD simulations

The simulations in the preceding section were carried out with esp-r which is a large program for simulation of the thermal performance of buildings including the constructions and installations. However, the model of the class rooms is rather rough – ie. 6 zones in each class room connected by a flow net work. The model gives thus only a rough impression of the temperature distribution in the rooms.

In order to investigate more in details the temperature distribution in the rooms when the sun hits the tables in the class rooms CFD (computational fluid dynamics) was been applied out. The program utilized for the purpose was ANSYS version 11 and the class rooms were divided in more than 140,000 nodes and over 775,000 tetrahedral elements. The simulation time step was 0.4 s.

Figure 6.21 shows the model of the class room. The infiltration is as earlier 23 m²/m. It is assumed that all solar radiation hits the tables. The external radiation level is as on day 241 investigated in the above simulations – ie a very sunny day. The tables are assumed to have a reflectance of 0.2. For the two investigated cases:

194.4 W/m² was absorbed on the tables in the room with the solar control window
92 W/m² was absorbed on the tables in the room with the MicroShade window

In figure 6.21 is also shown stars in a line from a window to the back wall. The stars are located right over tables as shown in figure 6.22. During the simulation the temperature is monitored in these eight points. The result of this monitoring is shown in figures 6.23-6.24.

The CFD simulation was rather unstable and convergence was not reached before the simulation had to be stopped. However, the temperature level seems to may reach the level of figure 6.4 and the max temperature difference is also in agreement with figure 6.4. However, figures

6.4 and 6.23-6.24 show the temperatures over the tables – ie the mean value of the room will as mentioned earlier be lower and thus more in agreement with the esp-r simulations.

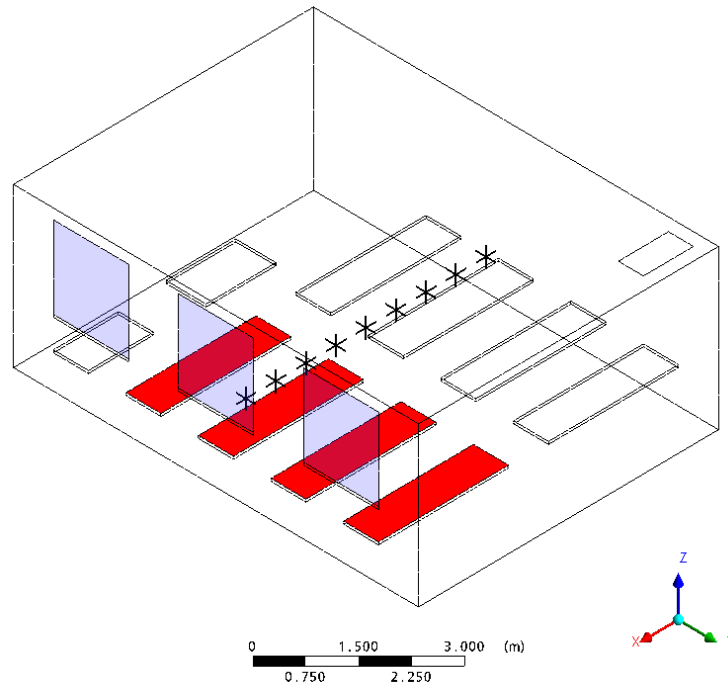


Figure 6.21. The CFD model of the room

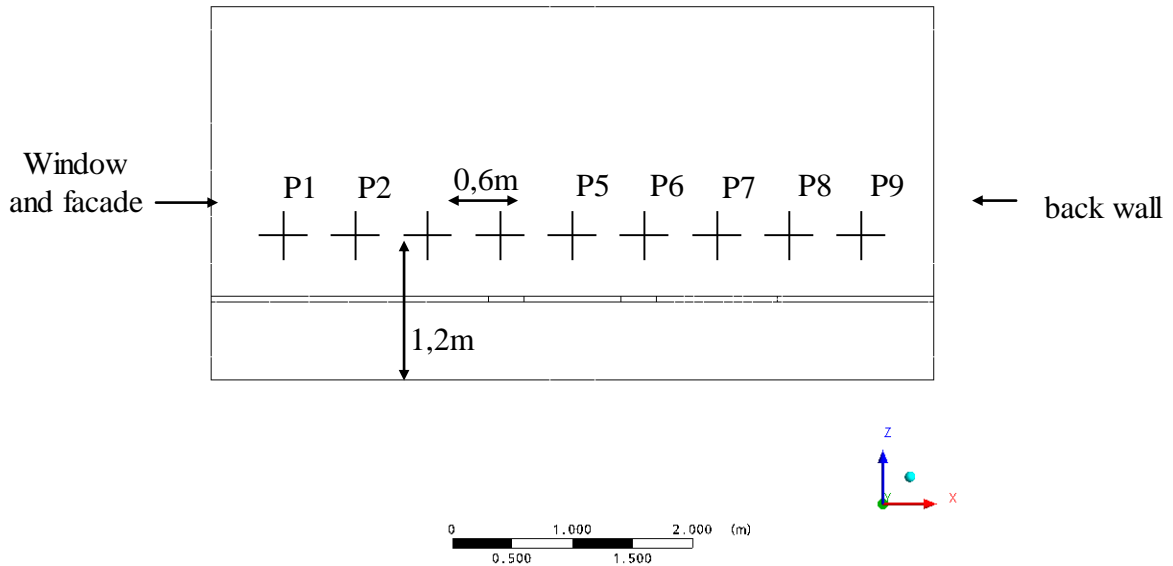


Figure 6.22. The points where the temperature has been monitored through the simulation.

High peak values are seen in figures 6.23-6.24 over the sun exposed table and the air temperature fluctuates much here. Highest for the room with the solar control window due to a higher radiation level on the tables. Figures 6.23-6.24 shows, however, only the temperature at this particular line across the table.

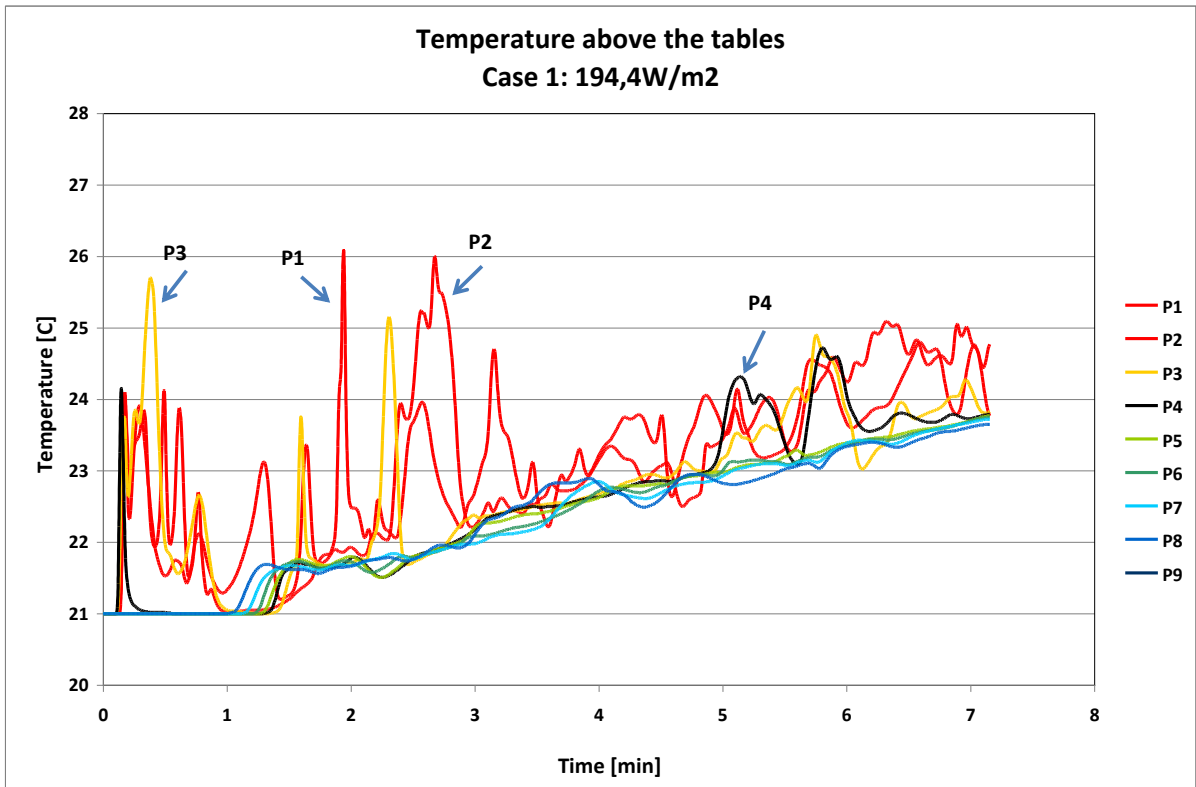


Figure 6.23. The temperature evolution for the case of the class room with the solar control window.

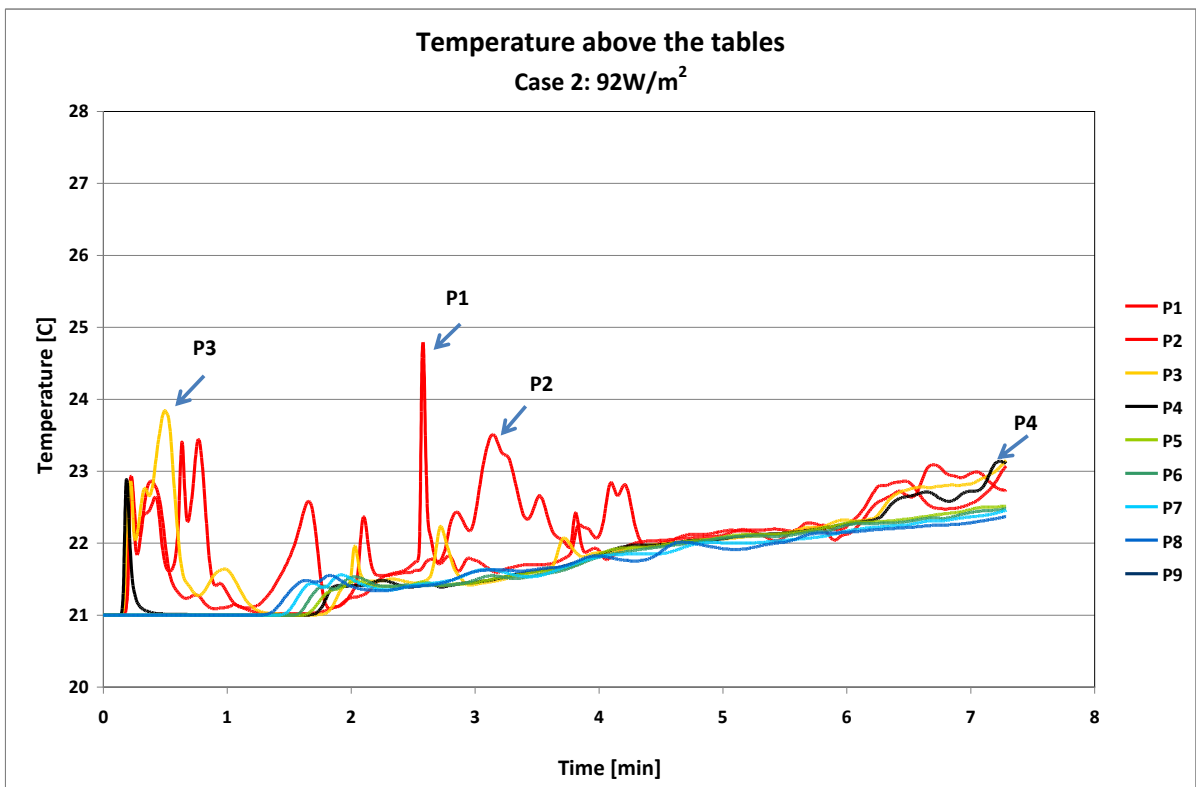


Figure 6.24. The temperature evolution for the case of the class room with the MicroShade window.

The temperature distribution over the tables is shown figure 6.25 which shows a snap shot after 5 minutes (real time). Figure 6.25 shows the border line where the temperature is above 26°C. Figure 6.25 shows that the tables in the room with the solar control windows heat more up than in the room with the MicroShade window.

The higher temperature in the class room with the solar control window may cause discomfort for all in the room. But further discomfort will be created for the pupils sitting at the warm tables along the façade and because they are being hit by more solar radiation.

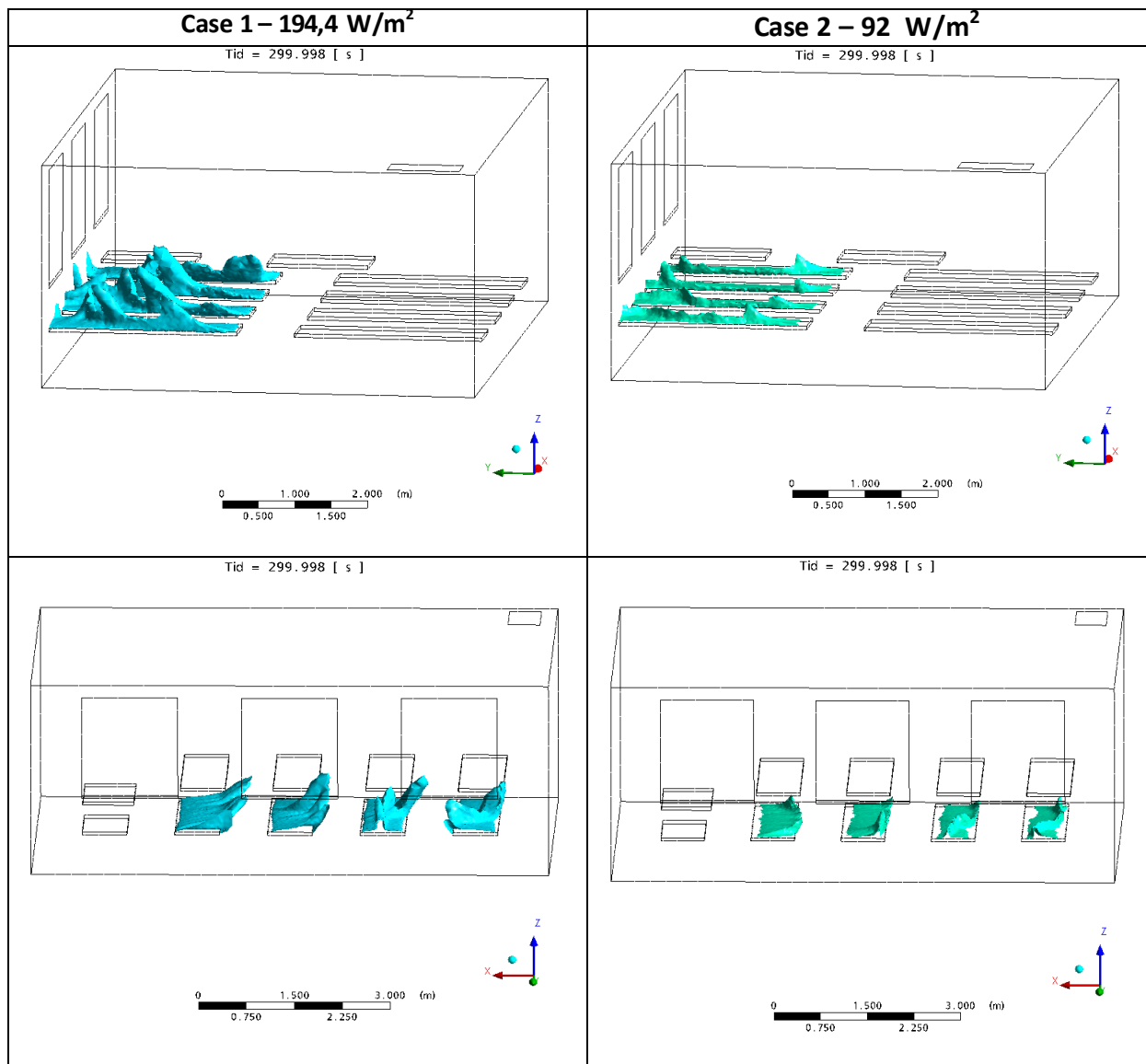


Figure 6.25. The border line of an air temperature of 26°C. Solar control window to the left and MicroShade window to the right.

Figure 6.26 shows the air circulation created by the solar radiation at two cross sections in the two class rooms. Discomfort is normally said to be a problem at air speeds above 0.20 m/s. This air speed is obtained under the ceiling and at an area between the tables in the class room with the Solar control window – the latter being a less occupied zone. However, higher air speeds may actually increase comfort if the air temperature is high.

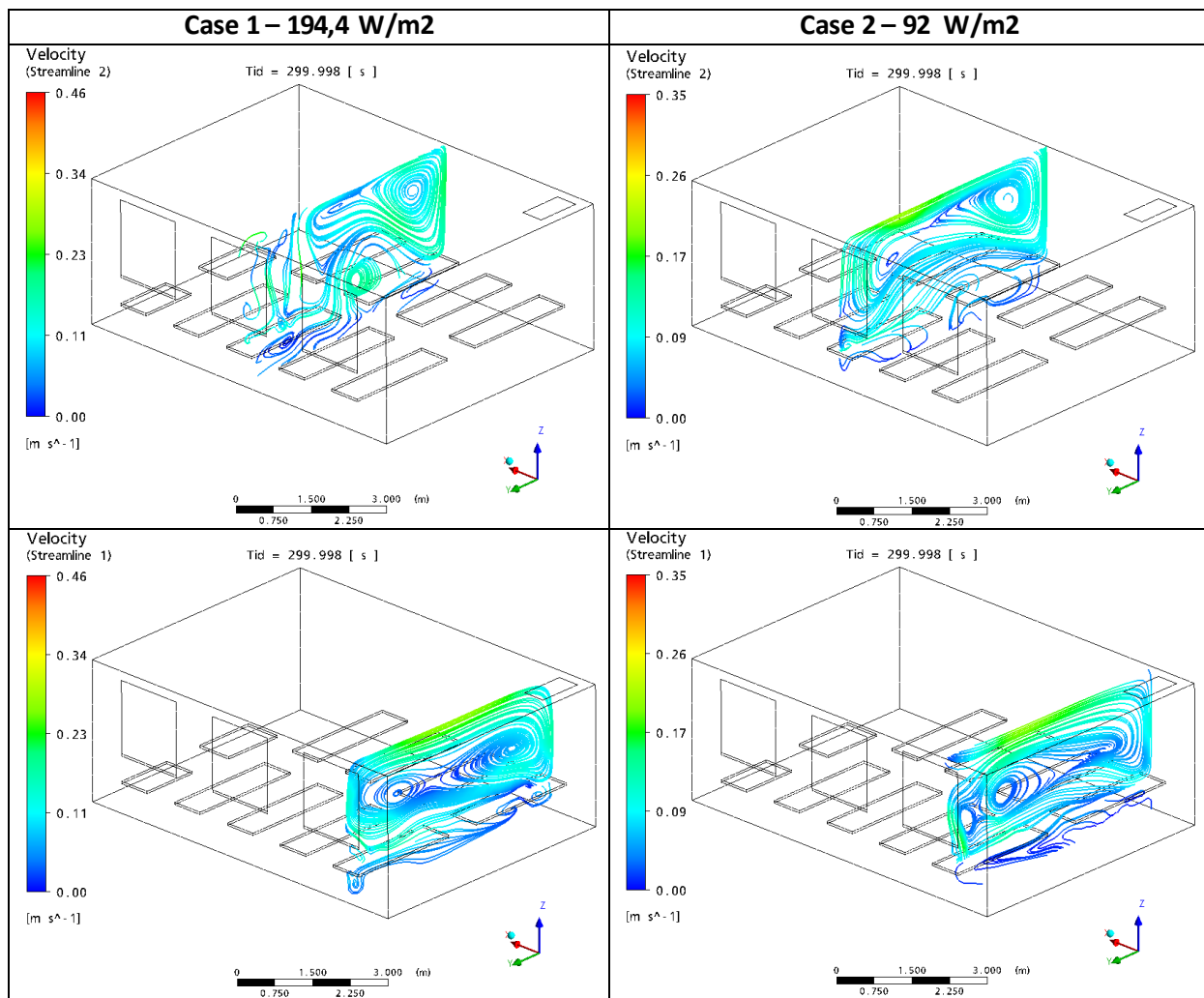


Figure 6.26. The temperature distribution across the room at two locations. Solar control window to the left and MicroShade window to the right.

The CFD simulations are in agreement with the measurements at Malling school – but also in agreement with the esp-r simulations when considering that the mean air temperature is lower than shown in figure 6.23-6.24.

The CFD simulations show that discomfort may arise in the room with the solar control windows due to high temperatures of the tables and just above the tables. The generated air streams seem not to cause problems.

The CFD simulations further show that it is a very complex problem to simulate the influence of solar radiation on the temperature distribution in a room.

6.4. Conclusions

The simulations show what is experienced by the users of the class rooms: that the temperature is lower in the room with MicroShades than in the room with the solar control windows. The simulations also show that the very high temperature differences reported in Appendix C

has more to do with people being hit by a higher radiation level and warmer tables in the room with the solar control windows than due to an elevated mean air temperature.

The investigation contains the first comparison between measurements and simulations for a real life situation. The comparison shows a reasonable agreement but no firm conclusions can be made as the measurements were of a too low quality – both with regard to the number of the measuring points and to the available information on the measurements. It is therefore recommended to perform carefully planned and more detailed measurements in buildings with MicroShade windows in order to gain valuable experience on the behaviour of MicroShade windows. The measurements should both include sensor measurements and questionnaires – the latter to make possible an evaluation of the subjective sensed thermal indoor climate.

7. The effect of solar radiation through windows on thermal comfort

Solar radiation is known to may cause considerable discomfort to people in buildings. This discomfort may be divided in three groups:

- discomfort due to elevation of the mean room temperature in the building
- discomfort due to temperature asymmetry – i.e. because one surface gets warmer than the other surfaces in the room e.g. a warm floor where the solar radiation hits or a warm window due to absorption of solar radiation in the window
- discomfort when people are directly hit by solar radiation

The discomfort of the first group may be reduced using cooling and solar shading devices, while the other two may be reduced using solar shading devices which however may create visual discomfort.

Much research has been carried out on the two first groups while less research has been performed on the relationship between comfort and solar radiation hitting people in buildings. Some studies have however been carried out concerning comfort and solar radiation in cars as the view here is mandatory and people therefore are hit by solar radiation.

The aim of this chapter is to transfer the results from one study concerning cars (Hodder and Parsons, 2006) to buildings. Especially buildings with MicroShades.

(Hodder and Parsons, 2006) investigates the effect of solar radiation hitting a person in the form of different radiation levels, different spectral distributions of the solar radiation at the same radiation level and different glazing exposed to an identical exterior radiation level.

The tests were carried out in two test rooms as shown in figure 7.1. The test persons were exposed to solar radiation on the torso, arms and thighs. But not at the head as cars have measures to protect the head against solar radiation.

Several values were measured and calculated and the test persons filled in questionnaires each five minutes. For a detailed description of the tests see (Hodder and Parsons, 2006). Here will mainly be dealt with PMV (predicted mean votes), AMV (actual mean vote), PPD (predicted percentage of dissatisfied) and APD (actual percentage of dissatisfied). PMV and PPD are calculated using the comfort equation (Fanger, 1982) while AMV and APD are based on the questionnaires filled in by the test persons.

The main result is that:

- when exposed to a solar radiation of 400 W/m² the spectral distribution has no effect on the comfort level. This is in the present paper further extended to conclude that it doesn't matter if the solar radiation is direct or diffuse if the radiation level is identical
- an increase of on scale unit (AMV) per increase of 200 W/m² solar radiation hitting the person
- the type of glass influence the comfort due to the level of transmitted solar radiation

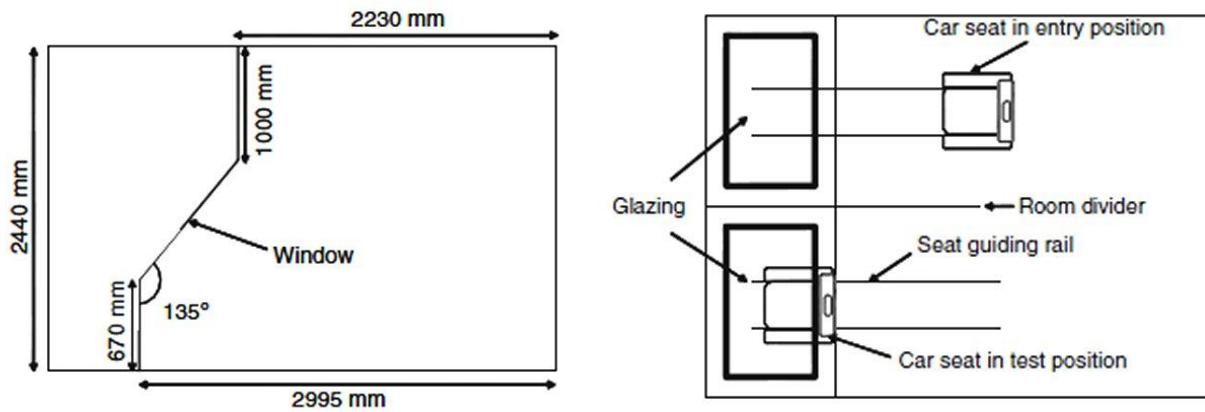


Figure 7.1. The test rooms in (Hodder and Parsons, 2006).

The below table shows the result of the study with different levels of radiation hitting the test persons.

Simulated solar radiation	600 Wm^{-2}	400 Wm^{-2}	200 Wm^{-2}	0 Wm^{-2}
t_a shielded ($^{\circ}\text{C}$)	24.0	23.4	23.4	22.8
t_r ($^{\circ}\text{C}$) derived from t_g	44.0	41.8	37.7	24.2
Air velocity (m/s)	0.1	0.1	0.1	0.1
Relative humidity (%)	49.6	51.0	51.4	48.3
PMV ^a	0.2	0.1	0.1	-0.1
PPD ^a	6.8	8.8	7.1	6.2
PMV ^b	2.8	2.3	1.9	0.2
PPD ^b	96.5	79.8	70.6	12.8
AMV	3.1	1.9	1.1	0.2
APD	100	75	62.5	12.5

t_a air temperature, t_g globe temperature, t_r mean radiant temperature derived from globe temperature (Parsons 2003 p 97), *PMV* predicted mean vote, *PPD* predicted percentage of dissatisfied, *AMV* actual mean vote, *APD* actual percentage dissatisfied

^aPMV calculated with $t_r=t_a$

PMV^b calculated with t_r =measured t_r

Table 7.1. The result from study 1 of (Hodder and Parsons, 2006) with different levels of solar radiation hitting the test persons.

Table 7.1 shows two PMVs and PPDs. The values with “a” are calculated with a mean radiant temperature equal to the air temperature: i.e. without solar radiation. The values with “b” are calculated with the measured mean radiant temperature: i.e. with solar radiation. From table 7.1 it is seen that the persons would have been in thermal comfort if no solar radiation was hitting them – PMV^a is between -0.5 and 0.5.

Figure 7.2 shows a graphical representation of PMV^b and AMV dependent on the solar radiation level hitting the test persons.

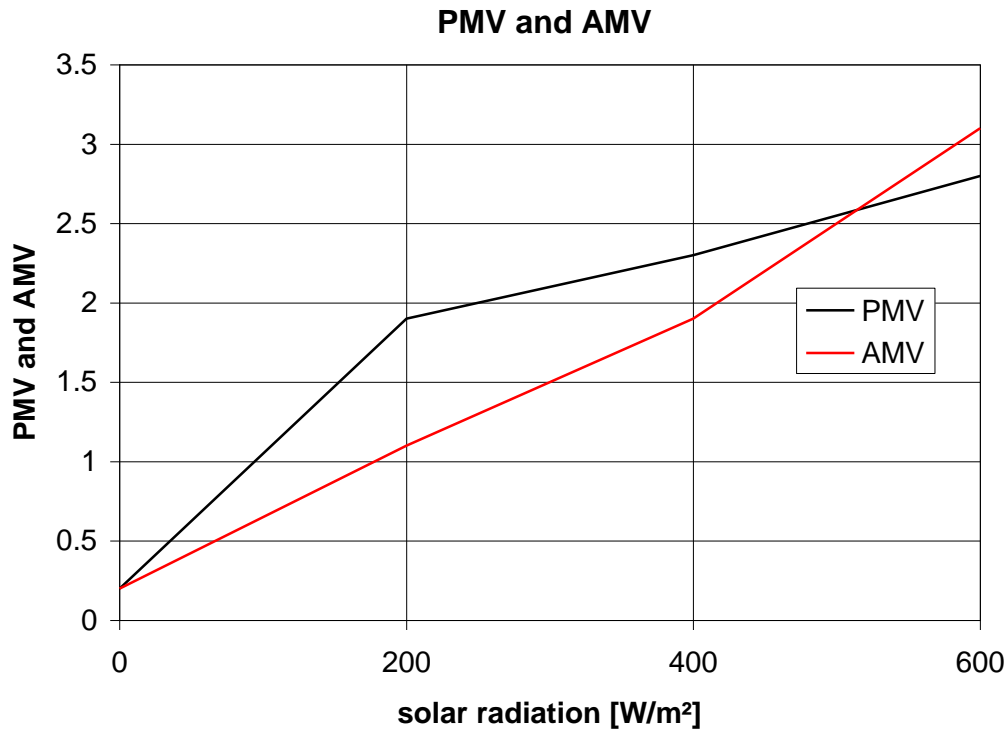


Figure 7.2. PMV^b and AMV dependent on the level of solar radiation.

PMV^b over predicts the discomfort at 200 and 400 W/m². This is in (Hodder and Parsons, 2006) explained with the fact that some people enjoy being hit by the sun up to a certain level after which these persons also start to feel uncomfortable.

Figure 7.3 shows a graphical representation of PPD^b and APD. Although PMV^b and AMV are quite different at 200 and 400 W/m² this is not the case for PPD^b and APD.

The solar transmittance for a normal low-E window is around 0.65 which means that a person behind such a window may be hit by 500-700 W/m² dependent on the time of the year – highest during wintertime. So figure 7.2 and 7.3 are within the range of what may be experienced in buildings.

Figure 7.2 shows that the conclusion in (Hodder and Parsons, 2006) “an increase of on scale unit (AMV) per increase of 200 W/m² solar radiation hitting the person” is based on AMV and not PMV.

7.1. MicroShades

A prototype of MicroShades was investigated in [Jensen, 2008b]. MicroShades decrease the transmittance of direct solar radiation at large solar altitudes (solar heights) as seen in figure 7.4. Figure 7.4 shows the ratio between incoming solar radiation through a PowerShade (MicroShade) window and a solar control (Velfac) window (g-value of 0.37). At low solar heights during the winter (11°) the two windows let in the same amount of solar radiation, while the Velfac window lets twice as much solar radiation in during the summer (solar height: 57°)

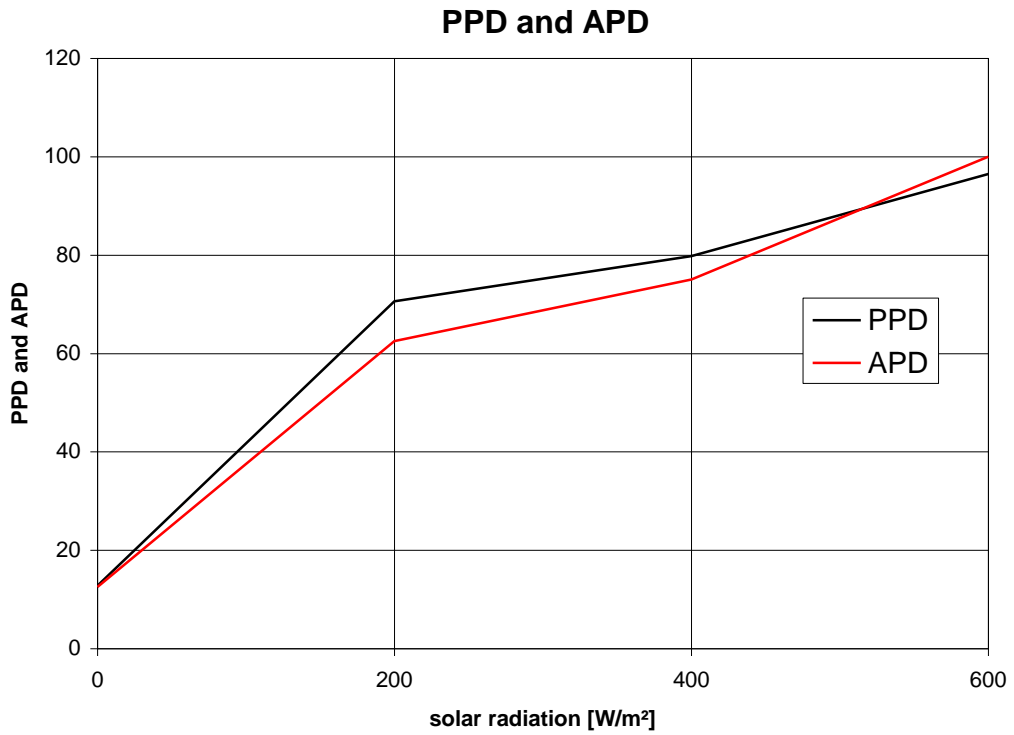


Figure 7.3. PPD^b and APD dependent on the level of solar radiation.

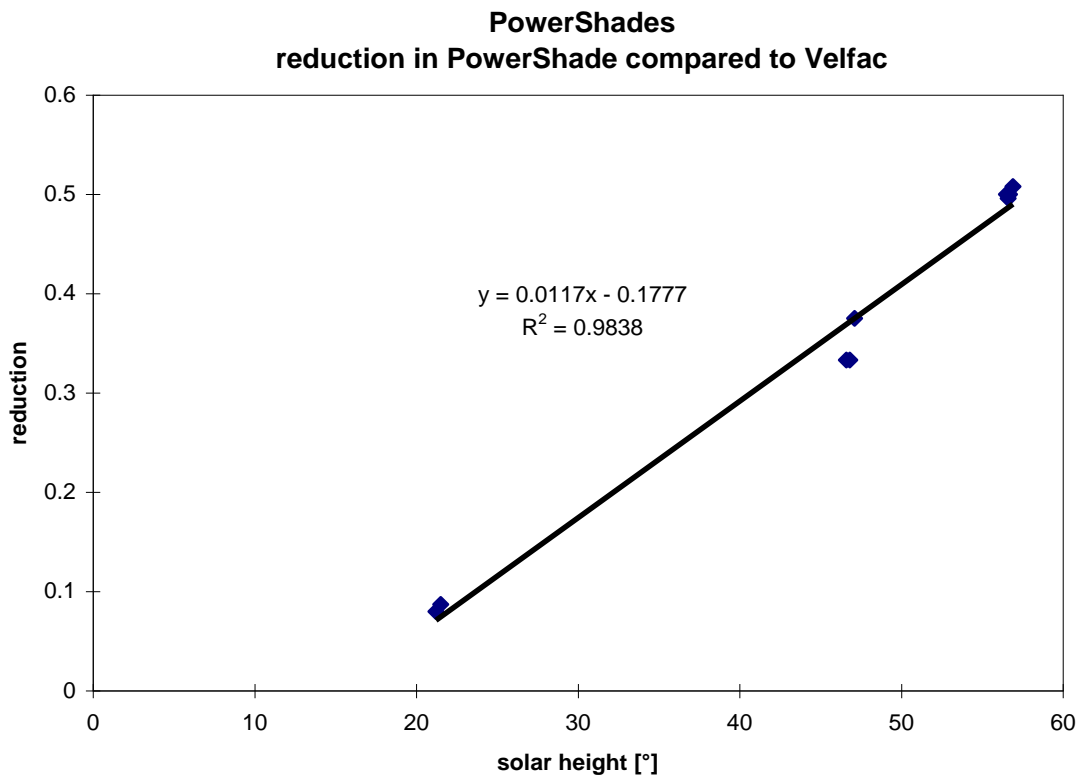


Figure 7.4 Ratio of solar radiation between solar radiation through a MicroShade window and a traditional solar control window at an azimuth of 0°.

The measured transmitted solar radiation at noon was:

	solar control window W/m ²	MicroShade window W/m ²
Winter	280	280
Summer	170	85

The increase in AMV (PMV) – the numbers above divided with 200 – is then:

	solar control window	MicroShade window
Winter	1.4	1.4
Summer	0.85	0.43

Figure 7.5 shows the relationship between PMV and PPD. The equation for the curve in figure 7.5 is:

$$PPD = 100 - 95 * \exp(- (0.03353 * PMV^4 + 0.2179 * PMV^2))$$

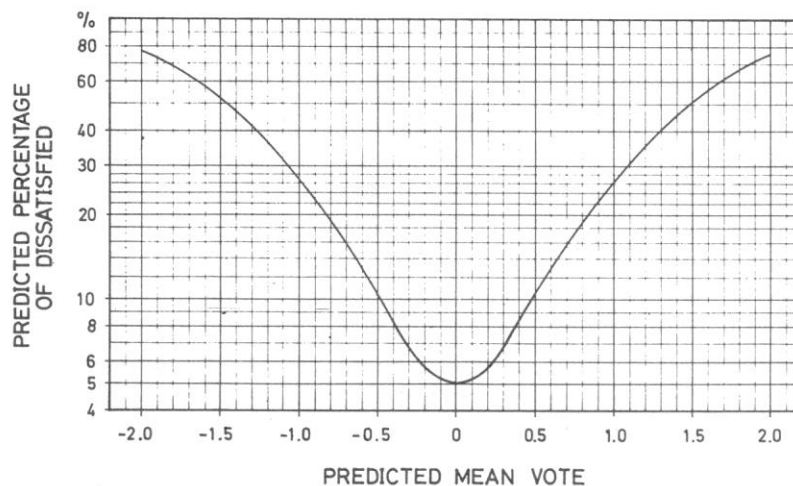


Figure 7.5. The relationship between PPD and PMV.

If perfect comfort in the room – i.e. PMV is 0 - the solar radiation will give 45% unsatisfied if hit by the solar radiation during the winter for both window types. During the summer a room with MicroShades will be inside the comfort range of ± 0.5 , while 20% will be dissatisfied in a room with the solar control window if hit by the sun.

7.2. Experiments in the two test rooms

Based on the above it was decided to design an experiment to verify the above findings.

The two test rooms were equipped with globe temperature sensors as shown in figure 7.6. The globe temperature sensors had a mat black globe with a standard diameter of 150 mm. The globes were made of thin plastic in order to increase the thermal response to variation in the solar radiation level.



Figure 7.6. Globe temperature sensors in test room B.

Based on the globe temperature and the room temperature it is possible to determine the mean radiation temperature which is necessary to know in order to calculate the comfort. The mean radiation temperature may be calculated using the below equation if the air speed along the globe is low which is assumed as the rooms are sealed:

$$t_r = ((t_g + 273)^4 + 0.4 \cdot 10^8 \cdot |t_g - t_a|^{0.25} \cdot (t_g - t_a))^{0.25} - 273^\circ\text{C} \quad [\text{Olesen, 1996}] \quad [1]$$

where: t_g is the globe temperature [$^\circ\text{C}$]
 t_a is the room temperature [$^\circ\text{C}$]

Two globe temperature sensors were located in each room – both in the middle compared to the not open able window (see figure 7.6). One 380 mm from the façade in a height so that solar radiation did hit the globe at an azimuth of 0° of the sun. The other globe was located 2 m from the façade in order to prevent it from being hit by the sun.

The measurements demanded clear sky conditions but this turned out to be difficult to obtain. Only 8 days of measurements are included in the investigations: 6 days in the period March 25-April 15 (in the following called spring) and June 3rd and 6th (in the following called summer). During spring the original Velfac sun 1/clear with solar control film [Jensen, 2008a] was still mounted in test room B. This window was in the beginning of May replaced with a traditional low-E window without solar control film in order to allow more solar radiation into the room. However, unfortunately clear sky conditions were first obtained a month later resulting in a less difference in incoming solar radiation between the two periods than hoped.

The test rooms do not have air conditions so it is not possible to control the air temperature and further the air temperature continued to incline after the solar radiation had peaked. So the measuring conditions were not stable. This is illustrated in table 7.2 containing the measurements from spring where for each day are shown two sets of measurements: one when the room temperature (troom) peaked and one when the incoming solar radiation (radiation) peaked. The mean radiation temperature (Tr) was calculated using equation [1]. The solar radiation has in table 7,2 not been corrected according to the findings in chapter 4.

Room A					Room B				
	Troom	Tr	radiation	ΔT		Troom	Tr	radiation	ΔT
day 84	26.3	33.27	170	6.97	day 84	27.84	38.61	244	10.77
	24.42	31.56	187	7.14		25.36	37.01	223	11.65
day 93	24.88	31.76	158	6.88	day 93	26.76	39.83	230	13.07
	23.79	31.17	184	7.38		26.13	39.28	254	13.15
day 97	24.86	31.77	156	6.91	day 97	26.08	38.65	232	12.57
	24.18	30.75	169	6.57		25.49	37.91	239	12.42
day 100	24.76	31.83	129	7.07	day 100	26.53	40.16	206	13.63
	23.55	30.34	163	6.79		26.27	39.68	243	13.41
day 104	28.61	35.51	148	6.9	day 104	30	43.34	227	13.34
	27.1	33.37	160	6.27		28.48	41.94	236	13.46
day 105	28.49	35.27	145	6.78	day 105	30.3	43.3	218	13
	27.42	34.02	162	6.6		28.94	42.12	241	13.18

Table 7.2. Measurements from spring.

If the values in table 7.2 are used in Fangers equation where the clo (level of clothing) and met (metabolism – ie level of activity) were adjusted in order to obtain thermal comfort at the measured room temperature and Tr equal to the room temperature a very scattered result is obtained as shown in figure 7.7.

However, the difference between the mean radiation temperature and the room temperature is very stable not depending on the air temperature as seen in figure 7.8. This has been utilized in order to compare with the findings in [Hodder, 2006]:

- room temperature 23.4°C from table 7.1
- met was kept at 1.2 while clo adjusted to create thermal comfort at 23.4°C – clo = 0.69
- mean radiant temperature: 23.4°C + the difference between the mean radiatnt temperature and the room temperature from the measurements

Figure 7.9 shows the result from these calculations. The 6 days in spring was averaged into one mean day which also was the case for the three days in summer. There are two values for each season/room: one for max incoming solar radiation and one for max room temperature as discussed earlier. The values in figure 7.9 have been corrected with respect to the solar radiation according to the findings in chapter 4. However, it has not been considered if the globe in room A received lees solar radiation through the MicroShade window as measured – see section 4.1.1. But an uncertainty of up to $\pm 10\%$ will not effect the following conclusions.

All values except the summer values from room B fall within the measurements/calculations by [Hodder, 2006]. However, while the values in [Hodder, 2006] shows a more or less linear dependency the values from the present investigation shows more a second order dependency on the incoming solar radiation – meaning that the discomfort at large radiation level is higher in the present study than in [Hodder, 2006]. This goes also for the PPD as seen in figure 7.10.

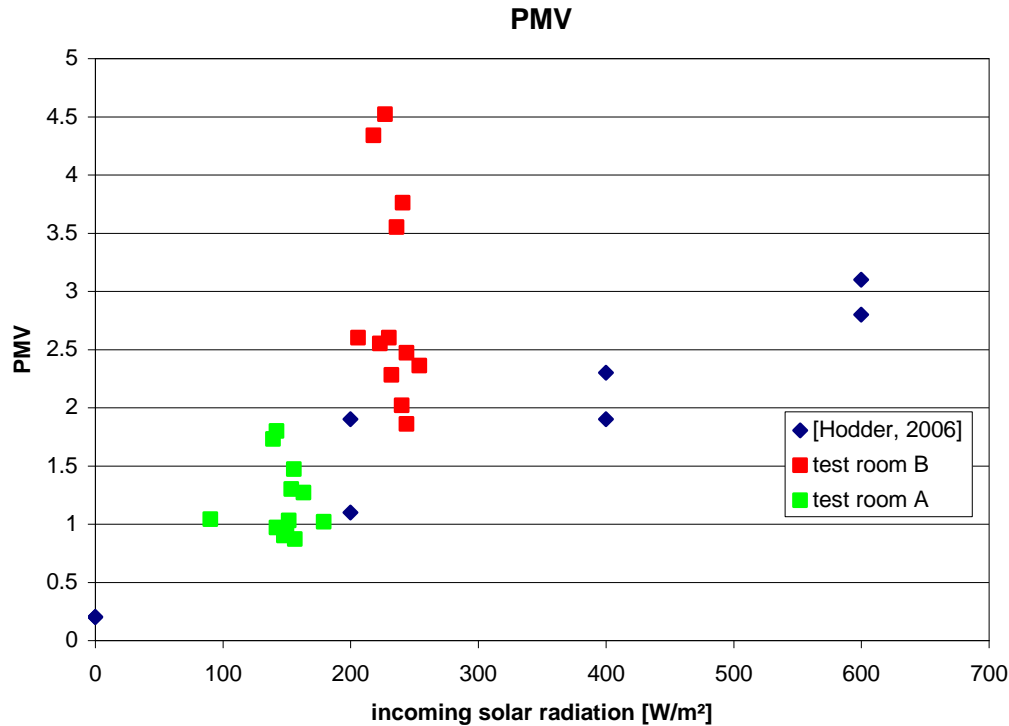


Figure 7.7. PMV when the values in table 7.2 are put in directly in Fangers equation.

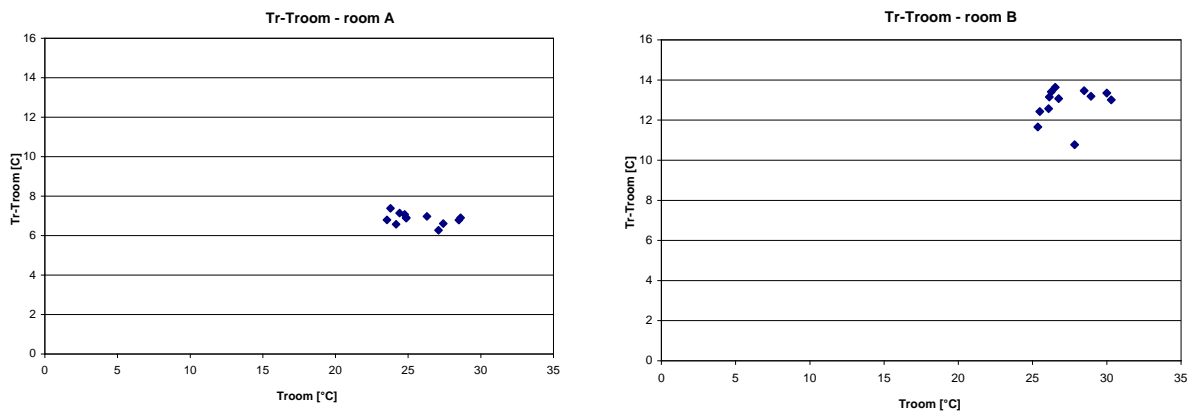


Figure 7.8. Tr minus Troom for the values in table 7.2.

The measurements from the globe temperature sensors at the back of the rooms showed that if a person is in thermal comfort the solar radiation through the window will not create discomfort while if a person is not in comfort (too hot) the radiation through the window will only increase the discomfort slightly.

This means that the radiation not surprisingly only/mainly influences the comfort level if the person is hit by the radiation.

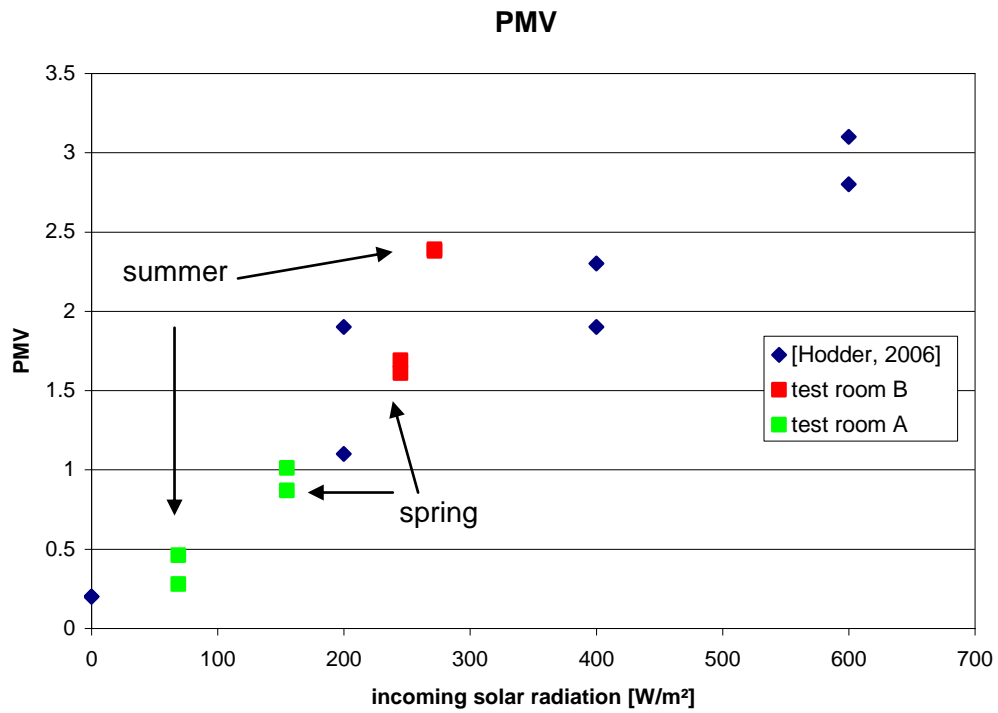


Figure 7.9. The PMV's dependency on the incoming solar radiation.

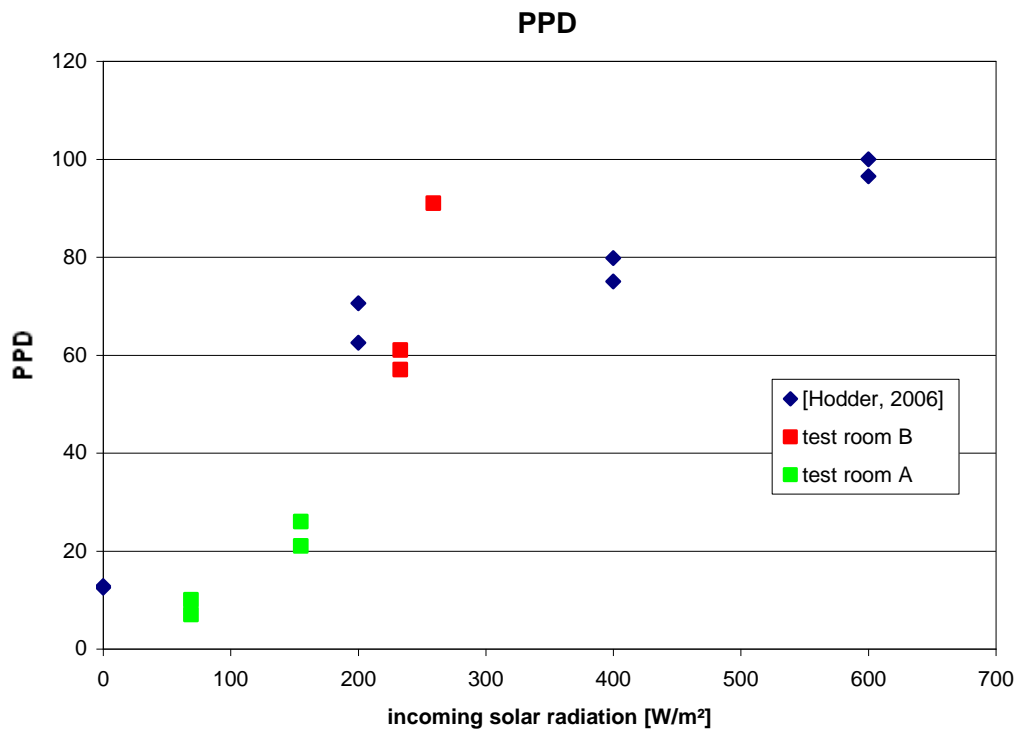


Figure 7.10. The PPD's dependency on the incoming solar radiation.

7.3. Conclusions

The result of the experiment in the two test rooms is in agreement with [Hodder, 2006] at incoming radiation levels below 230 W/m²: an increase of on scale unit (PMV) per increase of 200 W/m² solar radiation hitting the person. Above 230 W/m² the experiment indicates a larger influence on the PMV than shown in [Hodder, 2006], however, further experiments is necessary to verify this – especially experiments at larger levels of incoming radiation than obtained in the here reported experiment.

The experiments should also include test persons as [Hodder, 2006] concludes that many people likes moderate levels of incoming radiation – ie the calculated PMV is here higher than the voted AMV.

Until research has shown otherwise one may use the following equation:

$$\text{PMV(AMV)} = I/200 \quad [2]$$

where: I ist the incoming radiation through the window hitting a person [W/m²]
the person would have been in comfort without being hit by the radiation

The comfort level of persons not being hit by the radiation is not influenced by the radiation.

8. Daylight measurements

Three windows has been investigated in the two test rooms:

Room A: MicroShade window with MicroShade type MS-A

Room B: Until May 2010: the original Velfac sun 1/clear with solar control coating
From May 2010: a low-E window without solar control coating.

Light transmittance: Velfac: 0.67
Low_E window: 0.8

Figure 8.1 shows measured daylight factors for the three windows. Figure 8.1 shows a more uniform daylight distribution through the room at a lower level than the two other windows. This is in agreement with the findings in [Jensen, 2008b] – see Appendix E.

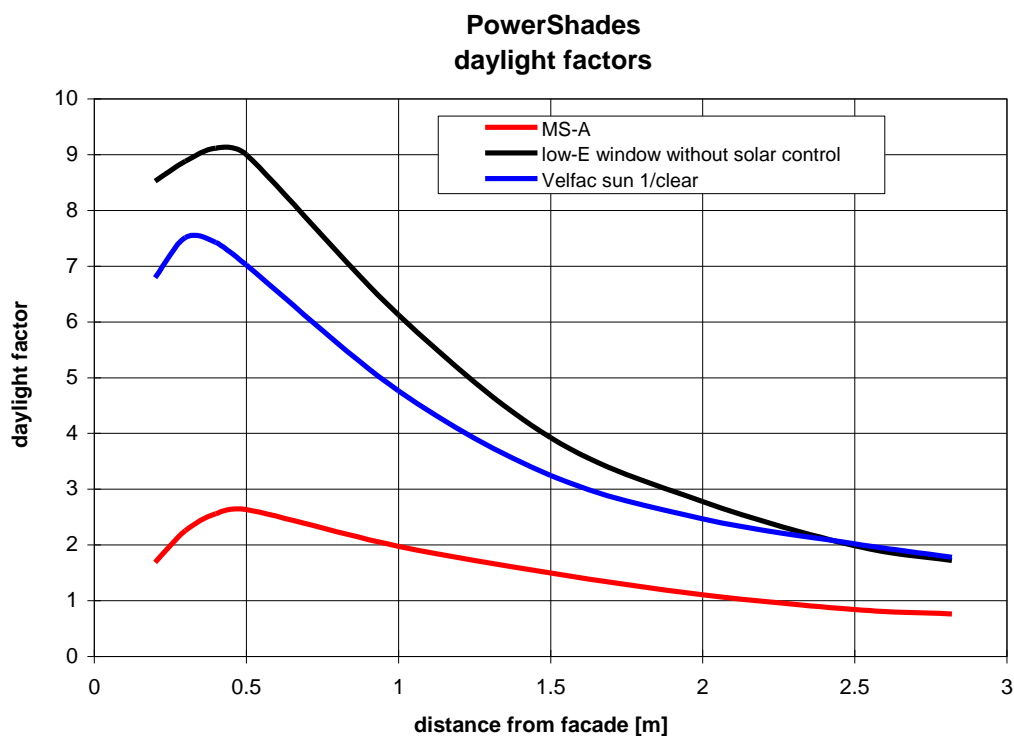


Figure 8.1. Daylight factors for the three windows investigated in the present project.

Figure 8.1 shows daylight factors measured at as close a possible to uniform overcast conditions. However, the figure does not tell about the daylight conditions at other weather conditions. In order to investigate this figure 8.2 has been generated based on measurements from November 10, 2009-July 7, 2010.

As no external Lux measurements was available figure 8.2 shows the ratio between the Lux measured in the two rooms: Lux room A divided with Lux room B. The Lux meters were located at a height of 0.7 m in the middle of the rooms.

Only values at a solar azimuth of 0° are included in figure 8.2 in order to avoid any influence of the fact that the test rooms are parallel reversed – see [Jensen, 2008a].

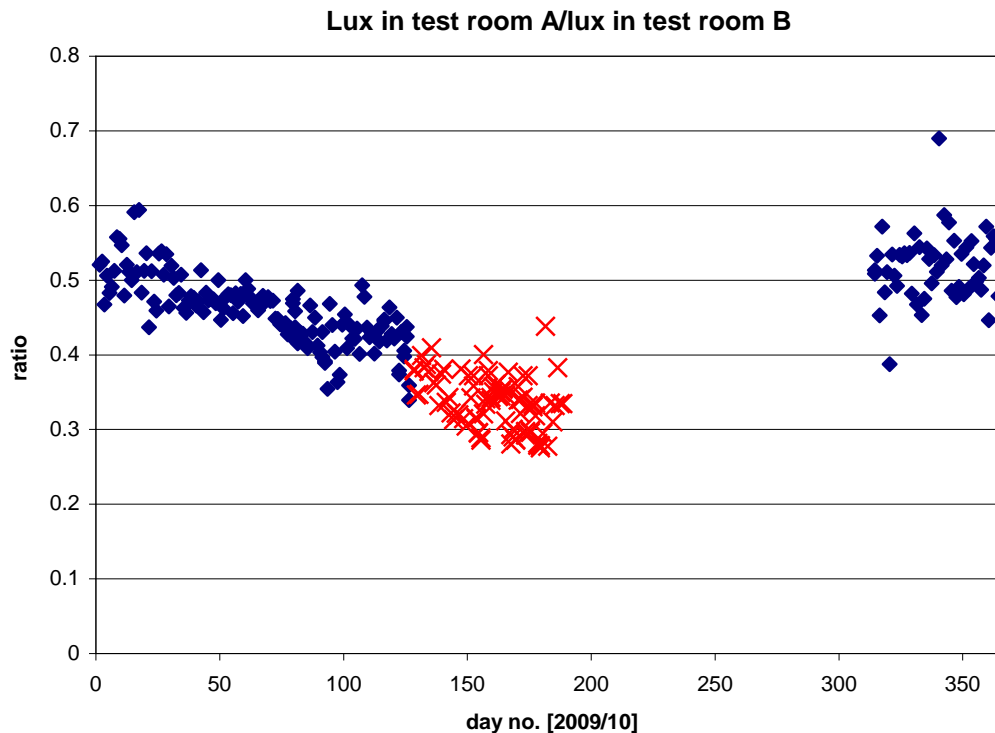


Figure 8.2. The ration between the Lux in room A and room B. Blue rhombs are with the Velfac window mounted in room B, while red crosses is with the low-E window mounted in room B.

Figure 8.2. shows a decreasing ration when going from winter toward summer and a increasing ration when going from summer towards winter – ie decreasing ratio with increasing solar heights. This was expected for sunny conditions as the MicroShades cut off more direct solar radiation at high solar angles than at low solar angles. But figure 8.2 includes both sunny and overcast conditions – this is investigated in figure 8.3. Figure 8.3 shows the ratio - for the situation with the low-E window in room B - dependent on the solar radiation hitting the façade. Figure 8.3 shows that the ratio decreases with increasing solar radiation on the façade – which based on theory also should be the case. At low solar radiation the ratio is around 0,375 which is identical to the ration found in figure 8.1 at 1.5 m which was the location of the Lux meters. The scattering in figure 8.2 is thus caused by different levels of solar radiation.

Figure 8.4 shows regression lines for the first half year of 2010 for the two cased of windows in room B. The slope of the regression lines is identical for the two cases: -0.0009 (will be $+0.009$ for the second half of the year – see figure 8.1), while the starting point is different due to the different light transmittance of the two windows in room B.

Figure 8.5 shows the slope of the solar ratio from [Jensen, 2008a] where room B was equipped with the Velfac window and room A with a MicroShade window with MicroShades of the type prototype 1 (with a 12 % higher openings area than MS-A but a glass more with a transmittance of 0.89 – see section 10.2) with similar daylight factors as seen when comparing figure 8.1 with figure 3.1 in Appendix E.

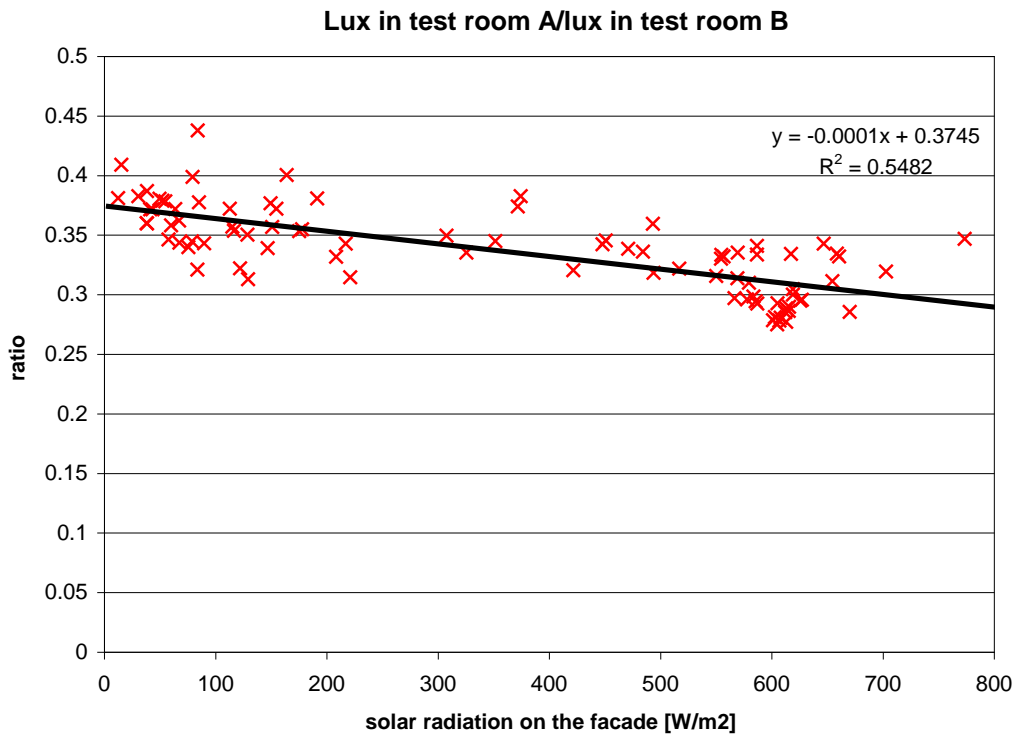


Figure 8.3. The Lux ration with the low-E window in room B dependent on the solar radiation on the façade.

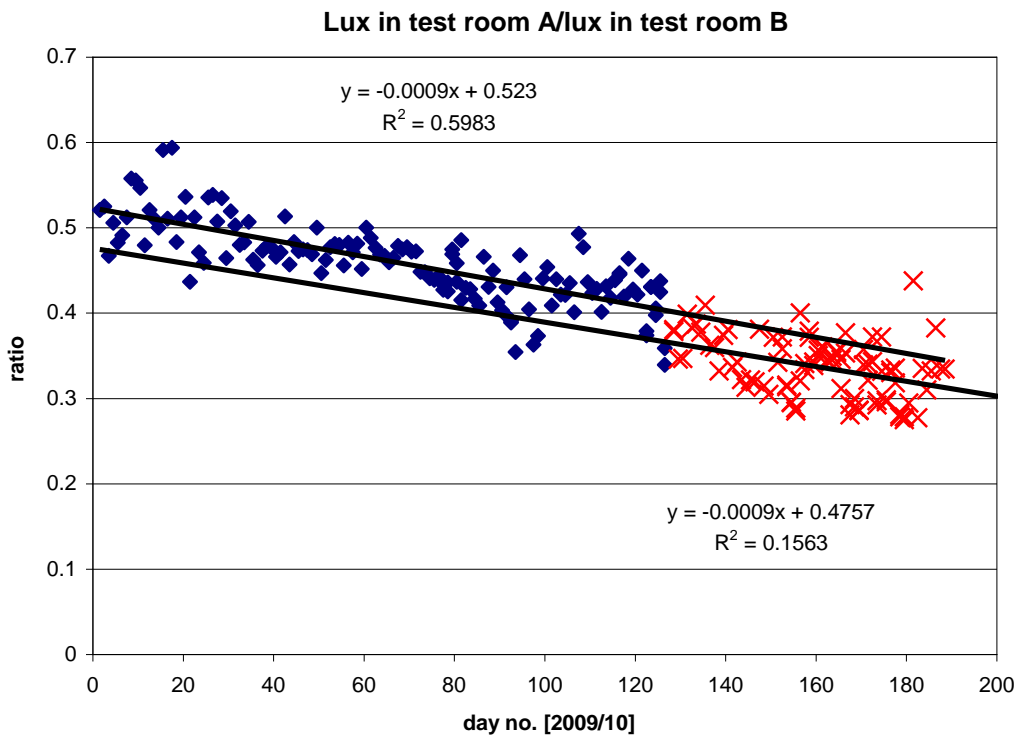


Figure 8.4. Regression lines for the Lux ratio for the two different windows in room B.

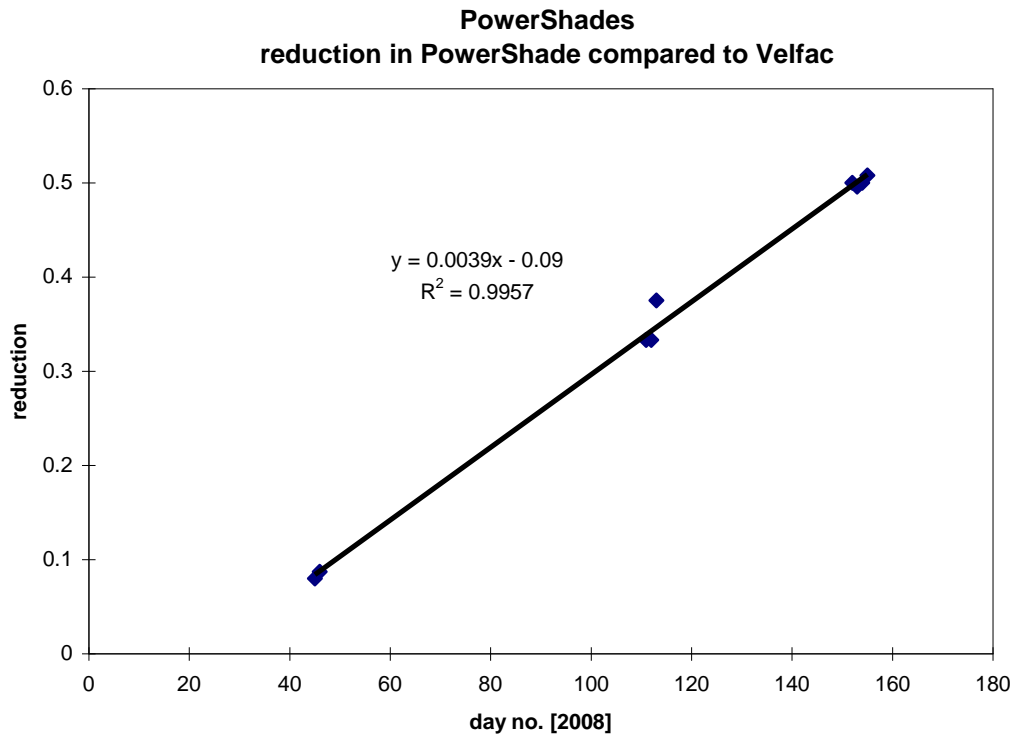


Figure 8.5. Solar ratio for MicroShade type prototype 1 in room A and the Velfac window in room B.

The trend in figure 8.5 is 0.0039 – ie about 4 times larger than for the Lux ratio. This means that the MicroShades influence 4 times more the solar radiation than the daylight in the middle of the room not hit by direct sunlight. This is positive as this may reduce the number of hours where electric lightning is necessary while still reducing the overheating considerably.

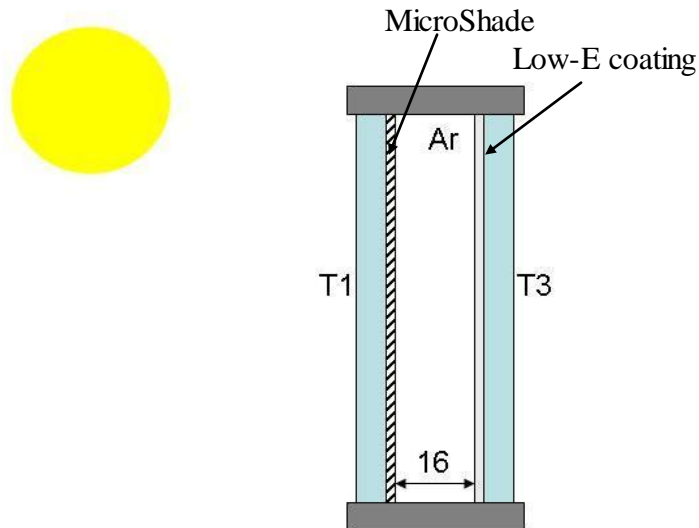
The daylight will not be investigated more in the present context but MicroShades are part of an ongoing investigation at the Danish Building Research Institute where the effect of solar cells in windows on visual comfort is investigated. MicroShades are one of the solutions being investigated both utilizing measurements and subject judgement from test persons. This investigation is part of the project: Thi-Fi-Tech, project no. 2008-1-0033 also financed Energinet.dk. A report of the investigations by the Building Research Institute is expected late 2010/early 2011.

9. Temperatures in windows with MicroShades

The temperature of the glass next to MicroShades has in this chapter been investigated for several different constructions.

9.1. MicroShade low-E window

This construction is a MicroShade low-E window with the MicroShades located behind the outer glass of the window - see figure 9.1.



PU = Planilux + Ultratherm

Figure 9.1. MicroShade low-E window with the MicroShade located behind the outer glass.

The MicroShade 101110-PU optical matrix has been used for the calculations – see figure 9.2. The resistance of the air gap is $0.743 \text{ m}^2\text{K/W}$.

Figure 9.3 shows the temperature of the outer glass in the construction of figure 9.1 over the year for Danish weather conditions. Figure 9.4 shows the same temperature set but as frequency curves.

The two figures show that the max temperature of the glass with the MicroShades reaches a max temperature just above 60°C .

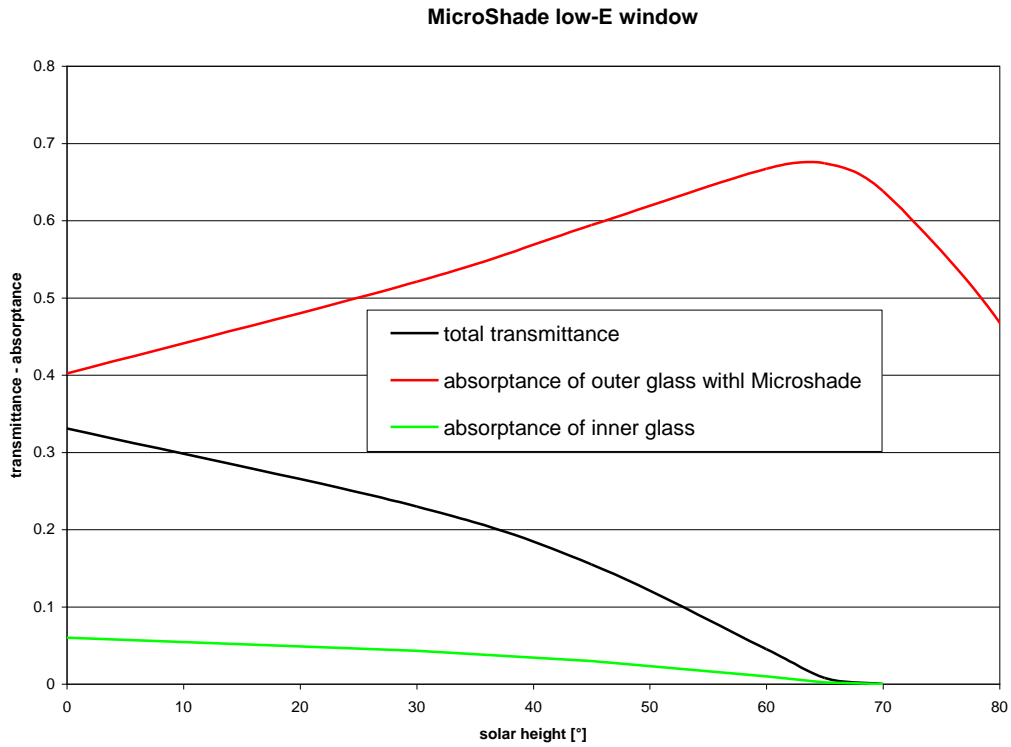


Figure 9.2. Optical properties of the MicroShade low-E window for an azimuth of 0° (ie. the horizontal incidence angle is 0°) for different solar heights (ie. vertical incidence angles).

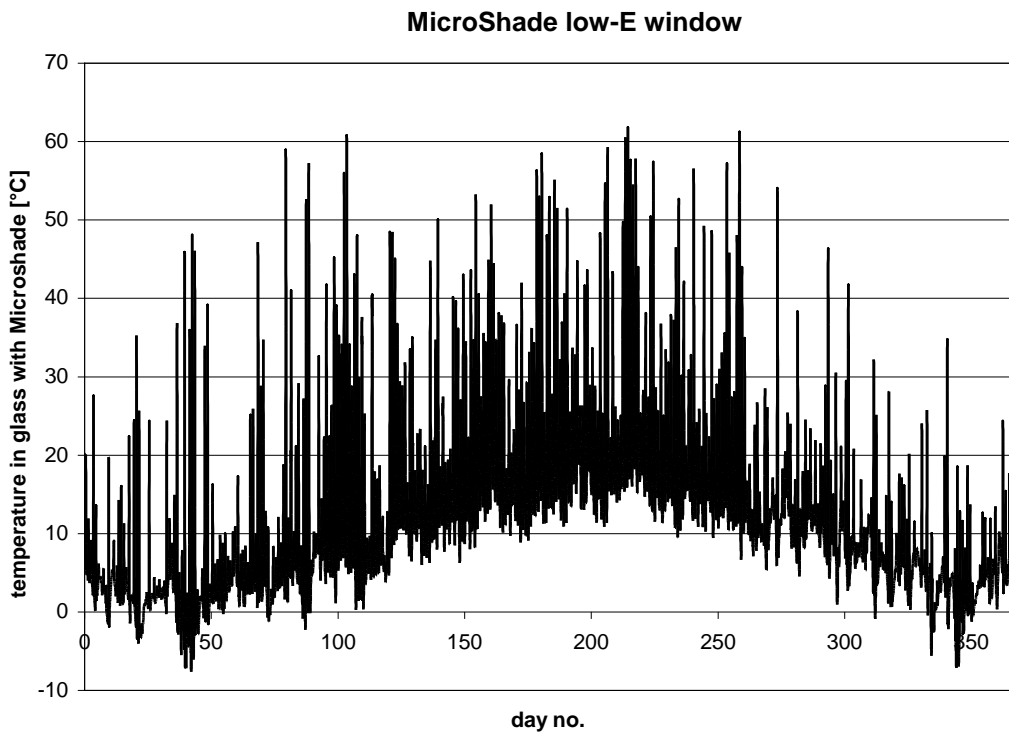


Figure 9.3. Temperatures over the year in the outer glass of the construction in figure 9.1.

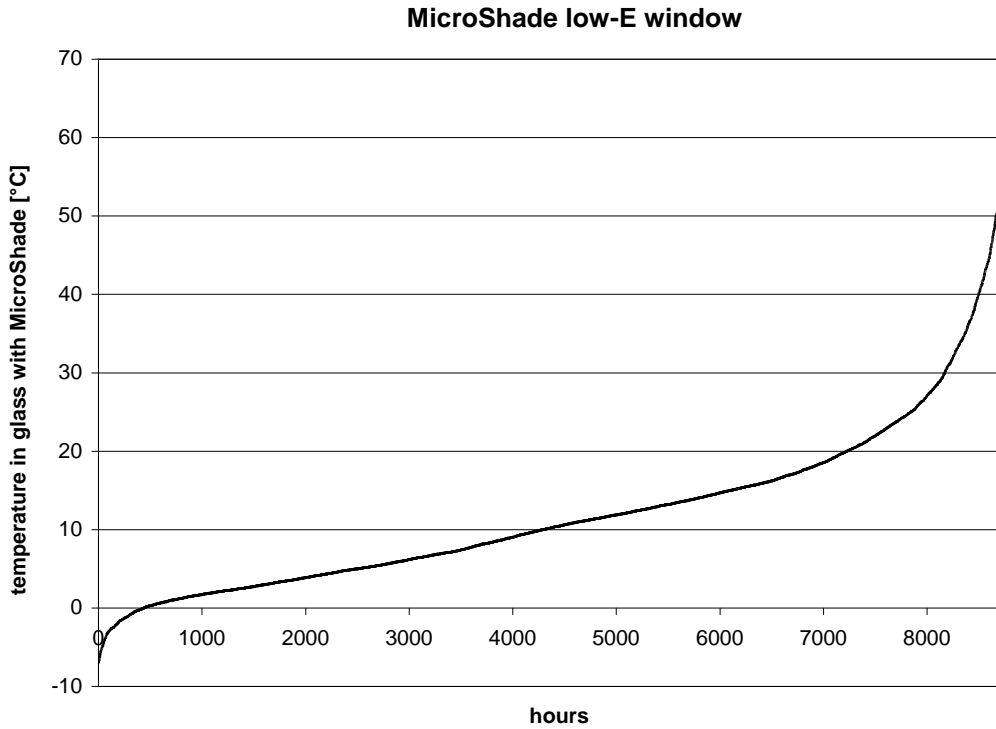


Figure 9.4. Temperatures in the outer glass of the construction in figure 9.1 as frequency curve.

9.2. MicroShade low-E window with a single layer of glass in front

In this construction the MicroShade low-E window is located behind a single glass as seen in figure 9.5.

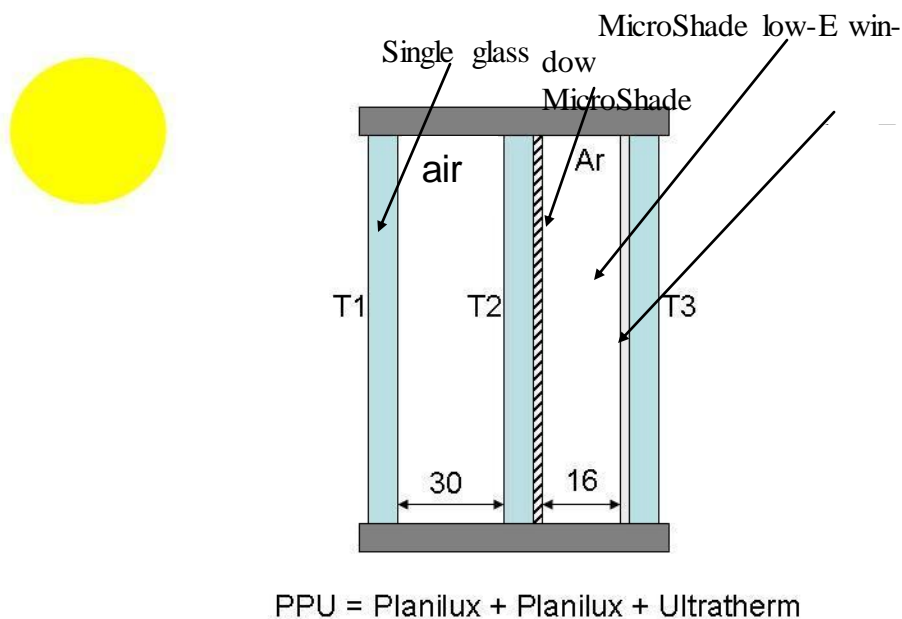


Figure 9.5. MicroShade low-E window located behind a single glass.

The spacing between the glazing is: single glass – MicroShade low-E window: 30 mm
between glasses in the MicroShade window: 16 mm

The thickness is 4 mm for all glasses.

Two different constructions have been investigated – with different thermal resistance in the air gap between the glasses:

- 1: the thermal resistance: single glass – MicroShade low-E window: 0.198 m²K/W
between glasses in the MicroShade window: 0.719 m²K/W
- 2: the thermal resistance: single glass – MicroShade low-E window: 0.268 m²K/W
between glasses in the MicroShade window: 0.808 m²K/W

The MicroShade 080610-PPU optical matrix has been used for the calculations – see figure 9.6.

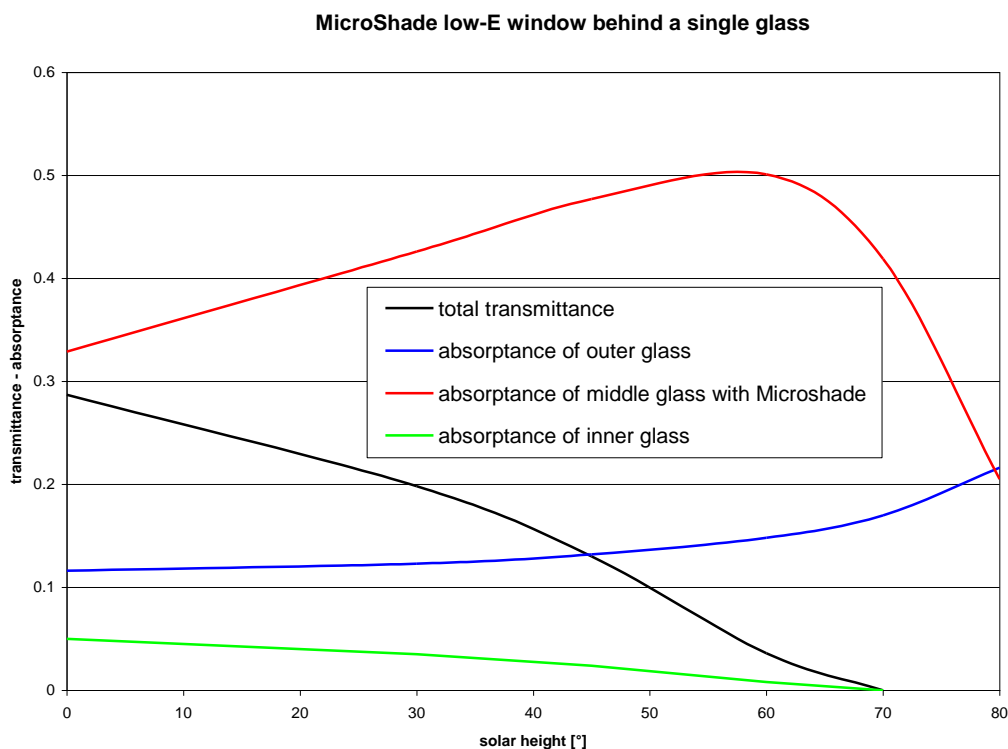


Figure 9.6. The optical properties of the MicroShade low-E window behind a single glass for an azimuth of 0° (ie. the horizontal incidence angle is 0°) for different solar heights (ie. vertical incidence angles).

Figures 9.7 and 9.8 show the temperature of the middle glass in the construction of figure 9.5 over the year for Danish weather conditions. Figures 9.9-10 show the same temperature sets but as frequency curves.

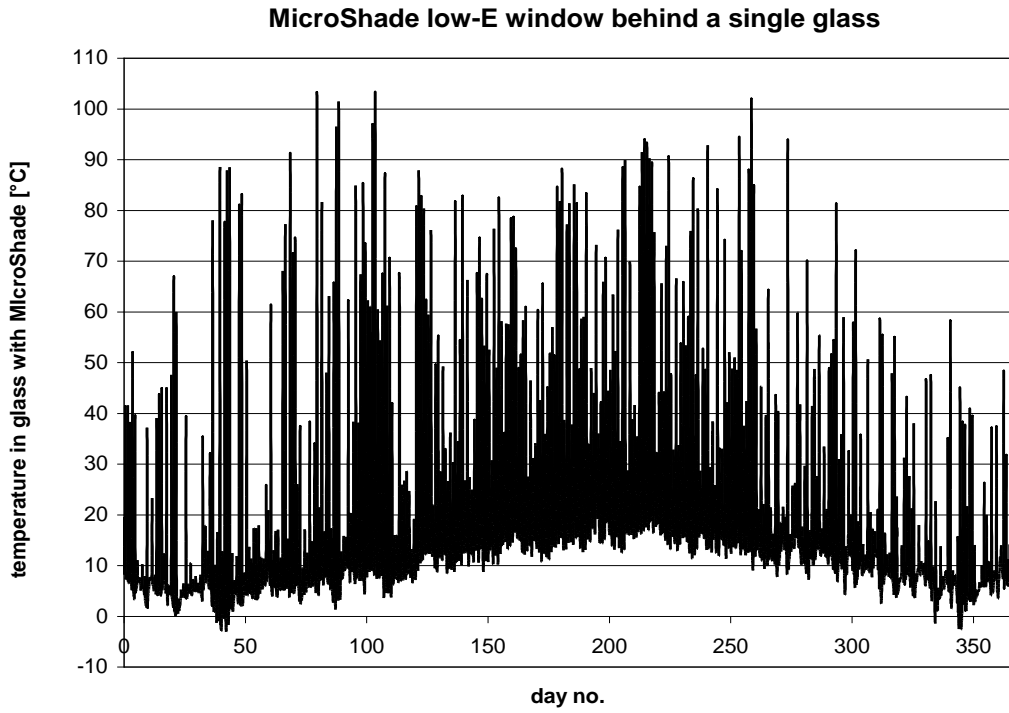


Figure 9.7. Temperatures over the year in the middle glass of the construction in figure 9.5 for construction 1.

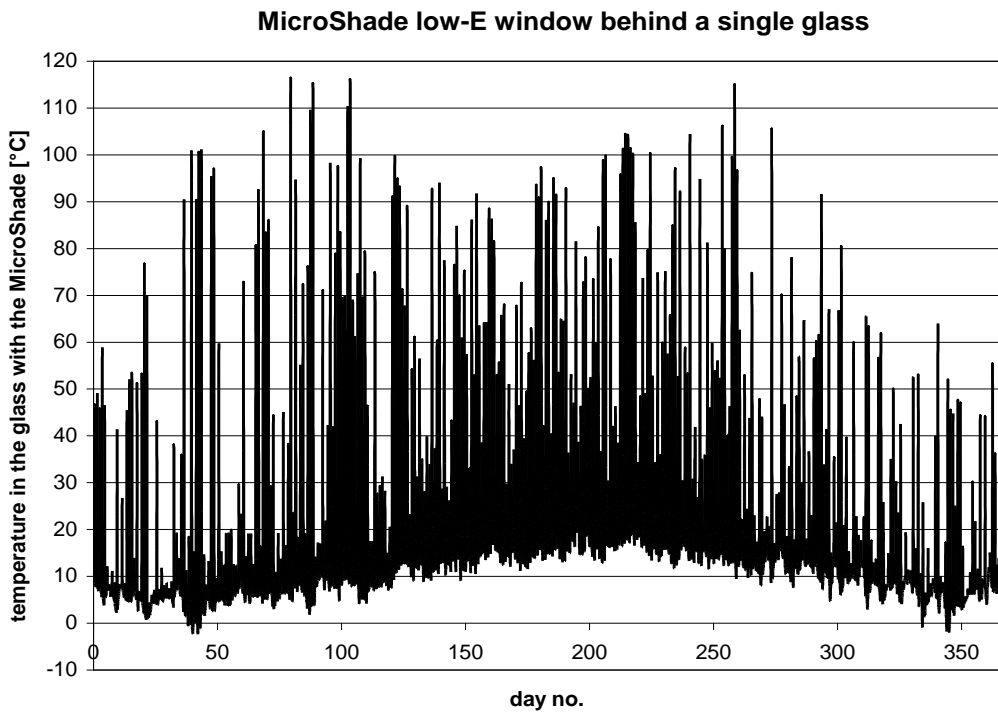


Figure 9.8. Temperatures over the year in the middle glass of the construction in figure 9.5 for construction 2.

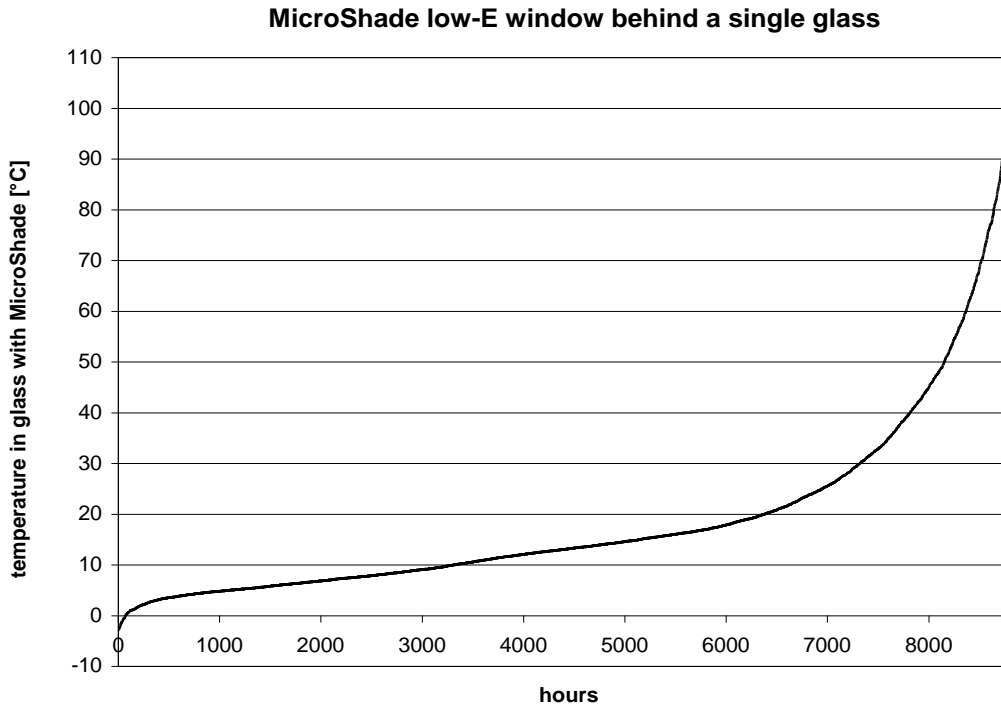


Figure 9.9. Temperatures in the middle glass of the construction in figure 9.5 for construction 1 as a frequency curve.

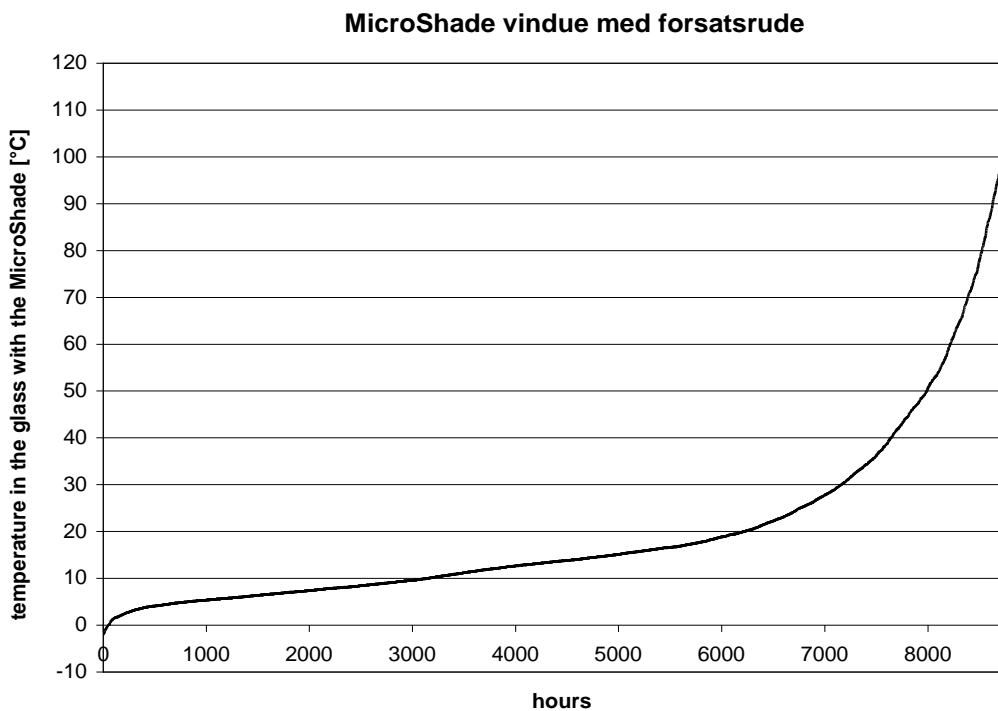


Figure 9.10. Temperatures in the middle glass of the construction in figure 9.5 for construction 2 as a frequency curve.

Figures 9.7 and 9.9 shows a max temperature of approx. 103°C, which occurs in spring (March-April) and late summer (September) for construction 1. The max temperature in con-

struction 2 is higher due to the lower heat transfer from the middle glass to both ambient and the room. The max temperature for construction 2 is approx. 117 (figures 9.8 and 9.10) and occurs at the same dates as for construction 1.

9.3. 3 pane low-E MicroShade window

In this construction the MicroShade is located behind the outer glass of a triple glazed low-E window as seen in figure 9.11.

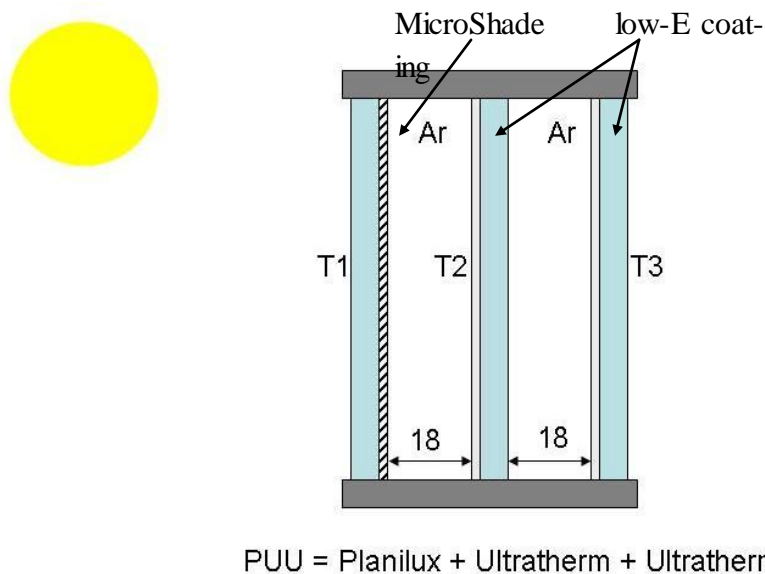


Figure 9.11. Triple glazed low-E window with MicroShade behind the outer glass.

The spacing between the glazing is for both spaces 18 mm and the glasses are all 4 mm thick.

The thermal resistance is: outer space: 0.892 m²K/W
inner space: 0.969 m²K/W

The MicroShade 110610-PUU optical matrix has been used for the calculations – see figure 9.12.

Figure 9.13 shows the temperature of outer glass in the construction of figure 9.11 over the year for Danish weather conditions. Figure 14 shows the same temperature set but as frequency curves. The two curves show a max temperature of approx. 64°C. The higher max temperature compared to the MicroShade low-E window is due to the lower heat transfer to the room behind the window.

Figures 9.15-16 shows the temperatures in the middle glass, where the highest temperature occurs.

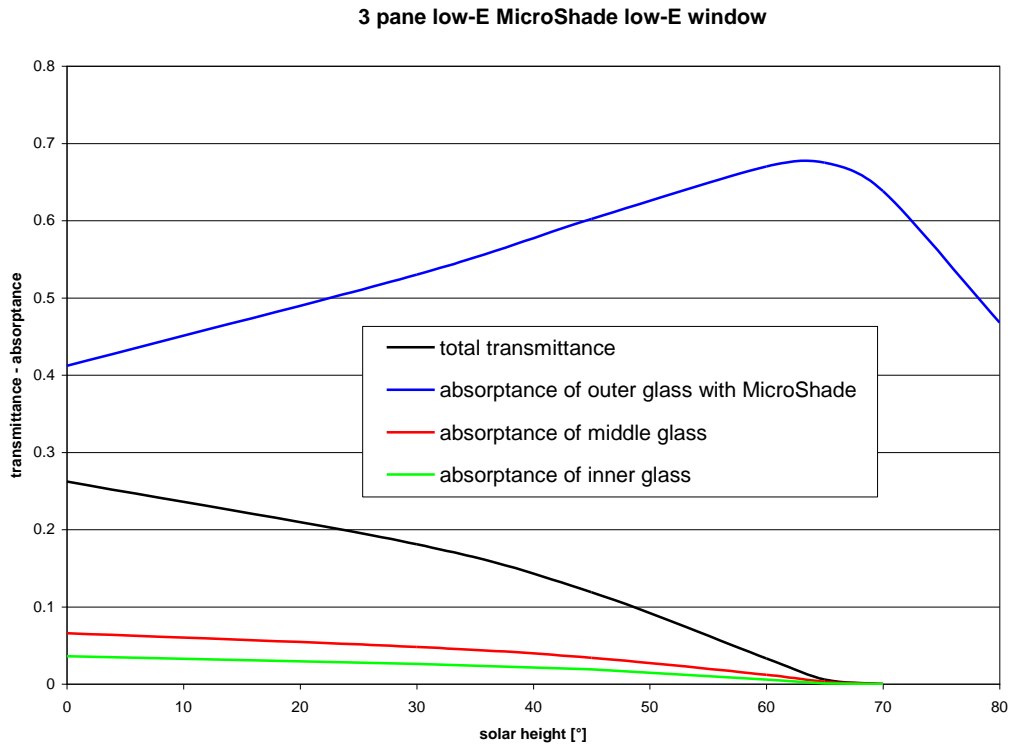


Figure 9.12. Optical properties for 3 pane low-E MicroShade window for an azimuth of 0° (ie. the horizontal incidence angle is 0°) for different solar heights (ie. vertical incidence angles).

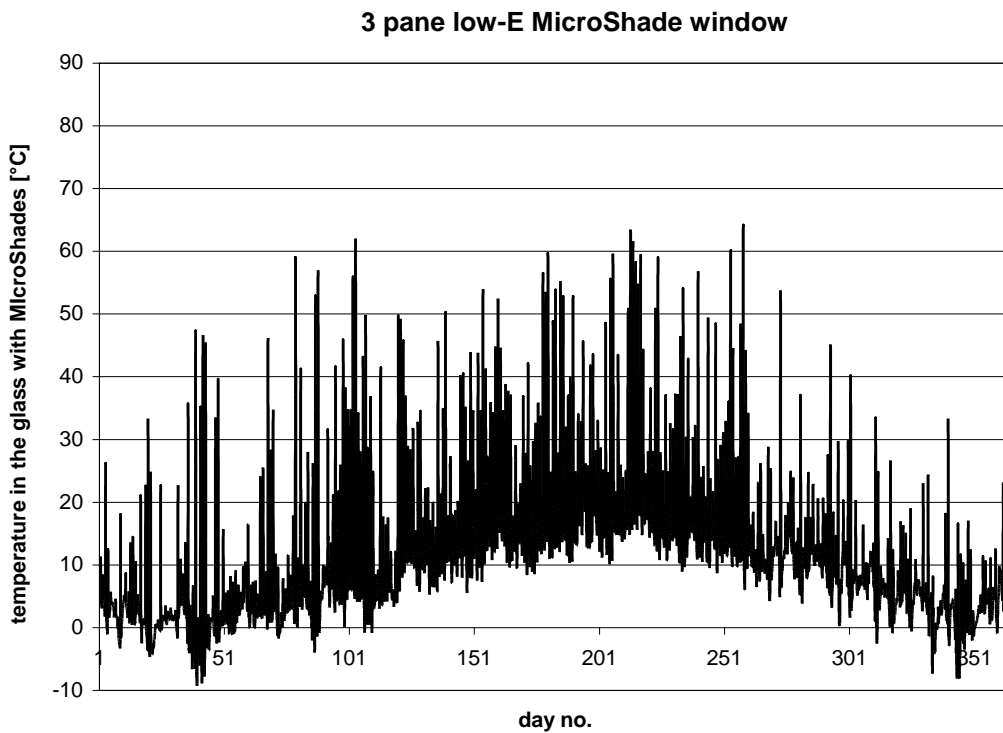


Figure 9.13. Temperatures over the year in the outer glass of the construction in figure 9.11.

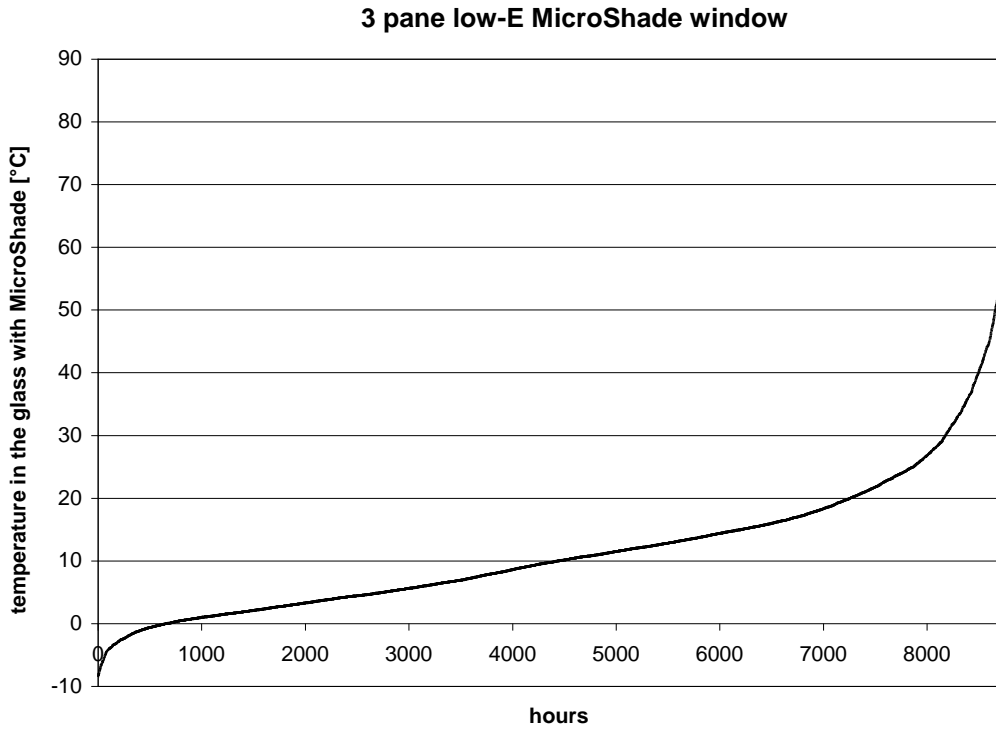


Figure 9.14. Temperatures in the outer glass of the construction in figure 9.11 as frequency curve.

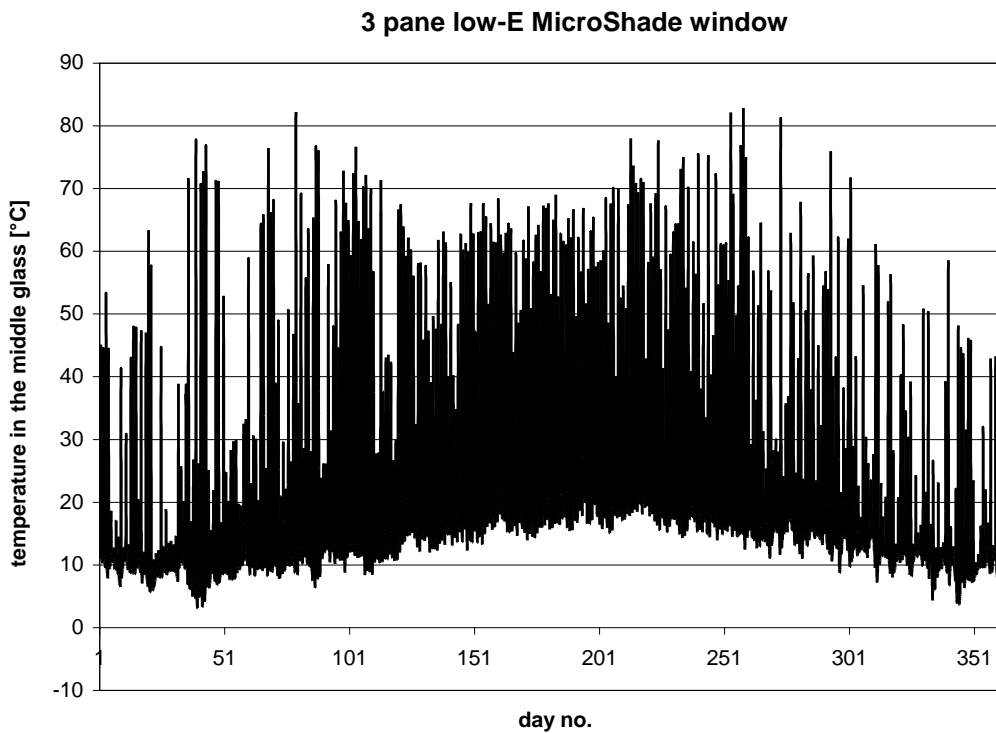


Figure 9.15. Temperatures over the year in the middle glass of the construction in figure 9.11.

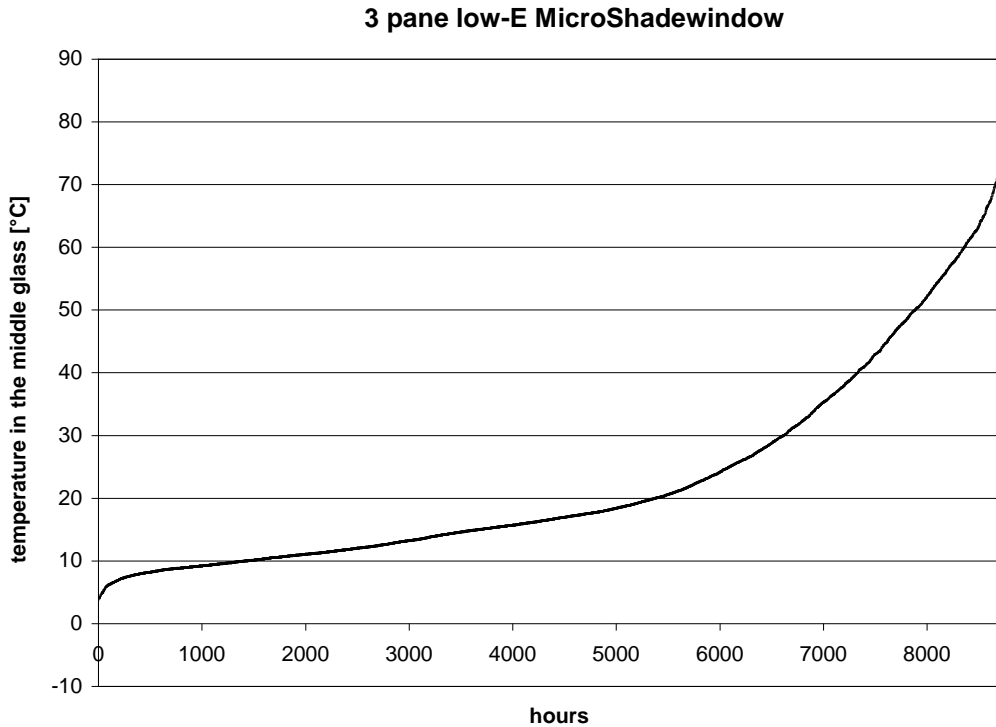


Figure 9.16. Temperatures in the middle glass of the construction in figure 9.11 as frequency curve.

Figure 9.15-16 show a max temperature of approx. 83°C although the absorptance in the middle glass is low - see figure 9.12. The reason for the high temperature is that the heat loss to the ambient and to the room is very low. If the MicroShade is removed from the construction in figure 9.11 the max temperature in the middle glass will raise to approx. 104°C as more solar radiation is hitting this glass as the shading from the MicroShade is removed.

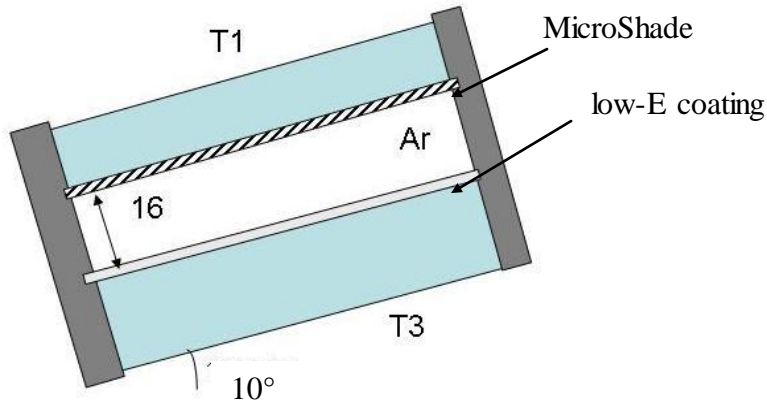
9.4. MicroShade low-E roof window

This construction is a MicroShade low-E window with the MicroShades located behind the outer glass of the window - see in figure 9.17.

For safety reasons the glasses are thicker than in a normal low-E window. The outer glass is 12 mm thick while the inner glass is 16 mm thick. The resistance in the gap is due to the nearly horizontal location 0.452 m²K/W.

The MicroShade 150610-P12U16 optical matrix has been used for the calculations – see figure 9.18.

Figure 9.19 shows the temperature of outer glass in the construction of figure 9.17 over the year for Danish weather conditions. Figure 9.20 shows the same temperature set but as frequency curves.



P12U16 = Planilux 12mm + Ultratherm 16mm

Figure 9.17. MicroShade low-E roof window.

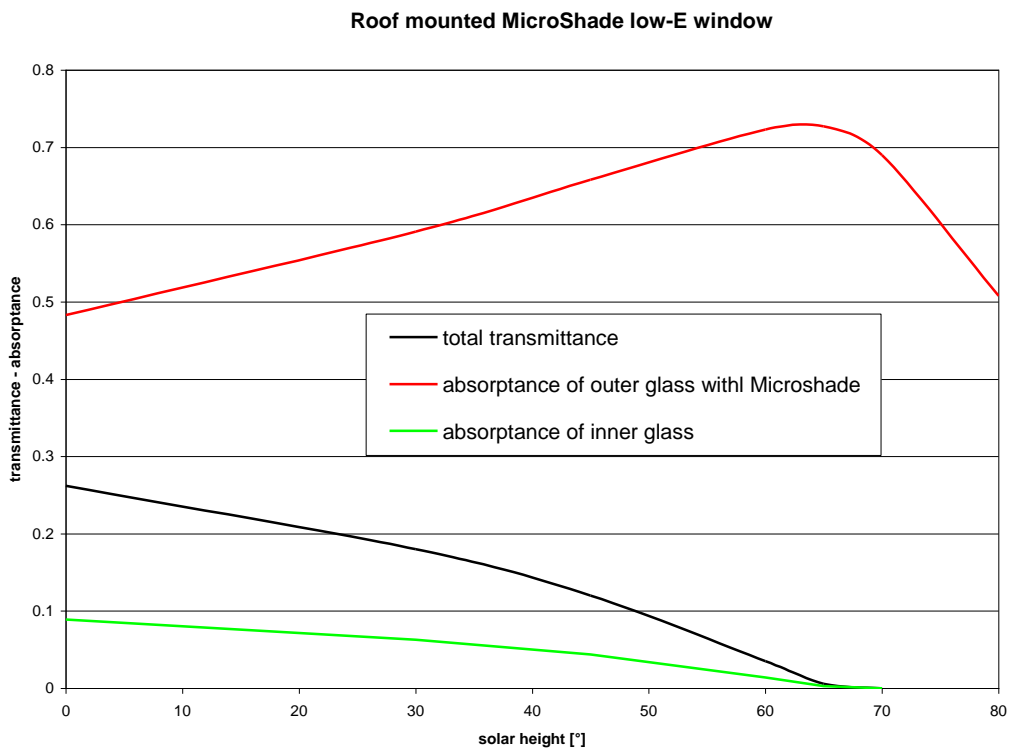


Figure 9.18. Optical properties of the roof mounted MicroShade low-E window for an azimuth of 0° (ie. the horizontal incidence angle is 0°) for different solar heights (ie. vertical incidence angles).

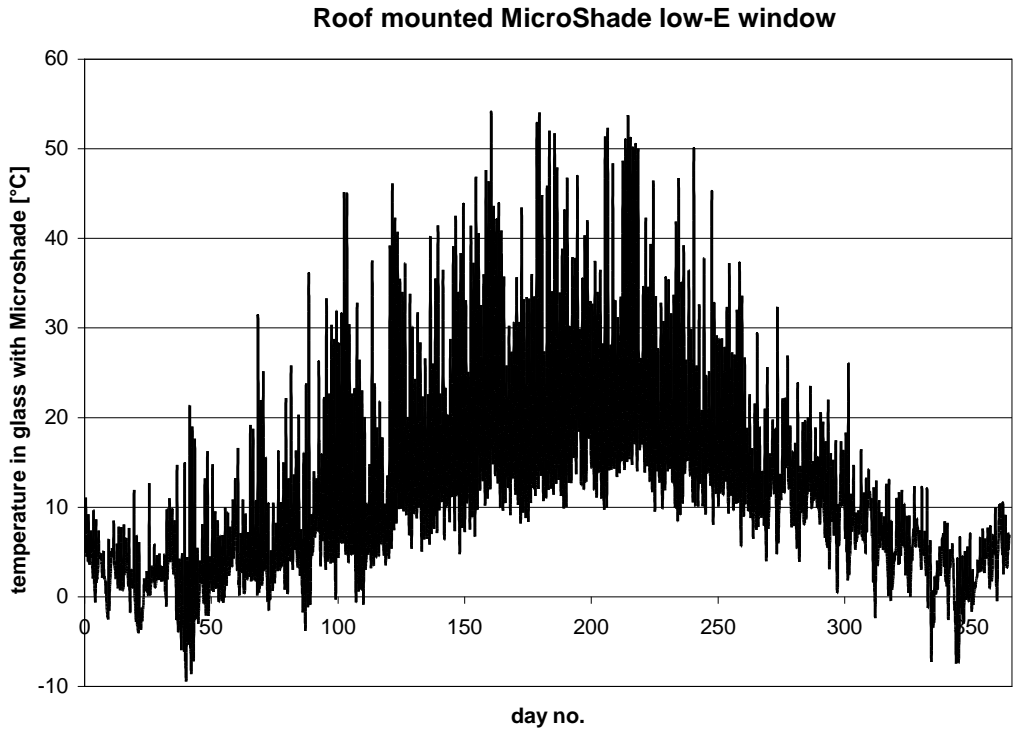


Figure 9.19. Temperatures over the year in the outer glass of the construction in figure 9.17.

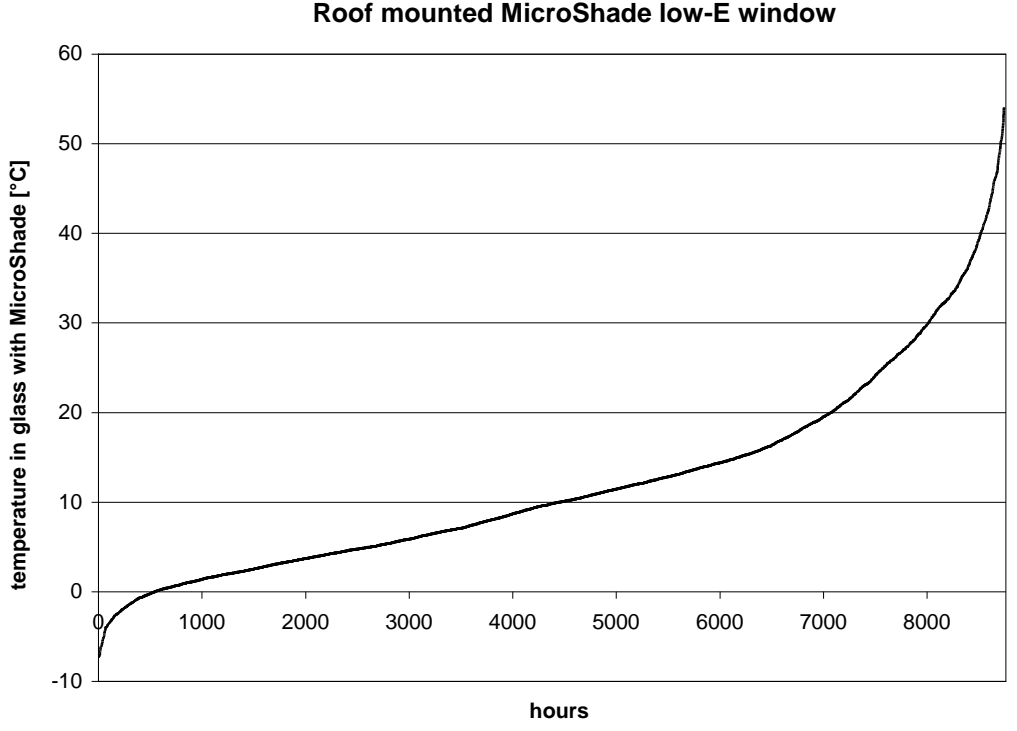


Figure 9.20. Temperatures in the outer glass of the construction in figure 9.17 as frequency curve.

Figures 9.19 and 9.20 show that the max temperature of the glass with the MicroShades reaches a max temperature approx. 54°C. The max temperature occurs due to the nearly horizontal location during the summer when the solar height is at maximum.

Although the higher absorptance due to a thicker outer glass the max temperature is lower than for the vertical mounted MicroShade low-E window – please compare figure 9.19 with 3. This is due to a higher heat loss from an almost vertical mounted window compared to a vertical mounted window.

9.5. Conclusions

The simulations show that when MicroShades is mounted on the inside of the outer glass in a low-E (double or triple glazed and vertical or horizontal) window the temperature of the MicroShades/outer glass will stay below 65°C under Danish weather conditions.

If the MicroShades are mounted in a low-E double glass window – again behind the outer glass – but with a single glazing in front, the temperature of the MicroShades/glass will in shorter periods reach a temperatures as high as nearly 120°C depending on the U-value of the low-E window.

10. Evaluation of measurements from the test rooms

The measurements with the MS-A type MicroShade window lasted from November 10, 2009 until July 15, 2010. Before this the Prototype 1 was installed in test room A. Measurements with the latter window are evaluated in [Jensen, 2008b] and will not be dealt with here.

10.1. Temperatures in the test rooms

The test rooms are almost identical but reversed regarding the windows. In [Jensen, 2008b] it was concluded that an extra layer of gypsum on the wall in room B facing another laboratory influenced the temperature difference between the two test rooms of up to 0.5 K. So in this project a gypsum plate was installed on the reverse wall in room A.

However, the empty laboratory next to the laboratory containing the two test rooms was again occupied which meant that the temperature of this laboratory could not any longer be controlled as in [Jensen, 2008b]. Figures 10.1-10.2 shows the temperatures of the zones surrounding the test rooms for the first half year of 2010. Except for the temperature of the laboratory next to room B (the curve labelled “left of B”) the surrounding temperatures are very similar. “left of B” is between 2-6 K higher than the other surrounding temperatures. The influence of this on the air temperature in room B is shown in figures 10.3-4. The figures show that during the night and overcast conditions the mean air temperature of room B is between 0.5 and 1 K higher than the mean air temperature in room A. This has to be considered when comparing air temperatures during solar radiation – ie using a simple assumption that this difference of 0.5-1 K should be subtracted the difference between the rooms at solar radiation.

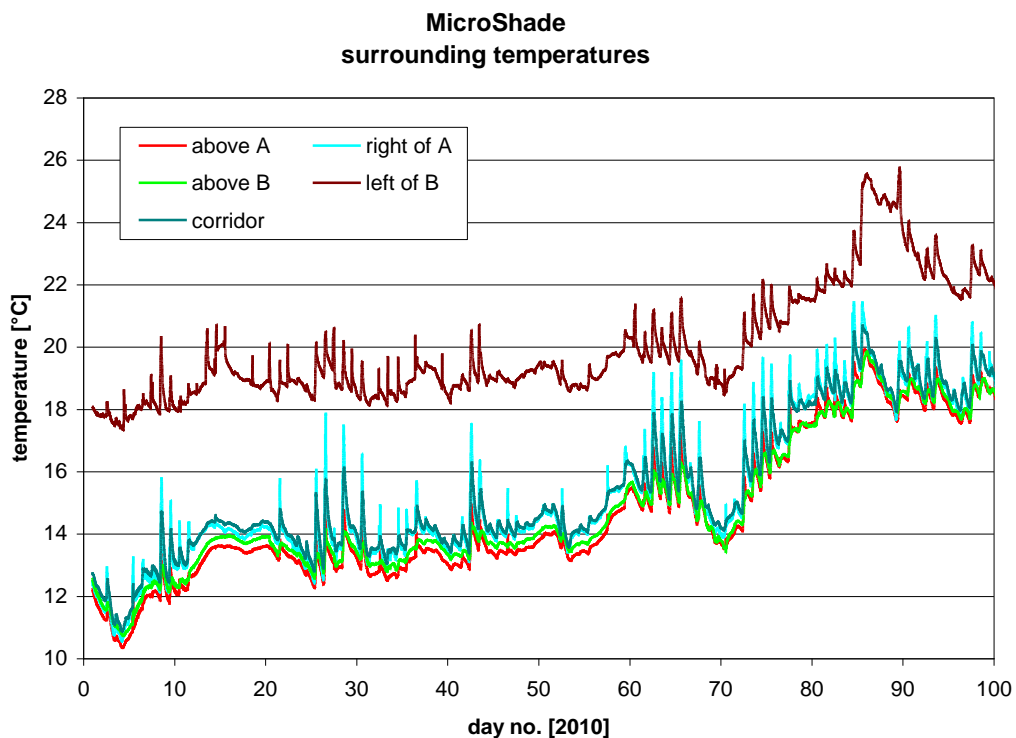


Figure 10.1. Temperatures surrounding the test rooms – January 1-April 9.

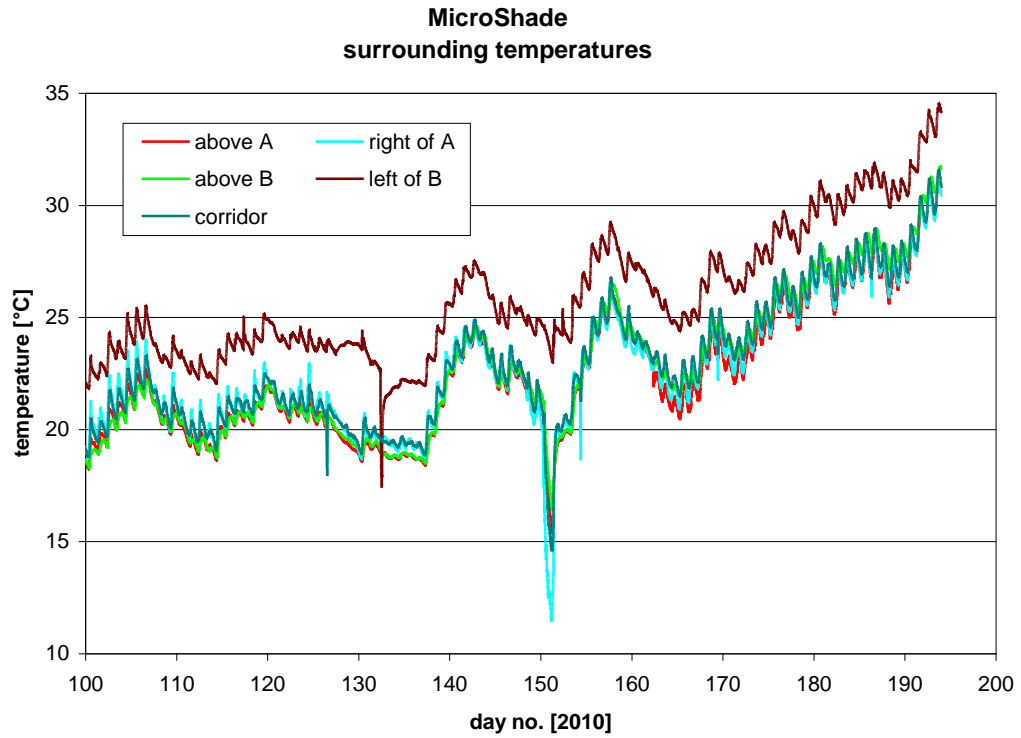


Figure 10.2. Temperatures surrounding the test rooms – April 10-July 11.

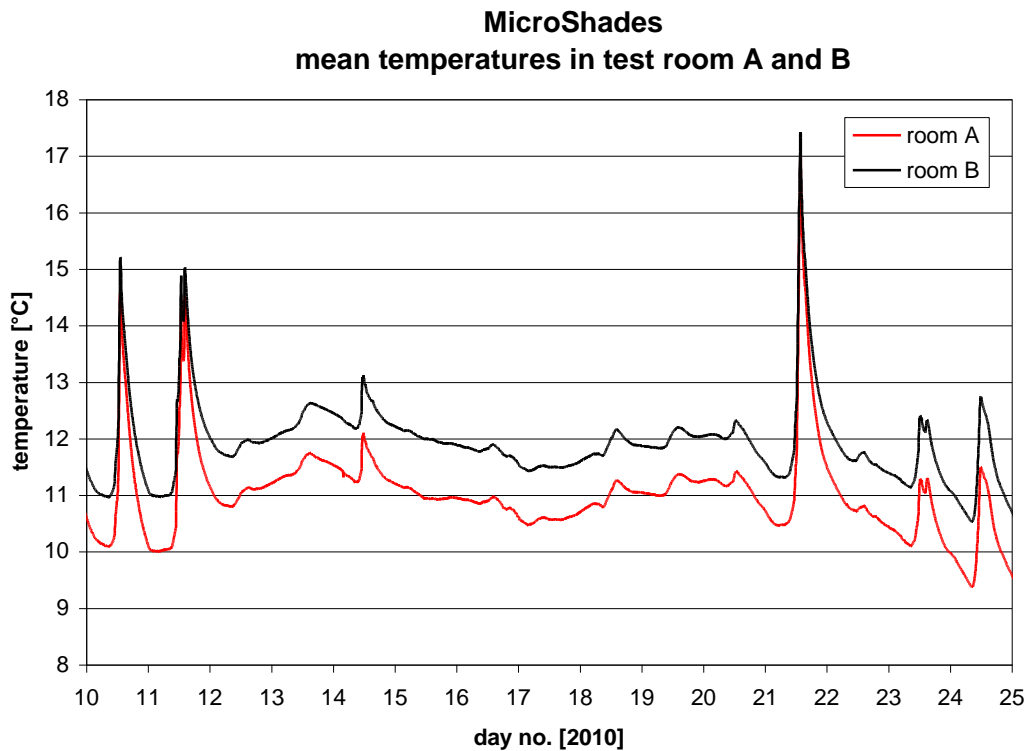


Figure 10.3. Mean air temperatures in the rooms during a period with large difference between “left of B” and “left of A”.

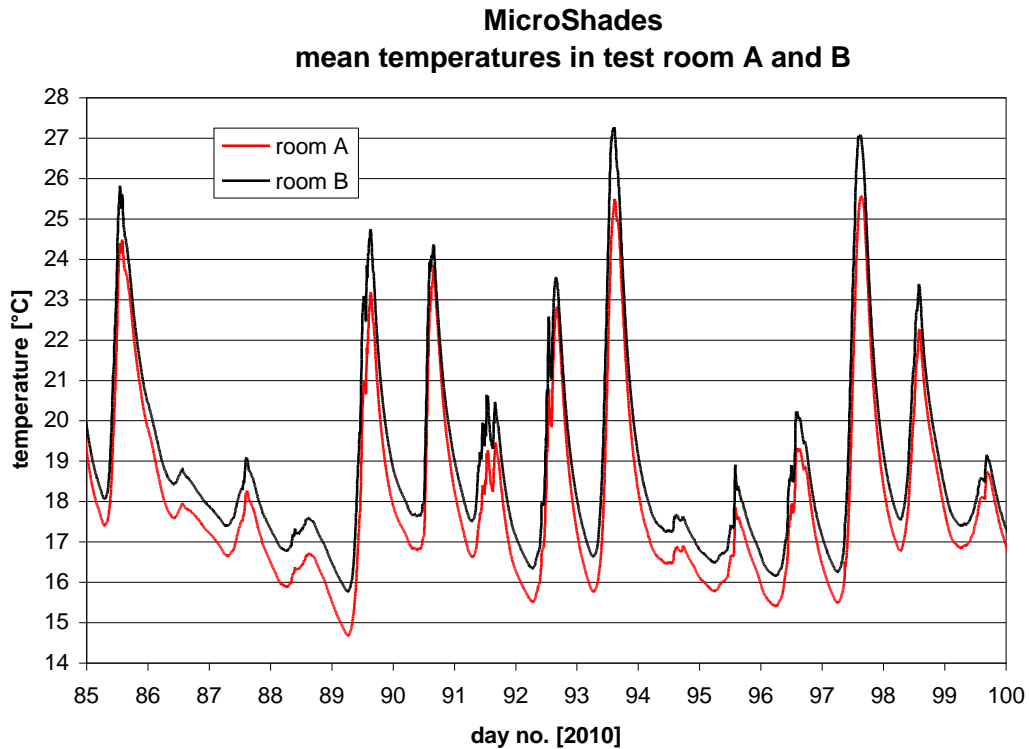


Figure 10.4. Mean air temperatures in the rooms during a period with smaller difference between “left of B” and “left of A”.

Figures 10.5-10.12 show the mean air temperature in the two test rooms during main part of the first half year of 2010. Figures 10.5-10.9 show the situation with the Velfac sun 1/clear window in test room B while figures 10.10-10.12 show the situation with the low-E window without solar control in room B.

The solar height varied between 11 and 49° in figures 10.5-10.9 and between 50.5 and 56.7° in figures 10.10.10.12.

10.1.1. Comparison with the Velfac window

Day 8 in figure 10.5 show that room A got 1 K warmer than room B + the 1 K difference during the night. This give a 2 K temperature difference with room A being the warmest. The temperature of the two test rooms should be identical as the same amount of radiation get into the two test rooms. This may be due to not known uncertainties within the test rooms.

Day 42 in figure 10.6 the above difference is decreased to 1.5 K and on day 65 in figures 10.7 the difference is further decreased to 1 K. On day 84 in figure 10.7 room B get warmer than room A with a difference of 0.5 K. This difference increase to 1 K on day 93 in figure 10.8 and holds in figure 10.9.

In the case study on Malling school in chapter a temperature difference of 0.7 K on the mean air temperatures was found. The solar height on August 28 is equal to the solar height on April 15 = day 115. In figure the temperature difference is found to 1 K – ie very similar to the case study.

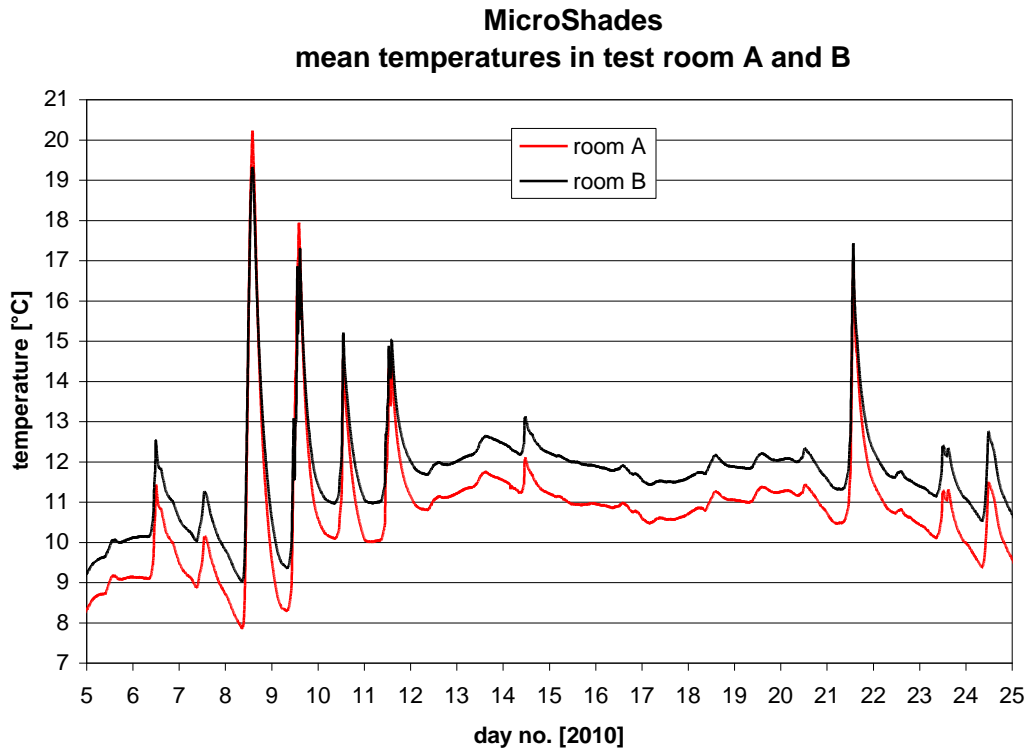


Figure 10.5. The mean air temperature in test rooms with the Velfac sun1/clear window in room B for the period January 5-24.

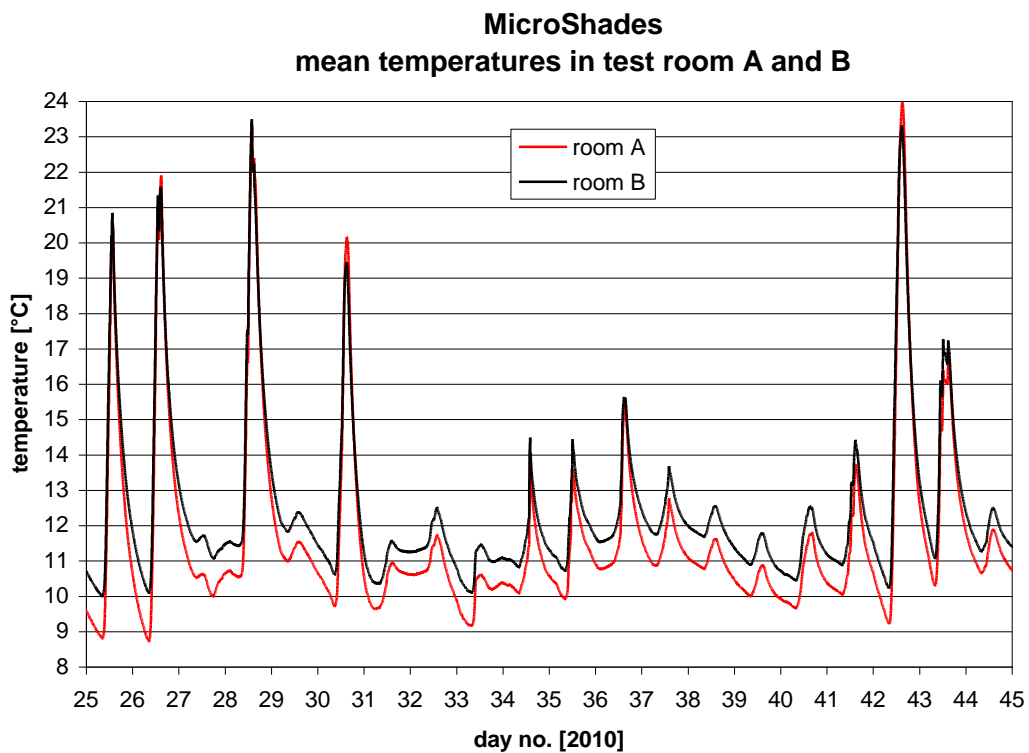


Figure 10.6. The mean air temperature in test rooms with the Velfac sun1/clear window in room B for the period January 25-February 13.

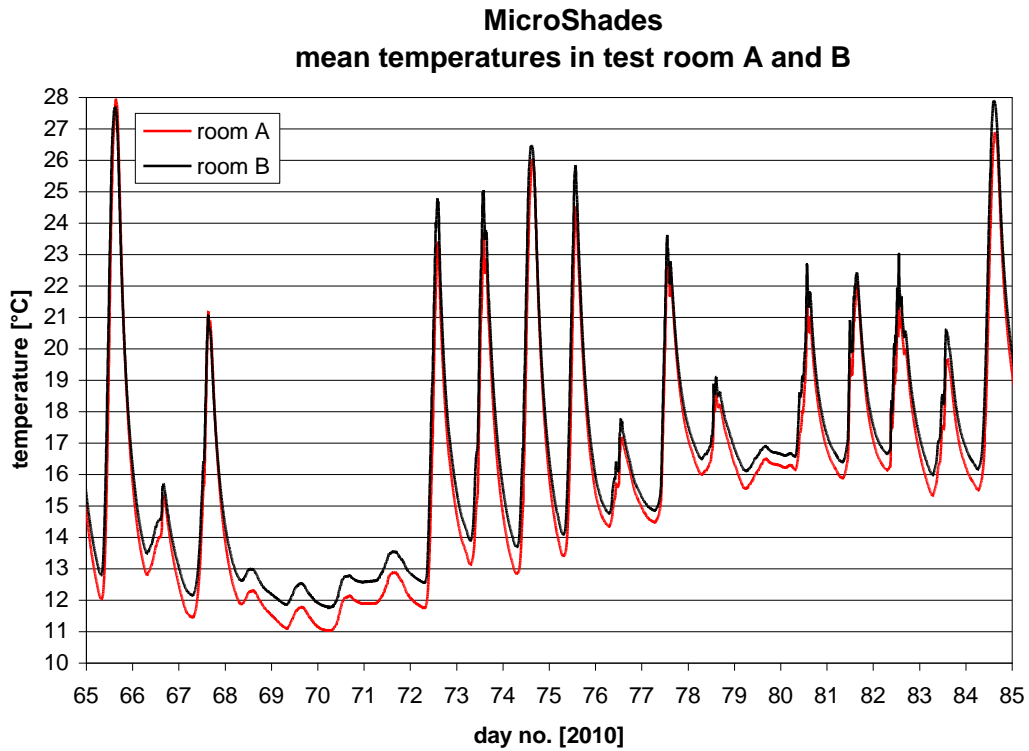


Figure 10.7. The mean air temperature in test rooms with the Velfac sun1/clear window in room B for the period March 6-25.

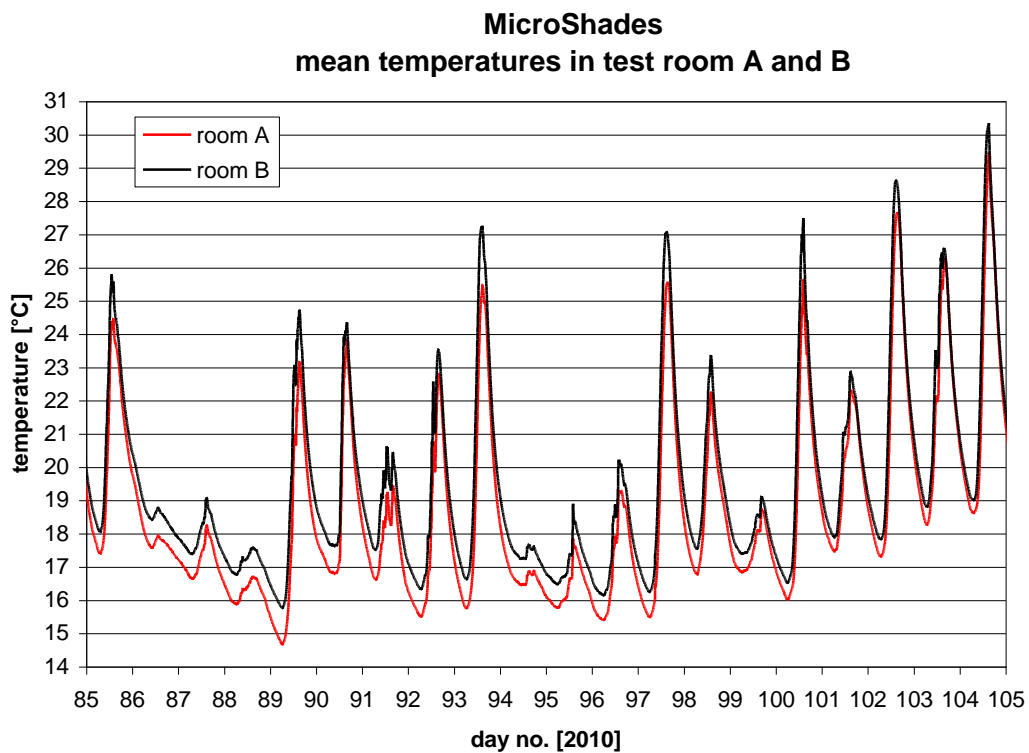


Figure 10.8. The mean air temperature in test rooms with the Velfac sun1/clear window in room B for the period March 26-April 14.

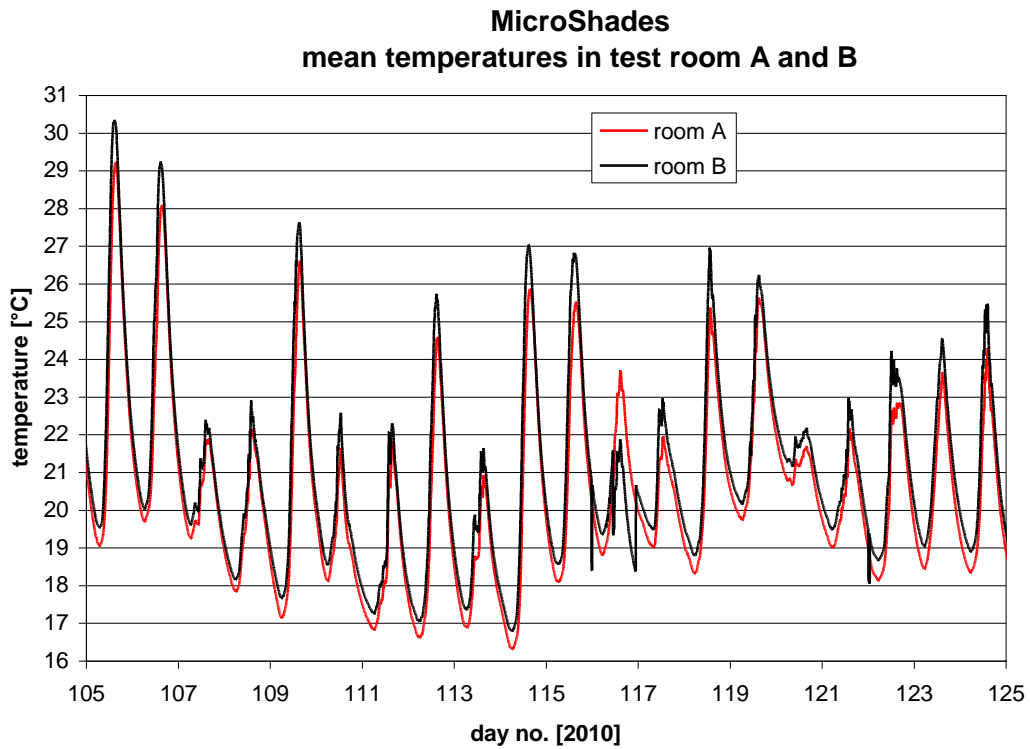


Figure 10.9. The mean air temperature in test rooms with the Velfac sun1/clear window in room B for the period April 15-May 4.

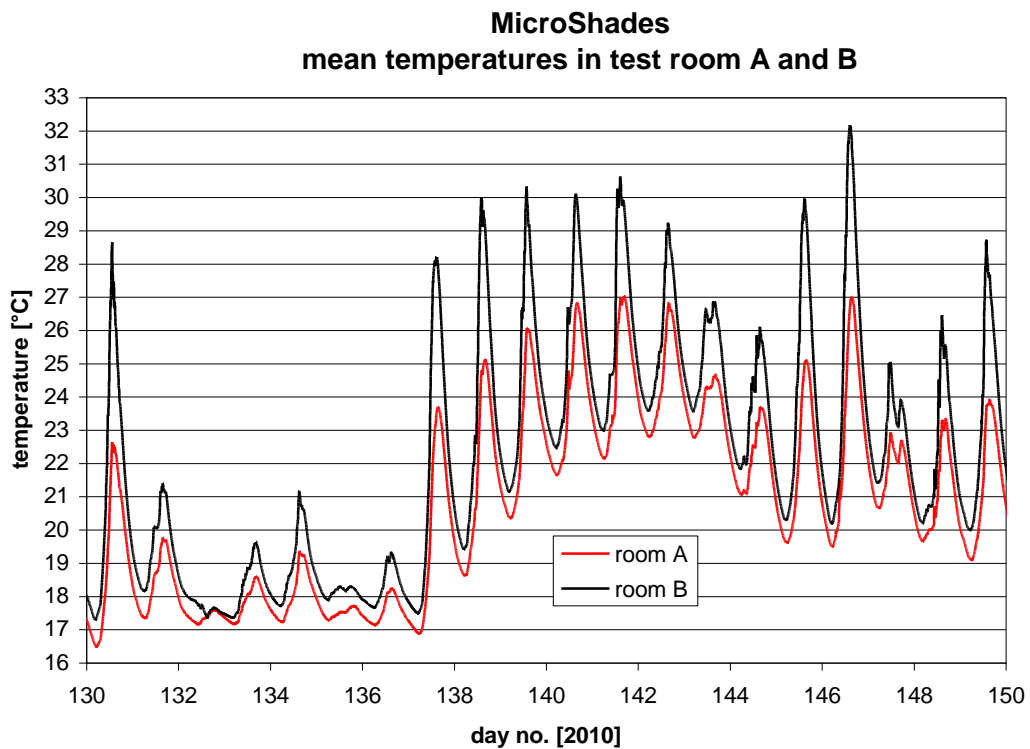


Figure 10.10. The mean air temperature in test rooms with the low-E window in room B for the period May 10-29.

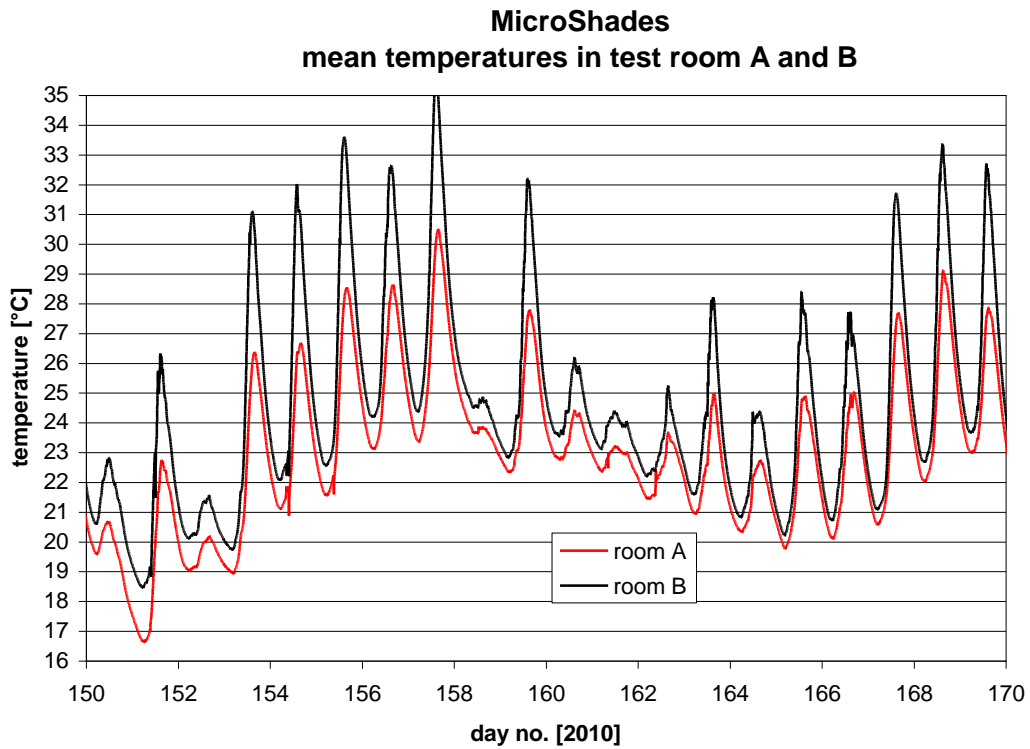


Figure 10.11. The mean air temperature in test rooms with the low-E window in room B for the period May 30-June 18.

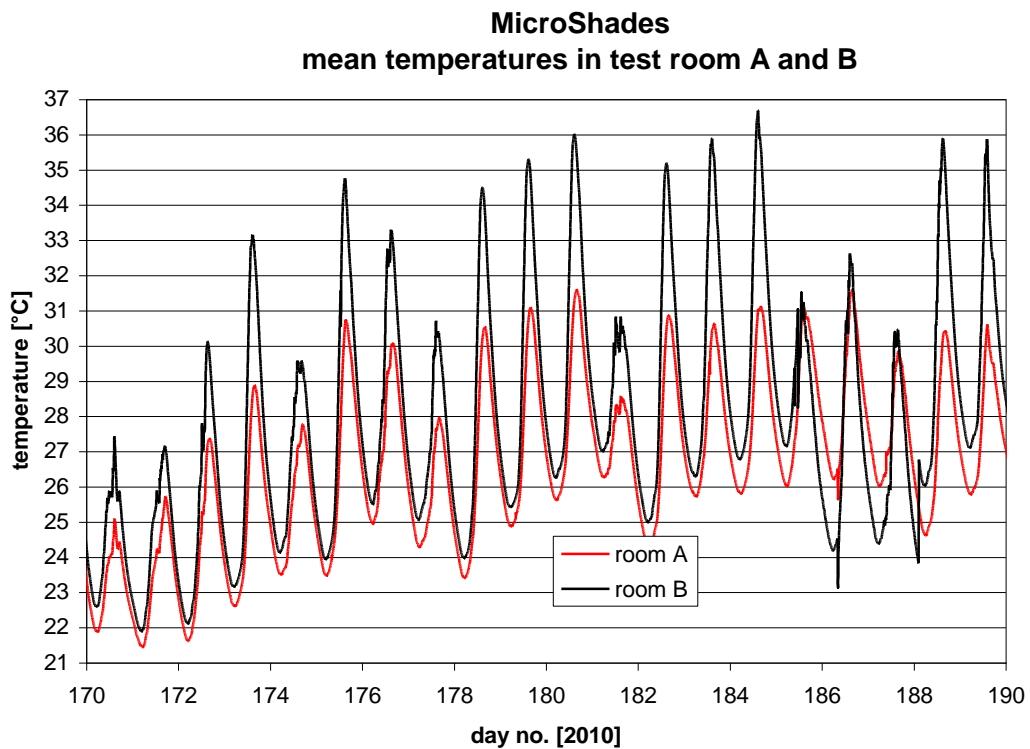


Figure 10.12. The mean air temperature in test rooms with the low-E window in room B for the period June 19-July 8.

10.1.2. Comparison with the low-E window

Figures 10.10-10.12 shows a very similar temperature difference between 4 and 5 K. This is because the solar height only varies slightly – ie between 50.5 and 56.7°.

Due to the larger solar height the temperature difference in figures 10.10-10.12 cannot directly be compared with the simulations in chapter 6. The found temperature difference of 1.1 K found in chapter 6 seems to be too small compared with the findings in figures 10.10-10.12 but matches as explained in chapter 6 very well the difference in transmittance between the Velfac window and the low-E window.

The reason for the very much larger temperature difference in the test rooms compared to the case study in chapter 6 is partly explained when comparing figure 10.17 (same solar height as in chapter 6) with figures 10.18-10.21 – although these figures cannot be compared directly due to different windows in room B. The cut off of solar radiation is much more drastic in figures 10.18-10.21 than in figure 10.17.

10.2. Solar radiation to the test rooms

Figures 10.13-10.21 show the incoming solar radiation through the MicroShade window divided with the incoming solar radiation to room B. Figures 10.13-10.17 show the situation with the Velfac window in room B while figures 10.18-10.21 shows the situation with the low-E window in room B. The figures also show the solar radiation on the façade.

Figures 10.13-10.21 show the behaviour of the MicroShade:

- during the morning and afternoon at large horizontal incidence angles the MicroShade cuts due to the hole structure off more solar radiation than the two other windows.
- around noon the reduction compared to the other windows describes a soft curve at lower solar heights – in figures 10.13-10.15 up to 32°
- in the morning and in the afternoon there is a cut in the curve. Between figures 10.15 and 10.16 – solar heights between 32 and 35.8° - this gets more noticeable and at solar heights around and above 55.3° (figure 10.18-10.21) the level of reduction increases drastically and the reduction occurs very sudden in the morning and stops very sudden in the afternoon.

The reduction at a horizontal incidence angle of 0° (azimuth = 0°) has been plotted into figure 10.22. Red squares for the Velfac window and black squares for the low-E window.

The red squares lay as seen on a straight line. The red line is actually the line found in [Jensen, 2008b] for the Prototype 1 MS and the Velfac window – also shown in figure 7.4. This not a surprise: MS-A has a hole area of 0.6 while Prototype 1 had a hole area of 0.675. But Prototype 1 had one more glass with an direct transitivity of 0.89. Multiplying 0.675 with 0.89 gives 0.6.

The values for the low-E window are gathered close around only one point which is rather close to the difference in direct solar transmittance of the Velfac and low-E window: values of $Velfac \cdot 0.54 / 0.34$. However, as the dependency on the incidence angle of the two windows is similar it can be concluded, that the slope of the black line should be similar to the slope of the red line. This has been drawn into figure 10.22.

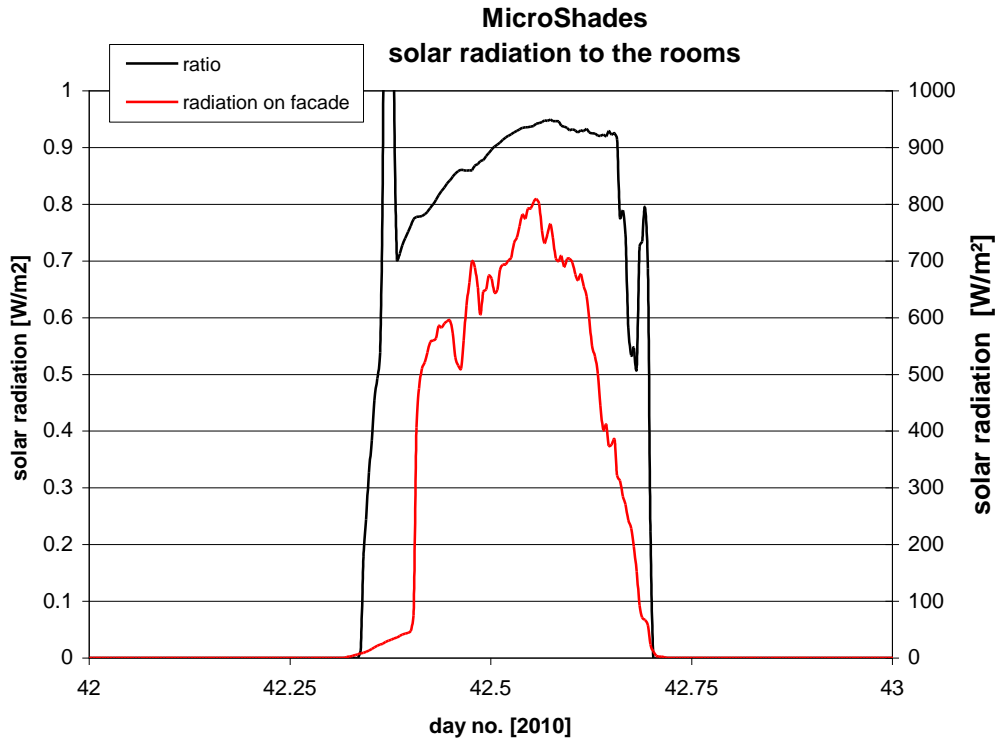


Figure 10.13. Ratio between the solar radiations to the two rooms with the Velfac sun 1/clear in room B. February 11.

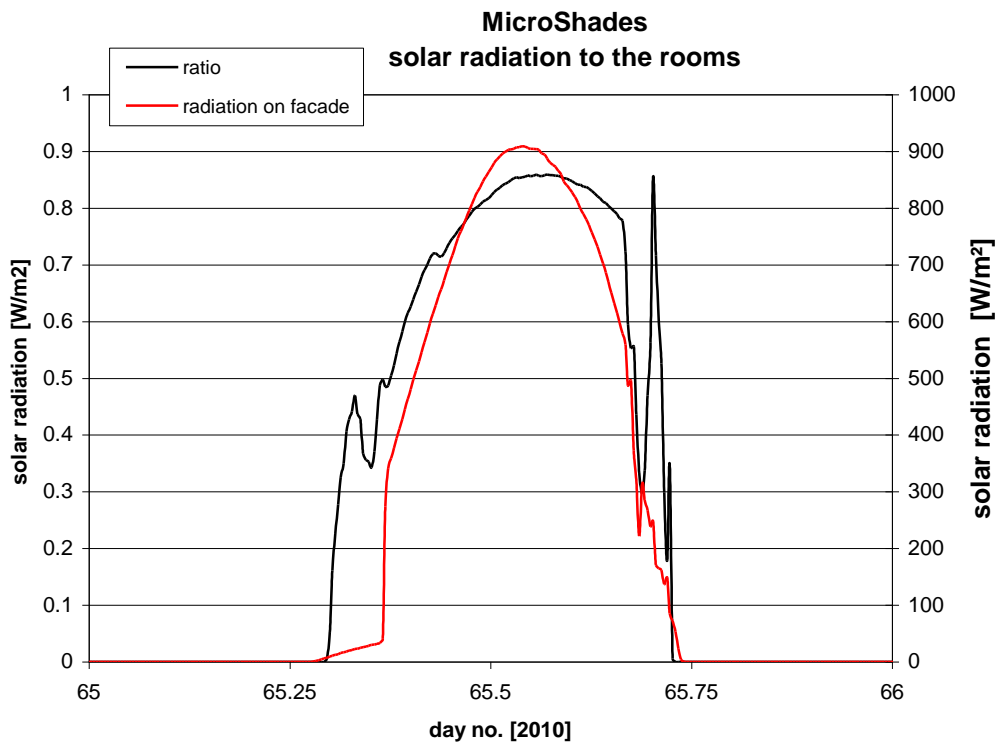


Figure 10.14. Ratio between the solar radiations to the two rooms with the Velfac sun 1/clear in room B. March 6.

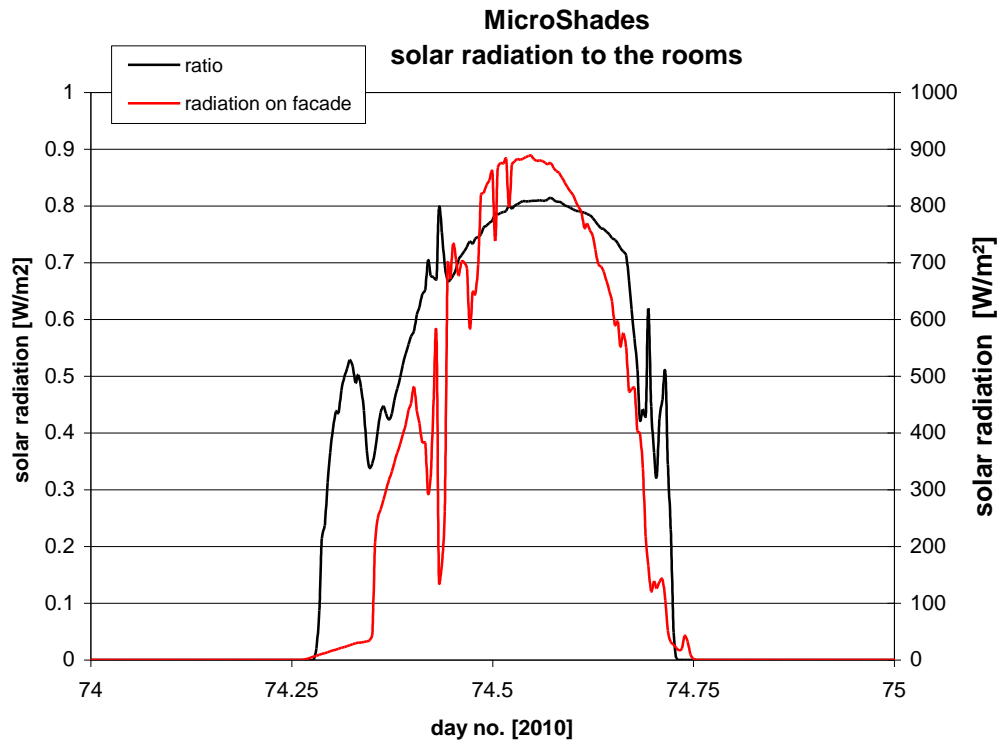


Figure 10.15. Ratio between the solar radiations to the two rooms with the Velfac sun 1/clear in room B. March 16.

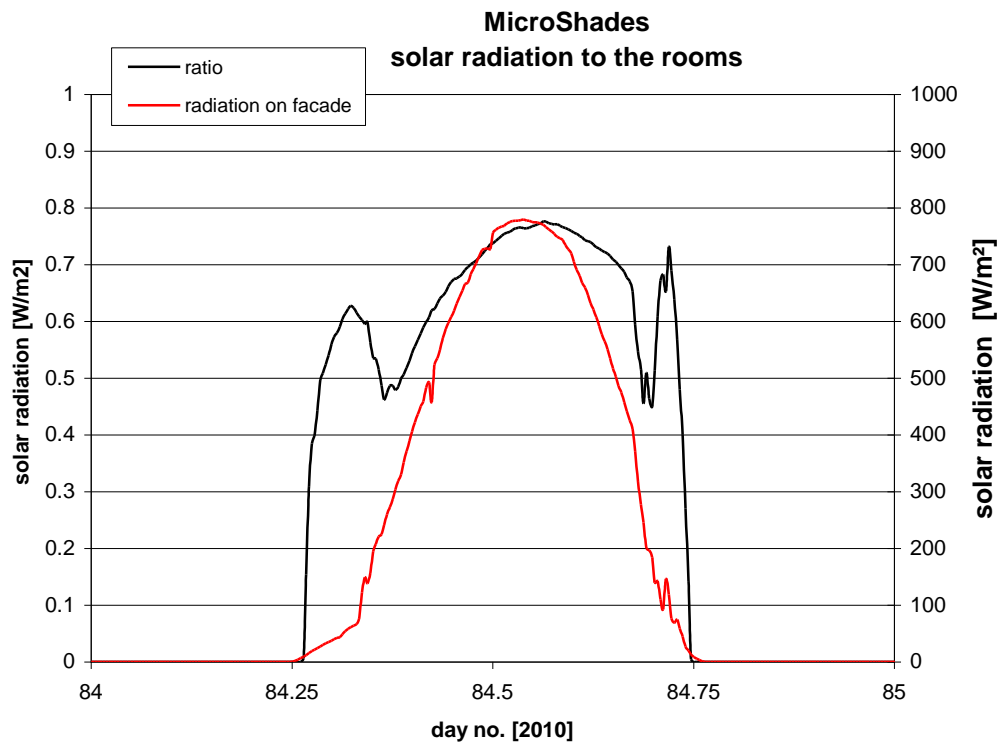


Figure 10.16. Ratio between the solar radiations to the two rooms with the Velfac sun 1/clear in room B. March 25.

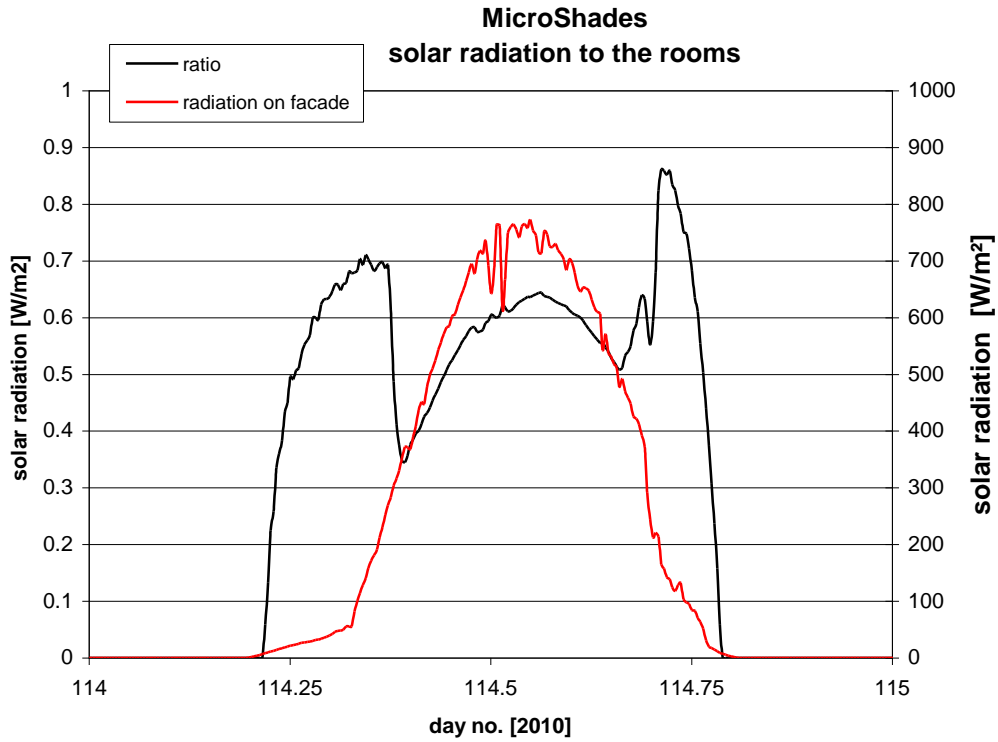


Figure 10.17. Ratio between the solar radiations to the two rooms with the Velfac sun 1/clear in room B. April 24.

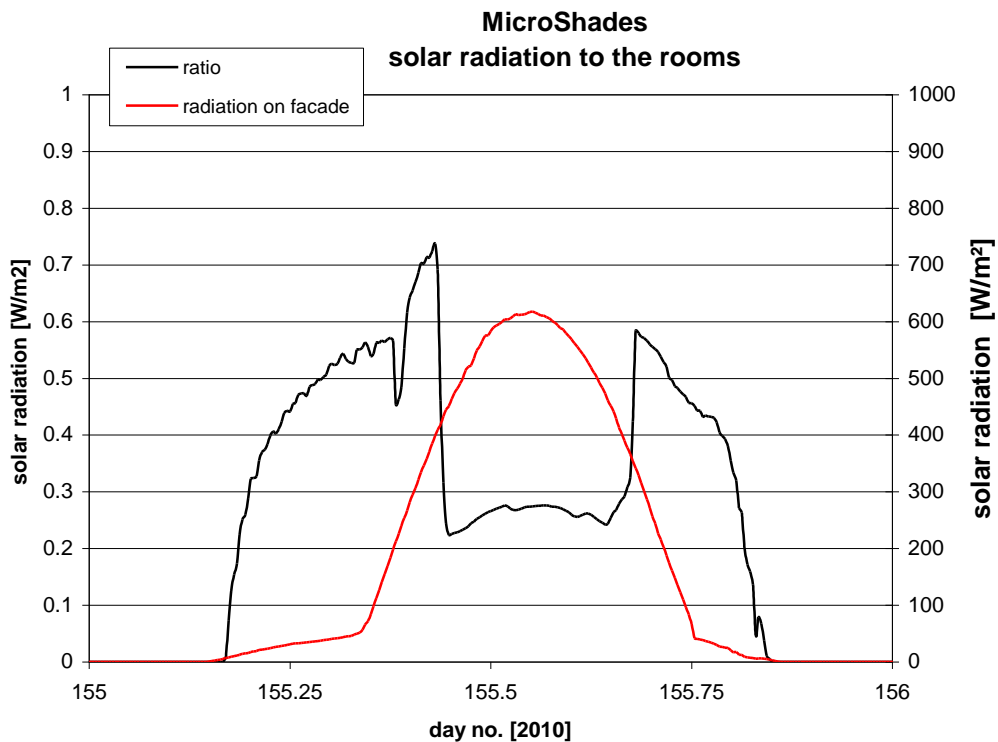


Figure 10.18. Ratio between the solar radiations to the two rooms with the low-E window in room B. June 4.

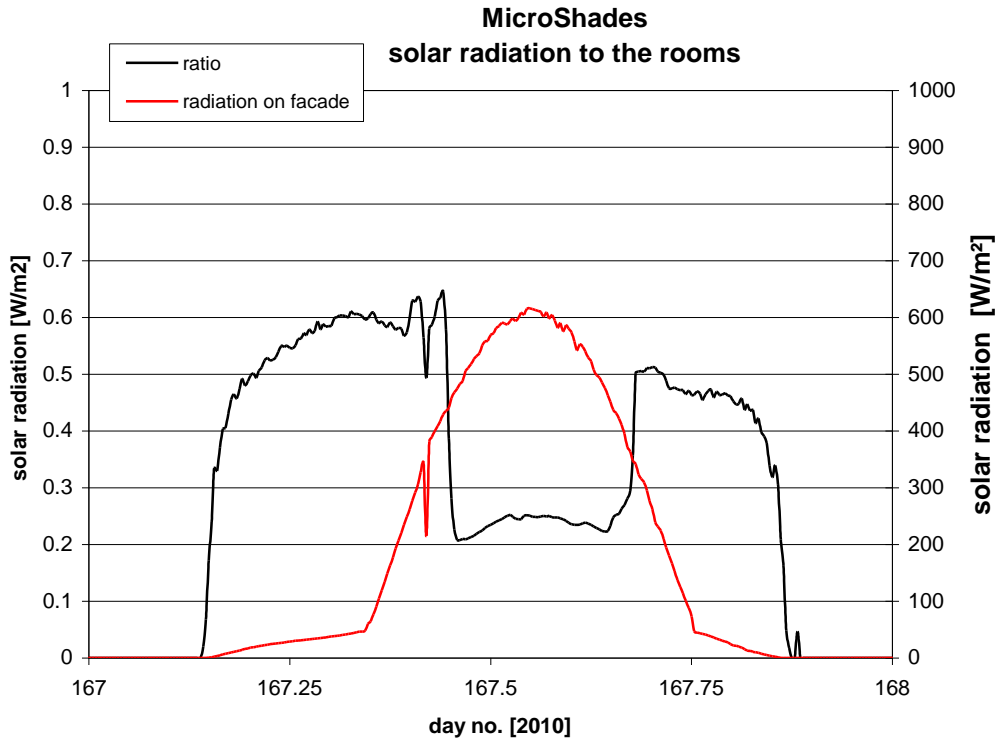


Figure 10.19. Ratio between the solar radiations to the two rooms with the low-E window in room B. June 16.

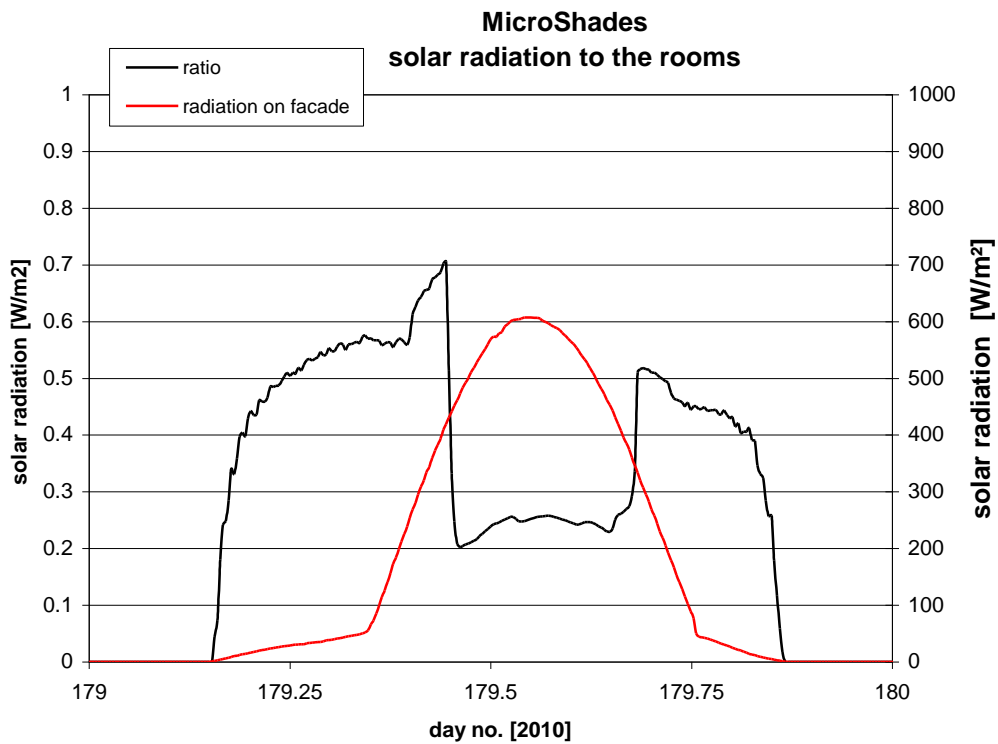


Figure 10.20. Ratio between the solar radiations to the two rooms with the low-E window in room B. June 28.

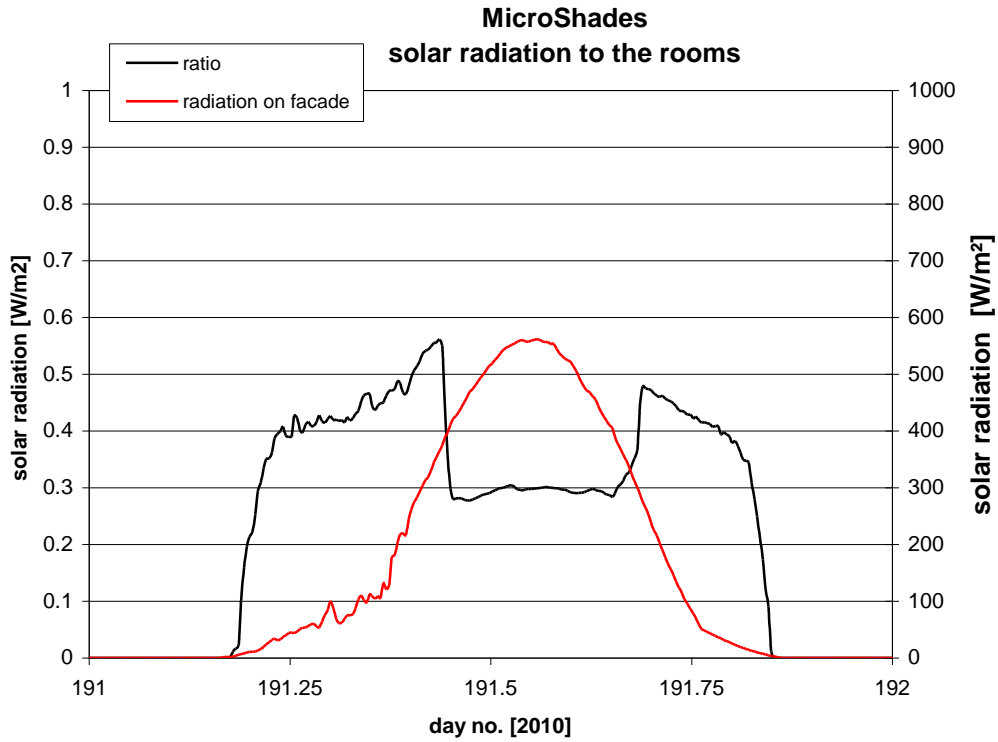


Figure 10.21. Ratio between the solar radiations to the two rooms with the low-E window in room B. July 10.

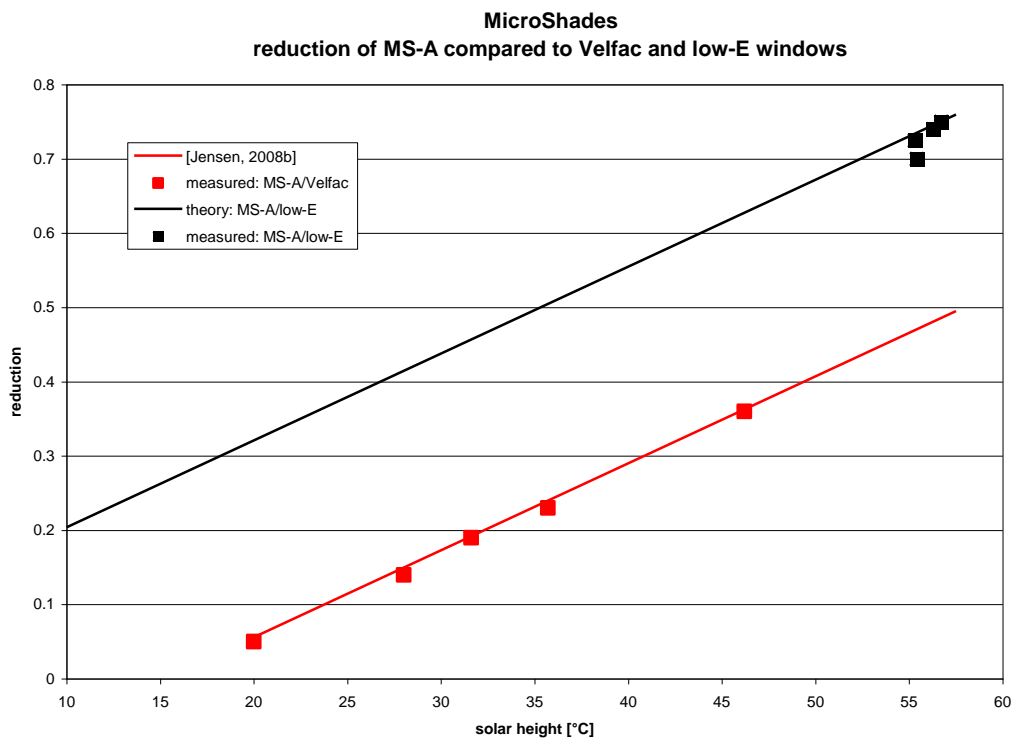


Figure 10.22. The reduction by the MicroShade window at an azimuth of 0° compared with the two windows in room B dependent on the solar height.

In figure 10.22 (and figures 10.13-10.21) the solar radiation measurements have not been corrected with the factors found in chapter 4 which would lead to a 9.3 % higher reduction than shown in figure 10.22. However, if it is assumed that the correction factors for the solar radiation measurements also goes for the measurements in [Jensen, 2008b] – which is a logical assumption as the physical nature of the windows in [Jensen, 2008b] (MS Prototype 1 and the Velfac window) are similar to the windows investigated in chapter 4 – figure 10.22 can be transformed to figure 10.23.

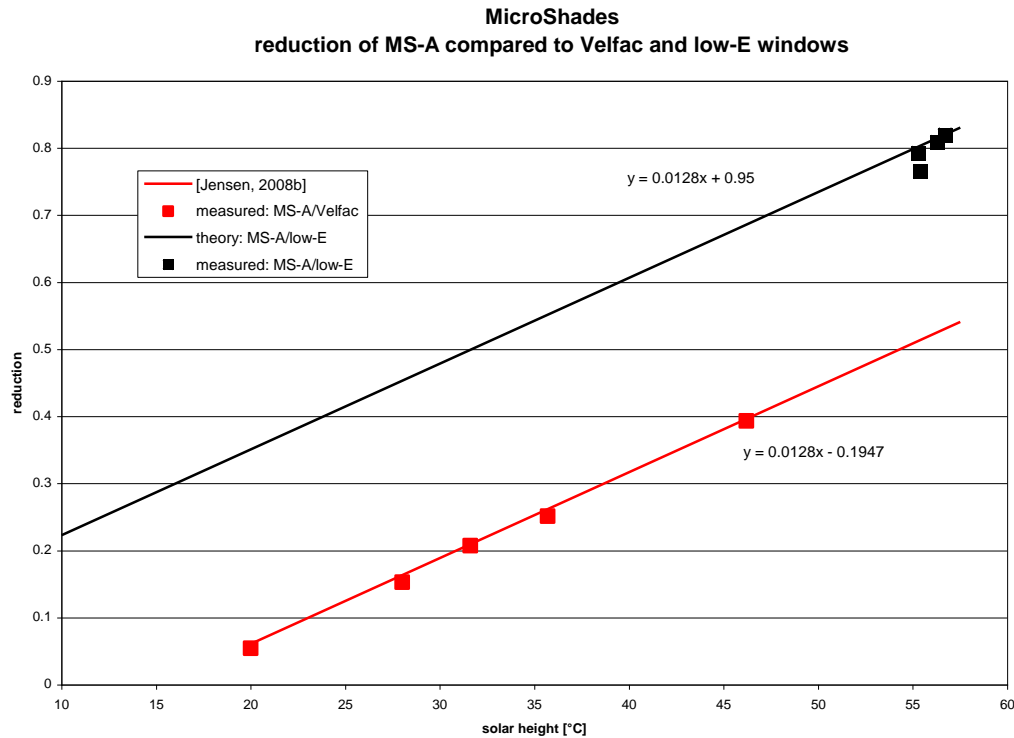


Figure 10.23. The reduction by the MicroShade window at an azimuth of 0° compared with the two windows in room B dependent on the solar height. Solar radiation measurements have been corrected according to chapter 4.

10.3 Conclusions

The measurements show moderate temperature differences between test room A with the MicroShade window and test room B with the Velfac window. Surprisingly test room A was up to 2 K warmer during solar radiation than test room B although they received the same amount of solar radiation. During late spring test room B got up to 1 K warmer than test room B which is in agreement with the calculations for the case study from Malling school in chapter 6. This however, changed drastically when the Velfac window was replaced by a low-E window without solar control. The temperature difference increased to 4-5 K with room B with the low-E window being the warmest.

The investigation of the solar radiation measurements showed a quite sudden reduction of the incoming solar radiation in the morning during the summer and again a sudden return to less reduction in the afternoon. This effect should be investigated in more detail.

The reduction when comparing the MS-A window with the Velfac window at an azimuth of 0° dependent on the solar height is in agreement with the earlier findings in [Jensen, 2008b]. Based on theory the reduction when comparing MS-A with a traditional low-E window without solar control dependent on the solar height has been developed.

11. Conclusions

Modelling of MicroShades is a non trivial task due to the rather complex structure of the MicroShades. A program for generation of a matrix representing the optical properties of windows with MicroShades has been developed. Measurements at both the Technological University of Denmark and University of Basel, Switzerland shows good agreement with the model for direct solar radiation. However, there is as yet no theory for determination of the transmittance of diffuse radiation and of the scattering in the MicroShades of the direct radiation.

The transmittance of diffuse radiation has for overcast conditions been measured for the MS-A MicroShades in a low-E window to 0,185 which shows good agreement for overcast conditions when comparing with measurements. However, a calculation method should be developed.

The scattering of direct solar radiation (transformation from direct to diffuse radiation) has a rather large impact on the calculated radiation through a MicroShade window during clear sky conditions. A fixed scattering factor of 3 % was chosen as the best value for the MS-A MicroShades in a low-E window, however, this value may very well be angular dependent – both vertical and horizontal. The scattering should, therefore, be investigated further in order to come up with a theory for calculation of this value for the matrix.

Although much work can be done in order to fully understand the optical properties of MicroShades it may – based on comparisons between measurements and simulations - be concluded that the investigated model of MicroShades very well represent the optical performance of MicroShades and may be used to investigate the thermal performance of MicroShade windows in real buildings. A tutorial on how to implement MicroShades in simulations with the program esp-r has been written.

The above conclusion relies on the correctness of the measurements of the solar radiation through the windows in the test rooms. So tests were carried out in order to validate the readings from the pyranometers in the test rooms. The tests show that the influence of inter-reflections between the pyranometer/white screen of the Epply pyranometer measuring the solar radiation through the MicroShade window may lead to an over estimation of the incoming solar radiation of 4 % while it seems to have no influence on the readings from the pv-pyranometer measuring the solar radiation through the traditional windows. The diffuse radiation from the room behind the pyranometers seems to have negligible influence. The solar radiation measurements have been corrected based on the above tests.

In order to test the validity of the model of MicroShade windows in real life simulations has been compared with measurements from a school which has both MicroShade and solar control windows. The simulations show what is experienced by the users of the class rooms: that the temperature is lower in the room with MicroShades than in the room with the solar control windows. The simulations also show that the very high temperature differences reported has more to do with people being hit by a higher radiation level and warmer tables in the room with the solar control windows than due to an elevated mean air temperature. The investigation contains the first comparison between measurements and simulations for a real life situation. The comparison shows a reasonable agreement but no firm conclusions can be made as the measurements were of a too low quality – both with regard to the number of the measuring points and to the available information on the measurements. It is therefore recommended

to perform carefully planned and more detailed measurements in buildings with MicroShade windows in order to gain valuable experience on the behaviour of MicroShade windows. The measurements should both include sensor measurements and questionnaires – the latter to make possible an evaluation of the subjective sensed thermal indoor climate.

The measurement and simulations for the school show that radiation hitting a person considerably influences the comfort senses by a person. Experiments in the test rooms has been carried out in order develop a theory for this influence on the comfort. The results have been compared to similar experiments for cars. The result of the experiment in the two test rooms is that the Predicted Mean Vote (PMV) increases with 200 divided with the incoming radiation in W/m^2 - ie with 1 for each step of $200 W/m^2$ solar radiation hitting a person. At least up to $230 W/m^2$. The experiments in the car conclude that this relation holds up to $600 W/m^2$, while the experiment in the test rooms suggest a much stronger increase in discomfort above $230 W/m^2$. However, further experiments are necessary to verify this – especially experiments at larger levels of incoming radiation than obtained in the experiments in the test rooms. The experiments should also include test persons as many people likes moderate levels of incoming radiation – ie the subjective senses discomfort may be lower than the calculated PMV. The comfort level of persons not being hit by the radiation is not influenced by the radiation.

The model of MicroShade windows has been use to study the temperature in windows with MicroShades. The simulations show that when MicroShades is mounted on the inside of the outer glass in a low-E (double or triple glazed and vertical or horizontal) window the temperature of the MicroShades/outer glass will stay below $65^{\circ}C$ under Danish weather conditions. If, however, the MicroShades are mounted in a low-E double glass window – again behind the outer glass – but with a single glazing in front, the temperature of the MicroShades/glass will in shorter periods reach a temperatures as high as nearly $120^{\circ}C$ depending on the U-value of the low-E window. This latter give problems with the durability of the window.

The measurements in the test rooms show moderate temperature differences between test room A with the MicroShade window and test room B with the Velfac window with solar control coating. During late spring test room B got up to 1 K warmer than test room A. This however, changed drastically when the Velfac window was replaced by a low-E window without solar control. The temperature difference increased to 4-5 K with room B with the low-E window being the warmest.

The measurements reveals a quite sudden reduction of the incoming solar radiation through the MicroShade window - when compared to the traditional windows - in the morning during the summer and again a sudden return to less reduction in the afternoon. This effect should be investigated in more detail.

The reduction in incoming solar radiation - when comparing the MS-A window with the traditional windows at an azimuth of 0° - forms straight lines dependent on the solar height. The reduction is of course largest when compared to the traditional window without solar control coating.

12. References

- ESRU, 2001. Data Model Summary – ESP-r – Version 9 series. Energy Systems Research Unit, University of Strathclyde, Scotland.
- Fanger, P.O., 1982. Thermal Comfort – Analysis and Applications in Environmental Engineering. Robert E. Krieger Publishing Company, Florida. ISBN 0-89874-446-6.
- Hodder, S.G. and Parsons, K., 2006. The effects of solar radiation on thermal comfort. International Journal of Biometeorol, 2007, Volume 51, pp 233-250.
- Jensen, S.Ø., 2008a. Test rooms for test of PowerShades. Danish Technological Institute. ISBN 87-7756-769-2
- Jensen, S.Ø., 2008b. Test of PowerShades and calibration of models with PowerShades. Danish Technological Institute. ISBN 87-7756-770-6.
- Olesen, B.W., 1996. Teknisk Arbejdshygiejne II, Kapitel 5: Termiske omgivelser. Arbejdsmiljøinstituttet

Appendix A

**Paper to IBPSA BS2009
27th-30th July, Glasgow, Scotland**

CALIBRATION OF MODELS WITH MICROSHADE

Søren Østergaard Jesnen
Soren.O.Jensen@teknologisk.dk
Danish Technological Institut, Industry and Energy Division
Gregersensvej, DK-26300 Taastrup, Denmark

ABSTRACT

This paper deals with the calibration of models capable of simulating the performance of MicroShade™. The function of MicroShade is similar to Venetian blinds, however, MicroShade is a microstructure embedded in a metal foil with a thickness of less than one mm. MicroShade has been modelled using a novel module in ESP-r for modelling bidirectional transmission through transparent multilayered constructions. Windows with and without MicroShade have been tested in two dedicated test rooms. The measurements from the test rooms have been used to calibrate the model of MicroShade. Finally simulations are used to show how MicroShade will perform in a real building.

INTRODUCTION

MicroShade™ is a microstructure of small holes. Figure 1 shows an example of MicroShade. MicroShade consists of many small super elliptic shaped holes manufactured in a thin stainless steel sheet – see figure 1. The holes have a tilting angle and resemble the way Venetian Blinds function. However, the appearance is different and so is the view out as seen in figure 3. Newer versions of MicroShade have twice the distance between the opaque stripes shown in figure 3. The screening off and view out through MicroShade are determined by the shape and tilting angle of the holes in figure 1.

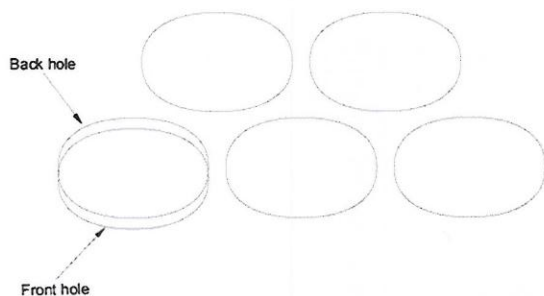


Figure 1 Example of the holes in MicroShade. The width of the holes are less than 1 mm.

Figure 24 shows MicroShade imbedded in a low-e window. The name of this product is MicroShade™ IG (Insulated Glazing) but will in the following be referred to as MicroShade windows.

The model of MicroShade is a matrix where the total direct transmission, the absorption in each layer of the window and the enhancement of incoming diffuse radiation due to the scattering of direct radiation in the MicroShade are listed for combinations of the horizontal and vertical incidence angle at steps of 5°. The values of the matrix are generated by a special purpose program where the main parameter is the projected hole area seen by the sun at different incidence angles and optical properties of MicroShade and glass. An example of the matrix is included at the end of the paper.



Figure 2 The view out of a traditional low-e window with solar control coating in test room B. g-value of the window: 0.37.



Figure 3 The view out of test room A with a low-e window with MicroShade.

Figure 4 shows the function of MicroShade. Figure 4 shows the transmittance of direct solar radiation through the two windows in figures 2 and 3 at an azimuth of 0°. During winter at low solar heights when solar heat is valuable the two windows let in almost the same amount of solar heat. But during summer at high solar heights and risk of overheating the MicroShade lets in considerably less solar heat than the traditional window with solar control coating.

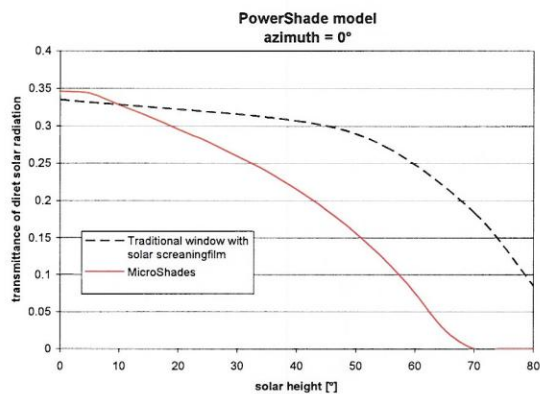


Figure 4 The transmittance of direct solar radiation through the two windows in figures 2 and 3 at an azimuth of 0°.

A special type of MicroShade is PowerShade. These are similar to MicroShade but are coated with solar cells on the surface facing the outside. PowerShades are currently under development. More information on PowerShade/MicroShade can be found on www.photosolar.dk.

TEST ROOMS

MicroShade and traditional windows were tested side-by-side in two well-defined and heavily monitored test rooms at Danish Technological Institute, Taastrup, Denmark. The floor area and volume of the test rooms were 6.84 m² and 16.73 m³ respectively. The window of each test room consisted of two transparent areas of totalling 1.98 m².

The test rooms, the thermo-physical properties of the materials of the test rooms and the monitoring system are described in detail in (Jensen, 2008a).

CALIBRATION OF THE MODELS

A model of the two test rooms was developed in the simulation program ESP-r (ESRU, 2001).

A step by step approach was applied in the calibration of the ESP-r and MicroShade models:

- Step 1. Calibration of the solar radiation on the facade
- Step 2. Calibration of the model of the traditional window
- Step 3. Calibration of the diffuse radiation through the MicroShade window
- Step 4. Calibration of the MicroShade model

Step 5. Calibration of the thermal model of the test rooms. However, this step will not be dealt with in this paper

The above calibration steps are documented in details in (Jensen, 2008b).

For the calibration exercises measurements from three periods in 2008 were chosen:

Table 1

The three measuring periods applied in the calibration exercise.

Season	Period	Solar height °
Winter	21/1-17/2 2008	14.4-22.7
Spring (autumn)	25/3-26/4 2008	36.1-47.8
Summer	1-28/6 2008	56.5-57.8

Calibration of the solar radiation on the facade

The input to the simulation program was the global solar radiation and the horizontal diffuse radiation on the roof just above the test rooms using calibrated precision pyranometers. The solar measuring station is shown in figure 5. The solar radiation on the facade was also measured with a calibrated precision pyranometer.



Figure 5 The solar measuring station.

Figure 6 shows an example of the comparison between measured and calculated solar radiation on the facade. The other periods show similar agreement (Jensen, 2008b). In order to obtain this very good agreement it was necessary to use an albedo of only 0.05. This is a low value but may be justified when considering that the facade faces a courtyard where the surfaces of the surrounding buildings are in the shade most of the time.

The standard solar algorithms in ESP-r for calculation of solar radiation were applied in the calibration

Calibration of the model of the traditional window

Calibrated precision pyranometers were applied for measuring the solar radiation entering the rooms.

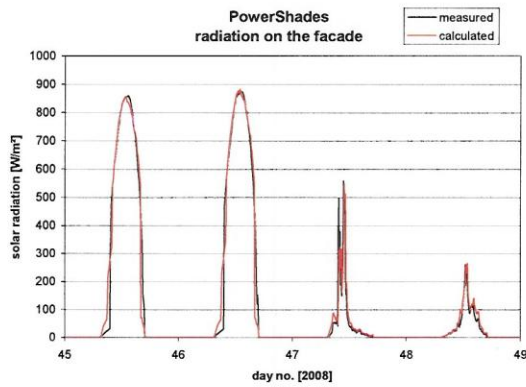


Figure 6 Comparison between measured and calculated solar radiation on the facade

Although the project concerned MicroShade the model of the traditional window was also calibrated. The reason for this was that both windows are low-e windows with at low-e coating. This coating changes the spectral distribution of solar radiation which might influence the accuracy of the pyranometers. However, the transmittance through a traditional window is very well-defined. So if good agreement is obtained between measured and calculated solar radiation for the traditional window it is implied that the pyranometers are capable of measuring the solar radiation coming through the MicroShade window. In fact such a calibration exercise is also a validation exercise on the pyranometers behind the windows.

Figure 7 shows a comparison between measured and calculated incoming solar radiation through the traditional window. The other periods show similar agreement (Jensen, 2008b).

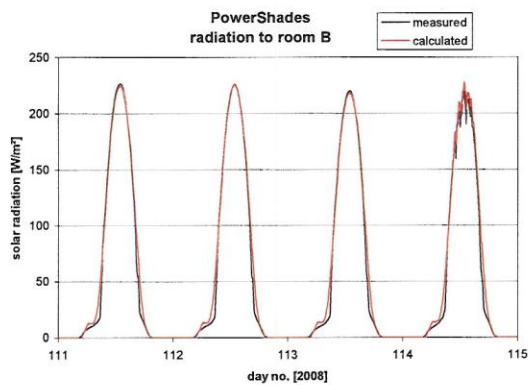


Figure 7 Comparison between measured and calculated solar radiation through the traditional window.

Based on the above it was concluded that the model of the traditional window was precise enough and that the measured solar radiation through the MicroShade window was applicable for calibration of the model of the MicroShade window.

Calibration of the diffuse radiation through the MicroShade

The matrix shown at the end of the paper is automatically generated by a special purpose program where the input is the geometry of the holes shown in figure 1. The program calculates for combinations of all vertical and horizontal incidence angles of the sun the total transmittance of direct radiation, the absorption in each layer of the window and the enhancement of the transmitted diffuse radiation due to scattering of direct radiation in the MicroShade. However, so far no model or experience exists on how to calculate the transmittance of diffuse radiation through MicroShades. Therefore, the transmittance of diffuse radiation is here found empirically by using the measured data from the test rooms. Days with only diffuse radiation have been chosen. During those days the ratio between the solar radiation on the façade and through the MicroShade window was calculated as shown in figure 8. That ratio is the transmittance of diffuse radiation.

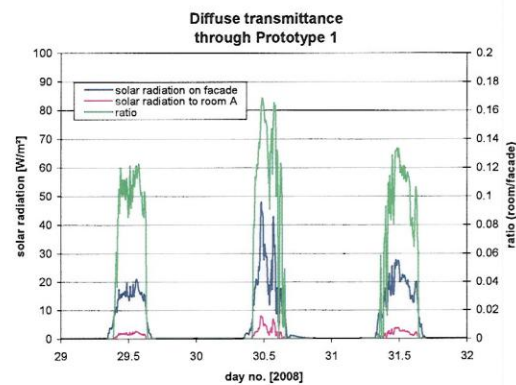


Figure 8 The solar radiation on the façade and to room A together with the ratio (= transmittance of diffuse radiation) for three days in January 2008 with overcast conditions.

Unfortunately, there were only few days with overcast conditions during the first half of 2008 – and that is not normal for Danish weather conditions. Figure 9 shows the calculated transmittance for those few days. The values in figure 9 should be similar or even higher during the winter due to the lower solar height but an opposite tendency is seen – increasing transmittance with increasing solar height. The increasing tendency is assumed to be caused by two facts:

1. solar radiation during January (two first points in figure 9) was very low and therefore the uncertainty is very high.
2. there might have been some direct radiation at high solar heights (two-three last points in figure 9).

Figure 9 shows that there is a need for the development of a rigid calculation method for the diffuse radiation through MicroShade. Such method are being developed when writing this. However, for the

calibration study a diffuse transmittance coefficient of 0.12 was chosen.

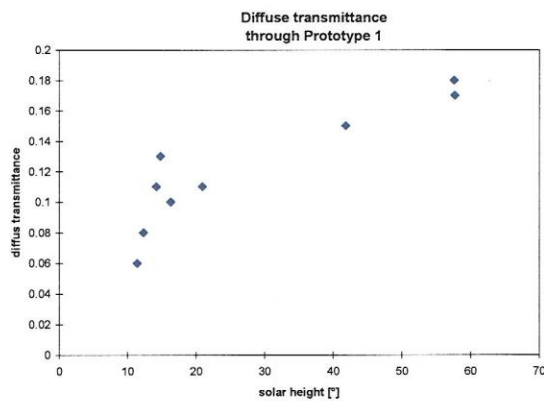


Figure 9 The transmittance of diffuse radiation dependent on solar height.

Calibration of the MicroShade model

A novel module for modelling bidirectional transmission through transparent multilayered constructions (developed in the project (Teknologisk Institute, 2005)) has been used in the following exercises. As input the module uses the matrix shown in figure 24. Using the special purpose program mentioned on the previous page the matrix for the actual MicroShade was generated and applied in the model of the test rooms. Figure 10 shows a comparison between measured and calculated solar radiation through the MicroShade window.

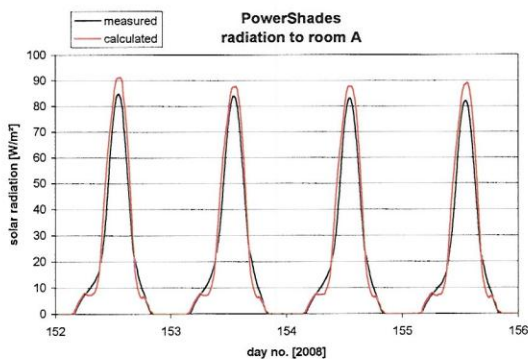


Figure 10 Measured and calculated solar radiation through the MicroShade window.

Figure 10 shows that the model overestimates the incoming solar radiation at noon and underestimates the incoming solar radiation at early morning and late afternoon. The main problem is the overestimation at noon as there is only a small amount of energy in the solar radiation at early morning and late afternoon.

As a first attempt the transmittance of direct solar radiation in the matrix was simply multiplied by an empirically found factor (using measurements from

all three measuring periods) dependent on the solar height:

$$f_s = -0.002 \cdot sh + 1.0529 \quad (1)$$

where: sh is the solar height

Figure 11 shows the result of applying this factor in the calculations.

The agreement is now much better but still not good enough as shown in figure 12. This close-up reveals that an overestimation also occurs before and after noon. Figure 13 shows the relative overestimation during six days in July 2006.

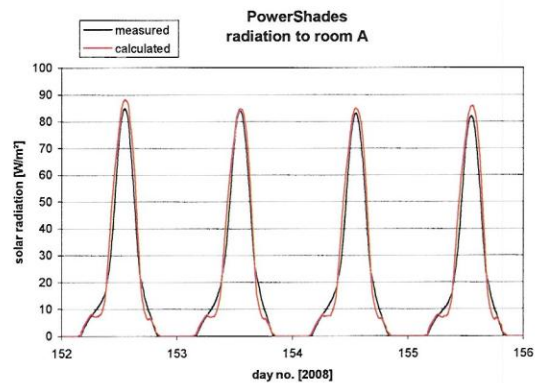


Figure 11 Measured and calculated solar radiation through the MicroShade window using the modified model - based on solar height.

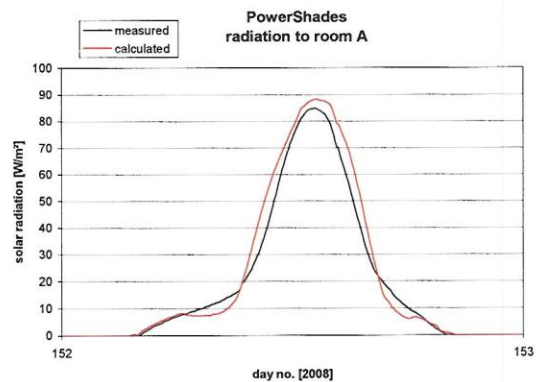


Figure 12 Close-up of figure 11.

Based on figure 13 a new correction factor dependent on the relative azimuth (azimuth relative to the facade) was developed:

$$f_a = -3.6223 \cdot 10^{-12} \cdot x^6 - 4.9168 \cdot 10^{-11} \cdot x^5 + 5.343 \cdot 10^{-8} \cdot x^4 + 5 \cdot 10^{-7} \cdot x^3 - 9.82 \cdot 10^{-4} \cdot x^2 - 9.108 \cdot 10^{-4} \cdot x + 1.0338 \quad (2)$$

for $f_a < 1$, for $f_a \geq 1$ f_a is set to 1

where: x is the relative azimuth. The relative azimuth is zero when the sun vertically is perpendicular to the facade.

Figures 14-15 shows the result of applying this factor in the calculations.

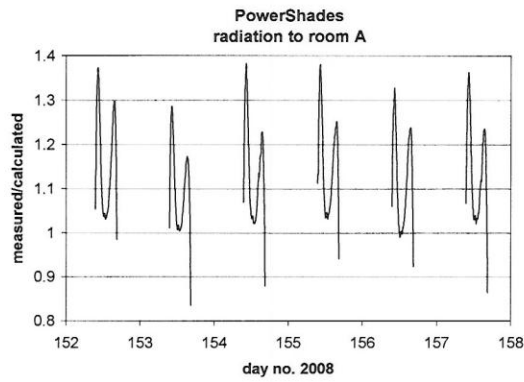


Figure 13 The relative overestimation.

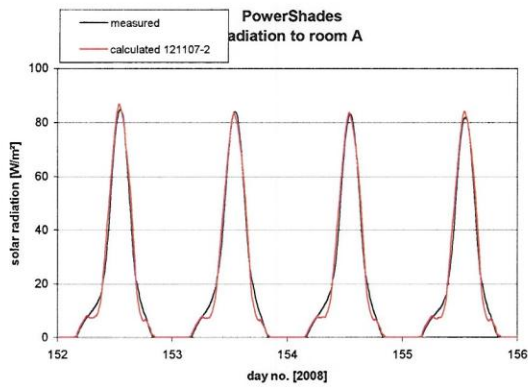


Figure 14 Measured and calculated solar radiation through the MicroShade window using the modified model called 121107-2 - based on solar height and relative azimuth.

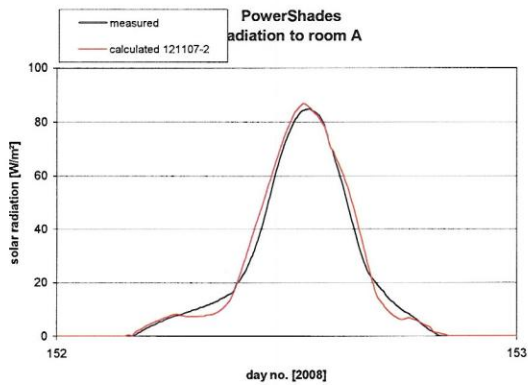


Figure 15 Clos- up of figure 14.

Figures 14 and 15 shows very good agreement between measured and calculated solar radiation through the MicroShade window.

The other periods show similar agreement (Jensen, 2008b) – both for clear sky and overcast conditions – as shown in the following figures. However, there was some underestimation during clear sky conditions at low solar heights as shown in figure 19.

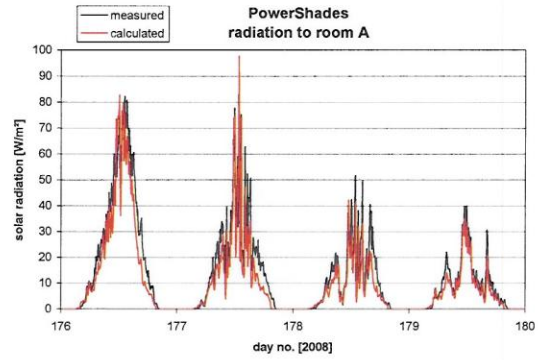


Figure 16 Measured and calculated solar radiation through the MicroShade window using the modified model 121107-2.

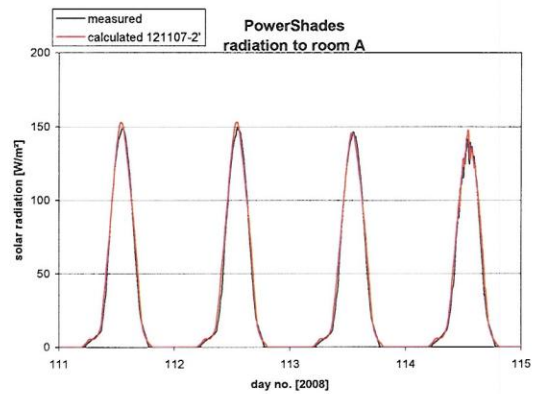


Figure 17 Measured and calculated solar radiation through the MicroShade window using the modified model 121107-2.

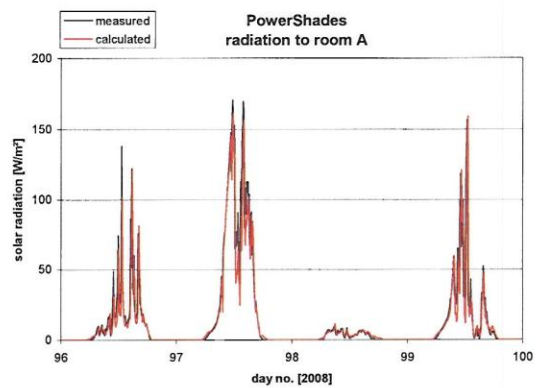


Figure 18 Measured and calculated solar radiation through the MicroShade window using the modified model 121107-2.

The above calibration exercise is to show that it is possible to generate a matrix/model of MicroShade windows, which represents the optical properties of MicroShade windows very well. The findings from the above calibration exercise will be utilized to modify the special purpose program that generates

the matrix so measurements no longer will be necessary in order to establish a well-matching matrix. The new version of the program will to more precisely describe the transmission of both direct and diffuse solar radiation through windows with MicroShades. The new program will be tested in a new validation exercise. A reliable program will ease the development of Micro- and PowerShade considerably as it is cheaper to perform parametric studies using a computer model than to perform measurements.

Figure 20 shows that the intention from figure 4 regarding MicroShade has been fulfilled. Figure 20 shows based on measurements that the investigated MicroShade during the summer at noon decreases the amount of incoming solar radiation with 50% compared to a traditional window with solar control coating, while letting the same amount of solar radiation in during the winter where solar heating most often is valuable

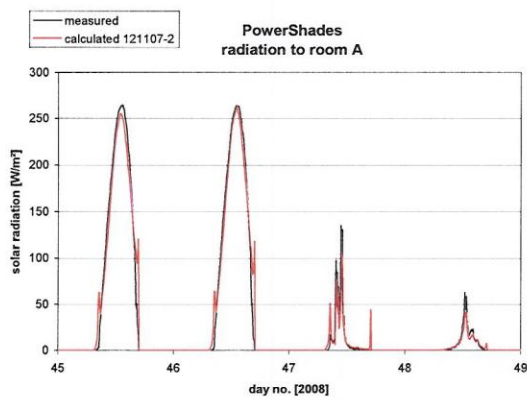


Figure 19 Measured and calculated solar radiation through the MicroShade window using the modified model 121107-2.

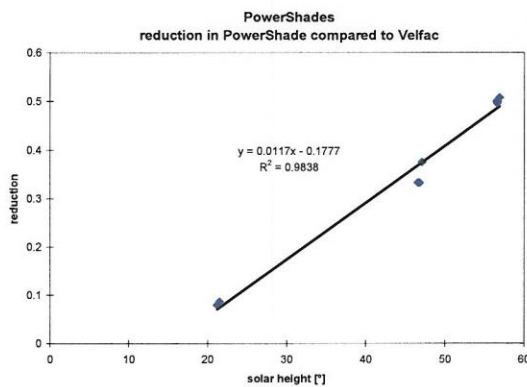


Figure 20 The measured reduction of the transmission of solar radiation due to MicroShade at noon compared to a traditional window with solar control coating.

Calibration of the thermal model of the test rooms

Although the test rooms are very simple the modelling of them is rather complex and the calibration of

this part of the model is difficult to perform due to the many parameters and large uncertainties. The calibration of the model of the test rooms will not be dealt with here, as the main purpose of the paper is to describe the calibration of the bidirectional model in ESP-r of MicroShade. Please refer to (Jensen, 2008b) if interested in step 5 of the calibration procedure.

Here it will only be stated that the investigated MicroShade (in the test room) is capable of lowering the peak temperature in the test room at noon with up to 2 K compared to the traditional window with solar control coating. MicroShade may thus reduce potential overheating risks and decrease the cooling demand. This is shown in the following paragraph.

THE PERFORMANCE OF MICRO-SHADES IN REAL BUILDINGS

It has been shown that although not perfect the model 121107-2 represent the optical performance of a MicroShade window rather well. Using this model it will in the following be shown how this type of solar control device performs compared to other solar shading measures.

ESP-r has been used to simulate the performance of MicroShade in a real Danish building. The building was designed by the world famous architects “Henning Larsen”. The building is the domicile of a bank and it is situated in the centre of Copenhagen. Figure 21 shows the north façade of the building. The figure shows the transparency of the building.

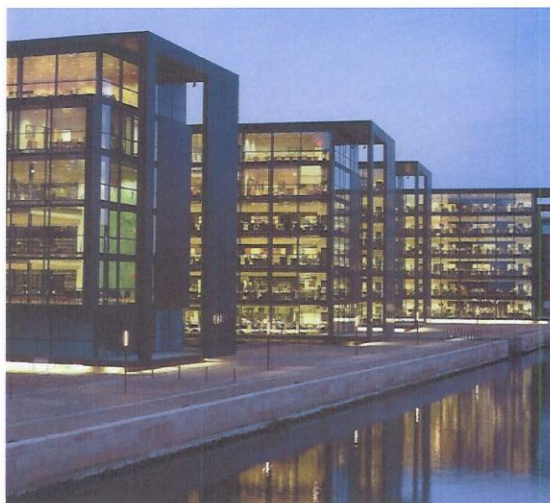


Figure 21 The north facing facades of the building.

90% of the south and north facades are transparent so extensive solar control is necessary in order to reduce the overheating problems and thereby reduce the cooling load and energy demand of the building. The glazing of the facades has solar control coating which reduces the g-value of the windows to 0.32 – ie rather similar to the original traditional window dealt with earlier in this paper. This very low g-value is, however, not sufficient for ensuring a comfortable indoor

climate in the building so external solar shading has been added to the south facades as seen in figure 22.



Figure 22 One south façade of the building.

As shown in figure 23 the external solar shading consists of movable lamellas made of glass with silk screen printing. The lamellas follow automatically the position of the sun (the solar height) over the day - ie the lamellas are always perpendicular to the beam radiation so that all direct solar radiation hits the lamellas before hitting the windows.



Figure 23 The external solar shading consisting of glass lamellas with silk screen printing.

Due to the silk screen printing on glass there is still some outlook through the window even when the lamellas are closed.

The combination of solar control glass and external solar shading gives an overall g-value of app. 0.17 – which is very low.

An ESP-r model of the building was developed in an earlier project (Danish Technological Institute, 2005) – please refer to this for further information. The U-value for the facades are 1.12 W/m^2 . The ventilation system maintain an air change rate of 5^{-h} . The internal heat gain is during office hours 49 W/m^2 .

In the present case, only one floor of the building has been simulated. The floor area is 642 m^2 .

Simulations have been carried out with four different types of south facades:

- the present south façade with at g-value of 0.17 – figure 23
- the present south façade without the external solar shading device
- MicroShade using the calibrated model 121107-2
- MicroShade using the non-calibrated model applied in figure 10 (called model 121107). The reason for this is to show the necessity of calibration of the MicroShade model.

Table 2 Absolute annual cooling demand and relative demand compared to the present situation. The column in % after the cooling demand in kWh states how much larger (in %) the cooling demand is compared to the present situation.

Facade	Cooling demand	
	kWh	%
Present, g-value: 0.17	6106	-
Present without external solar shade, g-value: 0.32	9091	49
MicroShade, 121107	7483	23
MicroShade, 121107-2	6584	8

121107-2 performs almost as well as the present rather complex solar control system and much better than traditional sun control glass.

In addition table 2 shows the importance of a correct model of the solar transmittance through the MicroShade. The cooling demand with 121107 is app. 15 % higher than with 121107-2.

The simulations also show that there is hardly any difference in the heating load between the four systems in table 2. The difference in electricity demand for artificial lightning should also be compared but is beyond the scope of the work behind this paper.

CONCLUSION

The described work shows that via calibration using measured data from test rooms it is possible to obtain a model that represents the complex optical performance of MicroShade very well. The model of MicroShade has been developed using the bidirectional transmission module for transparent multilayered constructions in the simulation program ESP-r.

The purpose of MicroShade is to reduce the overheating risk during the summer with large solar heights. The measurements show that the objective of MicroShade was met as the incoming solar energy was reduced by about 50% in the summer at noon compared to a traditional window with solar control coating and a g-value of 0.37.

Simulations on a real building show that the cooling demand in this particular building is in the same order of magnitude when using Micro-Shades as when considering the existing rather complex external solar shading system together with windows with solar control coating (g-value: 0.17).

ACKNOWLEDGEMENT

The work presented in this paper has been financed by Energinet.dk.

The described work was performed in cooperation with the Danish firm PhotoSolar that develops/produces MicroShade™ and PowerShade.

REFERENCES

ESRU, 2001. Data Model Summary – ESP-r – Version 9 series. Energy Systems Research Unit, University of Strathclyde. December 2001.

Jensen, S.Ø., 2008a. Test rooms for test of PowerShades. Danish Technological Institute. ISBN 87-7756-769-2

Jensen, S.Ø., 2008b. Test of PowerShades and calibration of models with PowerShades. Danish Technological Institute. ISBN 87-7756-770-6.

Technological Institute, 2005. Transparent solar cells – the electricity producing solar shading of the future (in Danish). PEC Group, Danish Technological Institute.

```

*BIDIRECTIONAL
*types,1
*item,121107
*layers,5,glass1,shading,glass2,air,glass3
*sets,1 # there is only this set of optical data
*start_set
*diffuse_abs,0.036,0.372,0.013,0.000,0.042
*diffuse_trn,0.12 ←----- diffuse transmittance
*direct_angs,37,37
*data
#Incidence angle, Total Glass 1, Shading device, Glass 2, Air, Glass 3, Converted diffuse fraction
#HorizontVertical, Transmittance, Absorb, Absorb, Absorb, Absorb, Absorb, Direct-diffuse
#Degrees, Degrees
-90 -90 0 0 0 0 0 0 0
-90 -85 0 0 0 0 0 0 0
-90 -80 0 0 0 0 0 0 0
-90 -75 0 0 0 0 0 0 0
-90 -70 0 0 0 0 0 0 0
-90 -65 0 0 0 0 0 0 0
-90 -60 0 0 0 0 0 0 0
-90 -55 0 0 0 0 0 0 0
-90 -50 0 0 0 0 0 0 0
-90 -45 0 0 0 0 0 0 0
-90 -40 0 0 0 0 0 0 0
-90 -35 0 0 0 0 0 0 0
-90 -30 0 0 0 0 0 0 0
-90 -25 0 0 0 0 0 0 0
-90 -20 0 0 0 0 0 0 0
-90 -15 0 0 0 0 0 0 0
-90 -10 0 0 0 0 0 0 0
-90 -5 0 0 0 0 0 0 0
-90 0 0 0 0 0 0 0 0
-90 5 0 0 0 0 0 0 0
-90 10 0 0 0 0 0 0 0
-90 15 0 0 0 0 0 0 0
-90 20 0 0 0 0 0 0 0
-90 25 0 0 0 0 0 0 0
-90 30 0 0 0 0 0 0 0
-90 35 0 0 0 0 0 0 0
-90 40 0 0 0 0 0 0 0
-90 45 0 0 0 0 0 0 0
-90 50 0 0 0 0 0 0 0
-90 55 0 0 0 0 0 0 0
-90 60 0 0 0 0 0 0 0
-90 65 0 0 0 0 0 0 0
-90 70 0 0 0 0 0 0 0
-90 75 0 0 0 0 0 0 0
-90 80 0 0 0 0 0 0 0
-90 85 0 0 0 0 0 0 0
-90 90 0 0 0 0 0 0 0
-85 -90 0 0 0 0 0 0 0
-85 -85 0 0.022 0 0 0 0 0
-85 -80 0 0.039 0.003 0 0 0 0
-85 -75 0 0.039 0.02 0 0 0 0.001
-85 -70 0 0.039 0.035 0 0 0 0.002
-85 -65 0 0.039 0.05 0 0 0 0.003

```

- 1th column: azimuth
- 2th column: solar height
- 3th column: total direct transmittance
- 4th column: absorption in the outer layer of glass
- 5th column: absorption in the PowerShade foil
- 6th column: absorption in the in the glass behind the PowerShade foil
- 7th column: absorption in the air gab of the window
- 8th column: absorption in the inner layer of glass
- 9th column: enhancement of diffuse radiation due to scattering of direct radiation in the PowerShade fail

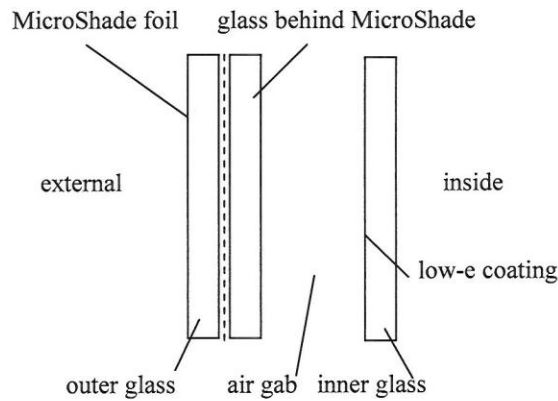


Figure 25 Example of a MicroShade matrix. The matrix covers azimuths and solar heights from -90 to 90° with steps of 5°.

Appendix B

Comparison between measured and calculated radiation through the MicroShade window with scattering factors of 0, 1 and 2 %

Winter period – scattering factor 0%

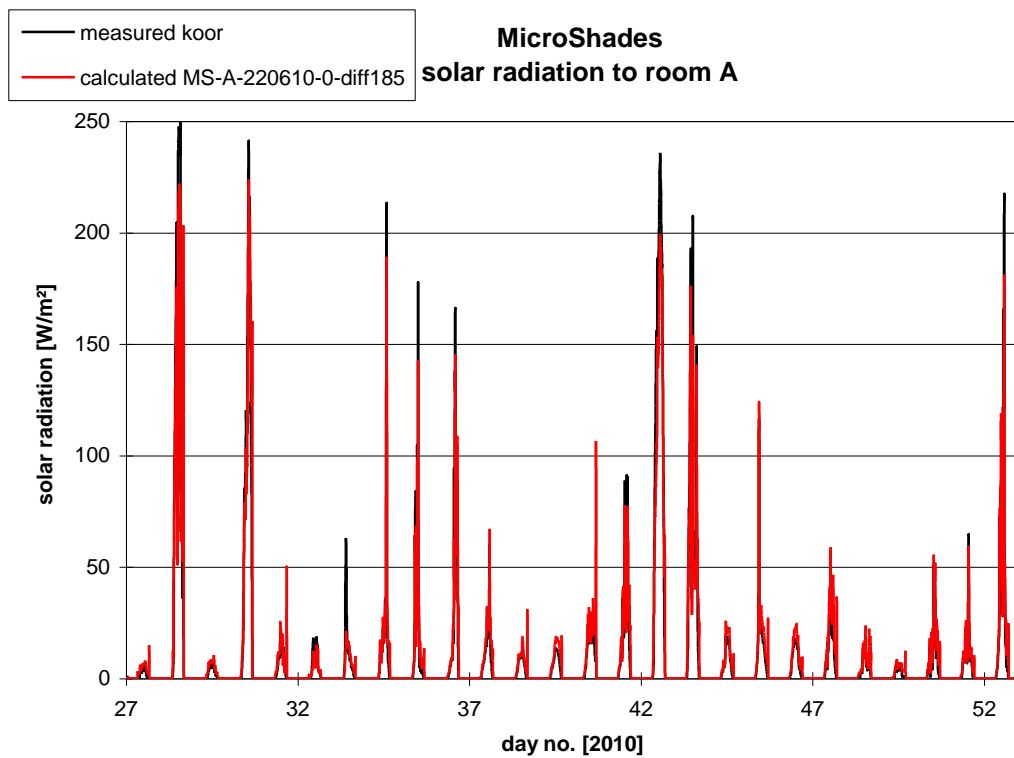


Figure B.1. Solar radiation through the MicroShade window during summer period. Scattering factor: 0%.

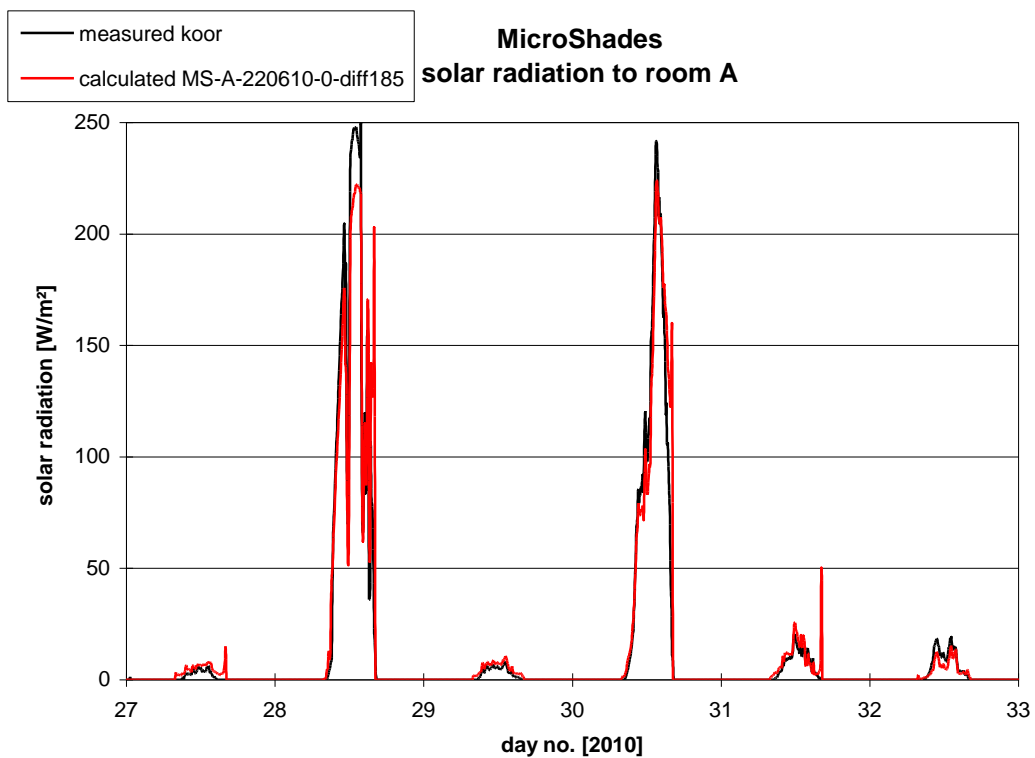


Figure B.2. Solar radiation through the MicroShade for 5 days in the winter (January 27-February 1, 2010). Scattering factor: 0%.

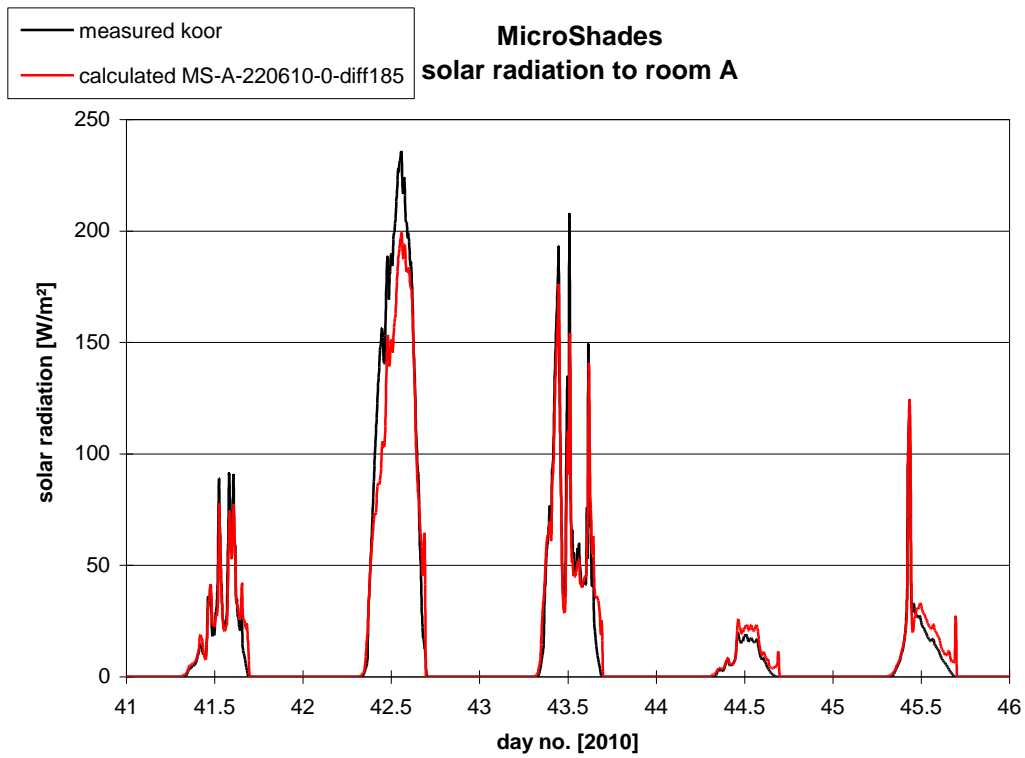


Figure B.3. Solar radiation through the MicroShade for 5 days in the winter (February 11-14, 2010). Scattering factor: 0%.

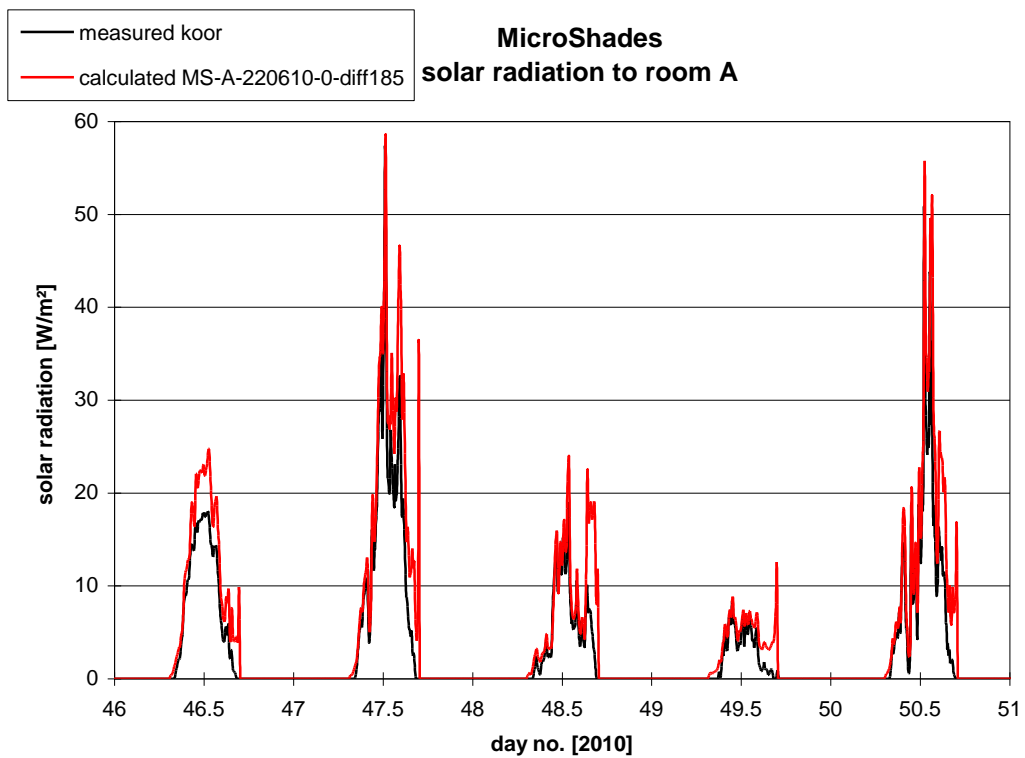


Figure B.4. Solar radiation through the MicroShade for 5 days in the winter (February 15-19, 2010). Scattering factor: 0%.

Winter period – scattering factor 1%

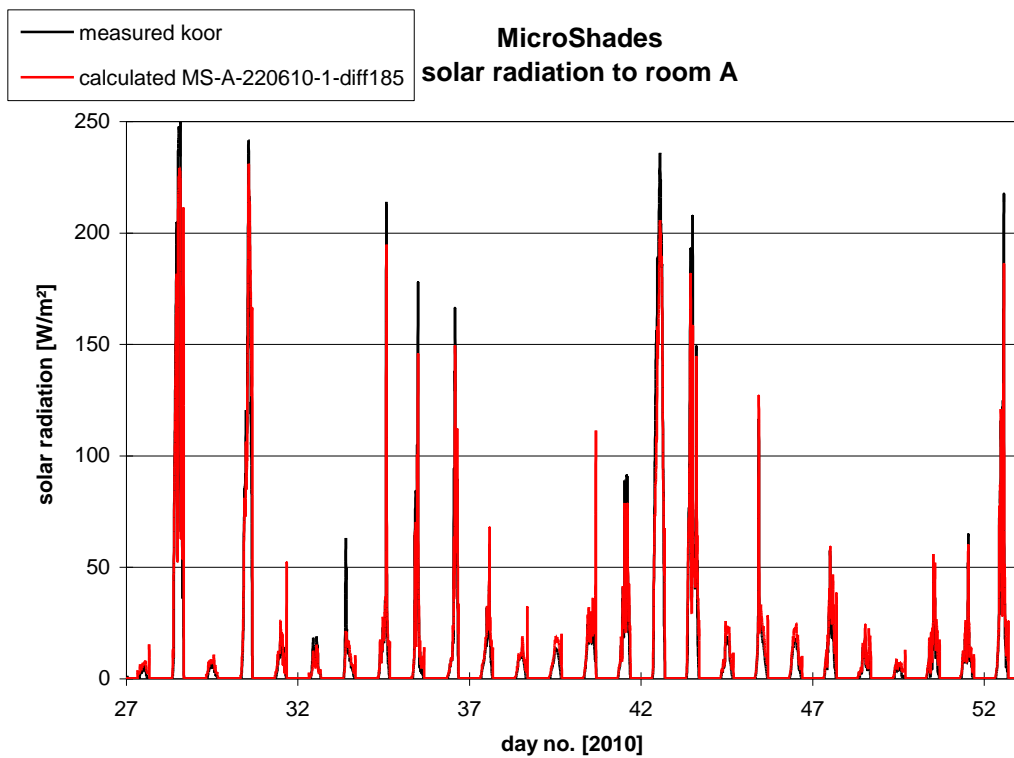


Figure B.5. Solar radiation through the MicroShade window during summer period. Scattering factor: 1%.

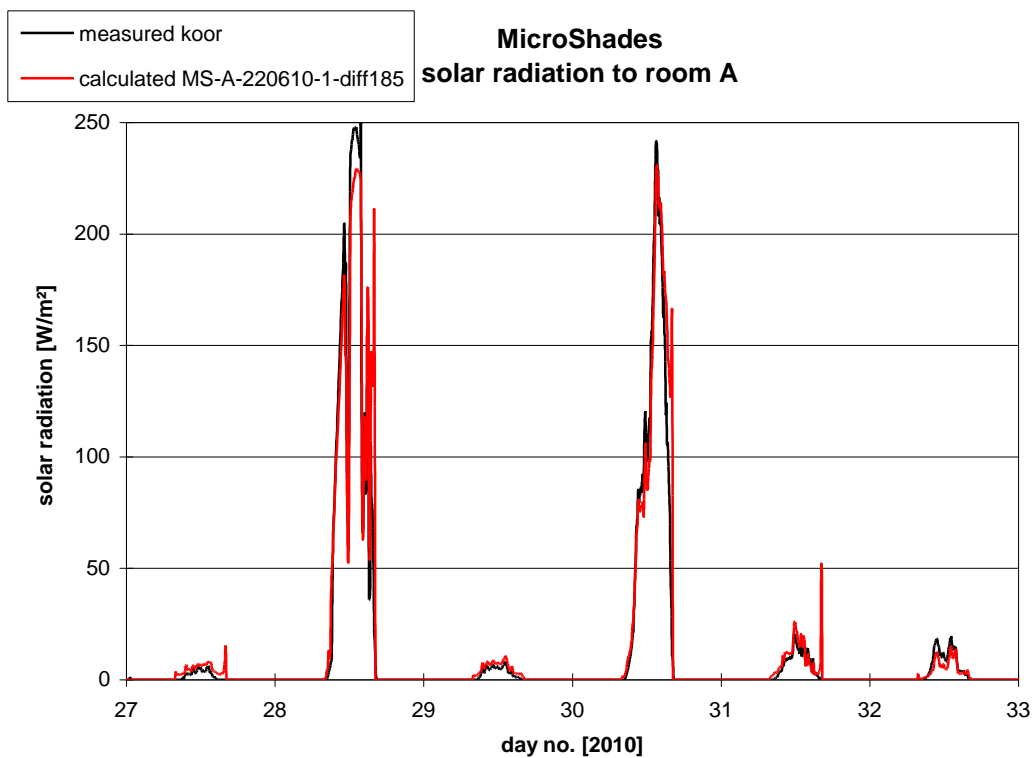


Figure B.6. Solar radiation through the MicroShade for 5 days in the winter (January 27-February 1, 2010). Scattering factor: 1%.

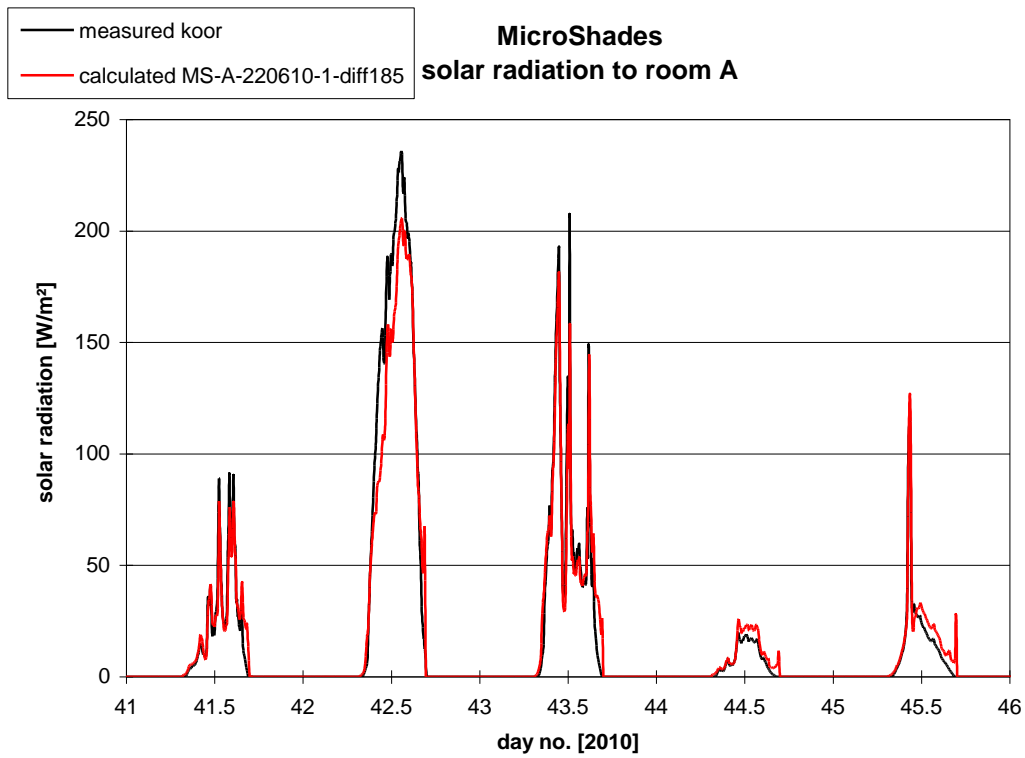


Figure B.7. Solar radiation through the MicroShade for 5 days in the winter (February 11-14, 2010). Scattering factor: 1%.

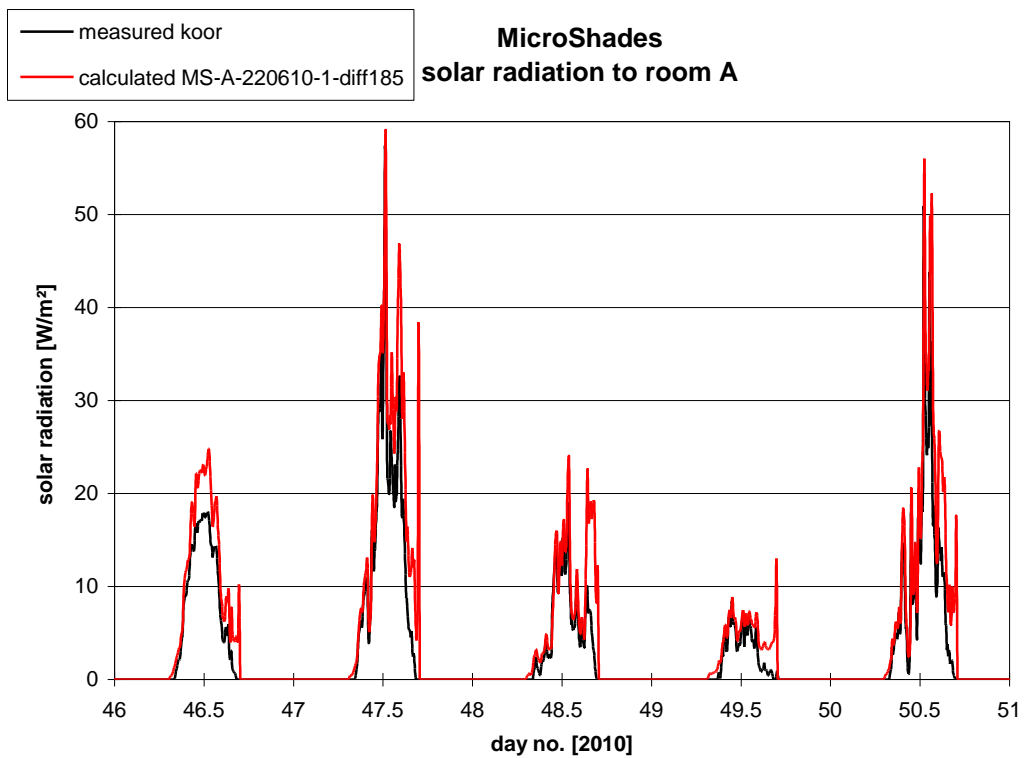


Figure B.8. Solar radiation through the MicroShade for 5 days in the winter (February 15-19, 2010). Scattering factor: 1%.

Winter period – scattering factor 2%

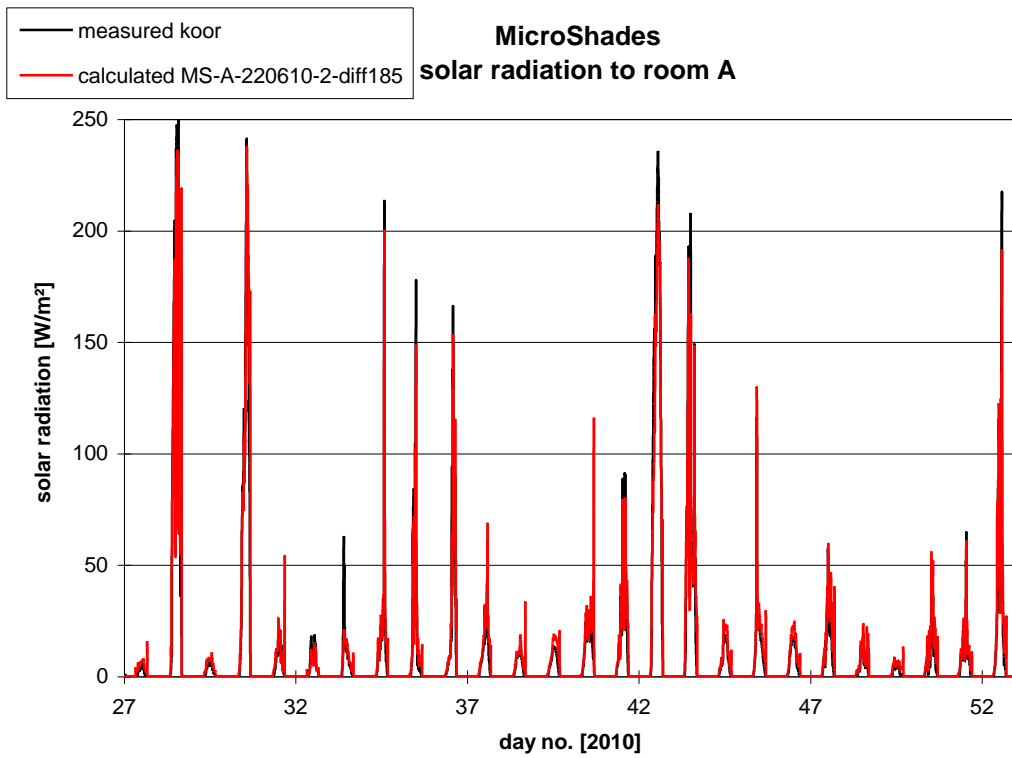


Figure B.9. Solar radiation through the MicroShade window during summer period. Scattering factor: 2%.

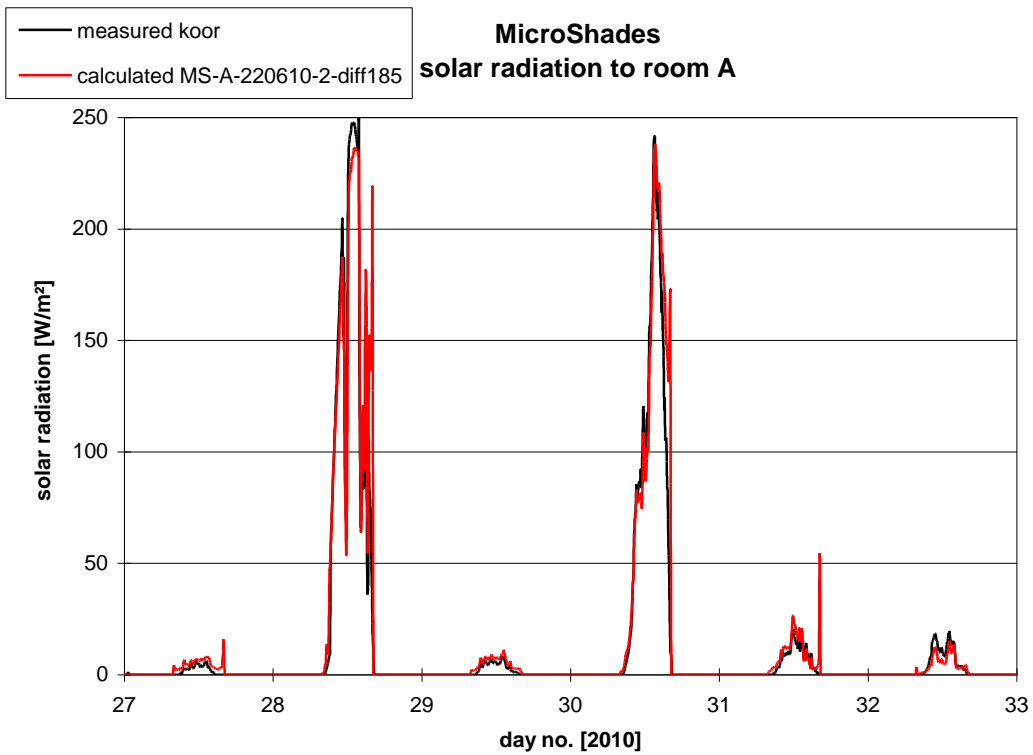


Figure B.10. Solar radiation through the MicroShade for 5 days in the winter (January 27-February 1, 2010). Scattering factor: 2%.

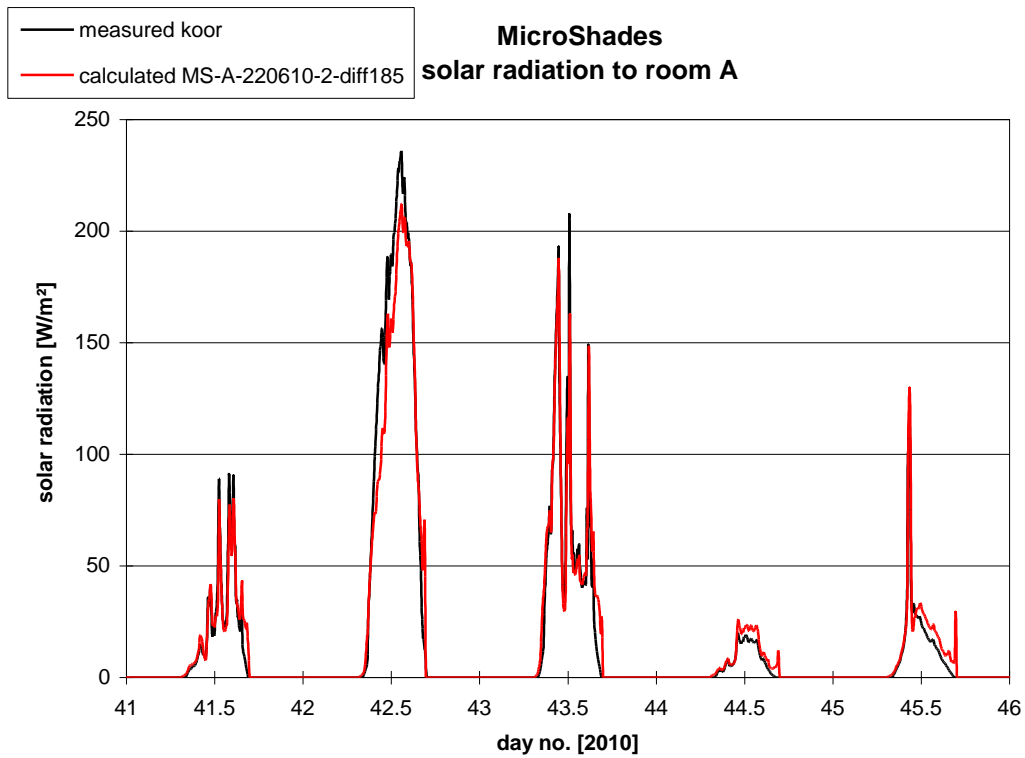


Figure B.11. Solar radiation through the MicroShade for 5 days in the winter (February 11-14, 2010). Scattering factor: 2%.

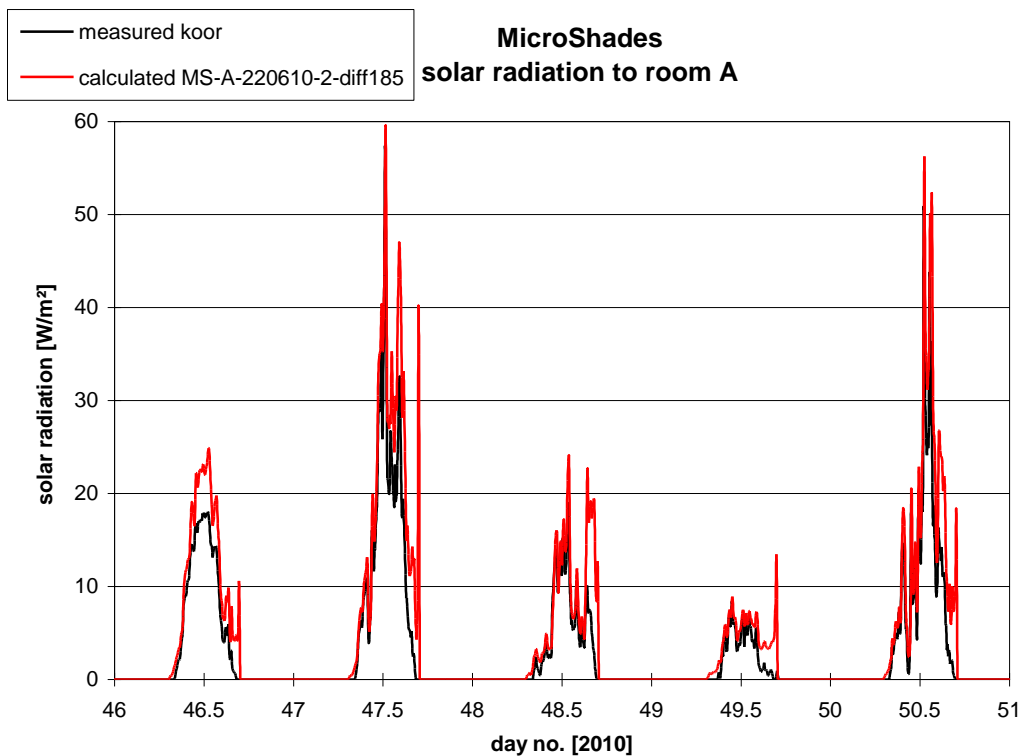


Figure B.12. Solar radiation through the MicroShade for 5 days in the winter (February 15-19, 2010). Scattering factor: 2%.

Spring period – scattering factor 0%

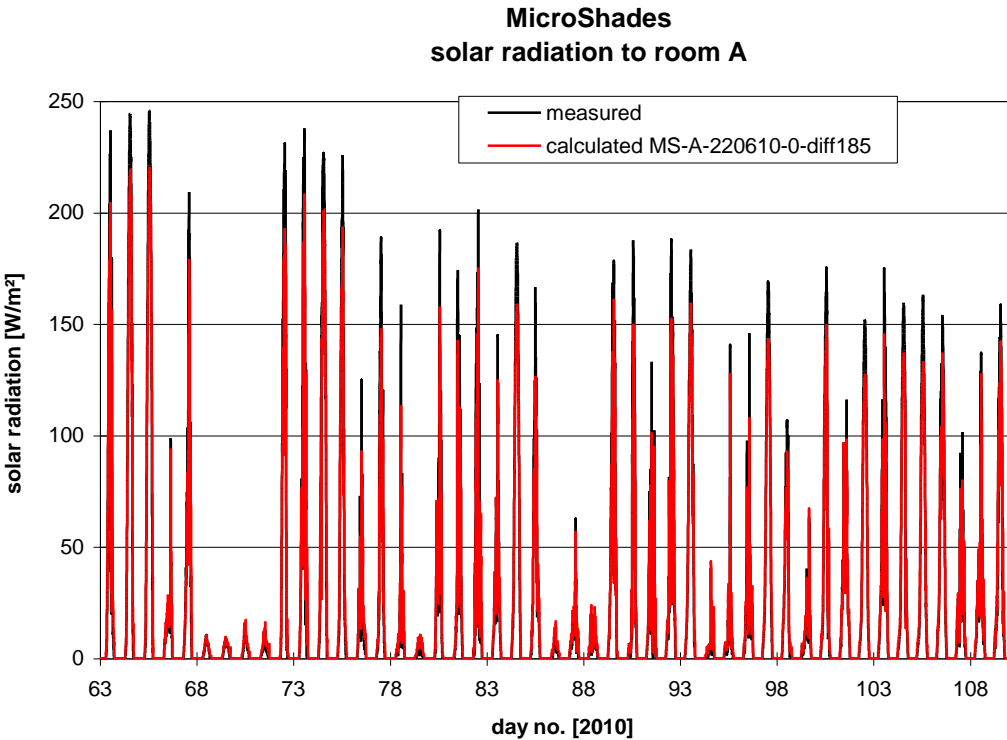


Figure B.13. Solar radiation through the MicroShade window during spring period. Scattering factor: 0%.

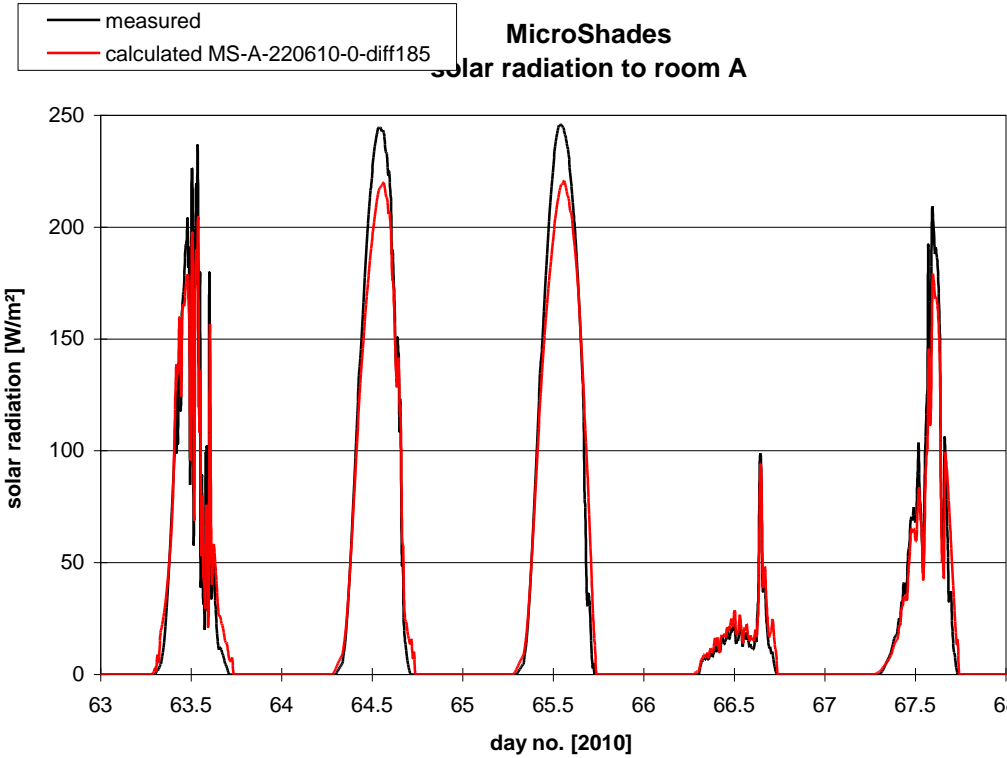


Figure B.14. Solar radiation through the MicroShade for 4 days in the spring (March 4-8, 2010). Scattering factor: 0%.

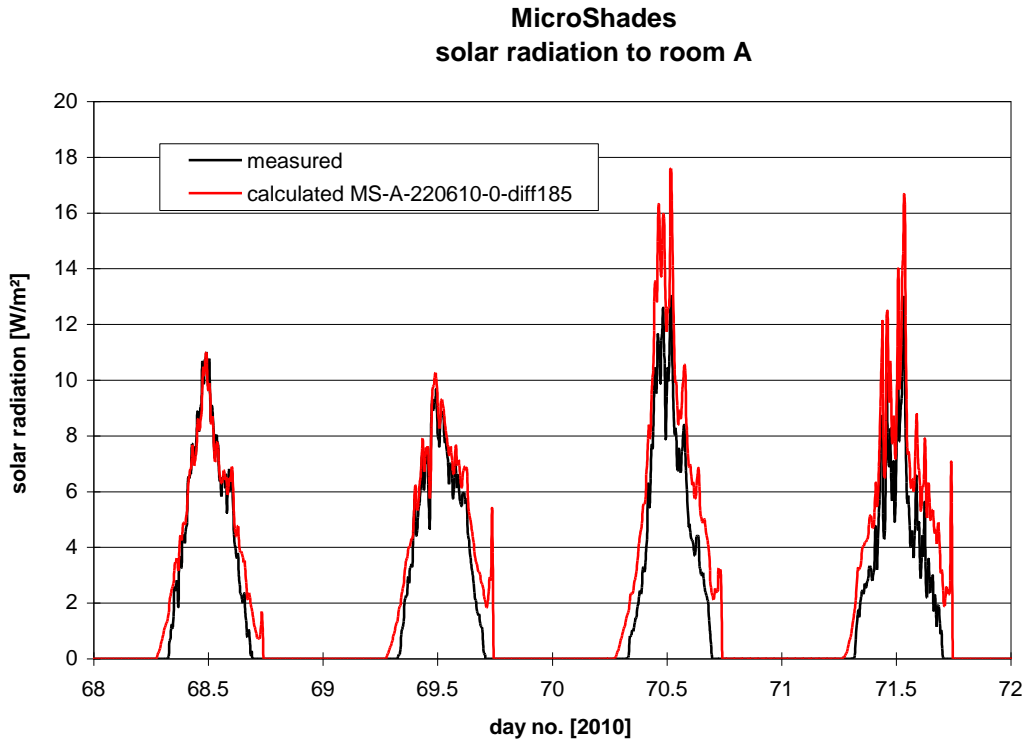


Figure B.15. Solar radiation through the MicroShade for 5 days in the spring (March 12-16, 2010). Scattering factor: 0%.

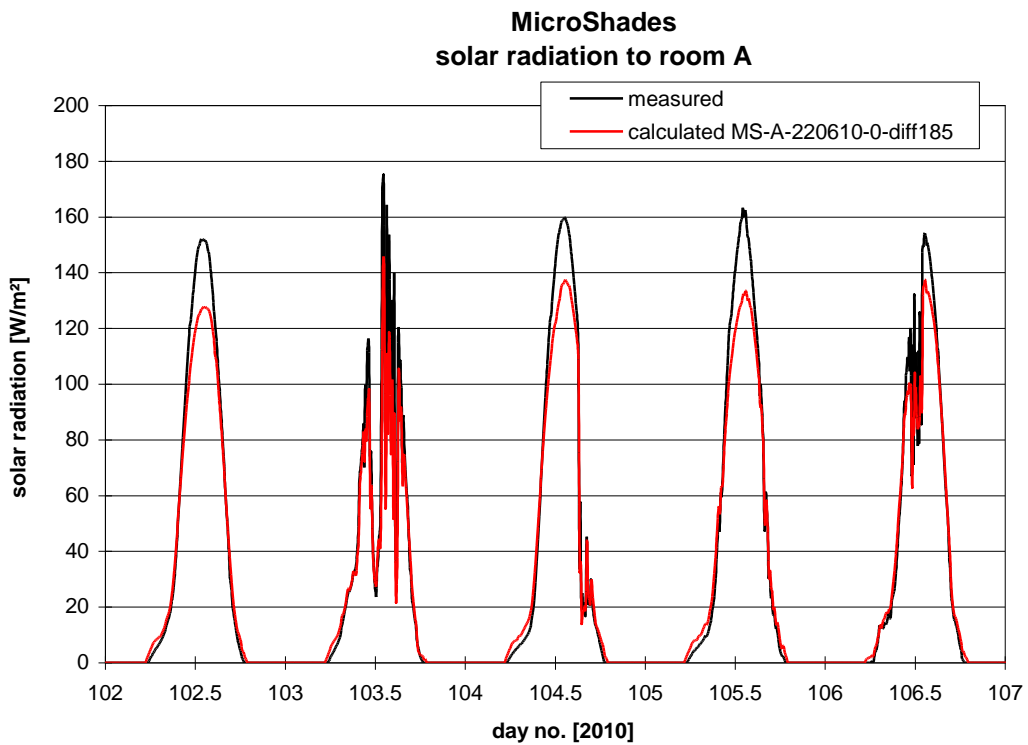


Figure B.16. Solar radiation through the MicroShade for 5 days in the spring (April 12-16, 2010). Scattering factor: 0%.

Spring period – scattering factor 1%

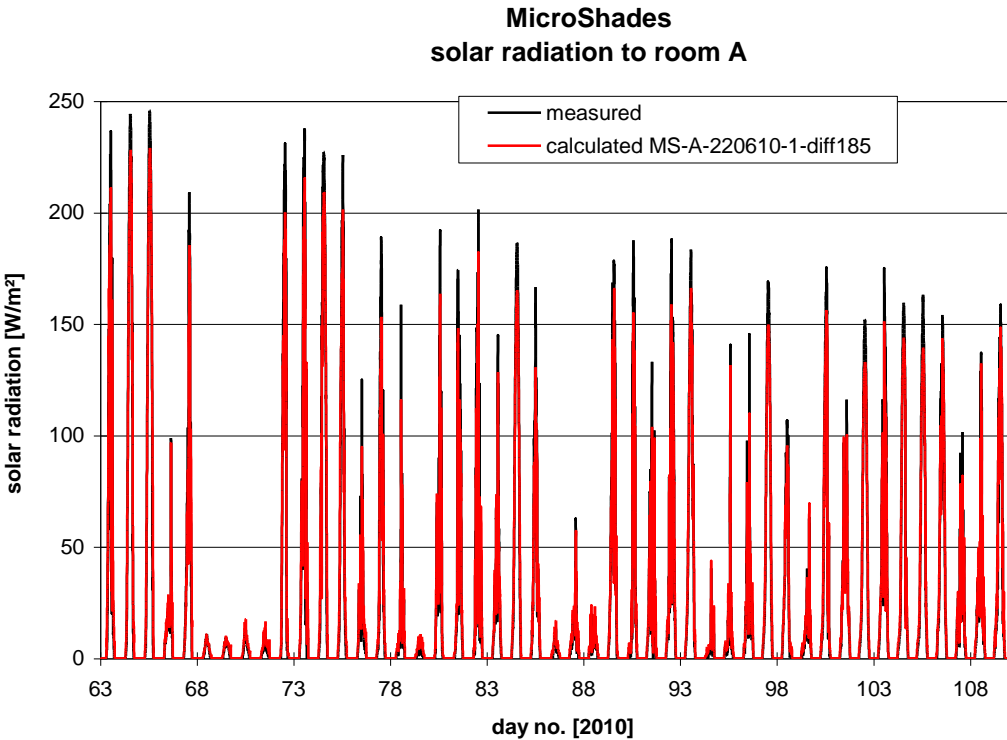


Figure B.17. Solar radiation through the MicroShade window during spring period. Scattering factor: 1%.

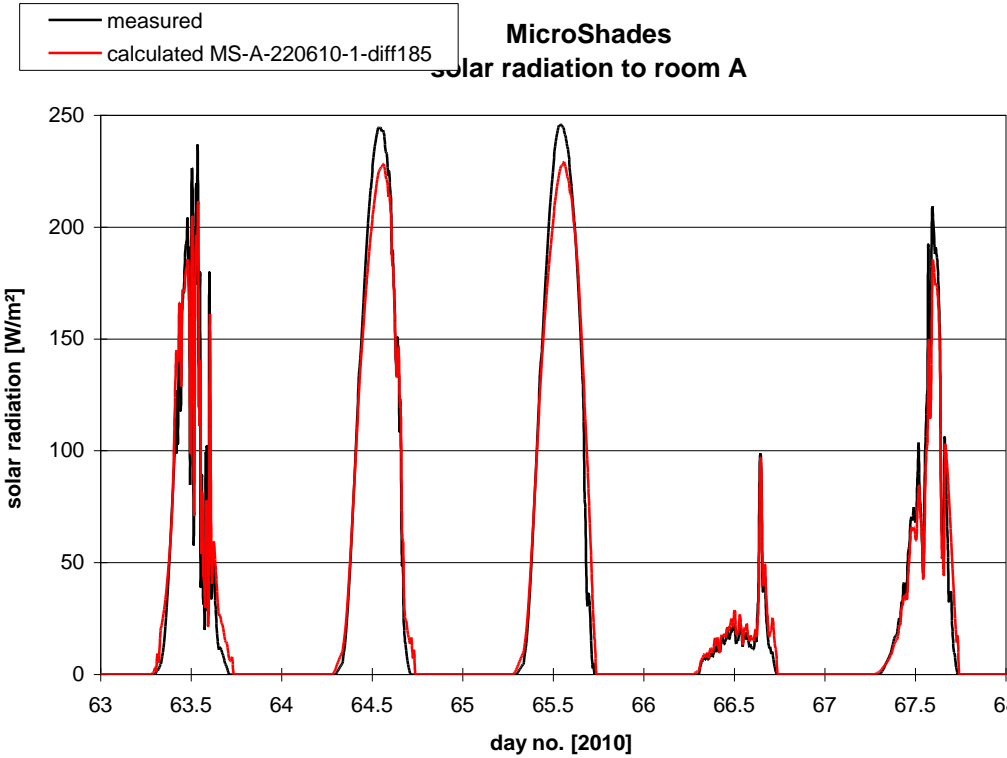


Figure B.18. Solar radiation through the MicroShade for 4 days in the spring (March 4-8, 2010). Scattering factor: 1%.

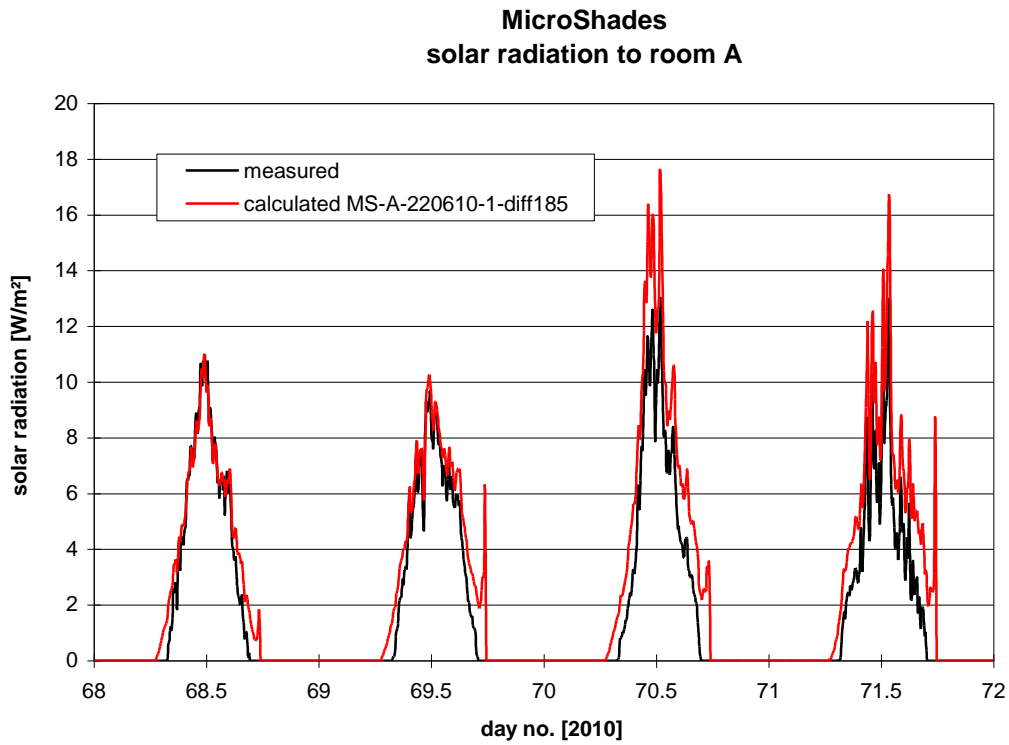


Figure B.19. Solar radiation through the MicroShade for 5 days in the spring (March 12-16, 2010). Scattering factor: 1%.

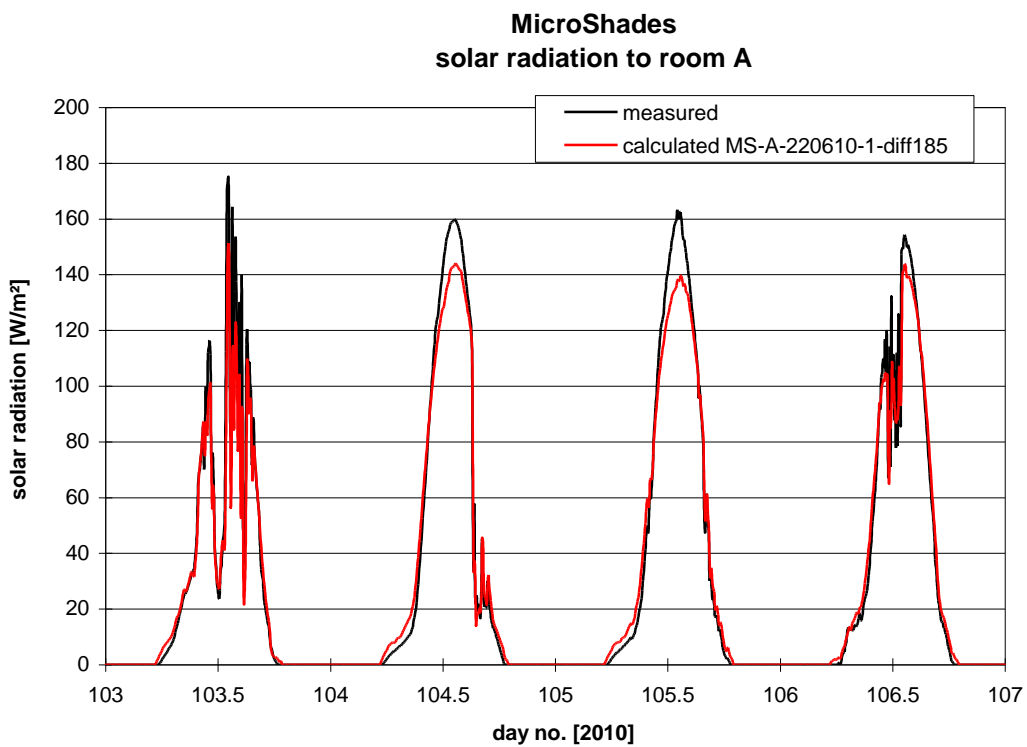


Figure B.20. Solar radiation through the MicroShade for 5 days in the spring (April 12-16, 2010). Scattering factor: 1%.

Spring period – scattering factor 2%

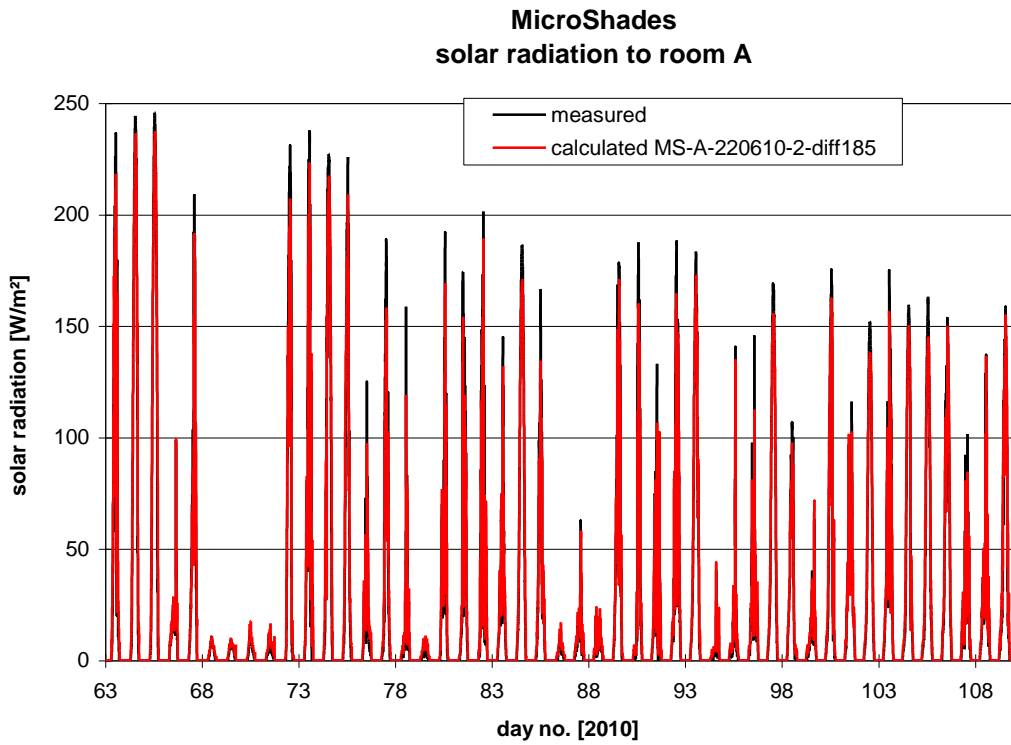


Figure B.21. Solar radiation through the MicroShade window during spring period. Scattering factor: 2%.

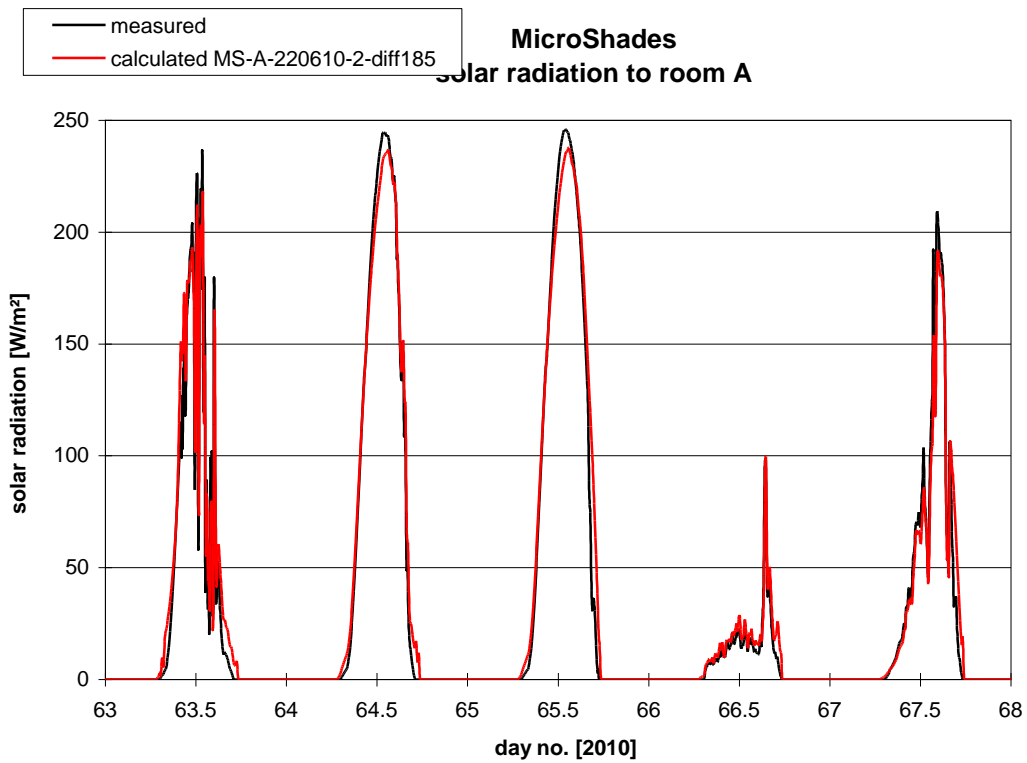


Figure B.22. Solar radiation through the MicroShade for 4 days in the spring (March 4-8, 2010). Scattering factor: 2%.

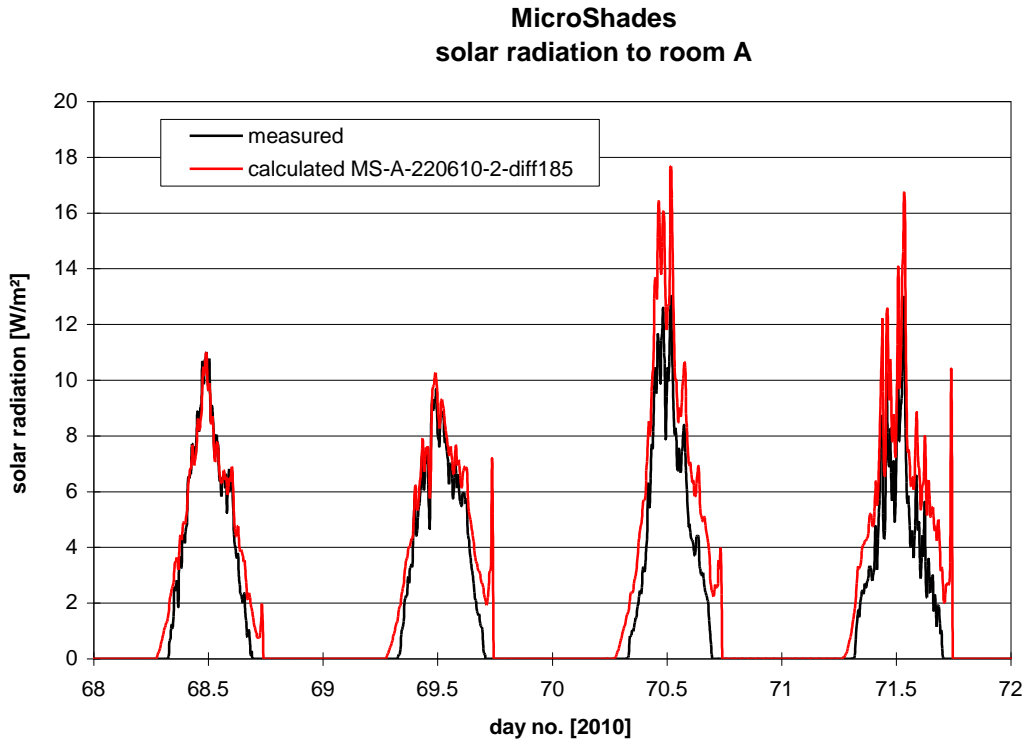


Figure B.23. Solar radiation through the MicroShade for 5 days in the spring (March 12-16, 2010). Scattering factor: 2%.

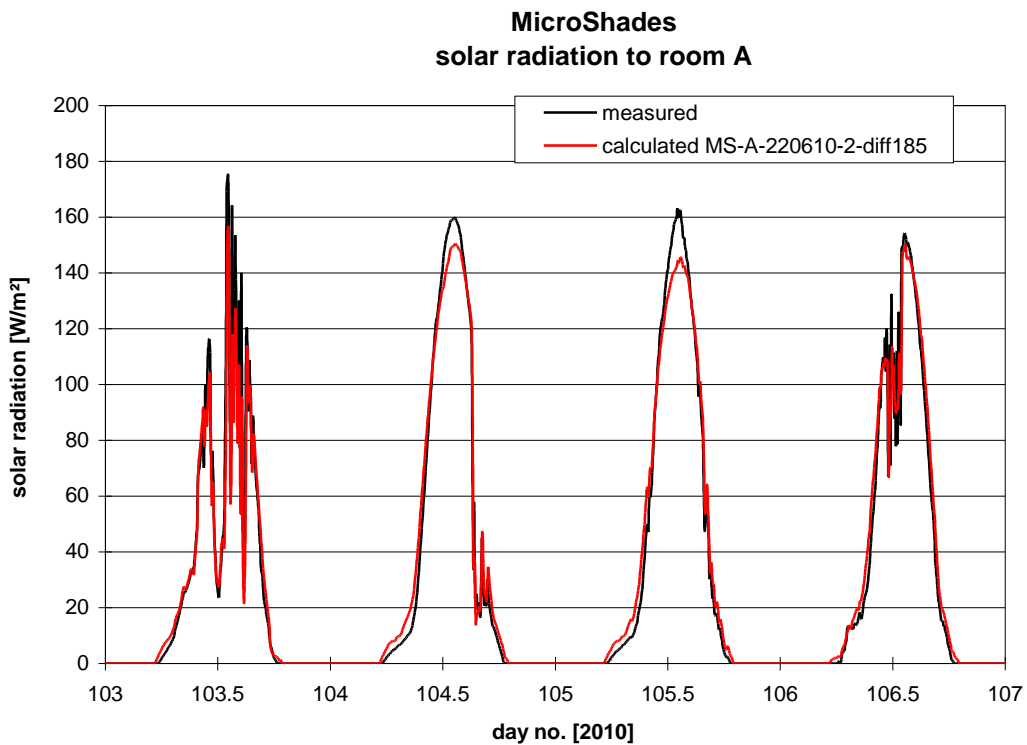


Figure B.24. Solar radiation through the MicroShade for 5 days in the spring (April 12-16, 2010). Scattering factor: 2%.

Summer period – scattering factor 0%

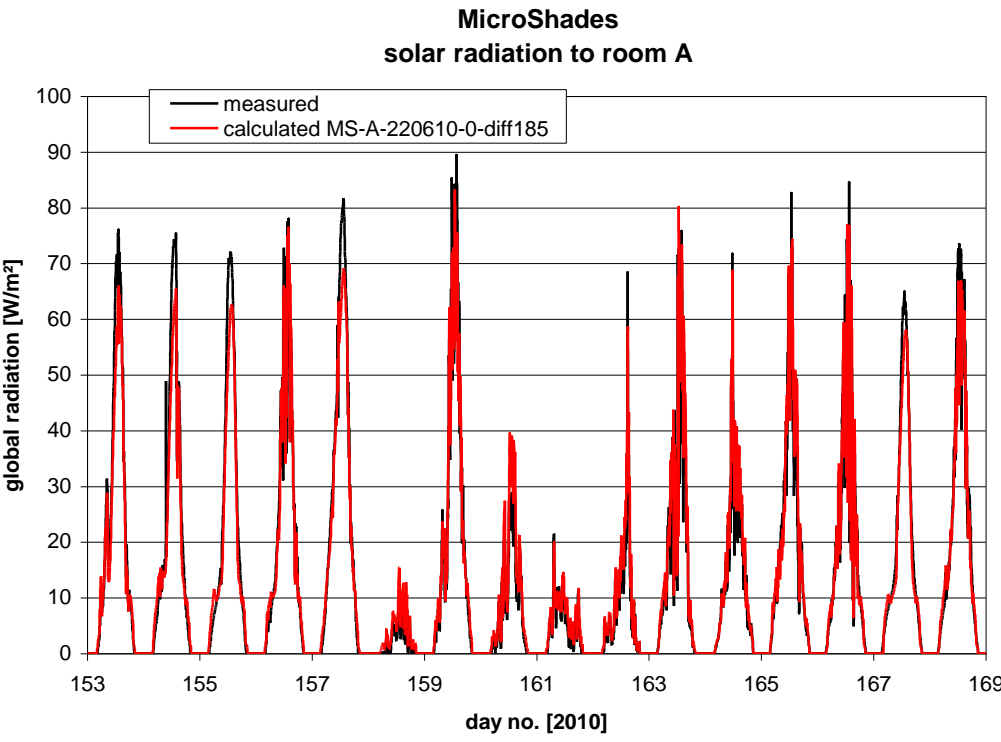


Figure B.25. Solar radiation through the MicroShade window during summer period. Scattering factor: 0%.

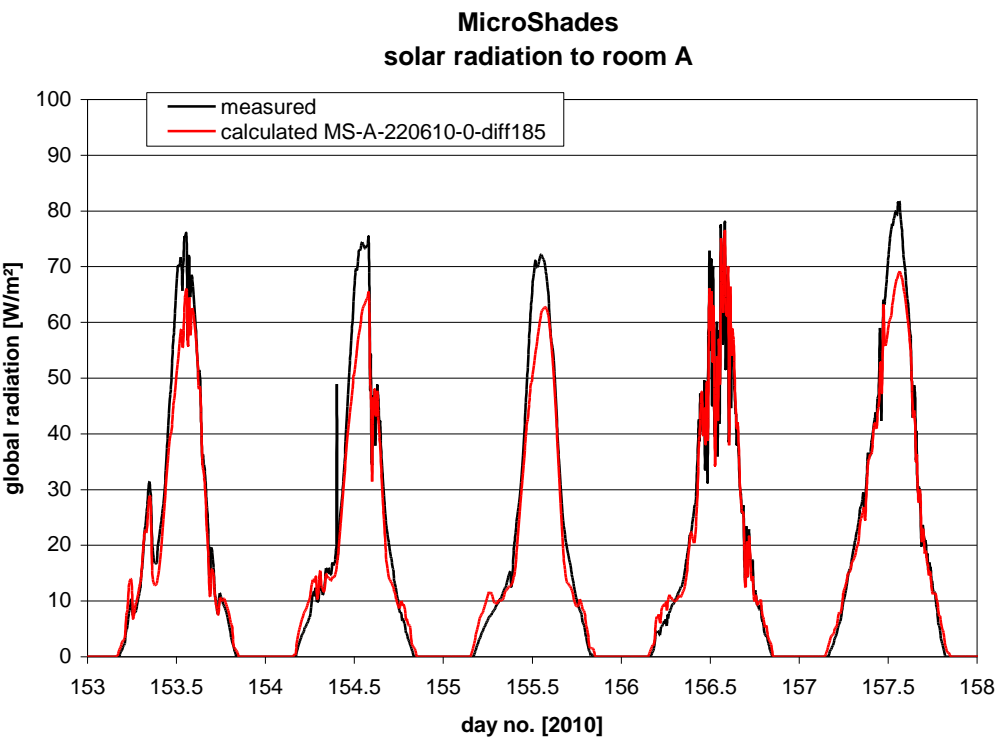


Figure B.26. Solar radiation through the MicroShade for 5 days in the summer (June 2-6, 2010). Scattering factor: 0%.

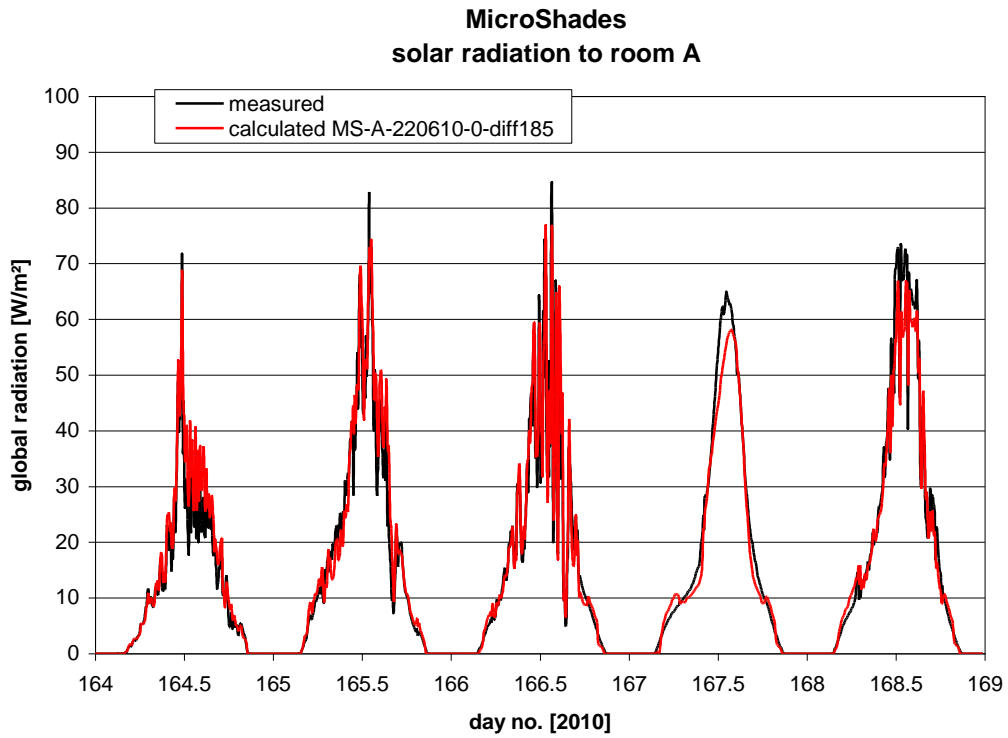


Figure B.27. Solar radiation through the MicroShade for 6 days in the summer (June 7-12, 2010). Scattering factor: 0%.

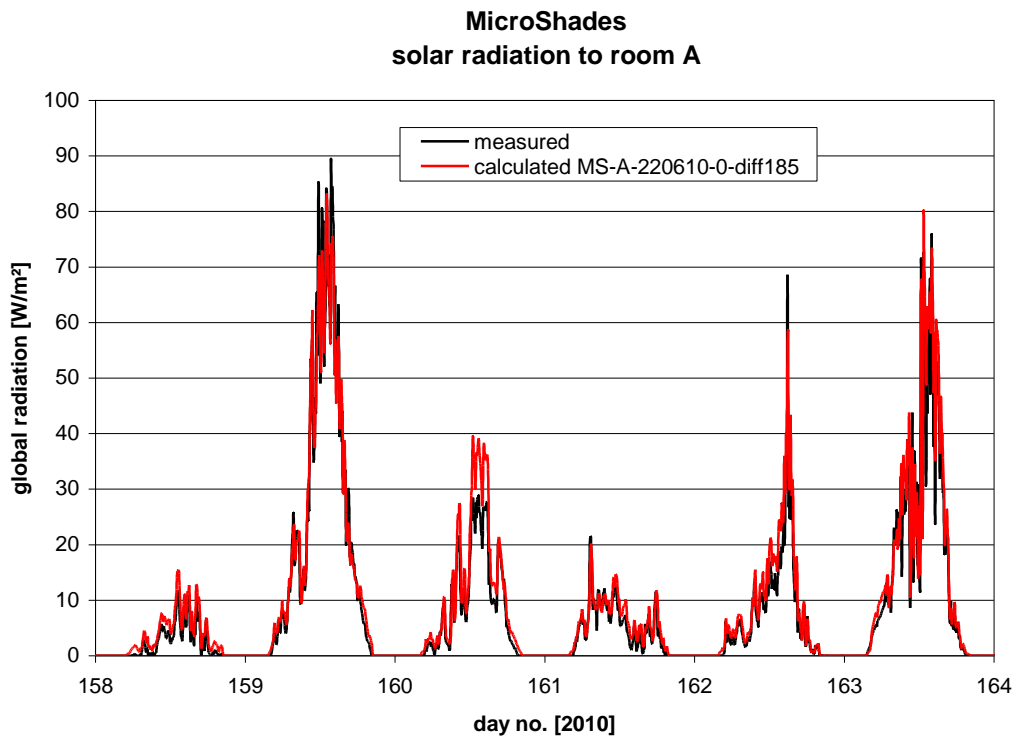


Figure B.28. Solar radiation through the MicroShade for 5 days in the summer (June 13-17, 2010). Scattering factor: 0%.

Summer period – scattering factor 1%

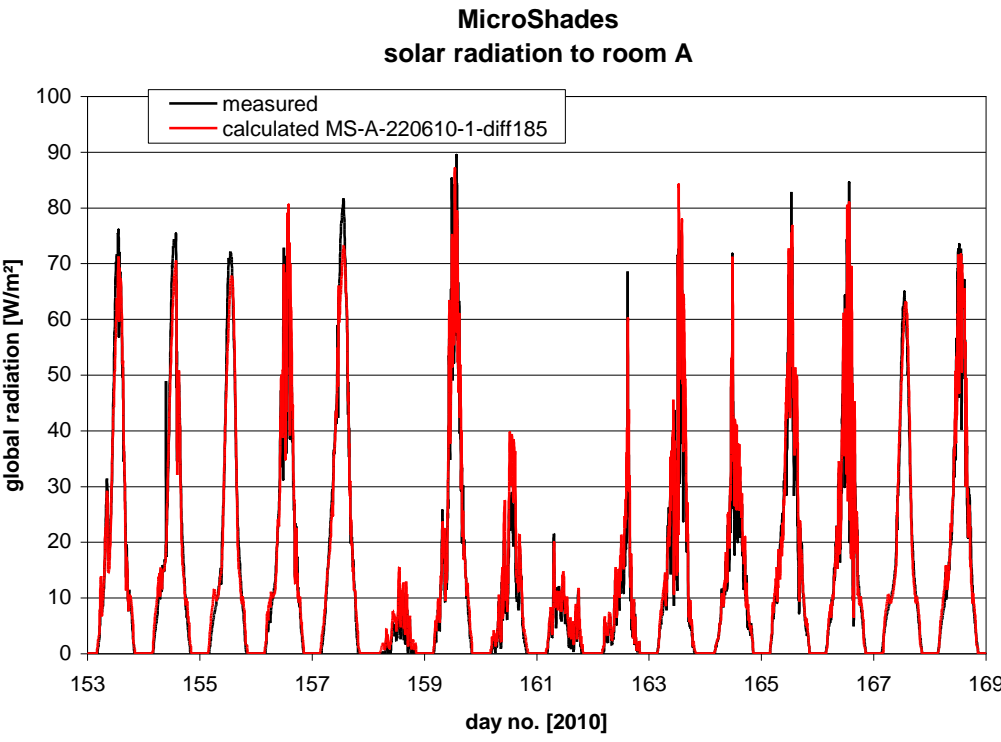


Figure B.29. Solar radiation through the MicroShade window during summer period. Scattering factor: 1%.

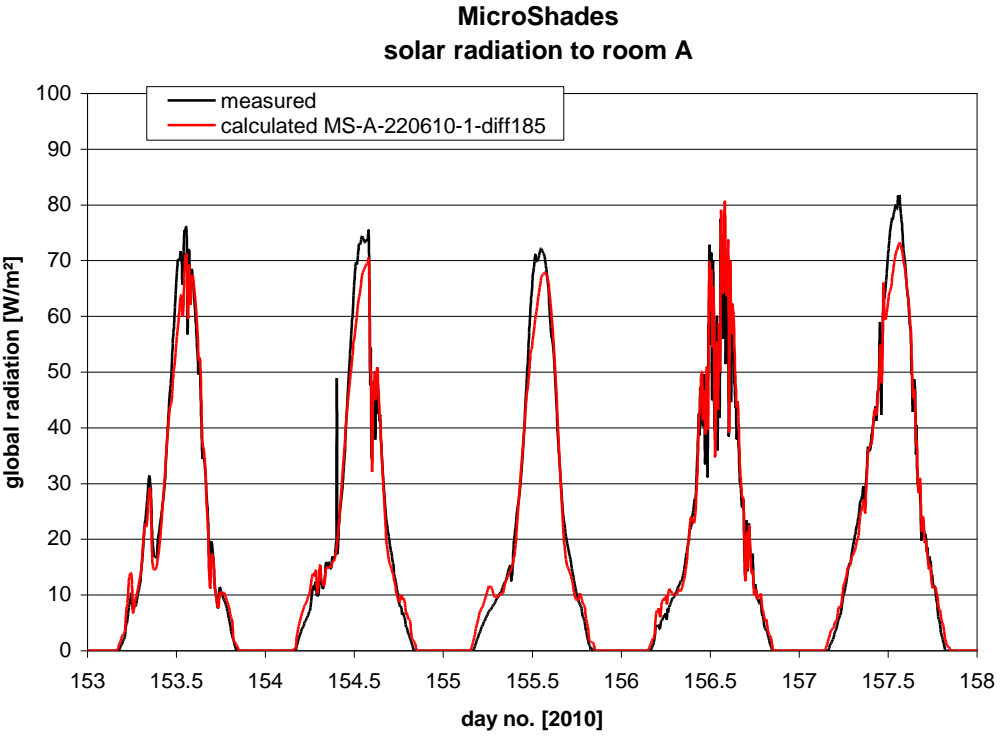


Figure B.30. Solar radiation through the MicroShade for 5 days in the summer (June 2-6, 2010). Scattering factor: 1%.

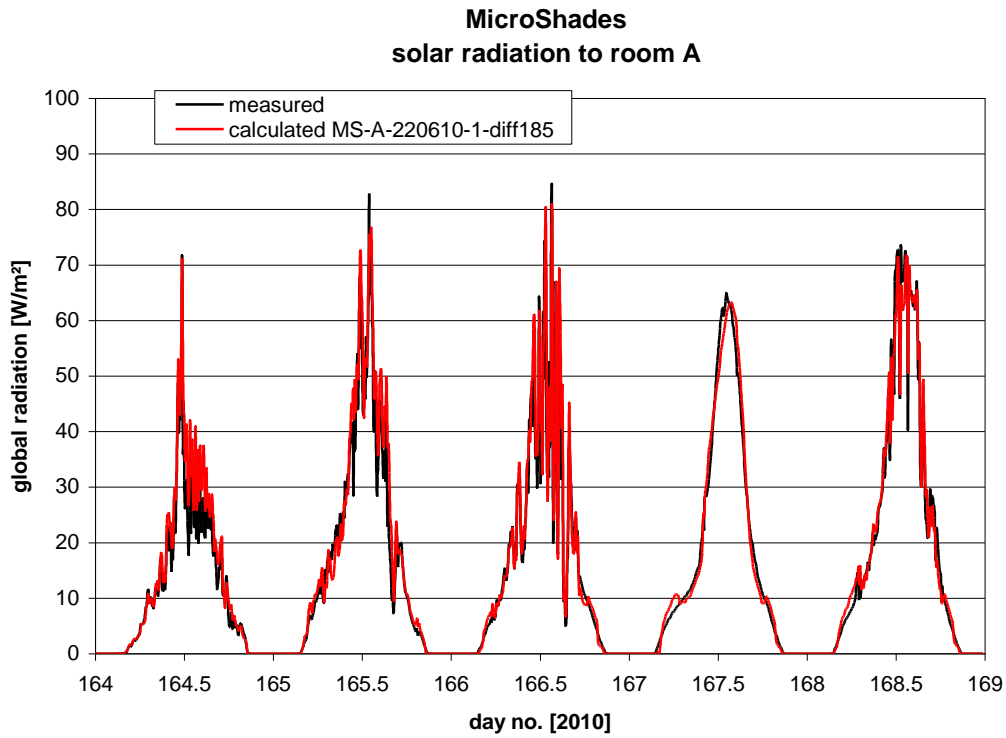


Figure B.31. Solar radiation through the MicroShade for 6 days in the summer (June 7-12, 2010). Scattering factor: 1%.

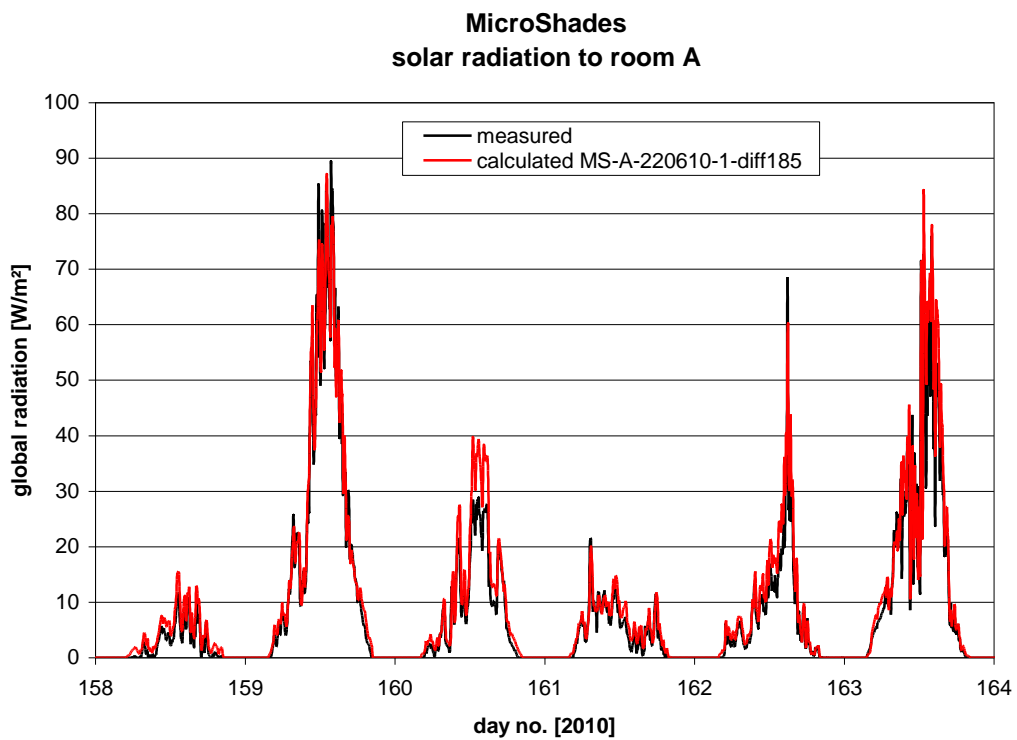


Figure B.32. Solar radiation through the MicroShade for 5 days in the summer (June 13-17, 2010). Scattering factor: 1%.

Summer period – scattering factor 2%

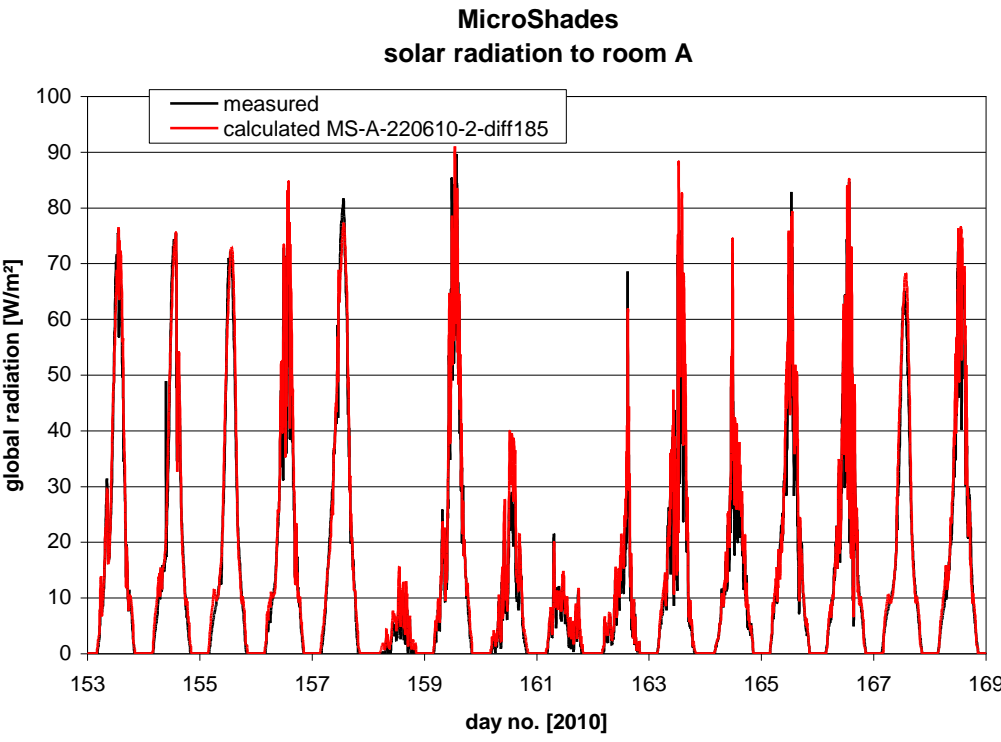


Figure B.33. Solar radiation through the MicroShade window during summer period. Scattering factor: 2%.

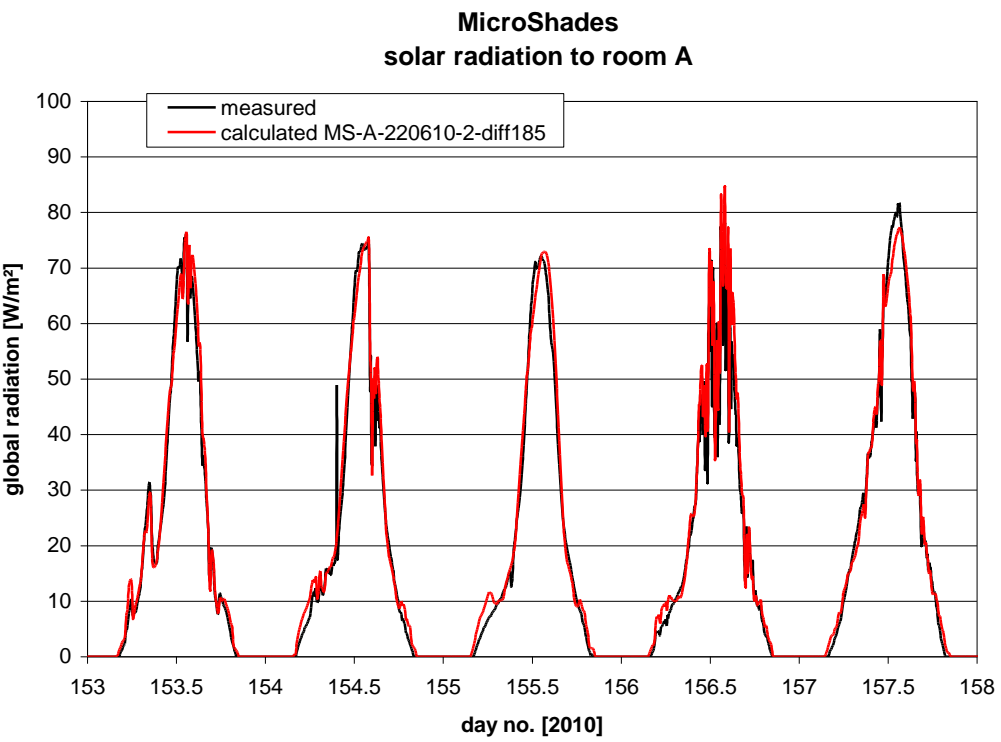


Figure B.34. Solar radiation through the MicroShade for 5 days in the summer (June 2-6, 2010). Scattering factor: 2%.

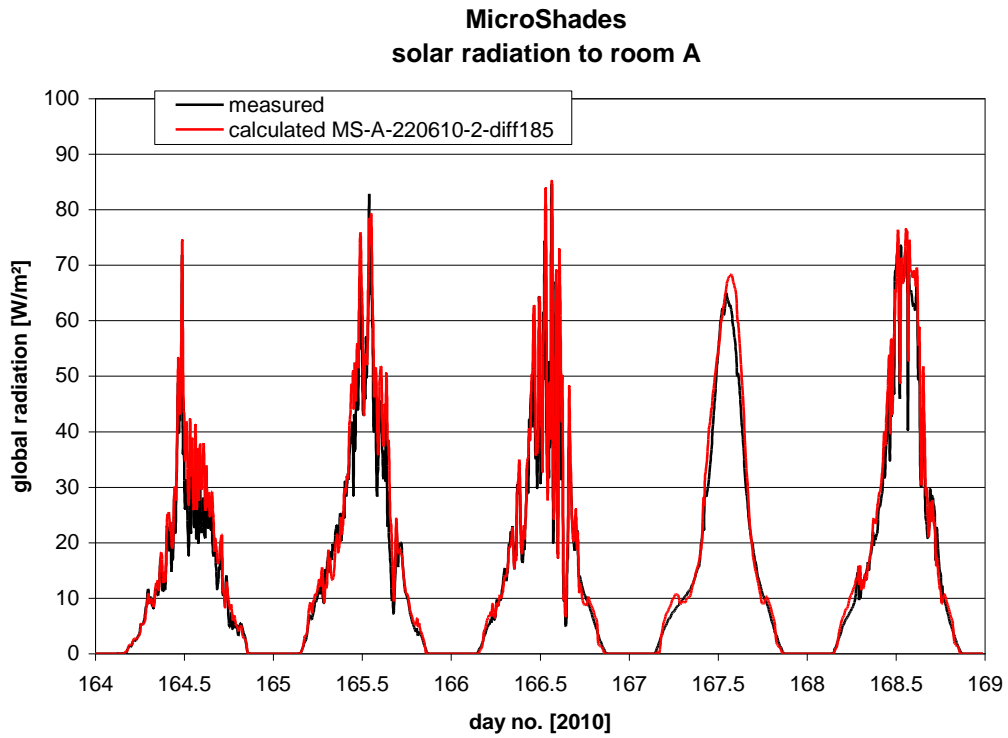


Figure B.35. Solar radiation through the MicroShade for 6 days in the summer (June 7-12, 2010). Scattering factor: 2%.

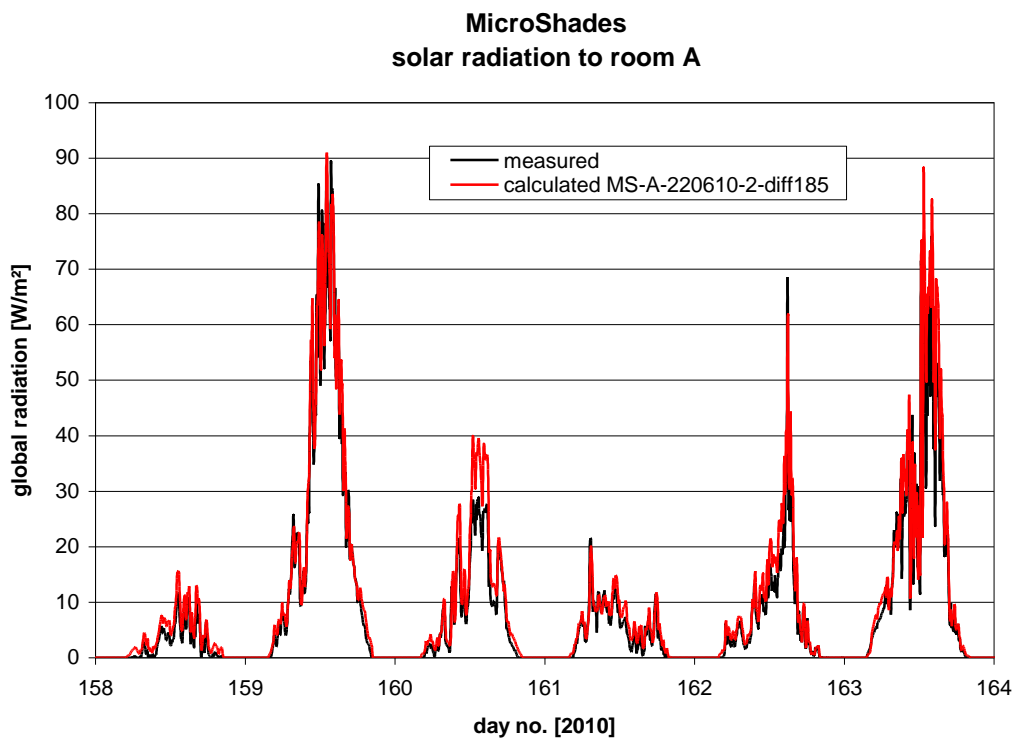


Figure B.36. Solar radiation through the MicroShade for 5 days in the summer (June 13-17, 2010). Scattering factor: 2%.

Appendix C

Brochure on applying MicroShades in windows at Malling school

At Malling School they are keeping their heads cool

There is nothing new about an overheated indoor climate in classrooms and pupils who are unable to focus. But at Malling School they have managed to lower the temperature by up to 4-5°C by changing to glazing units with integrated MicroShade™ solar shading.

Malling School, just south of Aarhus, had persistent problems with its indoor climate for some time, particularly in the south-facing classrooms, where the strong sun radiation coming through the windows sharply raised classroom temperatures and provided poor lighting. This was even though solar control glass had already been installed. The problem had to be fixed and it had to be done in the most cost-effective way, in terms of maintenance and investment.

As a result, Aarhus County had to look around for a less conventional solution, so that pupils and teachers could keep their heads cool. The end result was two-layered insulating glazing units that incorporated MicroShade™.

Significant reduction of temperature from day one

Pupils and teachers alike are delighted with MicroShade™. The indoor environment is now much improved, helping to improve levels of concentration. Gorm Albertsen, of Aarhus County, says: "Our own tests confirm that the temperature in the sun has been significantly reduced using MicroShade™, in some cases from 30°C to 25.5°C. It used to be boiling hot in the sun and it could be difficult to read the writing on the board. However, the problem has been solved and teachers and pupils now feel much more comfortable."

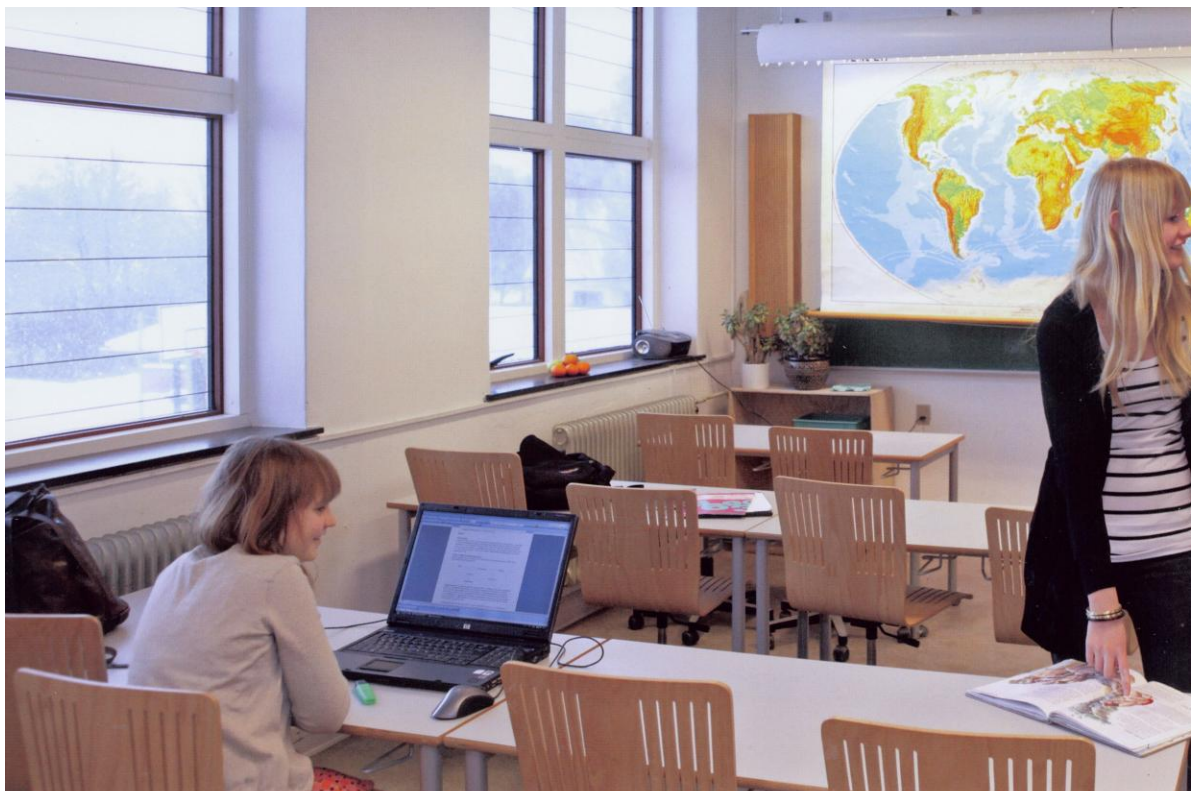




PROJEKTSTUDIE:

På Malling Skole holder de hovedet koldt

Alt for varmt indeklima i klasselokaler og ukoncentrerede skoleelever er ikke noget ukendt fænomen. Men på Malling Skole har de sænket temperaturen op til 4-5° C med solafskærmning integreret i termoruderne.



Problemer med indeklima

Malling Skole syd for Århus havde længe haft problemer med indeklimaet. Specielt i skolens sydvendte klasselokaler, hvor den kraftige solindstråling gav stærk opvarmning og dårligt lys i undervisningslokalerne på trods af, at der var installeret solkontrolglas. Der skulle gøres noget ved problemet, og det skulle ske mest økonomisk ud fra både drift og investering.

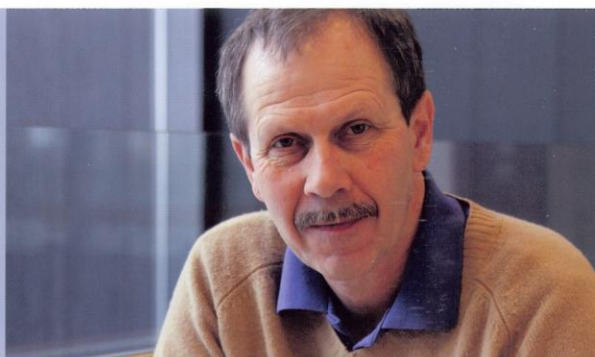
Gorm Albertsen, bygningskonsulent for skolerne i den sydlige del af Århus Kommune: "Det er et tilbagevendende problem, at der bliver for høje temperaturer i

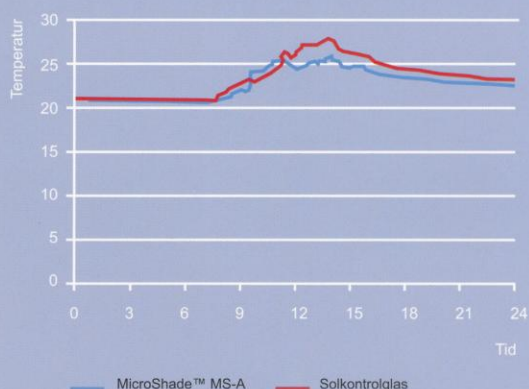
sydvendte klasselokaler, når solen står højt på himlen. Arbejdstilsynet gav os påbud om at finde en løsning til indeklimaet på dele af Malling Skole. Vi forkastede traditionelle løsninger med udvendig solafskærmning, fordi de blev vurderet som u hensigtsmæssige at vedligeholde i forbindelse med blandt andet leg i skolegårdene."

Resultatet blev, at Århus Kommune måtte gå på udkig efter andre, mere utraditionelle løsninger, så elever og lærere kunne holde hovedet koldt.

"Vores målinger bekræfter, at temperaturen i solen blev kraftigt reduceret, i nogle tilfælde fra 30 til 25,5° C med MicroShade™."

Gorm Albertsen, Århus Kommune.





Eksempel på temperaturforløb, Malling Skole

Måledata fra Malling Skole, temperaturmåling foretaget med afskyggede temperaturfølere.

Måledata omfatter to serier målt samtidigt i tilstødende og identiske klasselokaler. Lokale 1 udstyret med solkontrolglas, lokale 2 udstyret med MicroShade™ MS-A ruder.

De i eksemplet viste måledata er udført tirsdag 1. september 2009, en delvis skyet dag.

Undersøgte markedet for solafskærmning

Løsningen blev fundet i samarbejde med Bascon A/S, der var rådgiver på sagen. Mark Lund Andersen, Bascon A/S: "Vi blev via en omtale i et fagblad opmærksom på mulighederne i PhotoSolar og deres MicroShade™ solafskærmning af mikrolameller. Sammen med en af vores indeklimaeksperter og bygherren besøgte vi virksomheden og fandt den nye løsning spændende, fordi afskærmningen er bragt uden for fysisk kontakt og indbygget i termoruden, og derfor ikke har ulemperne ved udvendig solafskærmning."

En række fuldskalaforsøg direkte i miljøet blev gennemført, og MicroShade™ blev valgt, fordi PhotoSolar kunne fremvise en effektiv solafskærmning og en vurderet god totaløkonomi. Mark Lund Andersen uddyber: "Drifts- og vedligeholdelsesmæssigt er MicroShade™ i dette projekt et intelligent produkt med en rigtig god totaløkonomi set over tid."

Ingen vedligeholdelse og ingen hærværk

En vigtig årsag til valget af MicroShade™ var, at der ingen vedligeholdelse er - i modsætning til udvendig solafskærmning. En udvendig løsning vil være udsat i forbindelse med vejrlig, leg og eventuelt hærværk.

Markant reduktion af temperaturen fra dag 1

Både elever og lærere er glade for MicroShade. De oplever, at undervisningsklimaet er blevet meget bedre til gavn for koncentration og indlæring. Gorm Albertsen: "Vores målinger bekræfter, at temperaturen i solen blev kraftigt reduceret, i nogle tilfælde fra 30 til 25,5° C med MicroShade™. Tidligere var det stegende hedt at sidde i solskin, og det kunne samtidig være svært at læse, hvad der stod på tavlen. Det problem er løst og komforten er kraftigt forbedret."

Man måtte erkende, at de eksisterende ruder med traditionelle solkontrolglas havde deres begrænsninger. Med MicroShade™ er den belastende "punktvarmning" af elever og inventar i opholdszonerne væk, og i tilgift kan eleverne nu se, hvad læreren viser på tavlen. Kombineret med balanceret ventilation har løsningen forbedret indeklimaet – til Arbejdstilsynets fulde tilfredshed.



Med MicroShade™ er den belastende "punktopvarmning" af elever og inventar i opholdszonerne væk.

Mikrolameller stopper solen – ikke udsynet

Løsningen består af 50 m² 2-lags ruder med indlagt MicroShade™ solafskærmning, argonfyldning og U-værdi 1,1. Ruderne har en g-værdi helt ned til 0,10, hvilket i praksis svarer til maksimal afskærmning. Isætningen af ruderne er foregået på helt normal vis.

MicroShade™ afskærmning består af patenterede og transparente mikrolameller, der placeres som et indvendigt lag i termoruden. Afskærmningen er designet efter solens bevægelsesmønster og årstiden: Jo højere solen står, des større er afskærmningseffekten. Det transmitterede lys er godt naturligt dagslys.

Nyt projekt allerede på vej

Århus Kommune er meget tilfredse med projektets forløb, og med at indeklimaproblemerne på Malling Skole nu er løst. Derfor har kommunen også valgt MicroShade™ i forbindelse med et stort renoveringsprojekt på en anden af kommunens skoler, Solbjerg Skole. Her skal der under de samme betingelser installeres ca. 400 m² MicroShade™ 3-lagsruder i energiklasse 1 og U-værdi 0,76.

PhotoSolar A/S
Gregersensvej 1
2630 Taastrup
Danmark
Tel: +45 7214 4848
info@photosolar.dk
www.photosolar.dk

Alle oplysninger er vejledende.
Ret til ændringer forbeholdes.
Ingen af de foreliggende informationer er bindende for PhotoSolar A/S.

Appendix D

Description of two class rooms at Malling school

Malling Skole, Århus Kommune

Beskrivelse af klasselokaler, 416/417, sydvendt.

Rum 416 og 417 er placeret på første sal. Bygningen er opbygget som følger:

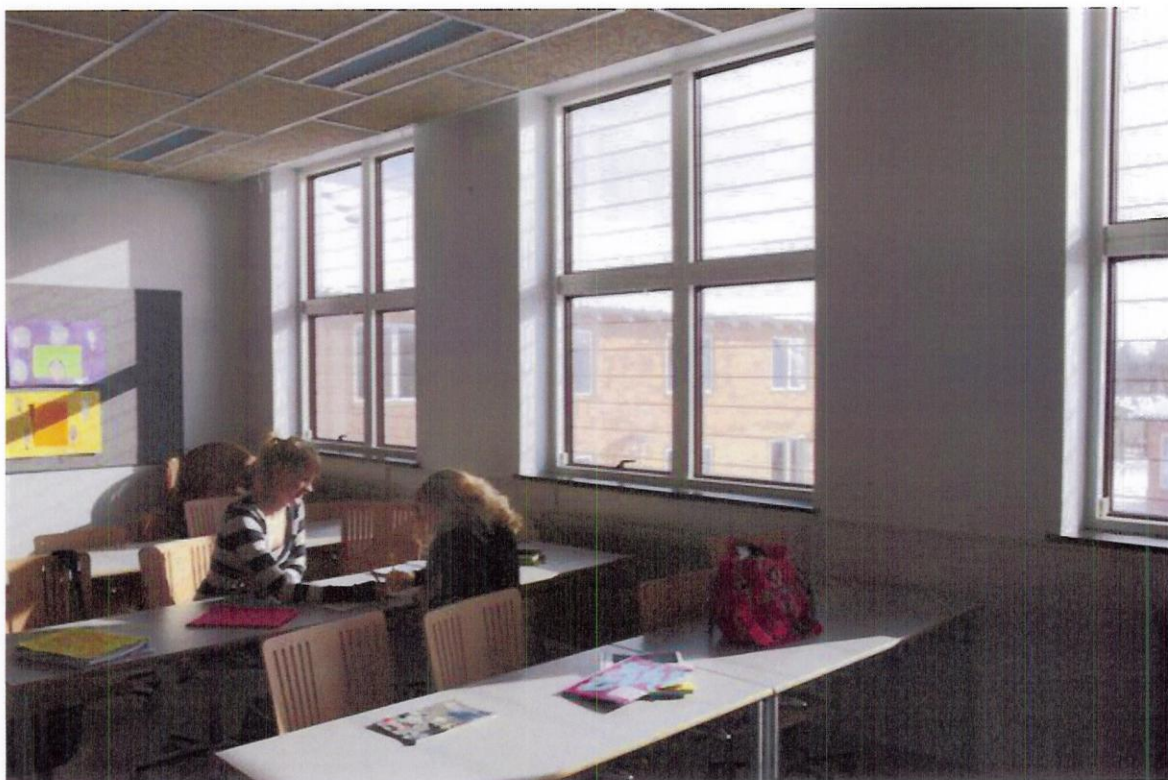
- 15 cm betondæk (anslået).
- Tunge vægge (hulmurskonstruktion i tegl).
- Bagvæg mod gang er 10 cm beton (anslået).
- Damploft på forskalling i loft og 150 mm mineraluld.
- Der var ikke nogen ventilation i rummene.

Lokalerne har følgende mål:

- 6,0 m dybde
- 8,1 m længde
- 3,1 m. loftshøjde

Plantegning og snit for bygningen er vist i figurerne nedenfor. Bemærk, at snittegningen stammer fra en fløj som kun er 1 etage, men tegningen er gældende også for disse rum, blot er der et tilsvarende lokale i stedet for krybekælder.

Jeg vedlægger desuden lidt billeder fra de omtalte rum, det viser lidt om bygningstypen.





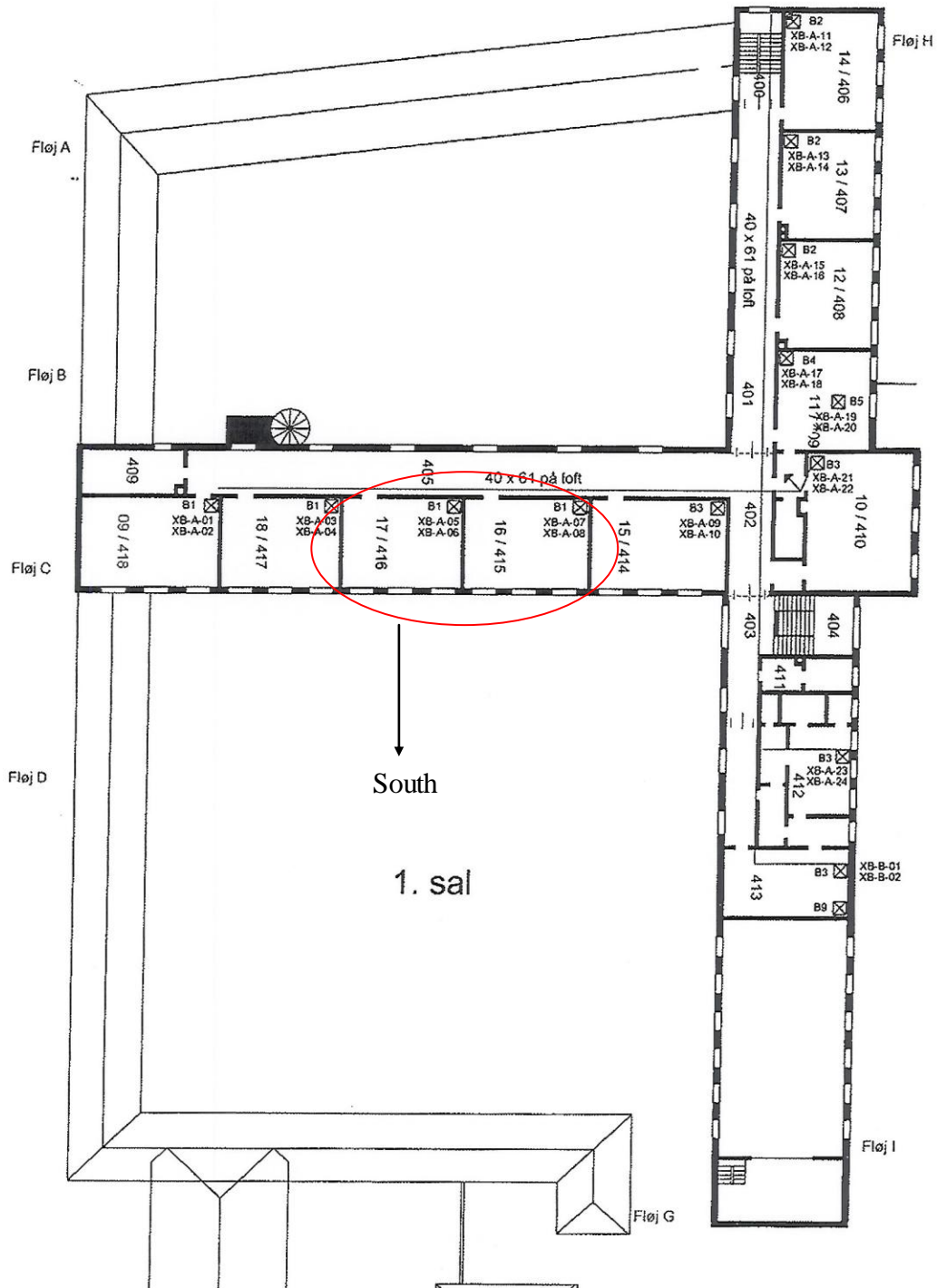


Figure D.1. Plan over Malling school. The two considered class rooms is room 16 and 17.

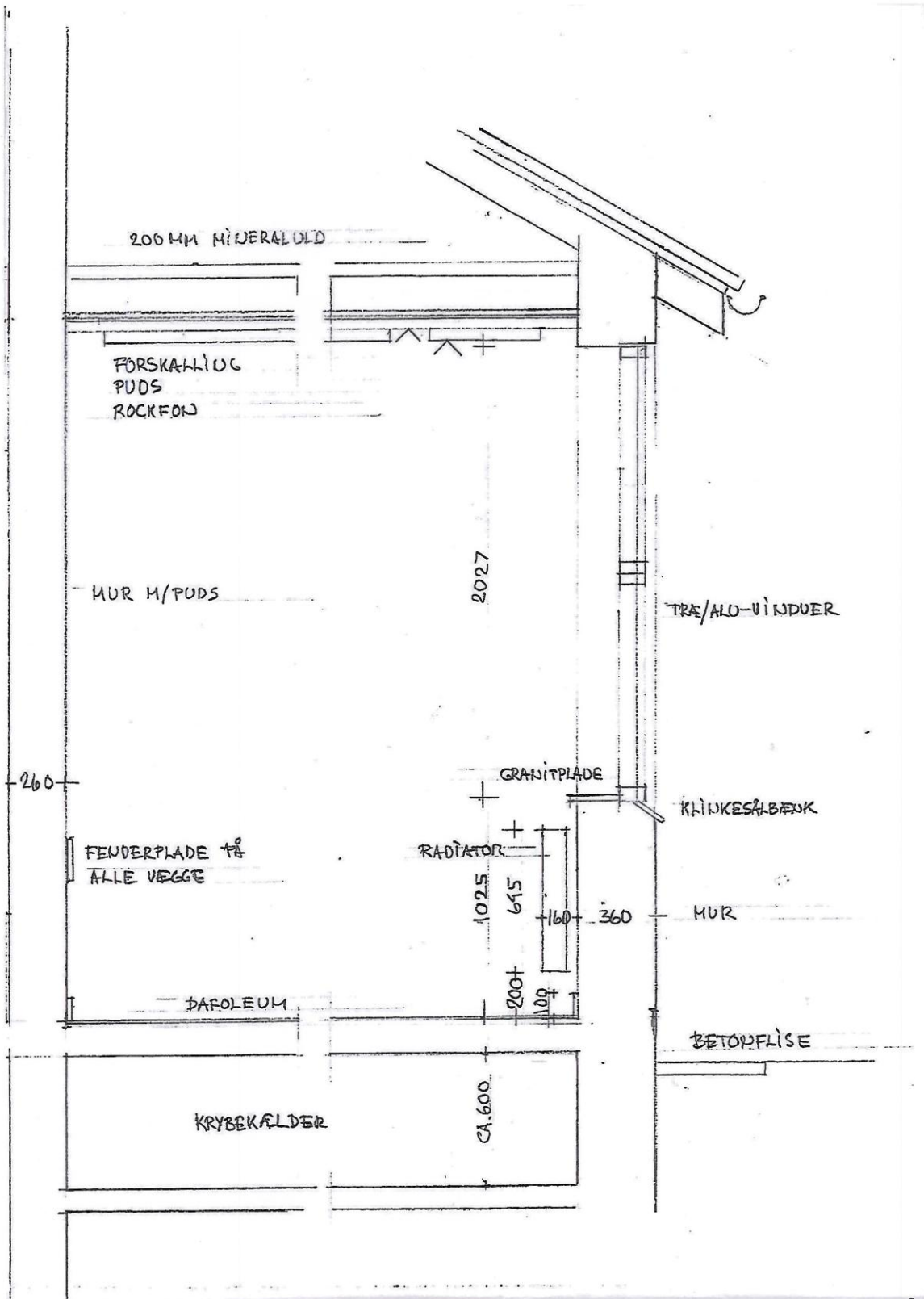


Figure D.2. Section of the class room 16 and 17.

Appendix E

Daylight measurements from [Jensen, 2008b]

3. Daylight factors

One of the purposes of installing the PowerShades in rooms of real room size was to be able to evaluate the influence of the PowerShades on the daylight conditions within a room behind the powerShades.

The dimensions of the test rooms are given in figure 1.6. The colour of the walls except the façade is light grey while the colour of the façade internally, the ceiling and the entrance door is white. The colour of the floor is brown. For more details please refer to (Jensen, 2008a).

Daylight factors are obtained in the following way: the horizontal Lux is measured in the room at a height of 0.7 m. At the same time the horizontal Lux on the roof without shading is measured. The measurements have to be conducted during cloudy conditions without any direct solar radiation. The daylight factor is the Lux in the room divided by the Lux at the roof and multiplied with 100. The unit is %.

Further the Lux meter in the room has been traversed through the room from the window to the back of the room.

The following daylight measurements have been conducted:

Daylight measurements	test room A	test room B
1	PS4060	Velfac sun 1/clear
2	PS4060	Computer curtains
3	PS4060	Velfac sun 1/clear + external solar screening from Faber
4	PS4060	Velfac sun 1/clear + external solar screening from Faber with half number of lamellas
5	Prototype 1	Velfac sun 1/clear

Table 3.1. The daylight measurements conducted in the test rooms.

The daylight factors may vary due to different sky conditions between the measurements and can, therefore, not be compared directly. Instead the daylight factors for the different measurements have been normalized based on measurement number 1 in table 3.1. The result is shown in figure 3.1.

- the Velfac window with computer curtain and with full Faber solar shading have the lowest and identical daylight factors
- PS4060 has the second lowest daylight factors
- Prototype 1 and Velfac window with half Faber solar shading have the second highest and almost identical daylight factors – this was anticipated as these two systems have similar screening effect
- the Velfac window without screening has the highest daylight factors

The daylight factor should preferably be above 2%. This is only achieved all through the room by the Velfac window, however, with a very high daylight factor at the window. The other windows lead to a more even daylight factor throughout the room. Two of them have daylight factor above 2% during half of the room. The two systems with the lowest daylight

factors will lead to a high electricity demand for artificial lightning – however, this will often not be the case with computer curtains, as they are pulled up when no direct sunlight is disturbing screen work.

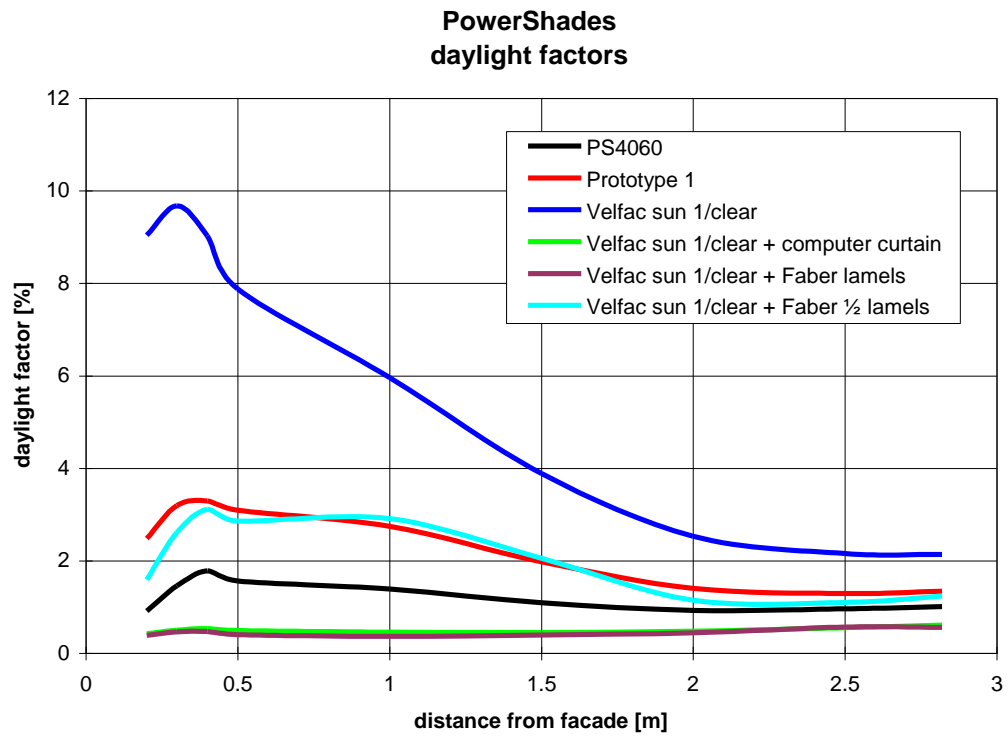


Figure 3.1. Daylight factors in the test rooms with different screening systems.